

**BOUNDS ON THE VOLUME OF AN INCLUSION IN
A BODY AND CLOAKING DUE TO ANOMALOUS
LOCALIZED RESONANCE**

by

Andrew E. Thaler

A dissertation submitted to the faculty of
The University of Utah
in partial fulfillment of the requirements for the degree of

Doctor of Philosophy

Department of Mathematics

The University of Utah

August 2014

Copyright © Andrew E. Thaler 2014

All Rights Reserved

The University of Utah Graduate School

STATEMENT OF DISSERTATION APPROVAL

The dissertation of Andrew E. Thaler
has been approved by the following supervisory committee members:

Graeme Milton, Chair May 19, 2014
Date Approved

Andrej Cherkaev, Member May 19, 2014
Date Approved

Elena Cherkaev, Member May 19, 2014
Date Approved

Fernando Guevara Vasquez, Member May 19, 2014
Date Approved

Hyeonbae Kang, Member May 19, 2014
Date Approved

and by Peter Trapa, Chair/Dean of
the Department/College/School of Mathematics

and by David B. Kieda, Dean of The Graduate School.

ABSTRACT

We study three problems in this dissertation. In the first problem, we derive bounds on the volume occupied by an inclusion in a body through the use of a single measurement of the complex voltage and current flux around the boundary of the body. We assume that the conductivities of the inclusion and the body are complex. In the second problem, we derive a formula that gives the exact volume fraction occupied by a linearly elastic inclusion in a linearly elastic body when both the inclusion and the body have the same shear modulus. The formula for the volume of the inclusion is based on an appropriate measurement of the displacement and traction around the boundary of the body, tailored to force the body to behave as if it were embedded in an infinite medium. In the third problem, we prove that the power dissipated in a nonsymmetric slab superlens blows up in the limit as the dissipation parameters in the lens and the surrounding medium go to zero when certain charge density distributions are placed within a critical distance of the slab. The critical distance that leads to this blow-up of the power dissipation depends nontrivially on the relative amount of dissipation in the slab and surrounding medium. This behavior of the power dissipation, in combination with the fact that the potential remains bounded far away from the slab as the dissipation parameters go to zero, leads to cloaking by anomalous localized resonance.

I dedicate this dissertation to my parents, Eric and Terrie Thaler. I will never be able to repay you for all of your love and support. I also dedicate this thesis to my wife, Chantelle, and my daughter, Bella. You both make every day beautiful.

CONTENTS

ABSTRACT	iii
LIST OF FIGURES	vii
LIST OF TABLES	ix
ACKNOWLEDGEMENTS	x
CHAPTERS	
1. INTRODUCTION	1
2. BOUNDS ON THE VOLUME OF AN INCLUSION IN A BODY FROM A COMPLEX CONDUCTIVITY MEASUREMENT	3
2.1 Introduction	3
2.2 Preliminaries	13
2.3 The Splitting Method	15
2.3.1 Null Lagrangians	15
2.3.2 Main Idea	18
2.4 Elementary Bounds	27
2.5 More Sophisticated Bounds	30
2.6 Additional Null Lagrangians in 2-D	38
2.6.1 Improved Elementary Bounds	38
2.6.2 Attainment of Improved Elementary Bounds	49
2.7 More Sophisticated Bounds in 2-D	53
2.7.1 Degenerate Cases	57
2.8 Numerical Example	57
3. EXACT DETERMINATION OF THE VOLUME OF AN INCLUSION IN A BODY HAVING CONSTANT SHEAR MODULUS	60
3.1 Introduction	60
3.2 Elasticity	64
3.2.1 Tensor Algebra	65
3.2.2 Linear Elasticity	66
3.2.3 The Effective Elasticity Tensor	67
3.3 Uniform Field Relations	68
3.4 Exact Volume Fraction	70
3.4.1 Behavior of $\Delta\phi$	72
3.4.2 Main Result	74
3.5 Finite Medium	74

3.5.1	Equivalent Boundary Value Problems	75
3.6	2-D Example	78
3.6.1	Exterior Dirichlet-to-Neumann Map	78
3.6.2	Nonlocal Boundary Condition	79
3.6.3	Previous Results	81
4.	SENSITIVITY OF ANOMALOUS LOCALIZED RESONANCE PHENOMENA TO DISSIPATION	82
4.1	Introduction	82
4.1.1	Our Results	93
4.2	Derivation of the Potential	102
4.2.1	The Solution in the Set \mathcal{C}	103
4.2.2	The Solution in the Set \mathcal{S}	104
4.2.3	The Solution in the Set \mathcal{M}	105
4.3	Some Properties of I_k	109
4.4	Some Useful Computations	115
4.5	Power Dissipation	117
4.6	Lower Bound on Power Dissipation	118
4.6.1	Numerical Discussion	125
4.6.1.1	Rectangle	125
4.6.1.2	Circle	126
4.7	Upper Bound on Power Dissipation	129
4.8	Boundedness of the Potential	137
4.8.1	The Potential V_c	140
4.8.2	The Potential V_m	142
 APPENDICES		
A.	APPENDIX TO CHAPTER 2	147
B.	APPENDIX TO CHAPTER 3	149
C.	APPENDIX TO CHAPTER 4	172
REFERENCES		202

LIST OF FIGURES

2.1	This heuristic picture illustrates the idea behind electrical impedance tomography.	4
2.2	In the example above, we know that either $\inf \mathcal{A}^* \leq f^{(1)} \leq \sup \mathcal{A}^*$ or $\inf \mathcal{A}^{**} \leq f^{(1)} \leq \sup \mathcal{A}^{**}$	26
2.3	In this figure, we sketch the region under consideration and provide an illustration of the elementary bounds.	31
2.4	The rectangle $\mathcal{F}_{f,e}$ (outlined in black) and the sets $\mathcal{E}_f^{(1)}$ (in red) and $\mathcal{E}_f^{(2)}$ (in blue) are drawn for several test values.	37
2.5	These are plots of the improved elementary bounds in 2-D.	46
2.6	The rectangle $\mathcal{F}_{f,e}$ (outlined in black) and the sets $\tilde{\mathcal{E}}_f^{(1)}$ (red) and $\tilde{\mathcal{E}}_f^{(2)}$ (blue) are drawn for several test values.	56
2.7	These are plots of the bounds in the case of an annulus (see Figure 2.3(a)) for several volume fractions ranging from $f^{(1)} = 0.01$ to $f^{(1)} = 0.99$	58
4.1	In this figure, we illustrate the behavior of light rays as they pass through a conventional (positive-index) slab lens and a slab superlens (with a negative index of refraction).	84
4.2	This is a sketch of the cylindrical superlens.	86
4.3	We illustrate the nonresonant potential in the case when the core and the surrounding medium have different dielectric constants.	88
4.4	This figure is the same as Figure 4.3, except now we have taken $\varepsilon_c = \varepsilon_m = 1$	89
4.5	This figure illustrates the method of images.	90
4.6	This figure is the same as Figure 4.3, except now the dipole is located within the critical radius, i.e., $r_s < r_0 < r_{\text{crit}}$	91
4.7	The parameters used in this figure are exactly the same as those in Figure 4.4, except now the dipole is located within the critical radius, i.e., $r_s < r_0 < r_*$ (since $\varepsilon_c = \varepsilon_m = 1$, the critical radius is now r_*).	92
4.8	We consider a slab geometry with a dielectric constant as illustrated in the figure.	94
4.9	(Rectangular ρ) In all of these figures we take $a = d_1/\tau(\beta)$ so ρ is completely within the region of influence.	127
4.10	(Circular ρ) In all of these figures we take $a = d_1/\tau(\beta)$ so ρ is completely within the region of influence.	130

4.11 (Rectangular ρ) In all of these figures we take $a = d_0/\tau(\beta)$ so ρ is completely outside the region of influence.	138
4.12 (Circular ρ) In all of these subfigures we take $a = d_0/\tau(\beta)$ so ρ is completely outside the region of influence.	139
B.1 The figure shows a plot of the cross-section of the cylinder discussed in the text.	152

LIST OF TABLES

2.1 This table provides a summary of our elementary bounds on the volume fraction.	57
2.2 This table gives a summary of our bounds corresponding to the test problem described in Figure 2.3.	59

ACKNOWLEDGEMENTS

I am sure I could write another dissertation about all of the wonderful help and support I have received over the years. I have become a better mathematician and also a better person due to everyone listed here.

I want to begin by thanking my advisor, Professor Graeme Milton. I can honestly say you are the best advisor anyone could ask for, and your guidance over the past several years has been truly invaluable.

My committee members, namely Professor Andrej Cherkaev, Professor Elena Cherkaev, Professor Fernando Guevara Vasquez, and Professor Hyeonbae Kang have been immensely helpful and supportive. All of you provided me with crucial insights and wonderful ideas. I greatly appreciate your willingness to meet with me and discuss this work — this dissertation could not have been written without your input.

Professor David Dobson at the University of Utah graciously helped me with many details. All of your answers to my questions can be found in this dissertation — I am greatly indebted to you for all of your help.

Professor Daniel Onofrei at the University of Houston deserves my sincerest gratitude. You inspired me to pursue a Ph.D., and I want to thank you for pointing me in Graeme's direction at the beginning of my graduate career. Your answers to my frequent emails and Skype calls are very much appreciated. Also, thank you so much for allowing me to visit you in Houston; the trip was wonderful, and much progress on the material in Chapter 4 was made on that trip. I cherish our friendship greatly.

I want to extend my thanks to Dr. Taoufik Meklachi and Gregory Funchess at the University of Houston for their collaboration on the material in Chapter 4. Gregory provided me with material for Figures 4.10 and 4.12.

I thank Professor Henryk Hecht and Professor James Keener for their outstanding courses. I enjoyed them thoroughly, and I hope to be able to approximate your teaching and mentoring skills someday.

There are several graduate students who deserve many thanks for their help and support over the years, including Jason Albright, Patrick Bardsley, Jack Jeffries, Michal Kordy, and Greg Rice at the University of Utah and Robbie Snellman at the University of California, San Diego. Robbie and Patrick, I appreciate our friendship more than you can know; there have been so many times you both have helped me by allowing me to discuss my problems (both mathematical and otherwise) with you. I could not have asked for anyone better with whom to share an office. Patrick, your willingness to listen to me and help me with this project can never be repaid.

Also, the secretaries and graduate advisors in the mathematics department at the University of Utah have been immensely helpful; thank you so much for all of your help. I also extend my thanks to the thesis editors for pointing out several errors and helping me create a more polished document.

I thank the University of Utah and the NSF for financial support through grants DMS-0707978 and DMS-1211359.

Of course, this project had no chance of being completed without the support of my friends and family. I extend heartfelt gratitude to my parents, grandparents, in-laws, and friends. Although there is not enough room here to list all of you by name, please be assured that I am greatly indebted to all of you for your love and encouragement. I wish there was a way for me to thank you all enough.

My wife, Chantelle, and daughter, Bella, have been incredible during this whole process. I cannot even begin to offer enough to either of you in return for your love, support, and all of the joy you give me.

Most importantly, I humbly thank God, who is everything to me. This dissertation is but a small token of gratitude I give to You in return for the immense favors You have bestowed upon me.

CHAPTER 1

INTRODUCTION

In this work we consider three problems. We provide a brief introduction to the problems here; we give a more thorough introduction to each problem in its respective chapter.

In the first problem, discussed in Chapter 2, we consider a body Ω that contains an inclusion D ; the body and inclusion are each characterized by a different complex conductivity. We apply an electrical current flux around the boundary of the body Ω and measure the resulting voltage around the boundary of Ω . (We may also apply a voltage around the body of Ω and measure the resulting current flux.) Such measurements are typical in the imaging modality known as *electrical impedance tomography*. Using this measurement of the voltage and current flux we derive bounds on the volume fraction occupied by the inclusion D .

In the second problem, we assume that the body Ω and inclusion D are linearly elastic materials with the same shear modulus but different Lamé moduli. Using a measurement of the displacement and traction around the boundary of Ω , we derive an exact formula for the volume fraction occupied by the inclusion D . In order to do this, the applied boundary conditions have to be tailored so that the body Ω behaves as if it were embedded in an infinite medium. We establish the required boundary conditions and obtain the exact volume fraction formula in Chapter 3.

In Chapter 4, we consider an unrelated problem. In particular, we study the effects of placing a charge density distribution ρ in the vicinity of a slab in 2-D. This slab, known as a “poor man’s superlens,” contains a material with a dielectric constant equal to $-1 + i\delta$, where δ is a small positive number that characterizes how the slab dissipates energy in the presence of slowly oscillating electric fields. The dielectric constants in the media to the left and to the right of the slab are $1 + i(\delta + \lambda\delta^\beta)$ and 1, respectively, where $\beta > 0$ and λ are parameters we are free to choose. The charge

density distribution ρ is placed in the medium to the right of the slab. We show that if ρ satisfies a certain explicit condition and is within a critical distance of the slab, then the power dissipated in the slab tends to infinity as δ goes to zero. However, the electric potential remains bounded far away from the slab in this limit; this leads to cloaking by anomalous localized resonance — see, e.g., the work by Milton and Nicorovici [91]. If ρ is further than the critical distance from the slab, then the power dissipation does not blow up as δ goes to zero. Perhaps one of our most interesting results is that the critical distance depends nontrivially on the parameter β .

CHAPTER 2

BOUNDS ON THE VOLUME OF AN INCLUSION IN A BODY FROM A COMPLEX CONDUCTIVITY MEASUREMENT

In this chapter we use a single measurement of the electrical potential and current flux around the boundary of a body to derive bounds on the volume fraction of an inclusion in the body.

2.1 Introduction

Electrical impedance tomography (EIT) is a noninvasive imaging technique in which one utilizes measurements of the voltage and current at the boundary of a body Ω to determine information about the electrical properties (such as the conductivity distribution) inside Ω . In particular, one typically places electrodes on the boundary of Ω (denoted $\partial\Omega$) and applies a current flux (or voltage) to $\partial\Omega$ and measures the corresponding voltage (or current flux) around $\partial\Omega$ — the idea is illustrated in Figure 2.1. One or several linearly independent current flux (or voltage) patterns may be applied to $\partial\Omega$ in practice. The measurements of the voltage and current flux around $\partial\Omega$ can then be used to reconstruct the conductivity distribution (or at least discover some information about it) inside Ω . Summaries of the theory and practice of electrical impedance tomography can be found in the article by Cheney, Isaacson, and Newell [27] and the book by Mueller and Siltanen [97]. The problem of determining the conductivity distribution inside a body Ω given knowledge of the voltage and current flux on $\partial\Omega$ is known as the *Calderón Problem* in honor of the mathematician Alberto Calderón who studied it in his famous 1980 paper [24].

The Calderón Problem is an example of an *inverse problem* (as opposed to a forward problem). In this case, the corresponding forward problem can be loosely

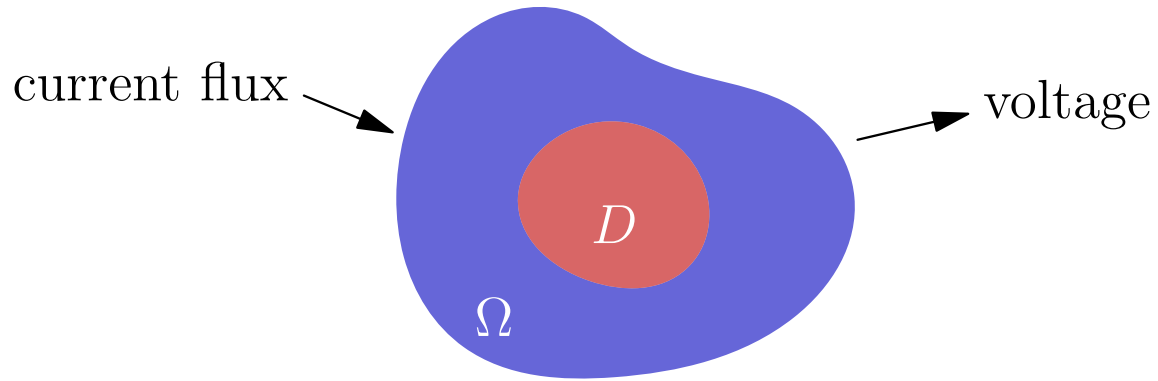


Figure 2.1. This heuristic picture illustrates the idea behind electrical impedance tomography. In practice one typically applies a current flux around $\partial\Omega$ and measures the corresponding voltage around $\partial\Omega$. The goal is to use this measurement in combination with the fact that the inclusion D (red) and the surrounding material $\Omega \setminus \bar{D}$ (blue) have different electrical properties to determine information about D .

stated as: given the conductivity distribution inside a bounded, open set Ω and appropriate boundary conditions on $\partial\Omega$ (e.g., specification of the voltage or current flux around $\partial\Omega$), determine the voltage inside Ω . The inverse problem (Calderón Problem) is: given knowledge of prescribed and measured boundary data (such as the voltage and current flux around $\partial\Omega$), determine the conductivity distribution inside Ω . Unfortunately the inverse problem is severely ill-posed; for instance, solutions may not be unique (this leads to cloaking — see the work by Greenleaf, Lassas, and Uhlmann [44] and the work of Kohn, Shen, Vogelius, and Weinstein [73]). As discussed by Mueller and Siltanen [97, Chapter 12], solutions may also be very sensitive to measurement errors. These issues have received a lot of attention in the mathematical literature — see the review article by Borcea [19] for a collection of several results regarding feasibility and uniqueness of the reconstruction of the conductivity inside Ω .

For example, Kohn and Vogelius [74] proved that boundary measurements of the voltage and current flux uniquely determine the (isotropic) conductivity and all of its normal derivatives on $\partial\Omega$ (assuming $\partial\Omega$ is smooth), and that this implies that the conductivity inside Ω can be uniquely reconstructed if it is a real-analytic function. Kohn and Vogelius [75] also extended their results to piecewise real-analytic conductivities.

Sylvester and Uhlmann [116] proved uniqueness results in the interior for smooth, isotropic conductivities (that are not necessarily real-analytic anywhere) in \mathbb{R}^d for $d \geq 3$. They were also able to prove uniqueness in 2-D if the conductivity was close enough to a constant [115]. In addition, Sylvester and Uhlmann [117] rederived the results of Kohn and Vogelius regarding uniqueness of the conductivity and its normal derivatives on $\partial\Omega$ using microlocal analysis. Sylvester and Uhlmann [117] also provided stability estimates — these estimates relate the error in measurements to the error in the reconstruction of the conductivity on $\partial\Omega$.

Nachman [100] extended the uniqueness results in the interior of Ω to domains with less regular boundaries and (isotropic) conductivities in dimension $d \geq 3$; he also provided a reconstruction algorithm. The question of whether or not conductivities could be uniquely reconstructed from boundary measurements in 2-D was answered in the affirmative by Nachman [101] for Lipschitz Domains Ω with isotropic conductivities that did not have to be too smooth. Brown and Uhlmann [22] extended this uniqueness result to even less smooth conductivities. Astala and Päivärinta [12] proved that the conductivity can be reconstructed uniquely from voltage and current flux measurements on $\partial\Omega$ assuming only that $\Omega \subset \mathbb{R}^2$ was bounded and simply connected and that the conductivity was bounded away from zero and infinity — in particular they assumed no smoothness of the boundary or the conductivity. Finally, Haberman and Tataru [47] proved uniqueness results in dimension $d \geq 3$ for continuously differentiable conductivities and Lipschitz conductivities close to the identity.

All of the above results were derived under the assumption that the conductivity inside Ω was isotropic and real which corresponds to the static case of zero frequency (direct currents) — this is discussed in more detail below. In the complex conductivity case (alternating currents), uniqueness of the reconstruction in 2-D was proved by Francini [35].

Electrical impedance tomography has applications in the nondestructive testing of materials, geophysical prospection, and medical imaging — see the review articles by Cheney et al. [27] and Borcea [19] as well as the book by Mueller and Siltanen [97] (and references therein). In the context of medical imaging, EIT can be used for breast

cancer detection as discussed by Cheney et al. [27]; according to Griffiths [46] and Beretta, Francini, and Vessella [14], EIT can also be used in the screening of organs for degradation prior to transplantation surgery. In these applications the complex conductivities of the healthy and cancerous/degraded tissues differ, so information about the conductivity distribution would allow one to estimate the location and/or size of the cancerous/degraded tissue. See the work by Hamilton and Mueller [49] for additional medical applications.

Our goal in this chapter is to find bounds on the volume fraction occupied by an inclusion D inside a body Ω . In the context of organ screening, for example, D could represent the degraded tissue and $\Omega \setminus \overline{D}$ could represent the healthy tissue; as pointed out by Griffiths [46] and Beretta et al. [14], it would be useful to estimate the volume of degraded tissue (the volume of D) before the organ is transplanted.

We assume that the complex conductivity inside Ω is of the form

$$\sigma = \sigma^{(1)}\chi(D) + \sigma^{(2)}\chi(\Omega \setminus \overline{D}),$$

where $\sigma^{(\alpha)} = \sigma_1^{(\alpha)} + i\sigma_2^{(\alpha)}$ for $\alpha = 1, 2$ and $\chi(D)$ is the indicator function of D . We require $\sigma_1^{(\alpha)} > 0$ for $\alpha = 1, 2$, which, as shown by Borcea [19], corresponds to energy dissipation. More generally, we follow Kang, Kim, and Milton [64] and consider a two-phase material with conductivity

$$\sigma(\mathbf{x}) = \sigma^{(1)}\chi^{(1)}(\mathbf{x}) + \sigma^{(2)}\chi^{(2)}(\mathbf{x})$$

where $\sigma^{(1)}$ and $\sigma^{(2)}$ are as before and $\chi^{(1)}$ is the characteristic function of phase 1, namely

$$\chi^{(1)}(\mathbf{x}) = 1 - \chi^{(2)}(\mathbf{x}) = \begin{cases} 1 & \text{if } \mathbf{x} \in \text{phase 1,} \\ 0 & \text{if } \mathbf{x} \in \text{phase 2.} \end{cases}$$

We also assume that each phase is homogeneous and isotropic, so $\sigma^{(1)}$ and $\sigma^{(2)}$ are constant complex scalars (as discussed by Beretta et al. [14], this is a reasonable assumption in the contexts of breast cancer detection and organ screening).

Electrical impedance tomography operates in the quasistatic regime, where the wavelengths of all relevant electric and magnetic fields are much larger than Ω . In EIT,

one typically prescribes either the voltage or current on $\partial\Omega$. Under these conditions, and assuming Ω is simply connected, the voltage V satisfies

$$\nabla \cdot (\sigma \nabla V) = 0 \quad \text{in } \Omega, \quad (2.1)$$

subject to either the Dirichlet Boundary Condition

$$V = V_0 \quad \text{on } \partial\Omega \quad (2.2)$$

or the Neumann Boundary Condition

$$\begin{cases} \sigma \frac{\partial V}{\partial n} = I_0 & \text{on } \partial\Omega, \\ \int_{\partial\Omega} I_0 = \int_{\partial\Omega} V = 0, \end{cases} \quad (2.3)$$

where \mathbf{n} is the outward unit normal to $\partial\Omega$ and $\frac{\partial V}{\partial n} = \nabla V \cdot \mathbf{n}$ — see the review article by Borcea [19].

The partial differential equation (PDE) (2.1) can be equivalently written in the form

$$\mathbf{E} = -\nabla V, \quad \nabla \cdot \mathbf{J} = 0, \quad \text{and} \quad \mathbf{J} = \sigma \mathbf{E}, \quad (2.4)$$

where \mathbf{E} is the electric field and \mathbf{J} is the current density — see the review article by Borcea [19].

Heuristically, these equations can be derived from the Maxwell Equations as follows (see the work by Francini [35]). The relevant Maxwell Equations are

$$\nabla \times \mathbf{E} = -\frac{\partial(\mu' \mathbf{H})}{\partial t} \quad \text{and} \quad \nabla \times \mathbf{H} = \sigma' \mathbf{E} + \frac{\partial(\varepsilon' \mathbf{E})}{\partial t}, \quad (2.5)$$

where \mathbf{E} is the electric field, \mathbf{H} is the magnetic field, μ' is the (real-valued) magnetic permeability, $\mathbf{J}' = \sigma' \mathbf{E}$ is the current field (by Ohm's Law), σ' is the (real-valued) conductivity, and ε' is the (real-valued) electric permittivity. We assume that ε' and μ' are independent of time. We also assume that the electric and magnetic fields are time-harmonic, i.e., that $\mathbf{E}(\mathbf{x}, t) = \widehat{\mathbf{E}}(\mathbf{x}, \omega) e^{-i\omega t}$ and $\mathbf{H}(\mathbf{x}, t) = \widehat{\mathbf{H}}(\mathbf{x}, \omega) e^{-i\omega t}$. Inserting these into (2.5) gives

$$\nabla \times \widehat{\mathbf{E}}(\mathbf{x}, \omega) = i\omega \mu'(\mathbf{x}, \omega) \widehat{\mathbf{H}}(\mathbf{x}, \omega), \quad (2.6a)$$

$$\nabla \times \widehat{\mathbf{H}}(\mathbf{x}, \omega) = \sigma'(\mathbf{x}, \omega) \widehat{\mathbf{E}}(\mathbf{x}, \omega) - i\omega \varepsilon'(\mathbf{x}, \omega) \widehat{\mathbf{E}}(\mathbf{x}, \omega) = \sigma(\mathbf{x}, \omega) \widehat{\mathbf{E}}(\mathbf{x}, \omega), \quad (2.6b)$$

where $\sigma(\mathbf{x}, \omega) \equiv \sigma'(\mathbf{x}, \omega) - i\omega \varepsilon'(\mathbf{x}, \omega)$ is the complex conductivity of the medium. In the literature, σ is often referred to as the admittivity and represented by γ . (The

electric and magnetic fields are sometimes assumed to have an $e^{i\omega t}$ time-dependence instead of an $e^{-i\omega t}$ time-dependence, which gives $\sigma(\mathbf{x}, \omega) = \sigma'(\mathbf{x}, \omega) + i\omega\varepsilon'(\mathbf{x}, \omega)$.) If $\omega = 0$, we refer to $\sigma(\mathbf{x}, 0) = \sigma'(\mathbf{x}, 0)$ as the real conductivity.

Hamilton [48] noted that μ' is quite small in many applications and thus performed a Taylor expansion of $\widehat{\mathbf{E}}(\mathbf{x}, \omega)$ and $\widehat{\mathbf{H}}(\mathbf{x}, \omega)$ around $\mu' = 0$ to derive (2.1). Previously, Cheney et al. [27] performed a scaling analysis to show that (2.1) gives a reasonable approximation to the operation of electrical impedance tomography machines (at low enough frequencies). The expression “low enough frequencies” deserves some comment here. In practice, quasistatics is a good approximation as long as the wavelengths and attenuation lengths of the electric and magnetic fields are large compared with the body in question (where the wavelength used is the wavelength of the field in the body, not the free space wavelength). For example, Cheney et al. [27] stated that one system they utilized operated at 28.8 kilohertz when used with bodies smaller than 1 meter and real conductivities smaller than $1 \text{ (Ohm-meter)}^{-1}$. (In particular, Cheney et al. [27] required that the quantity $\omega\mu'\sigma'[x]$ is negligible, where $[x]$ is a typical length in the body.) As was also mentioned in that paper, other systems work with higher real conductivities σ' but they operate at lower frequencies.

At any rate, the above works justify the disregard of the right-hand side of (2.6a) at low frequencies. Then $\nabla \times \widehat{\mathbf{E}}(\mathbf{x}, \omega) = 0$ in Ω , so $\widehat{\mathbf{E}}(\mathbf{x}, \omega) = -\nabla\widehat{V}(\mathbf{x}, \omega)$ for a potential \widehat{V} as long as Ω is simply connected. Since the divergence of a curl is always zero, if we take the divergence of (2.6b) we obtain

$$\nabla \cdot (\sigma(\mathbf{x}, \omega)\widehat{\mathbf{E}}(\mathbf{x}, \omega)) = 0. \quad (2.7)$$

We obtain (2.1) by inserting $\widehat{\mathbf{E}} = -\nabla\widehat{V}$ into (2.7); we obtain (2.4) by defining $\widehat{\mathbf{J}}(\mathbf{x}, \omega) = \sigma(\mathbf{x}, \omega)\widehat{\mathbf{E}}(\mathbf{x}, \omega)$. In both cases we remove the hats for notational convenience. For a derivation of the boundary conditions (2.2)–(2.3) see the works by Cheney et al. [27], Hamilton [48], and Mueller and Siltanen [97].

Our data are the measurements $(V_0, \sigma \frac{\partial V}{\partial n} \Big|_{\partial\Omega})$ (where $\sigma \frac{\partial V}{\partial n} \Big|_{\partial\Omega}$ is the current flux through $\partial\Omega$) when the Dirichlet boundary condition (2.2) is prescribed or $(I_0, V|_{\partial\Omega})$ when the Neumann Boundary Condition (2.3) is prescribed. (The measurements $\sigma \frac{\partial V}{\partial n} \Big|_{\partial\Omega}$ and $V|_{\partial\Omega}$ are known as the Dirichlet-to-Neumann and Neumann-to-Dirichlet Maps, respectively — see the review article by Borcea [19] and the references therein

for a more complete description and properties of these maps.) Note that we are assuming that we know the voltage and current around the entire boundary $\partial\Omega$ [19, 50]. Our goal is to use a single measurement of the voltage and current on $\partial\Omega$ to derive lower and upper bounds on the volume fraction of phase 1, namely $f^{(1)} = \langle \chi^{(1)} \rangle$, where

$$\langle \mathbf{u} \rangle = \frac{1}{|\Omega|} \int_{\Omega} \mathbf{u} \, d\mathbf{x} \quad (2.8)$$

denotes the average of a vector-valued (or scalar) function \mathbf{u} over Ω and $|\Omega|$ denotes the Lebesgue measure of Ω . We emphasize that we only apply one current flux (or voltage) and measure the corresponding voltage (or current flux) around $\partial\Omega$. It turns out that this single measurement gives us enough information to derive bounds on $f^{(1)}$. If more experiments are performed, that is, if several linearly independent current fluxes (or voltages) are prescribed around $\partial\Omega$ and the corresponding voltages (or current fluxes) are measured around $\partial\Omega$, then tighter bounds can be derived. For example, after our work was submitted, Kang, Kim, Lee, Li, and Milton [65] used two measurements to derive bounds on $f^{(1)}$ that are tighter than ours. If one assumes complete knowledge of the Neumann-to-Dirichlet or Dirichlet-to-Neumann Map, then more information about the conductivity distribution inside Ω can be obtained [19].

Several methods for deriving these bounds on $f^{(1)}$ have been explored in the literature. In the real conductivity case ($\omega = 0$), Kang, Seo, and Sheen [68], Alessandrini and Rosset [112], Ikehata [62], and Alessandrini, Rosset, and Seo [6] utilized a single boundary measurement of the voltage and current flux around $\partial\Omega$ and methods from elliptic PDE to bound the volume of an inclusion D in Ω . Alessandrini et al. [6, 112] made the technical assumption that

$$d(D, \partial\Omega) \geq d_0 > 0 \quad (2.9)$$

where $d(D, \partial\Omega)$ is the distance between D and $\partial\Omega$. The bounds they derived involve constants that are not easy to determine. Beretta et al. [14] used similar methods to derive bounds in the complex conductivity case — however they were able to remove the assumption (2.9) with certain restrictions on $\sigma^{(1)}$ and $\sigma^{(2)}$, which, as pointed out in their paper, is important in the application to organ screening as some of the degraded tissue may be present on the surface of the organ. Their bounds also

involve constants that in general may be difficult to determine, although they can be evaluated in some cases when special boundary conditions are imposed (see in particular Proposition 3.3 in their paper).

Capdeboscq and Vogelius [26] utilized multiple boundary measurements of the voltage and current flux around $\partial\Omega$ and the Lipton Bounds on polarization tensors [79] in the real conductivity case to find optimal asymptotic estimates on the volume of inclusions as the volume of the inclusions tends to 0. (To obtain multiple measurements in practice, multiple experiments are performed in which several different voltages or current fluxes are applied to the boundary and the corresponding current fluxes and voltages are measured.)

If the body Ω contains a statistically homogeneous or periodic composite, then bounds on the effective tensors of this composite can be used in an inverse fashion to bound the volume fraction — see the work of McPhedran, McKenzie, and Milton [85], Phan-Thien and Milton [111], McPhedran and Milton [86], and Cherkaeva and Golden [29]. Similarly, Milton [89] showed that the universal bounds of Nemat-Nasser and Hori [102] on the response of a body Ω containing two phases in any configuration can be easily inverted to bound the volume fraction. Moreover, Milton [89] used measurements of the voltage and current flux on $\partial\Omega$ with special boundary conditions to determine properties of the effective tensor of a composite containing rescaled copies of Ω packed to fill all space. Bounds on this effective tensor led to universal bounds on the response of the body when the special boundary conditions were applied; these bounds were then inverted to bound the volume fraction. We note that all of the bounds described in this paragraph can be computed in terms of known data (e.g., measurements of effective moduli or boundary measurements of the voltage and current flux).

In the real conductivity case, variational methods have also been used to bound the volume fraction. Berryman and Kohn [16] were the first to use variational methods in the context of EIT to determine information about the conductivity in a body. Kang et al. [64] used the translation method introduced by Murat and Tartar [98, 118, 119] and independently by Lurie and Cherkaev [80, 81] (see also the book by Milton [88]) to derive sharp bounds on the volume fraction using two boundary measurements of the

voltage and current flux in two dimensions. The bounds are easily computed in terms of these measurements. Kang et al. [64] also found geometries in which one of the bounds gives the true volume fraction. Kang and Milton [66] applied the translation method in three dimensions to find bounds on the volume fraction; these bounds can be computed using three boundary measurements. Kang, Milton, and Wang [67] also used the translation method to bound the size of an inclusion in the context of the shallow shell equations. We also mention that, in the complex conductivity case, several variational formulations of the PDE (2.1) were derived by Cherkaev and Gibiansky [28].

Rather than using variational principles, we use the fact that certain variations are nonnegative — see (2.23) and the paragraphs following it, for example. Matheron [84] used this idea to re-derive the famous Hashin–Shtrikman Bounds [55] on the effective conductivity of an isotropic composite — also see the book by Milton [88, Section 16.5]. We also apply the “splitting method,” introduced by Milton and Nguyen [90] in the context of elasticity, in which one derives bounds by splitting Ω into its constituent phases and correlating information about the facts that variations in each phase are nonnegative and averages of certain quantities (null Lagrangians) are known. Using this technique, in Theorems 2.1 and 2.3 we establish some elementary bounds that can be computed from the single voltage and current flux measurement on $\partial\Omega$.

In Theorems 2.2 and 2.4 we derive a method for numerically computing “better” bounds — we say “better” because these bounds may or may not be tighter than the above mentioned elementary bounds; see Sections 2.5 and 2.7. The method can be described as follows. Let $f \in \mathcal{A}_e \subseteq (0, 1)$, where \mathcal{A}_e is an interval determined by the elementary bounds. We call f a *test value*. The splitting method implies that f could potentially be the volume fraction of phase 1 if and only if certain 2×2 matrices $S_f^{(1)}(x, y)$ and $S_f^{(2)}(x, y)$ (one for each phase) are simultaneously positive-semidefinite at some point $(x, y) \in \mathbb{R}^2$. This, in turn, is equivalent to requiring that two elliptic disks in the xy -plane have a nonempty intersection. (By elliptic disk we mean an ellipse in the plane union its interior.) In other words, if the elliptic disks do intersect, f could be the true volume fraction; if the elliptic disks do not intersect, f cannot be the true volume fraction. This allows us to eliminate those values of $f \in \mathcal{A}_e$ for

which the elliptic disks do not intersect, leaving us with a set $\mathcal{A} \subseteq \mathcal{A}_e$ of *admissible* values. Any $f \in \mathcal{A}$ could be the true volume fraction of phase 1, so bounds on \mathcal{A} give us bounds on $f^{(1)}$. Unfortunately these “better” bounds must be computed numerically, but we emphasize that their computation is elementary and involves finding the interval (or intervals) of values where a certain function is positive and only requires a single measurement of the voltage and current flux on $\partial\Omega$.

We find the bounds are exceedingly tight for a particular 2-D geometry consisting of an annulus and surrounding material (the relative error between the true volume fraction and the upper and lower bounds on the volume fraction is approximately 0.0013%). At this stage we have not explored the question as to whether the bounds are tight for more general geometries nor the question as to how good the bounds are for three-dimensional geometries.

Finally, since we use the fact that variations are nonnegative rather than PDE methods or variational principles, we can easily determine attainability conditions for the bounds, i.e., conditions on the electric field that guarantee that the lower or upper elementary bound is exactly equal to the true volume fraction. Our method also enables us to remove the assumption that the distance between the inclusion and the boundary of the body is nonzero (2.9); in fact, as long as the PDE (2.1) subject to the boundary conditions (2.2) or (2.3) has a unique (weak) solution, our method can be applied.

It is worth mentioning the connection between the splitting method and the translation method. The translation method uses the classical variational principles in conjunction with constraints on the fields imposed by the null Lagrangians (or more generally quasiconvex functions): each constraint is taken into account with a Lagrange Multiplier. The classical variational principles can themselves be derived from the positivity of variations and using integration by parts, or equivalently by using the fact that certain quantities are null Lagrangians — see, for example, the book by Milton [88, Section 13.1]. The idea of the splitting method is to directly derive the bounds by using the positivity of the variations and the null Lagrangians. Since they use the same ingredients the bounds we derive here could presumably be derived using the translation method, but the application of this method when we

take into account all the null Lagrangians simultaneously is less transparent since we would need to introduce a Lagrange Multiplier for each of the many constraints. By contrast the splitting method is ideally suited to problems where there are a lot of null Lagrangians but relatively few relevant variations of which to keep track. Thus it is well suited to the complex conductivity problem where one measurement is used but less suited to the complex conductivity problem where two or more measurements are used. Recently Kang et al. [65] successfully applied the translation method to the two-measurement problem, but not while taking all null Lagrangians simultaneously into account.

The remainder of this chapter is organized as follows. In Section 2.2 we introduce our notation and assumptions. In Section 2.3 we apply the splitting method to several null Lagrangians, which are functionals of the electric field and current density that can be expressed in terms of the boundary voltage and current data. In Section 2.4 we derive the elementary bounds. We derive a geometrical method for computing “better” bounds in Section 2.5. Our work in Sections 2.2–2.5 applies in two or three dimensions. In Sections 2.6 and 2.7 we use two additional null Lagrangians to derive even better bounds in the 2-D case, and in Section 2.8 we apply our method to a test problem.

2.2 Preliminaries

As discussed in Section 2.1, we consider a two-phase mixture and also the case of an inclusion in a body. The region of interest (the unit cell of periodicity in the former case and the union of the inclusion and the body in the latter case) is denoted by Ω . We assume that the conductivity in each phase is homogeneous and isotropic; then for $\mathbf{x} \in \Omega$ we have

$$\sigma(\mathbf{x}) = \sigma^{(1)}\chi^{(1)}(\mathbf{x}) + \sigma^{(2)}\chi^{(2)}(\mathbf{x}),$$

where $\sigma^{(\alpha)} = \sigma_1^{(\alpha)} + i\sigma_2^{(\alpha)}$ for $\alpha = 1, 2$ are complex constants that we assume are known, $\sigma_1^{(\alpha)} > 0$ (as required physically), $0 < |\sigma^{(\alpha)}| < \infty$, and $\sigma^{(1)} \neq \sigma^{(2)}$. We will see later that, for technical reasons, we must also assume

$$\beta \equiv \sigma_1^{(1)}\sigma_2^{(2)} - \sigma_2^{(1)}\sigma_1^{(2)} \neq 0,$$

so $\text{Arg } \sigma^{(1)} \neq \text{Arg } \sigma^{(2)}$ (this condition ensures that a certain linear system has a unique solution). This implies that our results do not directly extend to the case when both phases have real conductivities.

The average value of an integrable vector field (or scalar function) \mathbf{u} is defined in (2.8). The volume fraction of phase α is denoted by $f^{(\alpha)}$, so

$$f^{(1)} = \langle \chi^{(1)} \rangle \quad \text{and} \quad f^{(2)} = 1 - f^{(1)} = \langle \chi^{(2)} \rangle.$$

The electric potential, electric field, and current density are denoted by $V = V_1 + iV_2$, $\mathbf{E} = \mathbf{E}_1 + i\mathbf{E}_2$, and $\mathbf{J} = \mathbf{J}_1 + i\mathbf{J}_2$, respectively (so for $m = 1, 2$, V_m , \mathbf{E}_m , and \mathbf{J}_m are real). Recall that if Ω is simply connected, then V satisfies (2.1) subject to either (2.2) or (2.3),

$$\mathbf{E} = -\nabla V, \quad \text{and} \quad \mathbf{J} = \sigma \mathbf{E}. \quad (2.10)$$

We emphasize that we assume Ω is simply connected throughout the remainder of this chapter.

As discussed by Borcea [19], the problem (2.1) with the Dirichlet Boundary Condition (2.2) has a unique solution $V \in H^1(\Omega)$ if $V_0 \in H^{1/2}(\partial\Omega)$; similarly, the problem (2.1) with the Neumann Boundary Condition (2.3) has a unique solution $V \in H^1(\Omega)$ if $I_0 \in H^{-1/2}(\partial\Omega)$. (For more on the Sobolev space $H^1(\Omega)$, see Section C.3.4 in Appendix C; for more on the fractional Sobolev Spaces $H^{1/2}(\partial\Omega)$ and $H^{-1/2}(\partial\Omega)$, see the book by Adams [1].) Thus we assume that $V \in H^1(\Omega)$ throughout this chapter.

Next, note that (2.1) implies that V is harmonic in each phase. Since $V \in H^1(\Omega)$, $V \in L^2(\Omega)$ by definition (see Section C.3.4 in Appendix C). The Cauchy–Schwarz Inequality then implies that $V \in L^1(\Omega)$, since

$$\|V\|_{L^1(\Omega)} = \int_{\Omega} |V| \leq \|V\|_{L^2(\Omega)} \|1\|_{\Omega} = |\Omega| \|V\|_{L^2(\Omega)} < \infty;$$

thus V is locally integrable in each phase. Then the Weyl Theorem (see Theorem 18.G in the book by Zeidler [125]) implies that V is infinitely continuously differentiable in each phase.

Let $\mathbf{u} = \mathbf{u}_1 + i\mathbf{u}_2$ be a complex-valued vector field in \mathbb{C}^2 or \mathbb{C}^3 . Then we set $\mathbf{u}^{(\alpha)}(\mathbf{x}) \equiv \chi^{(\alpha)}(\mathbf{x})\mathbf{u}(\mathbf{x})$ and $\mathbf{u}_m^{(\alpha)}(\mathbf{x}) \equiv \chi^{(\alpha)}(\mathbf{x})\mathbf{u}_m(\mathbf{x})$ for $\alpha, m = 1, 2$. The symbol “ \cdot ” denotes the usual Euclidean dot product on \mathbb{R}^2 or \mathbb{R}^3 , while the Euclidean norm of

a real-valued vector field $\mathbf{q}(\mathbf{x}) \in \mathbb{R}^2$ or \mathbb{R}^3 is denoted by $\|\mathbf{q}(\mathbf{x})\| = \sqrt{\mathbf{q}(\mathbf{x}) \cdot \mathbf{q}(\mathbf{x})}$. For any complex number $z = z_1 + iz_2$ the modulus of z is denoted by $|z| = \sqrt{z_1^2 + z_2^2}$.

2.3 The Splitting Method

We assume that we have full knowledge of a single applied boundary voltage V_0 and corresponding current flux $\sigma \frac{\partial V}{\partial n}|_{\partial\Omega}$ on $\partial\Omega$ (in the case of the Dirichlet Problem — in the case of the Neumann Problem, we assume that we have complete knowledge of the single applied current I_0 and corresponding voltage $V|_{\partial\Omega}$ on $\partial\Omega$). In order to derive bounds on the volume fraction $f^{(1)}$ (and, hence, on $f^{(2)} = 1 - f^{(1)}$) using these data, we make use of certain null Lagrangians, which are functionals that can be expressed in terms of boundary data.

2.3.1 Null Lagrangians

Recall that $\mathbf{J} = \sigma \mathbf{E}$ from (2.10). Then

$$\mathbf{J} = \mathbf{J}_1 + i\mathbf{J}_2 = (\sigma_1 + i\sigma_2)(\mathbf{E}_1 + i\mathbf{E}_2) = (\sigma_1\mathbf{E}_1 - \sigma_2\mathbf{E}_2) + i(\sigma_2\mathbf{E}_1 + \sigma_1\mathbf{E}_2);$$

in particular we have

$$\mathbf{J}_1 = \sigma_1\mathbf{E}_1 - \sigma_2\mathbf{E}_2 \quad \text{and} \quad \mathbf{J}_2 = \sigma_2\mathbf{E}_1 + \sigma_1\mathbf{E}_2. \quad (2.11)$$

Lemma 2.1 *For $k, l = 1, 2$ we have*

$$\langle \mathbf{E}_k \rangle = -\frac{1}{|\Omega|} \int_{\partial\Omega} V_k \mathbf{n} \, dS; \quad (2.12a)$$

$$\langle \mathbf{J}_l \rangle = \frac{1}{|\Omega|} \int_{\partial\Omega} \mathbf{x} (\mathbf{J}_l \cdot \mathbf{n}) \, dS; \quad (2.12b)$$

$$\langle \mathbf{E}_k \cdot \mathbf{J}_l \rangle = -\frac{1}{|\Omega|} \int_{\partial\Omega} V_k (\mathbf{J}_l \cdot \mathbf{n}) \, dS; \quad (2.12c)$$

\mathbf{n} is the outward unit normal to $\partial\Omega$ and, in the 2-D case, all boundary integrals are taken in the positive (counterclockwise) direction. In two dimensions we have the additional null Lagrangians

$$\langle \mathbf{E}_1 \cdot R_\perp \mathbf{E}_2 \rangle = \frac{1}{|\Omega|} \int_{\partial\Omega} V_1 \frac{\partial V_2}{\partial \mathbf{t}} \, dS \quad (2.13a)$$

$$\text{and} \quad \langle \mathbf{J}_1 \cdot R_\perp \mathbf{J}_2 \rangle = -\frac{1}{|\Omega|} \int_{\partial\Omega} \left[(\mathbf{J}_1 \cdot \mathbf{n}) \int_{\mathbf{x}_0}^{\mathbf{x}} (\mathbf{J}_2 \cdot \mathbf{n}) \, dS \right] \, dS, \quad (2.13b)$$

where R_\perp is the 2×2 matrix for a 90° clockwise rotation, namely

$$R_\perp = \begin{bmatrix} 0 & 1 \\ -1 & 0 \end{bmatrix}, \quad (2.14)$$

$\mathbf{t} = -R_\perp \mathbf{n} = R_\perp^T \mathbf{n}$ is the unit tangent vector to $\partial\Omega$, $\frac{\partial V_2}{\partial \mathbf{t}} = \nabla V_2 \cdot \mathbf{t}$, $\mathbf{x}_0 \in \partial\Omega$ is arbitrary, $\mathbf{x} \in \partial\Omega$, and both of the integrals over $\partial\Omega$ in (2.13) are taken in the positive (counterclockwise) direction.

Proof of Lemma 2.1: All three of the formulas in (2.12) are proven using integration by parts. In particular we use the scalar integration by parts formula

$$\int_\Omega (\nabla u) w \, d\mathbf{x} = - \int_\Omega u (\nabla w) \, d\mathbf{x} + \int_{\partial\Omega} u w \mathbf{n} \, dS, \quad (2.15)$$

and its vector generalizations

$$\int_\Omega (\nabla u) \cdot \mathbf{w} \, d\mathbf{x} = - \int_\Omega u (\nabla \cdot \mathbf{w}) \, d\mathbf{x} + \int_{\partial\Omega} u (\mathbf{w} \cdot \mathbf{n}) \, dS \quad (2.16)$$

and

$$\int_\Omega (\nabla \mathbf{u}) \cdot \mathbf{w} \, d\mathbf{x} = - \int_\Omega \mathbf{u} (\nabla \cdot \mathbf{w}) \, d\mathbf{x} + \int_{\partial\Omega} \mathbf{u} (\mathbf{w} \cdot \mathbf{n}) \, dS \quad (2.17)$$

(see the book by Evans [32]).

To see (2.12a), recall the definition of the average value of a field from (2.8) and that $\mathbf{E}_k = -\nabla V_k$ by (2.10). Then for $k = 1, 2$ we have

$$\langle \mathbf{E}_k \rangle = \frac{1}{|\Omega|} \int_\Omega \mathbf{E}_k \, d\mathbf{x} = -\frac{1}{|\Omega|} \int_\Omega (\nabla V_k) \mathbf{1} \, d\mathbf{x}.$$

Next we use (2.15) with $u = V_k$ and $w = 1$ to see that the above equation is equivalent to

$$\langle \mathbf{E}_k \rangle = -\frac{1}{|\Omega|} \left[- \int_\Omega V_k \nabla(1) \, d\mathbf{x} + \int_{\partial\Omega} V_k \mathbf{n} \, dS \right] = -\frac{1}{|\Omega|} \int_{\partial\Omega} V_k \mathbf{n} \, dS.$$

To prove (2.12b), we first note that $\nabla \mathbf{x} = \mathbf{I}$, where \mathbf{I} is the $d \times d$ identity tensor and $d = 2$ or $d = 3$ is the dimension. We use (2.17) with $\mathbf{u} = \mathbf{x}$ and $\mathbf{w} = \mathbf{J}_l$ to find

$$\langle \mathbf{J}_l \rangle = \frac{1}{|\Omega|} \int_\Omega \mathbf{J}_l \, d\mathbf{x} = \frac{1}{|\Omega|} \int_\Omega (\nabla \mathbf{x}) \cdot \mathbf{J}_l \, d\mathbf{x} = \frac{1}{|\Omega|} \left[- \int_\Omega \mathbf{x} (\nabla \cdot \mathbf{J}_l) \, d\mathbf{x} + \int_{\partial\Omega} \mathbf{x} (\mathbf{J}_l \cdot \mathbf{n}) \, dS \right]. \quad (2.18)$$

Since $0 = \nabla \cdot \mathbf{J} = \nabla \cdot \mathbf{J}_1 + i \nabla \cdot \mathbf{J}_2$ in Ω by (2.4), we have $\nabla \cdot \mathbf{J}_l = 0$ in Ω for $l = 1, 2$. Hence the first integral on the right-hand side of (2.18) vanishes and (2.18) becomes

$$\langle \mathbf{J}_l \rangle = \frac{1}{|\Omega|} \int_{\partial\Omega} \mathbf{x} (\mathbf{J}_l \cdot \mathbf{n}) \, dS.$$

Next we prove (2.12c). For $k, l = 1, 2$ we have

$$\langle \mathbf{E}_k \cdot \mathbf{J}_l \rangle \equiv \frac{1}{|\Omega|} \int_{\Omega} \mathbf{E}_k \cdot \mathbf{J}_l \, d\mathbf{x} = -\frac{1}{|\Omega|} \int_{\Omega} (\nabla V_k) \cdot \mathbf{J}_l \, d\mathbf{x}.$$

We use (2.16) with $u = V_k$ and $\mathbf{w} = \mathbf{J}_l$ to find that the above equation is equivalent to

$$\langle \mathbf{E}_k \cdot \mathbf{J}_l \rangle = -\frac{1}{|\Omega|} \left[-\int_{\Omega} V_k (\nabla \cdot \mathbf{J}_l) \, d\mathbf{x} + \int_{\partial\Omega} V_k (\mathbf{J}_l \cdot \mathbf{n}) \, dS \right] = -\frac{1}{|\Omega|} \int_{\partial\Omega} V_k (\mathbf{J}_l \cdot \mathbf{n}) \, dS$$

since $\nabla \cdot \mathbf{J}_l = 0$ in Ω .

Similarly, (2.13a) can be proved using (2.16). In particular we have

$$\langle \mathbf{E}_1 \cdot R_{\perp} \mathbf{E}_2 \rangle = \frac{1}{|\Omega|} \int_{\Omega} \mathbf{E}_1 \cdot R_{\perp} \mathbf{E}_2 \, d\mathbf{x} = -\frac{1}{|\Omega|} \int_{\Omega} (\nabla V_1) \cdot R_{\perp} \mathbf{E}_2 \, d\mathbf{x}.$$

If we take $u = V_1$ and $\mathbf{w} = R_{\perp} \mathbf{E}_2$ in (2.16) we see that the above equation is equivalent to

$$\langle \mathbf{E}_1 \cdot R_{\perp} \mathbf{E}_2 \rangle = -\frac{1}{|\Omega|} \left[-\int_{\Omega} V_1 (\nabla \cdot R_{\perp} \mathbf{E}_2) \, d\mathbf{x} + \int_{\partial\Omega} V_1 (R_{\perp} \mathbf{E}_2 \cdot \mathbf{n}) \, dS \right]. \quad (2.19)$$

For $p = 1, 2$ we let $E_{2,p}$ denote the p^{th} component of \mathbf{E}_2 . Then

$$\nabla \cdot R_{\perp} \mathbf{E}_2 = \nabla \cdot \begin{bmatrix} 0 & 1 \\ -1 & 0 \end{bmatrix} \begin{bmatrix} E_{2,1} \\ E_{2,2} \end{bmatrix} = \nabla \cdot \begin{bmatrix} E_{2,2} \\ -E_{2,1} \end{bmatrix} = \frac{\partial E_{2,2}}{\partial x_1} - \frac{\partial E_{2,1}}{\partial x_2} = \nabla \times \mathbf{E}_2. \quad (2.20)$$

By (2.4), $0 = \nabla \times \mathbf{E} = \nabla \times \mathbf{E}_1 + i(\nabla \times \mathbf{E}_2)$ in Ω , so $\nabla \times \mathbf{E}_1 = \nabla \times \mathbf{E}_2 = 0$ in Ω .

Combining (2.19) and (2.20) gives

$$\begin{aligned} \langle \mathbf{E}_1 \cdot R_{\perp} \mathbf{E}_2 \rangle &= -\frac{1}{|\Omega|} \left[-\int_{\Omega} V_1 (\nabla \times \mathbf{E}_2) \, d\mathbf{x} + \int_{\partial\Omega} V_1 (R_{\perp} \mathbf{E}_2 \cdot \mathbf{n}) \, dS \right] \\ &= -\frac{1}{|\Omega|} \int_{\partial\Omega} V_1 (R_{\perp} \mathbf{E}_2 \cdot \mathbf{n}) \, dS \end{aligned} \quad (2.21)$$

Note that

$$R_{\perp} \mathbf{E}_2 \cdot \mathbf{n} = \mathbf{E}_2 \cdot R_{\perp}^T \mathbf{n} = -\nabla V_2 \cdot (-R_{\perp} \mathbf{n}) = \nabla V_2 \cdot \mathbf{t} = \frac{\partial V_2}{\partial \mathbf{t}},$$

so (2.21) becomes

$$\langle \mathbf{E}_1 \cdot R_{\perp} \mathbf{E}_2 \rangle = -\frac{1}{|\Omega|} \int_{\partial\Omega} V_1 \frac{\partial V_2}{\partial \mathbf{t}} \, dS.$$

The following proof of (2.13b) is due to Kang et al. [64]. We begin by noting that

$$R_{\perp}^T R_{\perp} = \begin{bmatrix} 0 & -1 \\ 1 & 0 \end{bmatrix} \begin{bmatrix} 0 & 1 \\ -1 & 0 \end{bmatrix} = \begin{bmatrix} 1 & 0 \\ 0 & 1 \end{bmatrix},$$

so $R_{\perp}^{-1} = R_{\perp}^T$. Next, denoting the p^{th} component of \mathbf{J}_2 by $J_{2,p}$ (for $p = 1, 2$) we have

$$\nabla \times (R_{\perp} \mathbf{J}_2) = \nabla \times \begin{bmatrix} 0 & 1 \\ -1 & 0 \end{bmatrix} \begin{bmatrix} J_{2,1} \\ J_{2,2} \end{bmatrix} = \nabla \times \begin{bmatrix} J_{2,2} \\ -J_{2,1} \end{bmatrix} = -\frac{\partial J_{2,1}}{\partial x_1} - \frac{\partial J_{2,2}}{\partial x_2} = -\nabla \cdot \mathbf{J}_2 = 0.$$

As long as Ω is simply connected and because $\nabla \times (R_{\perp} \mathbf{J}_2) = 0$, there is a potential ϕ such that $R_{\perp} \mathbf{J}_2 = \nabla \phi$. Thus

$$\langle \mathbf{J}_1 \cdot R_{\perp} \mathbf{J}_2 \rangle \equiv \frac{1}{|\Omega|} \int_{\Omega} \mathbf{J}_1 \cdot R_{\perp} \mathbf{J}_2 \, d\mathbf{x} = \frac{1}{|\Omega|} \int_{\Omega} \mathbf{J}_1 \cdot \nabla \phi \, d\mathbf{x}.$$

Inserting this into (2.16) with $u = \phi$ and $\mathbf{w} = \mathbf{J}_1$ gives

$$\langle \mathbf{J}_1 \cdot R_{\perp} \mathbf{J}_2 \rangle = \frac{1}{|\Omega|} \left[-\int_{\Omega} \phi (\nabla \cdot \mathbf{J}_1) \, d\mathbf{x} + \int_{\partial\Omega} \phi (\mathbf{J}_1 \cdot \mathbf{n}) \, dS \right] = \frac{1}{|\Omega|} \int_{\partial\Omega} \phi (\mathbf{J}_1 \cdot \mathbf{n}) \, dS, \quad (2.22)$$

because $\nabla \cdot \mathbf{J}_1 = 0$ in Ω . In order to derive an expression for ϕ we note that

$$\nabla \phi \cdot \mathbf{t} = \nabla \phi \cdot (-R_{\perp} \mathbf{n}) = -R_{\perp}^T \nabla \phi \cdot \mathbf{n} = -R_{\perp}^{-1} \nabla \phi \cdot \mathbf{n} = -\mathbf{J}_2 \cdot \mathbf{n}.$$

Then for any fixed $\mathbf{x}_0 \in \partial\Omega$ and any $\mathbf{x} \in \partial\Omega$ we have

$$\phi(\mathbf{x}) = \int_{\mathbf{x}_0}^{\mathbf{x}} \nabla \phi \cdot \mathbf{t} \, dS = \int_{\mathbf{x}_0}^{\mathbf{x}} -(\mathbf{J}_2 \cdot \mathbf{n}) \, dS,$$

where the integral is taken from \mathbf{x}_0 to \mathbf{x} in the positive (counterclockwise) direction around $\partial\Omega$. Inserting the above expression for ϕ into (2.22) gives

$$\langle \mathbf{J}_1 \cdot R_{\perp} \mathbf{J}_2 \rangle = -\frac{1}{|\Omega|} \int_{\partial\Omega} \left[(\mathbf{J}_1 \cdot \mathbf{n}) \int_{\mathbf{x}_0}^{\mathbf{x}} (\mathbf{J}_2 \cdot \mathbf{n}) \, dS \right] \, dS,$$

as required. This completes the proof.

We emphasize here that the (real) values $V_k|_{\partial\Omega}$ and $(\mathbf{J}_l \cdot \mathbf{n})|_{\partial\Omega} = -\sigma \frac{\partial V_l}{\partial n}|_{\partial\Omega}$ are known from our measurement. We note that if the material under consideration is a periodic composite, it is well known that (2.12) and (2.13) become

$$\langle \mathbf{E}_k \cdot \mathbf{J}_l \rangle = \langle \mathbf{E}_k \rangle \cdot \langle \mathbf{J}_l \rangle, \quad \langle \mathbf{E}_1 \cdot R_{\perp} \mathbf{E}_2 \rangle = \langle \mathbf{E}_1 \rangle \cdot R_{\perp} \langle \mathbf{E}_2 \rangle, \quad \text{and} \quad \langle \mathbf{J}_1 \cdot R_{\perp} \mathbf{J}_2 \rangle = \langle \mathbf{J}_1 \rangle \cdot R_{\perp} \langle \mathbf{J}_2 \rangle.$$

2.3.2 Main Idea

For $\mathbf{x} \in \Omega$, $\mathbf{c}^{(\alpha)} \in \mathbb{R}^2$, and $\alpha = 1, 2$ we define

$$\mathbf{g}^{(\alpha)}(\mathbf{x}; \mathbf{c}^{(\alpha)}) \equiv \sum_{m=1}^2 c_m^{(\alpha)} \left[\mathbf{E}_m^{(\alpha)}(\mathbf{x}) - \frac{\chi^{(\alpha)}(\mathbf{x})}{f^{(\alpha)}} \langle \mathbf{E}_m^{(\alpha)} \rangle \right], \quad (2.23)$$

where $\mathbf{E}_m^{(\alpha)}(\mathbf{x}) = \chi^{(\alpha)}(\mathbf{x}) \mathbf{E}_m(\mathbf{x})$.

The meaning of the field $\mathbf{g}^{(\alpha)}$ can be understood in the following way. We let $\Omega^{(\alpha)}$ denote the set occupied by phase α and $|\Omega^{(\alpha)}|$ denote the Lebesgue measure of $\Omega^{(\alpha)}$. Then $1/|\Omega| = f^{(\alpha)}/|\Omega^{(\alpha)}|$ and

$$\langle \mathbf{E}_m^{(\alpha)} \rangle = \frac{1}{|\Omega|} \int_{\Omega} \chi^{(\alpha)}(\mathbf{x}) \mathbf{E}_m(\mathbf{x}) d\mathbf{x} = \frac{f^{(\alpha)}}{|\Omega^{(\alpha)}|} \int_{\Omega^{(\alpha)}} \mathbf{E}_m(\mathbf{x}) d\mathbf{x} = f^{(\alpha)} \langle \mathbf{E}_m \rangle_{\Omega^{(\alpha)}}, \quad (2.24)$$

where $\langle \mathbf{E}_m \rangle_{\Omega^{(\alpha)}}$ denotes the average of the field \mathbf{E}_m over phase α . This implies we can write $\mathbf{g}^{(\alpha)}$ as

$$\mathbf{g}^{(\alpha)}(\mathbf{x}; \mathbf{c}^{(\alpha)}) = \sum_{m=1}^2 c_m^{(\alpha)} [\chi^{(\alpha)}(\mathbf{x}) \mathbf{E}_m(\mathbf{x}) - \chi^{(\alpha)}(\mathbf{x}) \langle \mathbf{E}_m \rangle_{\Omega^{(\alpha)}}].$$

Thus, up to the constants $c_m^{(\alpha)}$, the field $\mathbf{g}^{(\alpha)}$ describes how the real and imaginary parts of the electric field \mathbf{E} vary from their average values over phase α . Also for any field $\mathbf{e}(\mathbf{x})$, and in particular for

$$\mathbf{e}(\mathbf{x}) = \sum_{m=1}^2 c_m^{(\alpha)} \mathbf{E}_m(\mathbf{x}),$$

the minimum of $\langle [\chi^{(\alpha)} \mathbf{e} - \chi^{(\alpha)} \mathbf{w}] \cdot [\chi^{(\alpha)} \mathbf{e} - \chi^{(\alpha)} \mathbf{w}] \rangle$ over constant vectors \mathbf{w} occurs when $\mathbf{w} = \langle \mathbf{e} \rangle_{\Omega^{(\alpha)}}$.

Note that $\langle \mathbf{g}^{(\alpha)} \rangle = 0$ for all $\mathbf{c}^{(\alpha)} \in \mathbb{R}^2$ because

$$\begin{aligned} \langle \mathbf{g}^{(\alpha)} \rangle &= \left\langle \sum_{m=1}^2 c_m^{(\alpha)} \left[\mathbf{E}_m^{(\alpha)}(\mathbf{x}) - \frac{\chi^{(\alpha)}(\mathbf{x})}{f^{(\alpha)}} \langle \mathbf{E}_m^{(\alpha)} \rangle \right] \right\rangle \\ &= \sum_{m=1}^2 \left\langle c_m^{(\alpha)} \left[\mathbf{E}_m^{(\alpha)}(\mathbf{x}) - \frac{\chi^{(\alpha)}(\mathbf{x})}{f^{(\alpha)}} \langle \mathbf{E}_m^{(\alpha)} \rangle \right] \right\rangle \\ &= \sum_{m=1}^2 c_m^{(\alpha)} \left[\langle \mathbf{E}_m^{(\alpha)} \rangle - \frac{\langle \chi^{(\alpha)} \rangle}{f^{(\alpha)}} \langle \mathbf{E}_m^{(\alpha)} \rangle \right] \\ &= \sum_{m=1}^2 c_m^{(\alpha)} \left[\langle \mathbf{E}_m^{(\alpha)} \rangle - \frac{f^{(\alpha)}}{f^{(\alpha)}} \langle \mathbf{E}_m^{(\alpha)} \rangle \right] \\ &= \sum_{m=1}^2 c_m^{(\alpha)} [\langle \mathbf{E}_m^{(\alpha)} \rangle - \langle \mathbf{E}_m^{(\alpha)} \rangle] \\ &= 0. \end{aligned}$$

It must also be the case that $\langle \mathbf{g}^{(\alpha)} \cdot \mathbf{g}^{(\alpha)} \rangle = \langle \|\mathbf{g}^{(\alpha)}\|^2 \rangle \geq 0$ for all $\mathbf{c}^{(\alpha)} \in \mathbb{R}^2$. In particular

$$\begin{aligned}
\langle \mathbf{g}^{(\alpha)} \cdot \mathbf{g}^{(\alpha)} \rangle &= \left\langle \left\{ \sum_{m=1}^2 c_m^{(\alpha)} \left[\mathbf{E}_m^{(\alpha)} - \frac{\chi^{(\alpha)}}{f^{(\alpha)}} \langle \mathbf{E}_m^{(\alpha)} \rangle \right] \right\} \cdot \left\{ \sum_{n=1}^2 c_n^{(\alpha)} \left[\mathbf{E}_n^{(\alpha)} - \frac{\chi^{(\alpha)}}{f^{(\alpha)}} \langle \mathbf{E}_n^{(\alpha)} \rangle \right] \right\} \right\rangle \\
&= \left\langle \sum_{m,n=1}^2 c_m^{(\alpha)} c_n^{(\alpha)} \left\{ \mathbf{E}_m^{(\alpha)} \cdot \mathbf{E}_n^{(\alpha)} - \frac{\chi^{(\alpha)}}{f^{(\alpha)}} \mathbf{E}_m^{(\alpha)} \cdot \langle \mathbf{E}_n^{(\alpha)} \rangle \right. \right. \\
&\quad \left. \left. - \frac{\chi^{(\alpha)}}{f^{(\alpha)}} \langle \mathbf{E}_m^{(\alpha)} \rangle \cdot \mathbf{E}_n^{(\alpha)} + \frac{[\chi^{(\alpha)}]^2}{[f^{(\alpha)}]^2} \langle \mathbf{E}_m^{(\alpha)} \rangle \cdot \langle \mathbf{E}_n^{(\alpha)} \rangle \right\} \right\rangle \\
&= \sum_{m,n=1}^2 c_m^{(\alpha)} c_n^{(\alpha)} \left\{ \langle \mathbf{E}_m^{(\alpha)} \cdot \mathbf{E}_n^{(\alpha)} \rangle - \frac{1}{f^{(\alpha)}} \langle \chi^{(\alpha)} \mathbf{E}_m^{(\alpha)} \rangle \cdot \langle \mathbf{E}_n^{(\alpha)} \rangle \right. \\
&\quad \left. - \frac{1}{f^{(\alpha)}} \langle \mathbf{E}_m^{(\alpha)} \rangle \cdot \langle \chi^{(\alpha)} \mathbf{E}_n^{(\alpha)} \rangle + \frac{\langle [\chi^{(\alpha)}]^2 \rangle}{[f^{(\alpha)}]^2} \langle \mathbf{E}_m^{(\alpha)} \rangle \cdot \langle \mathbf{E}_n^{(\alpha)} \rangle \right\}.
\end{aligned}$$

Since $\chi^{(\alpha)} \mathbf{E}_m^{(\alpha)} = \mathbf{E}_m^{(\alpha)}$ for $m = 1, 2$, $[\chi^{(\alpha)}]^2 = \chi^{(\alpha)}$, and $\langle \chi^{(\alpha)} \rangle = f^{(\alpha)}$, the above expression is equivalent to

$$\begin{aligned}
\langle \mathbf{g}^{(\alpha)} \cdot \mathbf{g}^{(\alpha)} \rangle &= \sum_{m,n=1}^2 c_m^{(\alpha)} c_n^{(\alpha)} \left\{ \langle \mathbf{E}_m^{(\alpha)} \cdot \mathbf{E}_n^{(\alpha)} \rangle - \frac{1}{f^{(\alpha)}} \langle \mathbf{E}_m^{(\alpha)} \rangle \cdot \langle \mathbf{E}_n^{(\alpha)} \rangle \right. \\
&\quad \left. - \frac{1}{f^{(\alpha)}} \langle \mathbf{E}_m^{(\alpha)} \rangle \cdot \langle \mathbf{E}_n^{(\alpha)} \rangle + \frac{\langle \chi^{(\alpha)} \rangle}{[f^{(\alpha)}]^2} \langle \mathbf{E}_m^{(\alpha)} \rangle \cdot \langle \mathbf{E}_n^{(\alpha)} \rangle \right\} \\
&= \sum_{m,n=1}^2 c_m^{(\alpha)} c_n^{(\alpha)} \left\{ \langle \mathbf{E}_m^{(\alpha)} \cdot \mathbf{E}_n^{(\alpha)} \rangle - \frac{2}{f^{(\alpha)}} \langle \mathbf{E}_m^{(\alpha)} \rangle \cdot \langle \mathbf{E}_n^{(\alpha)} \rangle \right. \tag{2.25} \\
&\quad \left. + \frac{f^{(\alpha)}}{[f^{(\alpha)}]^2} \langle \mathbf{E}_m^{(\alpha)} \rangle \cdot \langle \mathbf{E}_n^{(\alpha)} \rangle \right\}
\end{aligned}$$

$$\begin{aligned}
&= \sum_{m,n=1}^2 c_m^{(\alpha)} c_n^{(\alpha)} \left\{ \langle \mathbf{E}_m^{(\alpha)} \cdot \mathbf{E}_n^{(\alpha)} \rangle - \frac{1}{f^{(\alpha)}} \langle \mathbf{E}_m^{(\alpha)} \rangle \cdot \langle \mathbf{E}_n^{(\alpha)} \rangle \right\} \\
&= \mathbf{c}^{(\alpha)} \cdot S^{(\alpha)} \mathbf{c}^{(\alpha)}, \tag{2.26}
\end{aligned}$$

where

$$S^{(\alpha)} = \begin{bmatrix} A_{11}^{(\alpha)} - \frac{\langle \mathbf{E}_1^{(\alpha)} \rangle \cdot \langle \mathbf{E}_1^{(\alpha)} \rangle}{f^{(\alpha)}} & A_{12}^{(\alpha)} - \frac{\langle \mathbf{E}_1^{(\alpha)} \rangle \cdot \langle \mathbf{E}_2^{(\alpha)} \rangle}{f^{(\alpha)}} \\ A_{21}^{(\alpha)} - \frac{\langle \mathbf{E}_2^{(\alpha)} \rangle \cdot \langle \mathbf{E}_1^{(\alpha)} \rangle}{f^{(\alpha)}} & A_{22}^{(\alpha)} - \frac{\langle \mathbf{E}_2^{(\alpha)} \rangle \cdot \langle \mathbf{E}_2^{(\alpha)} \rangle}{f^{(\alpha)}} \end{bmatrix} \tag{2.27}$$

and

$$A_{mn}^{(\alpha)} = \langle \mathbf{E}_m^{(\alpha)} \cdot \mathbf{E}_n^{(\alpha)} \rangle \quad (2.28)$$

for $\alpha, m, n = 1, 2$. Since $\langle \mathbf{g}^{(\alpha)} \cdot \mathbf{g}^{(\alpha)} \rangle \geq 0$ for all $\mathbf{c}^{(\alpha)} \in \mathbb{R}^2$, (2.26) implies that

$$\mathbf{c}^{(\alpha)} \cdot \mathcal{S}^{(\alpha)} \mathbf{c}^{(\alpha)} \geq 0 \quad \text{for all } \mathbf{c}^{(\alpha)} \in \mathbb{R}^2. \quad (2.29)$$

Because $A_{mn}^{(\alpha)} = \mathbf{E}_m^{(\alpha)} \cdot \mathbf{E}_n^{(\alpha)} = \mathbf{E}_n^{(\alpha)} \cdot \mathbf{E}_m^{(\alpha)} = A_{nm}^{(\alpha)}$ and $\langle \mathbf{E}_m^{(\alpha)} \rangle \cdot \langle \mathbf{E}_n^{(\alpha)} \rangle = \langle \mathbf{E}_n^{(\alpha)} \rangle \cdot \langle \mathbf{E}_m^{(\alpha)} \rangle$ for $m, n, \alpha = 1, 2$, (2.27) and (2.28) imply that $\mathcal{S}^{(\alpha)}$ is symmetric for $\alpha = 1, 2$; $\mathcal{S}^{(\alpha)}$ must also be positive-semidefinite by (2.29).

Remark 2.1 In (2.23), we could have defined $\mathbf{g}^{(\alpha)}(\mathbf{x})$ in terms of the current field \mathbf{J} rather than the electric field \mathbf{E} without changing anything. To see this, note that (2.11) implies

$$\begin{aligned} & \sum_{m=1}^2 c_m^{(\alpha)} \left[\mathbf{J}_m^{(\alpha)}(\mathbf{x}) - \frac{\chi^{(\alpha)}(\mathbf{x})}{f^{(\alpha)}} \langle \mathbf{J}_m^{(\alpha)} \rangle \right] \\ &= c_1^{(\alpha)} \left[\mathbf{J}_1^{(\alpha)}(\mathbf{x}) - \frac{\chi^{(\alpha)}(\mathbf{x})}{f^{(\alpha)}} \langle \mathbf{J}_1^{(\alpha)} \rangle \right] + c_2^{(\alpha)} \left[\mathbf{J}_2^{(\alpha)}(\mathbf{x}) - \frac{\chi^{(\alpha)}(\mathbf{x})}{f^{(\alpha)}} \langle \mathbf{J}_2^{(\alpha)} \rangle \right] \\ &= c_1^{(\alpha)} \left[\sigma_1^{(\alpha)} \mathbf{E}_1^{(\alpha)}(\mathbf{x}) - \sigma_2^{(\alpha)} \mathbf{E}_2^{(\alpha)}(\mathbf{x}) - \frac{\chi^{(\alpha)}(\mathbf{x})}{f^{(\alpha)}} \langle \sigma_1^{(\alpha)} \mathbf{E}_1^{(\alpha)} - \sigma_2^{(\alpha)} \mathbf{E}_2^{(\alpha)} \rangle \right] \\ & \quad + c_2^{(\alpha)} \left[\sigma_2^{(\alpha)} \mathbf{E}_1^{(\alpha)}(\mathbf{x}) + \sigma_1^{(\alpha)} \mathbf{E}_2^{(\alpha)}(\mathbf{x}) - \frac{\chi^{(\alpha)}(\mathbf{x})}{f^{(\alpha)}} \langle \sigma_2^{(\alpha)} \mathbf{E}_1^{(\alpha)} + \sigma_1^{(\alpha)} \mathbf{E}_2^{(\alpha)} \rangle \right] \\ &= [c_1^{(\alpha)} \sigma_1^{(\alpha)} + c_2^{(\alpha)} \sigma_2^{(\alpha)}] \left[\mathbf{E}_1^{(\alpha)}(\mathbf{x}) - \frac{\chi^{(\alpha)}(\mathbf{x})}{f^{(\alpha)}} \langle \mathbf{E}_1^{(\alpha)} \rangle \right] \\ & \quad + [-c_1^{(\alpha)} \sigma_2^{(\alpha)} + c_2^{(\alpha)} \sigma_1^{(\alpha)}] \left[\mathbf{E}_2^{(\alpha)}(\mathbf{x}) - \frac{\chi^{(\alpha)}(\mathbf{x})}{f^{(\alpha)}} \langle \mathbf{E}_2^{(\alpha)} \rangle \right] \\ &= \tilde{c}_1^{(\alpha)} \left[\mathbf{E}_1^{(\alpha)}(\mathbf{x}) - \frac{\chi^{(\alpha)}(\mathbf{x})}{f^{(\alpha)}} \langle \mathbf{E}_1^{(\alpha)} \rangle \right] + \tilde{c}_2^{(\alpha)} \left[\mathbf{E}_2^{(\alpha)}(\mathbf{x}) - \frac{\chi^{(\alpha)}(\mathbf{x})}{f^{(\alpha)}} \langle \mathbf{E}_2^{(\alpha)} \rangle \right] \\ &= \sum_{m=1}^2 \tilde{c}_m^{(\alpha)} \left[\mathbf{E}_m^{(\alpha)}(\mathbf{x}) - \frac{\chi^{(\alpha)}(\mathbf{x})}{f^{(\alpha)}} \langle \mathbf{E}_m^{(\alpha)} \rangle \right], \end{aligned}$$

where

$$\tilde{c}_1^{(\alpha)} \equiv c_1^{(\alpha)} \sigma_1^{(\alpha)} + c_2^{(\alpha)} \sigma_2^{(\alpha)} \quad \text{and} \quad \tilde{c}_2^{(\alpha)} \equiv -c_1^{(\alpha)} \sigma_2^{(\alpha)} + c_2^{(\alpha)} \sigma_1^{(\alpha)}.$$

Since the constants $c_m^{(\alpha)}$ are arbitrary, we can use either the current field \mathbf{J} or the electric field \mathbf{E} in the definition of $\mathbf{g}^{(\alpha)}$.

We note that the quantities $\langle \mathbf{E}_m^{(\alpha)} \rangle$ are known; this can be seen as follows. Since the average of a function is computed using integration, we can “split” the average value of a field \mathbf{u} over Ω into two parts:

$$\langle \mathbf{u} \rangle = \langle \chi^{(1)} \mathbf{u} \rangle + \langle \chi^{(2)} \mathbf{u} \rangle. \quad (2.30)$$

Note that the averages in (2.30) are taken over Ω ; in particular $\langle \chi^{(\alpha)} \mathbf{u} \rangle$ is not the average of \mathbf{u} over phase 1, although it is equal to $f^{(\alpha)}$ times the average of \mathbf{u} over phase α .

We apply this “splitting method” to \mathbf{E} and \mathbf{J} and recall that the conductivity is homogeneous in each phase to obtain the system

$$\langle \mathbf{E} \rangle = \langle \mathbf{E}^{(1)} \rangle + \langle \mathbf{E}^{(2)} \rangle \quad \text{and} \quad \langle \mathbf{J} \rangle = \sigma^{(1)} \langle \mathbf{E}^{(1)} \rangle + \sigma^{(2)} \langle \mathbf{E}^{(2)} \rangle,$$

which is easily solved for $\langle \mathbf{E}^{(1)} \rangle$ and $\langle \mathbf{E}^{(2)} \rangle$:

$$\langle \mathbf{E}^{(1)} \rangle = \frac{\sigma^{(2)} \langle \mathbf{E} \rangle - \langle \mathbf{J} \rangle}{\sigma^{(2)} - \sigma^{(1)}} \quad \text{and} \quad \langle \mathbf{E}^{(2)} \rangle = \frac{-\sigma^{(1)} \langle \mathbf{E} \rangle + \langle \mathbf{J} \rangle}{\sigma^{(2)} - \sigma^{(1)}}. \quad (2.31)$$

Since $\langle \mathbf{E} \rangle$ and $\langle \mathbf{J} \rangle$ are null Lagrangians, they are known by Lemma 2.1. Therefore, the real and imaginary parts of $\langle \mathbf{E}^{(1)} \rangle$ and $\langle \mathbf{E}^{(2)} \rangle$ can be determined from (2.31) by equating the real and imaginary parts of the left- and right-hand sides of each equation.

Similarly, we may apply the splitting method to the null Lagrangians $\langle \mathbf{E}_k \cdot \mathbf{J}_l \rangle$; for $k, l = 1, 2$ this gives

$$\langle \mathbf{E}_k \cdot \mathbf{J}_l \rangle = \langle \chi^{(1)} \mathbf{E}_k \cdot \mathbf{J}_l \rangle + \langle \chi^{(2)} \mathbf{E}_k \cdot \mathbf{J}_l \rangle. \quad (2.32)$$

Using (2.11) and the fact that $\sigma^{(\alpha)}$ is constant, the equations in (2.32) can be shown to be equivalent to the linear system

$$\begin{bmatrix} \sigma_1^{(1)} & \sigma_1^{(2)} & -\sigma_2^{(1)} & -\sigma_2^{(2)} & 0 & 0 \\ \sigma_2^{(1)} & \sigma_2^{(2)} & \sigma_1^{(1)} & \sigma_1^{(2)} & 0 & 0 \\ 0 & 0 & \sigma_1^{(1)} & \sigma_1^{(2)} & -\sigma_2^{(1)} & -\sigma_2^{(2)} \\ 0 & 0 & \sigma_2^{(1)} & \sigma_2^{(2)} & \sigma_1^{(1)} & \sigma_1^{(2)} \end{bmatrix} \begin{bmatrix} A_{11}^{(1)} \\ A_{11}^{(2)} \\ A_{21}^{(1)} \\ A_{21}^{(2)} \\ A_{22}^{(1)} \\ A_{22}^{(2)} \end{bmatrix} = \begin{bmatrix} \langle \mathbf{E}_1 \cdot \mathbf{J}_1 \rangle \\ \langle \mathbf{E}_1 \cdot \mathbf{J}_2 \rangle \\ \langle \mathbf{E}_2 \cdot \mathbf{J}_1 \rangle \\ \langle \mathbf{E}_2 \cdot \mathbf{J}_2 \rangle \end{bmatrix}. \quad (2.33)$$

Recall that the right-hand side of this system is known from our measurement (see (2.12c)). Since this is an underdetermined system with infinitely many solutions, we set $x \equiv A_{11}^{(1)}$ and $y \equiv A_{11}^{(2)}$ and solve the system (2.33) in terms of the “free variables” x and y . In particular, we solve the system

$$\begin{bmatrix} -\sigma_2^{(1)} & -\sigma_2^{(2)} & 0 & 0 \\ \sigma_1^{(1)} & \sigma_1^{(2)} & 0 & 0 \\ \sigma_1^{(1)} & \sigma_1^{(2)} & -\sigma_2^{(1)} & -\sigma_2^{(2)} \\ \sigma_2^{(1)} & \sigma_2^{(2)} & \sigma_1^{(1)} & \sigma_1^{(2)} \end{bmatrix} \begin{bmatrix} A_{21}^{(1)} \\ A_{21}^{(2)} \\ A_{22}^{(1)} \\ A_{22}^{(2)} \end{bmatrix} = \begin{bmatrix} \langle \mathbf{E}_1 \cdot \mathbf{J}_1 \rangle - \sigma_1^{(1)}x - \sigma_1^{(2)}y \\ \langle \mathbf{E}_1 \cdot \mathbf{J}_2 \rangle - \sigma_2^{(1)}x - \sigma_2^{(2)}y \\ \langle \mathbf{E}_2 \cdot \mathbf{J}_1 \rangle \\ \langle \mathbf{E}_2 \cdot \mathbf{J}_2 \rangle \end{bmatrix}. \quad (2.34)$$

The system (2.34) has a unique solution if and only if the determinant of the matrix on the left-hand side is nonzero, i.e., if and only if $\beta \equiv \sigma_1^{(1)}\sigma_2^{(2)} - \sigma_2^{(1)}\sigma_1^{(2)} \neq 0$, so for the remainder of this paper we assume that $\beta \neq 0$.

Remark 2.2 *We chose $x = A_{11}^{(1)}$ and $y = A_{11}^{(2)}$ arbitrarily. We could have taken $x = A_{mn}^{(\alpha)}$ for α, m, n either 1 or 2 and $y = A_{mn}^{(\alpha)}$ such that $y \neq x$. In any of these cases, we would still have arrived at an underdetermined system like that in (2.33); this would have reduced to a system with a unique solution if and only if $\beta \neq 0$ similar to that in (2.34). Thus the condition that $\beta \neq 0$ is independent of how x and y are defined.*

Remark 2.3 *The requirement that $\beta \neq 0$ implies that the results of this chapter cannot be applied if $\sigma^{(1)}$ and $\sigma^{(2)}$ are both real (more precisely, the results of this chapter cannot be applied if $\sigma^{(1)}$ and $\sigma^{(2)}$ lie on the same line in the complex plane).*

Using Maple, we solve (2.34) in terms of x and y , insert the results into the matrices $S^{(1)}$ and $S^{(2)}$ (see (2.27)), and replace $f^{(1)}$ by a *test value* f . Denoting the resulting matrices by $S_f^{(1)}$ and $S_f^{(2)}$ we find

$$\begin{aligned} S_f^{(1)}(x, y) &\equiv \begin{bmatrix} x - \frac{\|\langle \mathbf{E}_1^{(1)} \rangle\|^2}{f} & S_{21}^{(1)}(x, y, f) \\ S_{21}^{(1)}(x, y, f) & -x + \eta^{(1)} - \frac{\|\langle \mathbf{E}_2^{(1)} \rangle\|^2}{f} \end{bmatrix} \\ \text{and } S_f^{(2)}(x, y) &\equiv \begin{bmatrix} y - \frac{\|\langle \mathbf{E}_1^{(2)} \rangle\|^2}{1-f} & S_{21}^{(2)}(x, y, f) \\ S_{21}^{(2)}(x, y, f) & -y + \eta^{(2)} - \frac{\|\langle \mathbf{E}_2^{(2)} \rangle\|^2}{1-f} \end{bmatrix} \end{aligned} \quad (2.35)$$

for $f \in (0, 1)$, where

$$\left\{ \begin{array}{l} S_{21}^{(1)}(x, y, f) = -\gamma x - \psi^{(1)}y + \xi^{(1)} - \frac{\langle \mathbf{E}_1^{(1)} \rangle \cdot \langle \mathbf{E}_2^{(1)} \rangle}{f}; \\ S_{21}^{(2)}(x, y, f) = \psi^{(2)}x + \gamma y - \xi^{(2)} - \frac{\langle \mathbf{E}_1^{(2)} \rangle \cdot \langle \mathbf{E}_2^{(2)} \rangle}{1-f}; \\ \beta = \sigma_1^{(1)}\sigma_2^{(2)} - \sigma_2^{(1)}\sigma_1^{(2)}; \quad \gamma = \frac{\sigma_1^{(1)}\sigma_1^{(2)} + \sigma_2^{(1)}\sigma_2^{(2)}}{\beta}; \\ \psi^{(1)} = \frac{|\sigma^{(2)}|^2}{\beta}; \quad \psi^{(2)} = \frac{|\sigma^{(1)}|^2}{\beta}; \\ \xi^{(1)} = \frac{\sigma_2^{(2)}\langle \mathbf{E}_1 \cdot \mathbf{J}_2 \rangle + \sigma_1^{(2)}\langle \mathbf{E}_1 \cdot \mathbf{J}_1 \rangle}{\beta}; \quad \xi^{(2)} = \frac{\sigma_2^{(1)}\langle \mathbf{E}_1 \cdot \mathbf{J}_2 \rangle + \sigma_1^{(1)}\langle \mathbf{E}_1 \cdot \mathbf{J}_1 \rangle}{\beta}; \\ \eta^{(1)} = \frac{\sigma_1^{(2)}(\langle \mathbf{E}_2 \cdot \mathbf{J}_1 \rangle - \langle \mathbf{E}_1 \cdot \mathbf{J}_2 \rangle) + \sigma_2^{(2)}(\langle \mathbf{E}_1 \cdot \mathbf{J}_1 \rangle + \langle \mathbf{E}_2 \cdot \mathbf{J}_2 \rangle)}{\beta}; \\ \eta^{(2)} = \frac{\sigma_1^{(1)}(\langle \mathbf{E}_1 \cdot \mathbf{J}_2 \rangle - \langle \mathbf{E}_2 \cdot \mathbf{J}_1 \rangle) - \sigma_2^{(1)}(\langle \mathbf{E}_1 \cdot \mathbf{J}_1 \rangle + \langle \mathbf{E}_2 \cdot \mathbf{J}_2 \rangle)}{\beta}. \end{array} \right. \quad (2.36)$$

Note that β , γ , $\psi^{(1)}$, $\psi^{(2)}$, $\xi^{(1)}$, $\xi^{(2)}$, $\eta^{(1)}$, and $\eta^{(2)}$ are known since they only depend on null Lagrangians and the (constant) conductivities of each phase.

We can use the relationship $\mathbf{J} = \sigma\mathbf{E}$ to rewrite $\eta^{(\alpha)}$ as

$$\eta^{(\alpha)} = \langle \chi^{(\alpha)} (\|\mathbf{E}_1\|^2 + \|\mathbf{E}_2\|^2) \rangle = \langle \|\mathbf{E}_1^{(\alpha)}\|^2 \rangle + \langle \|\mathbf{E}_2^{(\alpha)}\|^2 \rangle. \quad (2.37)$$

To see this, note that (2.11) and the fact that the conductivity in each phase is constant imply

$$\begin{aligned} \langle \mathbf{E}_2 \cdot \mathbf{J}_1 \rangle - \langle \mathbf{E}_1 \cdot \mathbf{J}_2 \rangle &= \langle \mathbf{E}_2 \cdot (\sigma_1\mathbf{E}_1 - \sigma_2\mathbf{E}_2) \rangle - \langle \mathbf{E}_1 \cdot (\sigma_2\mathbf{E}_1 + \sigma_1\mathbf{E}_2) \rangle \\ &= \langle \sigma_1\mathbf{E}_2 \cdot \mathbf{E}_1 \rangle - \langle \sigma_2\mathbf{E}_2 \cdot \mathbf{E}_2 \rangle - \langle \sigma_2\mathbf{E}_1 \cdot \mathbf{E}_1 \rangle - \langle \sigma_1\mathbf{E}_1 \cdot \mathbf{E}_2 \rangle \\ &= -\langle \sigma_2\|\mathbf{E}_2\|^2 \rangle - \langle \sigma_2\|\mathbf{E}_1\|^2 \rangle \\ &= -\sigma_2^{(1)}\langle \|\mathbf{E}_2^{(1)}\|^2 \rangle - \sigma_2^{(2)}\langle \|\mathbf{E}_2^{(2)}\|^2 \rangle - \sigma_2^{(1)}\langle \|\mathbf{E}_1^{(1)}\|^2 \rangle - \sigma_2^{(2)}\langle \|\mathbf{E}_1^{(2)}\|^2 \rangle \end{aligned} \quad (2.38)$$

and, similarly,

$$\langle \mathbf{E}_1 \cdot \mathbf{J}_1 \rangle + \langle \mathbf{E}_2 \cdot \mathbf{J}_2 \rangle = \sigma_1^{(1)}\langle \|\mathbf{E}_1^{(1)}\|^2 \rangle + \sigma_1^{(2)}\langle \|\mathbf{E}_1^{(2)}\|^2 \rangle + \sigma_1^{(1)}\langle \|\mathbf{E}_2^{(1)}\|^2 \rangle + \sigma_1^{(2)}\langle \|\mathbf{E}_2^{(2)}\|^2 \rangle. \quad (2.39)$$

Inserting (2.38) and (2.39) into (2.36) we find

$$\eta^{(1)} = \frac{\sigma_1^{(2)}(\langle \mathbf{E}_2 \cdot \mathbf{J}_1 \rangle - \langle \mathbf{E}_1 \cdot \mathbf{J}_2 \rangle) + \sigma_2^{(2)}(\langle \mathbf{E}_1 \cdot \mathbf{J}_1 \rangle + \langle \mathbf{E}_2 \cdot \mathbf{J}_2 \rangle)}{\beta}$$

$$\begin{aligned}
&= \frac{1}{\sigma_1^{(1)}\sigma_2^{(2)} - \sigma_2^{(1)}\sigma_1^{(2)}} \cdot \\
&\quad \left\{ -\sigma_1^{(2)} \left[\sigma_2^{(1)} \langle \|\mathbf{E}_2^{(1)}\|^2 \rangle + \sigma_2^{(2)} \langle \|\mathbf{E}_2^{(2)}\|^2 \rangle + \sigma_2^{(1)} \langle \|\mathbf{E}_1^{(1)}\|^2 \rangle + \sigma_2^{(2)} \langle \|\mathbf{E}_1^{(2)}\|^2 \rangle \right] \right. \\
&\quad \left. + \sigma_2^{(2)} \left[\sigma_1^{(1)} \langle \|\mathbf{E}_1^{(1)}\|^2 \rangle + \sigma_1^{(2)} \langle \|\mathbf{E}_1^{(2)}\|^2 \rangle + \sigma_1^{(1)} \langle \|\mathbf{E}_2^{(1)}\|^2 \rangle + \sigma_1^{(2)} \langle \|\mathbf{E}_2^{(2)}\|^2 \rangle \right] \right\} \\
&= \frac{1}{\sigma_1^{(1)}\sigma_2^{(2)} - \sigma_2^{(1)}\sigma_1^{(2)}} \cdot \\
&\quad \left\{ -\sigma_1^{(2)} \left[\sigma_2^{(1)} \langle \|\mathbf{E}_2^{(1)}\|^2 \rangle + \sigma_2^{(1)} \langle \|\mathbf{E}_1^{(1)}\|^2 \rangle \right] \right. \\
&\quad \left. + \sigma_2^{(2)} \left[\sigma_1^{(1)} \langle \|\mathbf{E}_1^{(1)}\|^2 \rangle + \sigma_1^{(1)} \langle \|\mathbf{E}_2^{(1)}\|^2 \rangle \right] \right\} \\
&= \frac{\left[\sigma_1^{(1)}\sigma_2^{(2)} - \sigma_2^{(1)}\sigma_1^{(2)} \right] \left[\langle \|\mathbf{E}_1^{(1)}\|^2 \rangle + \langle \|\mathbf{E}_2^{(1)}\|^2 \rangle \right]}{\sigma_1^{(1)}\sigma_2^{(2)} - \sigma_2^{(1)}\sigma_1^{(2)}} \\
&= \langle \|\mathbf{E}_1^{(1)}\|^2 \rangle + \langle \|\mathbf{E}_2^{(1)}\|^2 \rangle.
\end{aligned}$$

Similarly, from (2.36), (2.38), and (2.39) we have

$$\eta^{(2)} = \langle \|\mathbf{E}_1^{(2)}\|^2 \rangle + \langle \|\mathbf{E}_2^{(2)}\|^2 \rangle.$$

Note from (2.37) that $\eta^{(\alpha)} \geq 0$ with equality if and only if $\mathbf{E}^{(\alpha)} = \mathbf{E}_1^{(\alpha)} + i\mathbf{E}_2^{(\alpha)} \equiv 0$ (up to a set of measure 0); that is, $\eta^{(\alpha)} = 0$ if and only if the electric field is 0 in phase α . In two dimensions with D having smooth boundary the condition that the field is zero in one phase implies that it is zero everywhere; thus $\eta^{(\alpha)} = 0$ only for trivial boundary conditions. In three dimensions the situation is less clear [5], but in practice the field will almost always be zero in one of the phases only for trivial boundary conditions. Therefore we assume throughout the rest of this paper that $\eta^{(1)} \neq 0$ and $\eta^{(2)} \neq 0$.

Definition 2.1 For $f \in (0, 1)$ we set

$$\mathcal{F}_f^{(\alpha)} \equiv \{(x, y) \in \mathbb{R}^2 : S_f^{(\alpha)}(x, y) \text{ is positive-semidefinite}\}.$$

Then the set $\mathcal{F}_f \equiv \mathcal{F}_f^{(1)} \cap \mathcal{F}_f^{(2)}$ is called the feasible region associated with f . In addition, the set $\mathcal{A} \equiv \{f \in (0, 1) : \mathcal{F}_f \neq \emptyset\}$ is called the set of admissible test values.

Because there must be at least one $(x, y) \in \mathbb{R}^2$ at which $S_{f^{(1)}}^{(1)}(x, y)$ and $S_{f^{(1)}}^{(2)}(x, y)$ are both positive-semidefinite (see (2.29)), given $f \in (0, 1)$ we check to see whether or not there are regions in the xy -plane for which $S_f^{(1)}(x, y)$ and $S_f^{(2)}(x, y)$ are simultaneously positive-semidefinite — that is, whether or not $\mathcal{F}_f \neq \emptyset$. If the feasible region \mathcal{F}_f is nonempty, then f is an admissible test value, so $f \in \mathcal{A}$; that is, f may be the true volume fraction of phase 1. If $\mathcal{F}_f = \emptyset$ we can conclude that f is *not* the true volume fraction of phase 1. This will leave us with an interval (or set of intervals) of admissible test values, which we have defined as \mathcal{A} .

Our goal is to find the set \mathcal{A} . If \mathcal{A} is connected, the desired lower and upper bounds on $f^{(1)}$ will be $\inf \mathcal{A}$ and $\sup \mathcal{A}$, respectively. If \mathcal{A} is not connected, the structure of the bounds will be more complicated — see Figure 2.2. In Figure 2.2(b), the set of admissible test values is $\mathcal{A} = \mathcal{A}^* \cup \mathcal{A}^{**}$. In the examples we have encountered \mathcal{A} has always been connected.

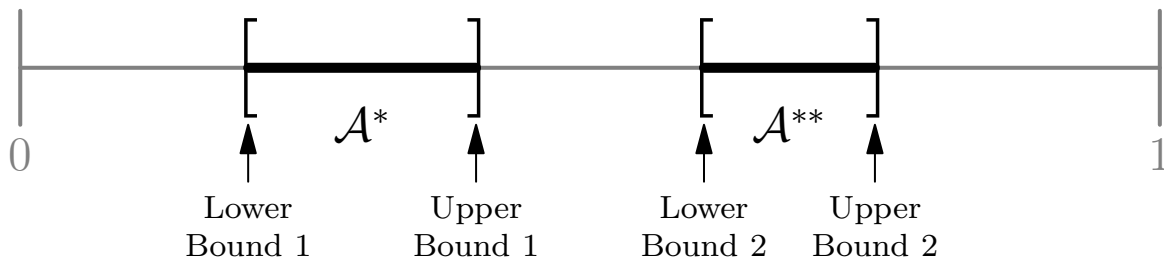
(a) \mathcal{A} connected(b) \mathcal{A} disconnected

Figure 2.2. In the example above, we know that either $\inf \mathcal{A}^* \leq f^{(1)} \leq \sup \mathcal{A}^*$ or $\inf \mathcal{A}^{**} \leq f^{(1)} \leq \sup \mathcal{A}^{**}$. (a) When \mathcal{A} (the darkened interval) is connected, we have $\inf \mathcal{A} \leq f^{(1)} \leq \sup \mathcal{A}$. (b) When $\mathcal{A} = \mathcal{A}^* \cup \mathcal{A}^{**}$ is disconnected, there will be multiple bounds on $f^{(1)}$.

2.4 Elementary Bounds

Recall that a symmetric 2×2 matrix

$$L = \begin{bmatrix} a & b \\ b & c \end{bmatrix}$$

is positive-semidefinite if and only if $a \geq 0$, $c \geq 0$, and $ac - b^2 = \det L \geq 0$. In this section we use the above requirements on the diagonal components of the matrices $S_f^{(1)}(x, y)$ and $S_f^{(2)}(x, y)$ to derive elementary bounds on $f^{(1)}$.

By Definition 2.1 and the above statement, $f \in \mathcal{A}$ only if there is at least one point $(x, y) \in \mathbb{R}^2$ such that $S_{f,mm}^{(\alpha)}(x, y) \geq 0$ for $\alpha, m = 1, 2$. That is, the following inequalities must hold for all admissible volume fractions f (see (2.35)):

$$\frac{\|\langle \mathbf{E}_1^{(1)} \rangle\|^2}{f} \leq x \leq \eta^{(1)} - \frac{\|\langle \mathbf{E}_2^{(1)} \rangle\|^2}{f} \quad (2.40a)$$

$$\frac{\|\langle \mathbf{E}_1^{(2)} \rangle\|^2}{1-f} \leq y \leq \eta^{(2)} - \frac{\|\langle \mathbf{E}_2^{(2)} \rangle\|^2}{1-f}. \quad (2.40b)$$

Definition 2.2 For $f \in (0, 1)$, the set

$$\mathcal{F}_{f,e} \equiv \{(x, y) \in \mathbb{R}^2 : \text{both (2.40a) and (2.40b) hold}\}$$

is called the elementary feasible region associated with f . The set

$$\mathcal{A}_e \equiv \{f \in (0, 1) : \mathcal{F}_{f,e} \neq \emptyset\}$$

is called the elementary set of admissible test values.

Geometrically, for each admissible $f \in (0, 1)$, the set $\mathcal{F}_{f,e}$ will be the closed rectangle in \mathbb{R}^2 defined by the inequalities in (2.40a) and (2.40b). For a given $f \in (0, 1)$, the set $\mathcal{F}_{f,e}$ will be nonempty if and only if both of the following inequalities hold:

$$\frac{\|\langle \mathbf{E}_1^{(1)} \rangle\|^2}{f} \leq \eta^{(1)} - \frac{\|\langle \mathbf{E}_2^{(1)} \rangle\|^2}{f} \quad (2.41a)$$

$$\frac{\|\langle \mathbf{E}_1^{(2)} \rangle\|^2}{1-f} \leq \eta^{(2)} - \frac{\|\langle \mathbf{E}_2^{(2)} \rangle\|^2}{1-f}. \quad (2.41b)$$

As stated earlier we assume that $\eta^{(\alpha)} \neq 0$ ($\Leftrightarrow \mathbf{E}^{(\alpha)} \neq 0$) for $\alpha = 1, 2$. Then the inequalities in (2.41a) and (2.41b) may be rewritten as

$$f \geq f_{e,l} \equiv \frac{\|\langle \mathbf{E}_1^{(1)} \rangle\|^2 + \|\langle \mathbf{E}_2^{(1)} \rangle\|^2}{\eta^{(1)}} \quad (2.42a)$$

$$f \leq f_{e,u} \equiv 1 - \frac{\|\langle \mathbf{E}_1^{(2)} \rangle\|^2 + \|\langle \mathbf{E}_2^{(2)} \rangle\|^2}{\eta^{(2)}}, \quad (2.42b)$$

so $\mathcal{A}_e = [f_{e,l}, f_{e,u}]$. We obtain elementary bounds on $f^{(1)}$ by combining (2.42a) and (2.42b) and noting that $f^{(1)}$ must be in \mathcal{A}_e :

$$f_{e,l} \leq f^{(1)} \leq f_{e,u}. \quad (2.43)$$

We emphasize that $f_{e,l}$ and $f_{e,u}$ can be computed from the boundary measurements — see (2.31) and (2.36).

To avoid minor technical difficulties, we henceforth assume $f_{e,l} \neq 0$ (i.e., that $\|\langle \mathbf{E}_1^{(1)} \rangle\|^2 + \|\langle \mathbf{E}_2^{(1)} \rangle\|^2 \neq 0$) and $f_{e,u} \neq 1$ (i.e., that $\|\langle \mathbf{E}_1^{(2)} \rangle\|^2 + \|\langle \mathbf{E}_2^{(2)} \rangle\|^2 \neq 0$) — see (2.42). Note that $0 \leq f_{e,l}$ and $f_{e,u} \leq 1$. Also note that

$$\left\langle \left\| \mathbf{E}_m^{(\alpha)} - \frac{\chi^{(\alpha)}}{f^{(\alpha)}} \langle \mathbf{E}_m^{(\alpha)} \rangle \right\|^2 \right\rangle \geq 0 \quad \Leftrightarrow \quad \|\langle \mathbf{E}_m^{(\alpha)} \rangle\|^2 \leq f^{(\alpha)} \langle \|\mathbf{E}_m^{(\alpha)}\|^2 \rangle. \quad (2.44)$$

To see this we expand the left-hand side:

$$\begin{aligned} & \left\langle \left\| \mathbf{E}_m^{(\alpha)} - \frac{\chi^{(\alpha)}}{f^{(\alpha)}} \langle \mathbf{E}_m^{(\alpha)} \rangle \right\|^2 \right\rangle \\ &= \left\langle \left[\mathbf{E}_m^{(\alpha)} - \frac{\chi^{(\alpha)}}{f^{(\alpha)}} \langle \mathbf{E}_m^{(\alpha)} \rangle \right] \cdot \left[\mathbf{E}_m^{(\alpha)} - \frac{\chi^{(\alpha)}}{f^{(\alpha)}} \langle \mathbf{E}_m^{(\alpha)} \rangle \right] \right\rangle \\ &= \langle \mathbf{E}_m^{(\alpha)} \cdot \mathbf{E}_m^{(\alpha)} \rangle - \frac{2}{f^{(\alpha)}} \langle \chi^{(\alpha)} \mathbf{E}_m^{(\alpha)} \rangle \cdot \langle \mathbf{E}_m^{(\alpha)} \rangle + \frac{1}{f^{(\alpha)}} \langle [\chi^{(\alpha)}]^2 \rangle \langle \mathbf{E}_m^{(\alpha)} \rangle \cdot \langle \mathbf{E}_m^{(\alpha)} \rangle \\ &= \langle \|\mathbf{E}_m^{(\alpha)}\|^2 \rangle - \frac{1}{f^{(\alpha)}} \|\langle \mathbf{E}_m^{(\alpha)} \rangle\|^2, \end{aligned}$$

from which (2.44) follows. In particular (2.37), (2.42), and (2.44) imply that $f_{e,l} \leq f_{e,u}$ since

$$\begin{aligned} f_{e,l} - f_{e,u} &= \frac{\|\langle \mathbf{E}_1^{(1)} \rangle\|^2 + \|\langle \mathbf{E}_2^{(1)} \rangle\|^2}{\eta^{(1)}} + \frac{\|\langle \mathbf{E}_1^{(2)} \rangle\|^2 + \|\langle \mathbf{E}_2^{(2)} \rangle\|^2}{\eta^{(2)}} - 1 \\ &\leq \frac{f^{(1)} [\langle \|\mathbf{E}_1^{(1)}\|^2 \rangle + \langle \|\mathbf{E}_2^{(1)}\|^2 \rangle]}{\langle \|\mathbf{E}_1^{(1)}\|^2 \rangle + \langle \|\mathbf{E}_2^{(1)}\|^2 \rangle} + \frac{f^{(2)} [\langle \|\mathbf{E}_1^{(2)}\|^2 \rangle + \langle \|\mathbf{E}_2^{(2)}\|^2 \rangle]}{\langle \|\mathbf{E}_1^{(2)}\|^2 \rangle + \langle \|\mathbf{E}_2^{(2)}\|^2 \rangle} - 1 \\ &= f^{(1)} + f^{(2)} - 1 \\ &= 0. \end{aligned}$$

We also note that (2.44) leads to a simpler proof of the elementary bounds. In particular, (2.44) implies that

$$\|\langle \mathbf{E}_1^{(\alpha)} \rangle\|^2 + \|\langle \mathbf{E}_2^{(\alpha)} \rangle\|^2 \leq f^{(\alpha)} \left[\|\langle \mathbf{E}_1^{(\alpha)} \rangle\|^2 + \|\langle \mathbf{E}_2^{(\alpha)} \rangle\|^2 \right] = f^{(\alpha)} \eta^{(\alpha)}.$$

The first and second inequalities in (2.43) follow from this by taking $\alpha = 1$ and $\alpha = 2$, respectively (recall $f^{(2)} = 1 - f^{(1)}$).

Now (2.44) holds as an equality if and only if

$$\mathbf{E}_m^{(\alpha)}(\mathbf{x}) = \chi^{(\alpha)}(\mathbf{x}) \frac{\langle \mathbf{E}_m^{(\alpha)} \rangle}{f^{(\alpha)}};$$

that is, (2.44) holds as an equality if and only if \mathbf{E}_m is a constant (almost everywhere) in phase α . From this we see that $f_{e,l} = f^{(1)}$ if and only if $\mathbf{E}^{(1)} = \chi^{(1)}\mathbf{E}$ is a constant (which must be nonzero since we are assuming $\eta^{(1)} \neq 0 \Leftrightarrow \mathbf{E}^{(1)} \neq 0$) and $f_{e,u} = f^{(1)}$ if and only if $\mathbf{E}^{(2)} = \chi^{(2)}\mathbf{E}$ is a (nonzero) constant. This implies that the bounds in (2.43) are sharp in the sense that the lower bound (upper bound) is satisfied as an equality for geometries in which the electric field is constant in phase 1 (phase 2).

For example, if phase 1 is a disk of radius r centered at the origin and phase 2 is a concentric disk of radius $R > r$, then $\mathbf{E}^{(1)}$ will be a constant for the affine Dirichlet Boundary Condition $V_0 = \mathbf{u} \cdot \mathbf{x}$, where $\mathbf{u} \neq 0 \in \mathbb{C}^2$. In this case $f_{e,l} = f^{(1)}$. If we relabel the phases then $\mathbf{E}^{(2)}$ will be a constant, so $f_{e,u} = f^{(1)}$. A simple laminate of materials with conductivities $\sigma^{(1)}$ and $\sigma^{(2)}$ has the property that the electric field is constant in both phases, so $f_{e,l} = f_{e,u} = f^{(1)}$ in that case. In 2-D there are many examples of inclusions inside which the electric field is constant for certain boundary conditions. Kang et al. [64] provided elegant constructions of these so-called E_Ω inclusions; although their argument was applied in the real conductivity case, it extends to the complex conductivity case as well. So for appropriate boundary conditions the field inside an E_Ω inclusion will be uniform even when the conductivities are complex. We have thus proven the following theorem, which states that $\mathcal{A}_e = [f_{e,l}, f_{e,u}]$.

Theorem 2.1 *Assume that $\beta \neq 0$ (where β is defined in (2.36)), $\eta^{(\alpha)} \neq 0$ ($\Leftrightarrow \mathbf{E}^{(\alpha)} \neq 0$) for $\alpha = 1, 2$, $f_{e,l} \neq 0$, and $f_{e,u} \neq 1$ (where $f_{e,l}$ and $f_{e,u}$ are defined in (2.42)). Then $f_{e,l} \leq f^{(1)} \leq f_{e,u}$. Moreover, $f_{e,l} = f^{(1)}$ if and only if $\mathbf{E}^{(1)}$ is a nonzero constant and $f_{e,u} = f^{(1)}$ if and only if $\mathbf{E}^{(2)}$ is a nonzero constant.*

We illustrate these ideas by considering an example, shown in Figure 2.3. We consider an annular ring with conductivity $\sigma^{(2)}$ and a discontinuous “inclusion phase” D consisting of the core and surrounding material outside the annulus with conductivity $\sigma^{(1)}$. Figure 2.3(a) is a sketch of the region Ω . In Figure 2.3(b) we plot the bounds from (2.40a) and (2.40b) versus f . In particular, the lower bound in (2.40a) is plotted as a red dashed line while the upper bound is plotted as a red solid line. The red shaded region indicates the values of f for which the bounds in (2.40a) hold, i.e., the values of f for which there is at least one value of x such that (2.40a) holds. Similarly, the lower bound in (2.40b) is plotted as a blue dash-dotted line while the upper bound is plotted as a blue dotted line. The blue shaded region indicates the values of f for which there is at least one value of y such that the bounds in (2.40b) hold. The left and right black vertical lines indicate the elementary lower and upper bounds $f_{e,l}$ and $f_{e,u}$, respectively; the dashed magenta line indicates the true volume fraction $f^{(1)}$. The elementary set of admissible test values, \mathcal{A}_e , is indicated by the darkened interval between $f_{e,l}$ and $f_{e,u}$.

2.5 More Sophisticated Bounds

Throughout this section, we assume that $\eta^{(1)}$ and $\eta^{(2)}$ are both nonzero and that $f_{e,l} \neq 0$ and $f_{e,u} \neq 1$. We derive a method to determine bounds by using the additional requirement that $S_f^{(\alpha)}(x, y)$ is positive-semidefinite only if $\det S_f^{(\alpha)}(x, y) \geq 0$. Using (2.35) we find, for $\alpha = 1, 2$, that

$$p_f^{(\alpha)}(x, y) \equiv \det S_f^{(\alpha)}(x, y) = a_1^{(\alpha)}x^2 + 2a_2^{(\alpha)}xy + a_3^{(\alpha)}y^2 + 2a_4^{(\alpha)}x + 2a_5^{(\alpha)}y + a_6^{(\alpha)} \quad (2.45)$$

where

$$\left\{ \begin{array}{l} a_1^{(1)} = -(1 + \gamma^2); \quad a_2^{(1)} = -\gamma\psi^{(1)}; \quad a_3^{(1)} = -[\psi^{(1)}]^2; \\ a_4^{(1)} = \frac{1}{2} \left\{ \eta^{(1)} - \frac{\|\langle \mathbf{E}_2^{(1)} \rangle\|^2}{f} + \frac{\|\langle \mathbf{E}_1^{(1)} \rangle\|^2}{f} + 2\gamma \left[\xi^{(1)} - \frac{\langle \mathbf{E}_1^{(1)} \rangle \cdot \langle \mathbf{E}_2^{(1)} \rangle}{f} \right] \right\}; \\ a_5^{(1)} = \psi^{(1)} \left[\xi^{(1)} - \frac{\langle \mathbf{E}_1^{(1)} \rangle \cdot \langle \mathbf{E}_2^{(1)} \rangle}{f} \right]; \\ a_6^{(1)} = - \left\{ \frac{\|\langle \mathbf{E}_1^{(1)} \rangle\|^2}{f} \left[\eta^{(1)} - \frac{\|\langle \mathbf{E}_2^{(1)} \rangle\|^2}{f} \right] + \left[\xi^{(1)} - \frac{\langle \mathbf{E}_1^{(1)} \rangle \cdot \langle \mathbf{E}_2^{(1)} \rangle}{f} \right]^2 \right\} \end{array} \right. \quad (2.46)$$

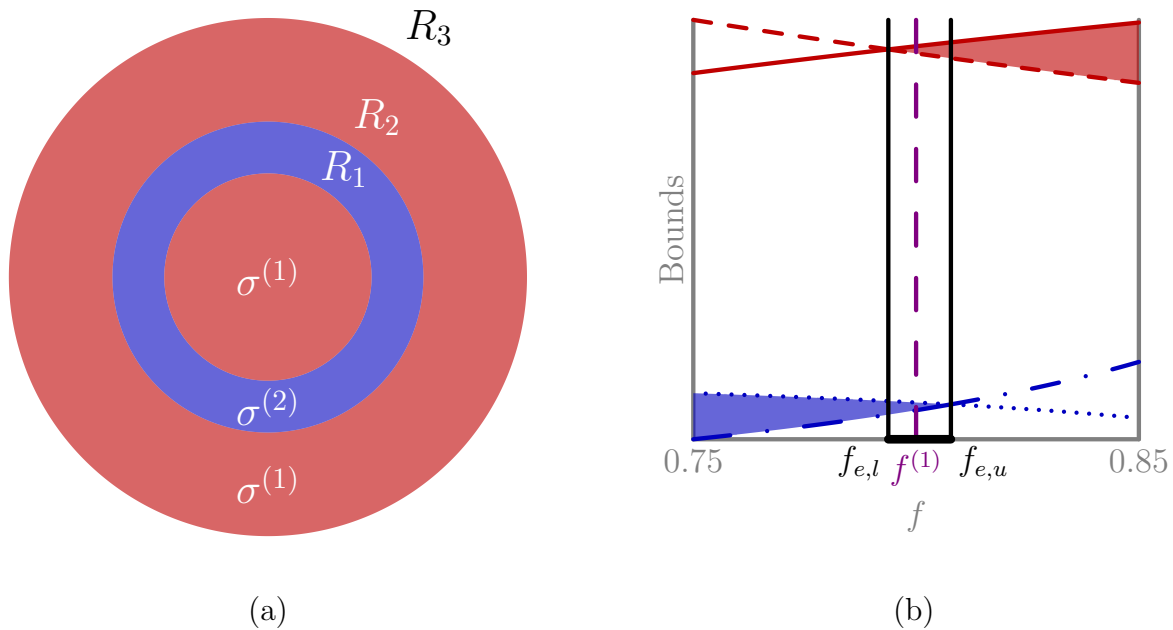


Figure 2.3. In this figure, we sketch the region under consideration and provide an illustration of the elementary bounds. (a) A sketch of the region under consideration — our discontinuous “inclusion phase” D (with conductivity $\sigma^{(1)}$ and volume fraction $f^{(1)}$) is the core plus the surrounding material outside the annulus. (b) Construction of the elementary bounds. The parameters that were used to create these plots are: radii $R_1 = 2$; $R_2 = 3$; $R_3 = 5$; conductivities $\sigma^{(1)} = 3 + 8i$; $\sigma^{(2)} = 8 + 6i$; the Dirichlet Boundary Condition was $V_0 = \mathbf{u} \cdot \mathbf{x}$, where $\mathbf{u} = \left(-2 + i, \frac{3}{5} - \frac{7}{5}i\right)^T$. The elementary lower and upper bounds are $f_{e,l} \approx 0.794$ and $f_{e,u} \approx 0.808$, respectively. The true volume fraction is $f^{(1)} = 0.8$.

and

$$\begin{cases} a_1^{(2)} = -[\psi^{(2)}]^2; & a_2^{(2)} = -\gamma\psi^{(2)}; & a_3^{(2)} = -(1 + \gamma^2); \\ a_4^{(2)} = \psi^{(2)} \left[\xi^{(2)} + \frac{\langle \mathbf{E}_1^{(2)} \rangle \cdot \langle \mathbf{E}_2^{(2)} \rangle}{1-f} \right]; \\ a_5^{(2)} = \frac{1}{2} \left\{ \eta^{(2)} - \frac{\|\langle \mathbf{E}_2^{(2)} \rangle\|^2}{1-f} + \frac{\|\langle \mathbf{E}_1^{(2)} \rangle\|^2}{1-f} + 2\gamma \left[\xi^{(2)} + \frac{\langle \mathbf{E}_1^{(2)} \rangle \cdot \langle \mathbf{E}_2^{(2)} \rangle}{1-f} \right] \right\}; \\ a_6^{(2)} = - \left\{ \frac{\|\langle \mathbf{E}_1^{(2)} \rangle\|^2}{1-f} \left[\eta^{(2)} - \frac{\|\langle \mathbf{E}_2^{(2)} \rangle\|^2}{1-f} \right] + \left[\xi^{(2)} + \frac{\langle \mathbf{E}_1^{(2)} \rangle \cdot \langle \mathbf{E}_2^{(2)} \rangle}{1-f} \right]^2 \right\}. \end{cases} \quad (2.47)$$

Definition 2.3 For $\alpha = 1, 2$ and for $f \in \mathcal{A}_e (= [f_{e,l}, f_{e,u}])$ we define

$$\mathcal{E}_f^{(\alpha)} \equiv \{(x, y) \in \mathbb{R}^2 : p_f^{(\alpha)}(x, y) \geq 0\} \quad \text{and} \quad \mathcal{E}_f \equiv \mathcal{E}_f^{(1)} \cap \mathcal{E}_f^{(2)}.$$

We now prove several lemmas in order to establish some useful properties of the sets $\mathcal{E}_f^{(\alpha)}$.

Lemma 2.2 Assume that $\beta \neq 0$, $\eta^{(\alpha)} \neq 0$ for $\alpha = 1, 2$, $f_{e,l} \neq 0$, and $f_{e,u} \neq 1$. Then the following properties hold.

- (1) For $f \in (f_{e,l}, f_{e,u})$ and $\alpha = 1, 2$, $\mathcal{E}_f^{(\alpha)}$ is a closed elliptic disk; its boundary is the ellipse $\partial\mathcal{E}_f^{(\alpha)} = \{(x, y) \in \mathbb{R}^2 : p_f^{(\alpha)}(x, y) = 0\}$;
- (2) $\mathcal{E}_{f_{e,l}}^{(1)}$ is a point and $\mathcal{E}_{f_{e,l}}^{(2)}$ is a closed elliptic disk;
- (3) $\mathcal{E}_{f_{e,u}}^{(1)}$ is a closed elliptic disk and $\mathcal{E}_{f_{e,u}}^{(2)}$ is a point.

Proof of Lemma 2.2: The discriminant of $p_f^{(\alpha)}$ is

$$a_1^{(\alpha)}a_3^{(\alpha)} - [a_2^{(\alpha)}]^2 = [\psi^{(\alpha)}]^2 > 0$$

for all $f \in \mathcal{A}_e$ by (2.36). Thus the graph of $p_f^{(\alpha)}$ is an elliptic paraboloid for all $f \in \mathcal{A}_e$.

The Hessian matrix of $p_f^{(\alpha)}$ is

$$H_f^{(\alpha)} \equiv \begin{bmatrix} 2a_1^{(\alpha)} & 2a_2^{(\alpha)} \\ 2a_2^{(\alpha)} & 2a_3^{(\alpha)} \end{bmatrix}.$$

By (2.36), (2.46), and (2.47), $a_1^{(\alpha)} < 0$ and

$$\det H_f^{(\alpha)} = 4 [\psi^{(\alpha)}]^2 > 0,$$

so $H_f^{(\alpha)}$ is negative-definite for all $f \in \mathcal{A}_e$; thus $p_f^{(\alpha)}$ is concave for all $f \in \mathcal{A}_e$. By Definition 2.3, therefore, $\mathcal{E}_f^{(\alpha)}$ is the intersection of the plane $z = 0$ with the graph of $p_f^{(\alpha)}$.

For $f \in \mathcal{A}_e$ we define

$$p_{f,\max}^{(\alpha)} \equiv \max_{(x,y) \in \mathbb{R}^2} p_f^{(\alpha)}(x,y).$$

Then $\mathcal{E}_f^{(\alpha)}$ will be a closed elliptic disk with boundary

$$\partial\mathcal{E}_f^{(\alpha)} = \{(x,y) \in \mathbb{R}^2 : p_f^{(\alpha)}(x,y) = 0\}$$

if and only if $p_{f,\max}^{(\alpha)} > 0$, a point if and only if $p_{f,\max}^{(\alpha)} = 0$, or the empty set if and only if $p_{f,\max}^{(\alpha)} < 0$. Using calculus (i.e., setting the gradient of $p_f^{(\alpha)}(x,y)$ equal to 0 and solving for (x,y)), we find that the maximum of $p_f^{(\alpha)}$ occurs at the point

$$\mathbf{r}_f^{(\alpha)} \equiv (\bar{x}_f^{(\alpha)}, \bar{y}_f^{(\alpha)}) \equiv \left(\frac{a_2^{(\alpha)} a_5^{(\alpha)} - a_3^{(\alpha)} a_4^{(\alpha)}}{[\psi^{(\alpha)}]^2}, \frac{a_2^{(\alpha)} a_4^{(\alpha)} - a_1^{(\alpha)} a_5^{(\alpha)}}{[\psi^{(\alpha)}]^2} \right). \quad (2.48)$$

Then we have

$$p_{f,\max}^{(\alpha)} = p_f^{(\alpha)}(\bar{x}_f^{(\alpha)}, \bar{y}_f^{(\alpha)}) = \frac{1}{4f_*^2} \left\{ \eta^{(\alpha)} f_* - [\|\langle \mathbf{E}_1^{(\alpha)} \rangle\|^2 + \|\langle \mathbf{E}_2^{(\alpha)} \rangle\|^2] \right\}^2, \quad (2.49)$$

where

$$f_* \equiv \begin{cases} f & \text{if } \alpha = 1 \\ 1 - f & \text{if } \alpha = 2. \end{cases} \quad (2.50)$$

Thus $p_{f,\max}^{(\alpha)} \geq 0$ for all $f \in \mathcal{A}_e$; in particular, from (2.49), $p_{f,\max}^{(1)} = 0$ if and only if $f = f_{e,l}$ (see (2.42a)) while $p_{f,\max}^{(2)} = 0$ if and only if $f = f_{e,u}$ (see (2.42b)). Therefore $\mathcal{E}_f^{(\alpha)}$ is a closed elliptic disk for $f \in (f_{e,l}, f_{e,u})$, $\mathcal{E}_{f_{e,l}}^{(1)}$ is a point and $\mathcal{E}_{f_{e,l}}^{(2)}$ is a closed elliptic disk, and $\mathcal{E}_{f_{e,u}}^{(1)}$ is a closed elliptic disk and $\mathcal{E}_{f_{e,u}}^{(2)}$ is a point. This completes the proof.

Lemma 2.3 *Suppose $\beta \neq 0$, $\eta^{(\alpha)} \neq 0$ for $\alpha = 1, 2$, $f_{e,l} \neq 0$, and $f_{e,u} \neq 1$. Then for each $f \in \mathcal{A}_e (= [f_{e,l}, f_{e,u}])$, $\mathcal{E}_f \subseteq \mathcal{F}_{f,e}$.*

Remark 2.4 *This lemma states that, for each $f \in \mathcal{A}_e$, the intersection of the elliptic disks (the set \mathcal{E}_f) is contained in the elementary feasible region associated with f (the set $\mathcal{F}_{f,e}$). Thus the feasible region associated with f (the set \mathcal{F}_f) is simply the set \mathcal{E}_f . In other words, if the elliptic disks $\mathcal{E}_f^{(1)}$ and $\mathcal{E}_f^{(2)}$ intersect so that $\mathcal{E}_f \neq \emptyset$, then $f \in \mathcal{A}$; if the elliptic disks do not intersect so that $\mathcal{E}_f = \emptyset$, then $f \notin \mathcal{A}$.*

Proof of Lemma 2.3: For each $f \in [f_{e,l}, f_{e,u}]$ the set $\mathcal{F}_{f,e}$ contains $\mathcal{F}_f^{(1)}$. The boundary of the set $\mathcal{F}_f^{(1)}$ is described by the equation $p_f^{(1)}(x, y) = 0$ which, according to Lemma 2.2, is either an ellipse, a point, or the empty set. Therefore $\mathcal{E}_f^{(1)} = \mathcal{F}_f^{(1)} \subseteq \mathcal{F}_{f,e}$. A similar argument shows that $\mathcal{E}_f^{(2)} = \mathcal{F}_f^{(2)} \subseteq \mathcal{F}_{f,e}$. This completes the proof.

Remark 2.5 *In fact, motivated by (2.40a) one can show that the ellipse $\partial\mathcal{E}_f^{(1)}$ is tangent to the boundary of the set*

$$X_f \equiv \left\{ (x, y) \in \mathbb{R}^2 : \frac{\|\langle \mathbf{E}_1^{(1)} \rangle\|^2}{f} \leq x \leq \eta^{(1)} - \frac{\|\langle \mathbf{E}_2^{(1)} \rangle\|^2}{f} \right\} \quad (2.51)$$

for $f \in (f_{e,l}, f_{e,u}]$. Similarly, motivated by (2.40b) one can also show that the ellipse $\partial\mathcal{E}_f^{(2)}$ is tangent to the boundary of the set

$$Y_f \equiv \left\{ (x, y) \in \mathbb{R}^2 : \frac{\|\langle \mathbf{E}_1^{(2)} \rangle\|^2}{1-f} \leq y \leq \eta^{(2)} - \frac{\|\langle \mathbf{E}_2^{(2)} \rangle\|^2}{1-f} \right\} \quad (2.52)$$

for $f \in [f_{e,l}, f_{e,u})$. The set $X_f \cap Y_f$ is in fact the rectangle $\mathcal{F}_{f,e}$ and the test values f where this rectangle collapses to a line segment are the elementary bounds.

See Appendix A for a proof of Remark 2.5.

Lemma 2.4 *Suppose $\beta \neq 0$, $\eta^{(\alpha)} \neq 0$ for $\alpha = 1, 2$, $f_{e,l} \neq 0$, and $f_{e,u} \neq 1$. Then for each $f \in \mathcal{A}_e$ the set $\partial\mathcal{E}_f^{(1)} \cap \partial\mathcal{E}_f^{(2)}$ contains at most two points.*

Proof of Lemma 2.4: Fix $f \in \mathcal{A}_e$ and suppose that the point $(x, y) \in \partial\mathcal{E}_f^{(1)} \cap \partial\mathcal{E}_f^{(2)}$ (note that $\partial\mathcal{E}_f^{(\alpha)} \neq \emptyset$ by Lemma 2.2). Then for $\alpha = 1, 2$ we must have $p_f^{(\alpha)}(x, y) = 0$, where $p_f^{(\alpha)}$ is defined in (2.45). This implies that

$$0 = |\sigma^{(1)}|^2 p_f^{(1)}(x, y) - |\sigma^{(2)}|^2 p_f^{(2)}(x, y) = \mu_4 x + \mu_5 y + \mu_6, \quad (2.53)$$

where

$$\mu_k \equiv |\sigma^{(1)}|^2 a_k^{(1)} - |\sigma^{(2)}|^2 a_k^{(2)}$$

for $k = 1, 3$, and 6 , and

$$\mu_k \equiv 2|\sigma^{(1)}|^2 a_k^{(1)} - 2|\sigma^{(2)}|^2 a_k^{(2)}$$

for $k = 2, 4$, and 5 . By (2.46) and (2.47), $\mu_1 = \mu_2 = \mu_3 = 0$ for all $f \in \mathcal{A}_e$. We solve (2.53) for y to find

$$y = -\frac{\mu_4 x + \mu_6}{\mu_5}. \quad (2.54)$$

Because $f_{e,l} > 0$ and $f_{e,u} < 1$, Lemma 2.3 implies that y is finite for all $f \in \mathcal{A}_e$ since the set $\mathcal{F}_{f,e}$ is compact and $(\mathcal{E}_f^{(1)} \cap \mathcal{E}_f^{(2)}) \subset \mathcal{F}_{f,e}$. Inserting (2.54) into the equation $p^{(1)}(x, y) = 0$ we find that x must be a root of the quadratic

$$q(x) \equiv \nu_1 x^2 + \nu_2 x + \nu_3,$$

where

$$\begin{cases} \nu_1 = a_1^{(1)} \mu_5^2 - 2a_2^{(1)} \mu_4 \mu_5 + a_3^{(1)} \mu_4^2; \\ \nu_2 = 2 \left[-a_2^{(1)} \mu_5 \mu_6 + a_3^{(1)} \mu_4 \mu_6 + a_4^{(1)} \mu_5^2 - a_5^{(1)} \mu_4 \mu_5 \right]; \\ \nu_3 = a_3^{(1)} \mu_6^2 - 2a_5^{(1)} \mu_5 \mu_6 + a_6^{(1)} \mu_5^2. \end{cases}$$

(Note that ν_1, ν_2 , and ν_3 are all functions of f .) The discriminant of q is

$$\Delta_f \equiv \nu_2^2 - 4\nu_1 \nu_3. \quad (2.55)$$

Therefore the set $\partial\mathcal{E}_f^{(1)} \cap \partial\mathcal{E}_f^{(2)}$ will be two (real) points if $\Delta_f > 0$, one (real) point if $\Delta_f = 0$, and zero (real) points if $\Delta_f < 0$. This completes the proof.

Lemma 2.2 implies that $\mathcal{E}_f^{(1)}$ and $\mathcal{E}_f^{(2)}$ are nonempty for all $f \in \mathcal{A}_e$, and Lemma 2.3 implies that $\mathcal{F}_f = \mathcal{E}_f$ for all $f \in \mathcal{A}_e$. Therefore $f \in \mathcal{A}$ if $\Delta_f \geq 0$, since $\Delta_f \geq 0$ implies $\mathcal{E}_f \neq \emptyset$. If $\Delta_f < 0$, \mathcal{E}_f may be empty or nonempty. For example, if one of the elliptic disks is completely inside the other, $\Delta_f < 0$ but $\mathcal{E}_f \neq \emptyset$.

To determine whether or not \mathcal{E}_f is empty when $\Delta_f < 0$ we examine the following four possibilities (recall that $\mathbf{r}^{(\alpha)}$ is defined in (2.48)):

- (1) if $p_f^{(1)}(\mathbf{r}^{(2)}) < 0$ and $p_f^{(2)}(\mathbf{r}^{(1)}) < 0$, then the elliptic disks (which may be points) are disjoint since neither elliptic disk contains the center of the other. Thus $\mathcal{E}_f = \emptyset$, which implies that $f \notin \mathcal{A}$;
- (2) if $p_f^{(1)}(\mathbf{r}^{(2)}) \geq 0$ and $p_f^{(2)}(\mathbf{r}^{(1)}) < 0$, then the elliptic disk $\mathcal{E}_f^{(1)}$ contains the center of the elliptic disk $\mathcal{E}_f^{(2)}$ but not vice versa. In this case $\mathcal{E}_f^{(2)} \subsetneq \mathcal{E}_f^{(1)} \Rightarrow \mathcal{E}_f \neq \emptyset \Rightarrow f \in \mathcal{A}$;
- (3) if $p_f^{(1)}(\mathbf{r}^{(2)}) < 0$ and $p_f^{(2)}(\mathbf{r}^{(1)}) \geq 0$, then $\mathcal{E}_f^{(1)} \subsetneq \mathcal{E}_f^{(2)} \Rightarrow \mathcal{E}_f \neq \emptyset \Rightarrow f \in \mathcal{A}$;
- (4) if $p_f^{(1)}(\mathbf{r}^{(2)}) \geq 0$ and $p_f^{(2)}(\mathbf{r}^{(1)}) \geq 0$, we can conclude that $\mathcal{E}_f \neq \emptyset$ and so $f \in \mathcal{A}$.

Unfortunately Δ_f is a complicated function of f , so it is difficult if not impossible to determine the sign of Δ_f analytically. The expressions for $p^{(1)}(\mathbf{r}^{(2)})$ and $p^{(2)}(\mathbf{r}^{(1)})$ are nontrivial as well, so the above steps must be carried out numerically. (For example, for the configuration considered in Figure 2.3, Δ_f is essentially a rational function with an irreducible polynomial of degree 8 in the numerator and an irreducible polynomial of degree 2 in the denominator. The functions $p_f^{(1)}(\mathbf{r}^{(2)})$ and $p_f^{(2)}(\mathbf{r}^{(1)})$ are rational functions with irreducible polynomials of degree 4 in the numerator.) We have thus proven the following theorem.

Theorem 2.2 *Suppose $\beta \neq 0$, $\eta^{(\alpha)} \neq 0$ for $\alpha = 1, 2$, $f_{e,l} \neq 0$, and $f_{e,u} \neq 1$. Then for $f \in \mathcal{A}_e (= [f_{e,l}, f_{e,u}])$, if $\Delta_f \geq 0$ then $f \in \mathcal{A}$, where Δ_f is defined in (2.55). If $\Delta_f < 0$, then $f \notin \mathcal{A}$ if and only if $p_f^{(1)}(\mathbf{r}^{(2)}) < 0$ and $p_f^{(2)}(\mathbf{r}^{(1)}) < 0$.*

The bounds derived in this section may or may not be tighter than the elementary bounds from Section 2.4. For example, the bounds from this section would be the same as the elementary bounds if $\Delta_f \geq 0$ for all $f \in \mathcal{A}_e$. We also note that Lemmas 2.2 and 2.4 hold for all $f \in (0, 1)$. This shows the importance of the elementary bounds: if we did not take them into account and only looked at the set \mathcal{E}_f for all $f \in (0, 1)$, it may be that $\mathcal{E}_f \neq \emptyset$ for all $f \in (0, 1)$ (we found this to be the case for certain parameters in the configuration in Figure 2.3). This would only give the trivial bounds $0 < f^{(1)} < 1$. Although we do not know if this is generally the case, in all of the 2-D examples we have encountered thus far the “more sophisticated” bounds determined using the elliptic disks have been the same as the elementary bounds. So it is not clear if the “more sophisticated” bounds are ever better than the elementary bounds. Irrespective of this, the analysis presented here is useful for the treatment presented in the next section where we do obtain tighter bounds using elliptic disks. Also, the more sophisticated bounds developed here are beneficial for periodic composite materials, where one may be given the volume fraction and wish to determine bounds on the possible values of the complex pair $(\langle \mathbf{E} \rangle, \langle \mathbf{J} \rangle)$.

In Figures 2.4(a)–2.4(h) we plot the sets $\mathcal{E}_f^{(1)}$ (red) and $\mathcal{E}_f^{(2)}$ (blue) at various values of $f \in \mathcal{A}_e = [f_{e,l}, f_{e,u}]$; the centers of each ellipse are indicated by dots. The black box is the boundary of the set $\mathcal{F}_{f,e}$, defined by the inequalities (2.40a) and (2.40b).

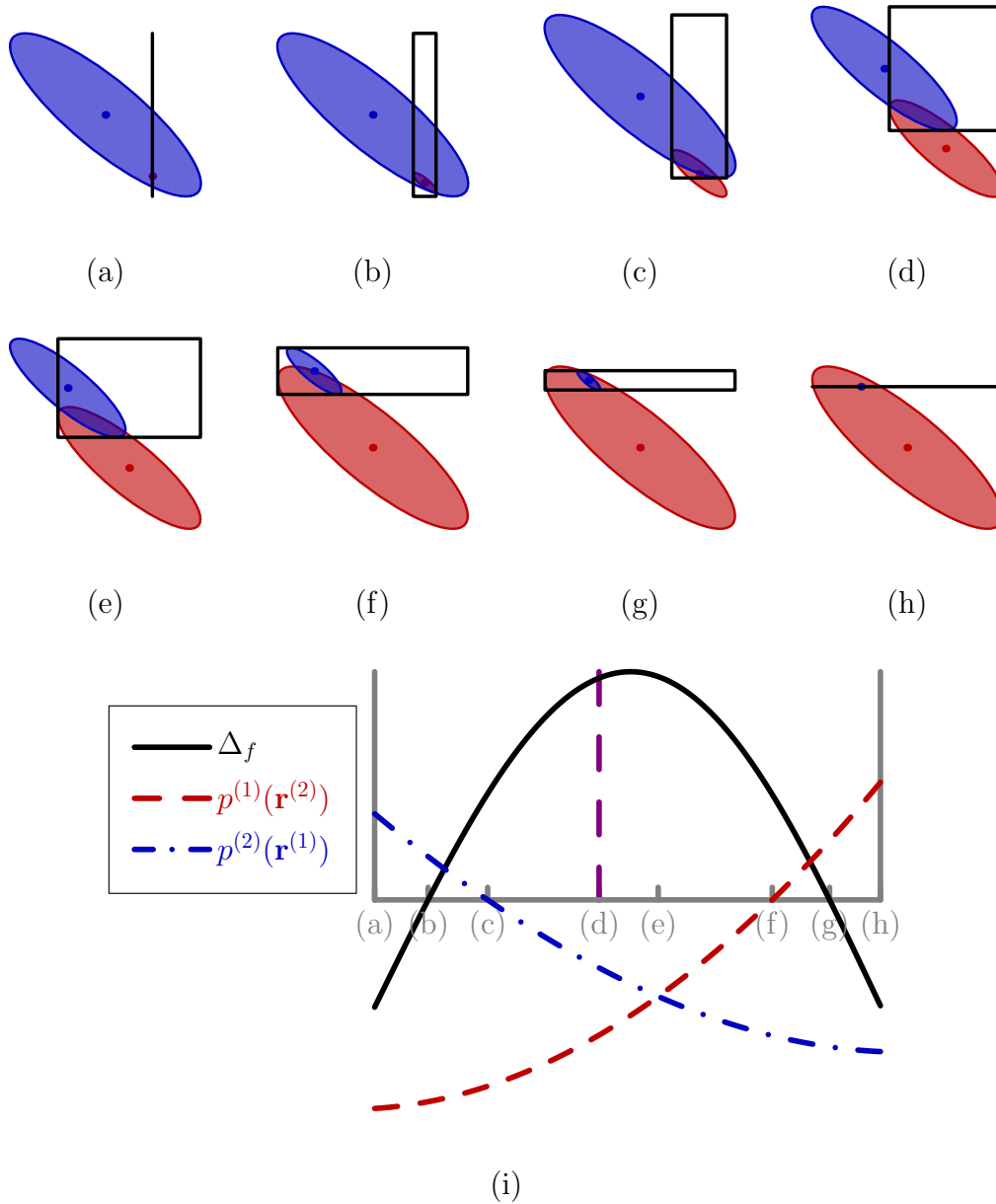


Figure 2.4. The rectangle $\mathcal{F}_{f,e}$ (outlined in black) and the sets $\mathcal{E}_f^{(1)}$ (in red) and $\mathcal{E}_f^{(2)}$ (in blue) are drawn for several test values. We took: (a) $f = f_{e,l} \approx 0.794$; (b) $f \approx 0.795$ (where $\Delta_f = 0$); (c) $f \approx 0.797$ (where $p_f^{(2)}(\mathbf{r}^{(1)}) = 0$); (d) $f = f^{(1)} = 0.80$; (e) $f \approx 0.802$ (intersection of $p_f^{(1)}(\mathbf{r}^{(2)})$ and $p_f^{(2)}(\mathbf{r}^{(1)})$); (f) $f \approx 0.805$ (where $p_f^{(1)}(\mathbf{r}^{(2)}) = 0$); (g) $f \approx 0.806$ (where $\Delta_f = 0$); (h) $f = f_{e,u} \approx 0.808$. (i) this is a plot of Δ_f (black solid line), $p_f^{(1)}(\mathbf{r}^{(2)})$ (red dashed line), and $p_f^{(2)}(\mathbf{r}^{(1)})$ (blue dash-dotted line) for $f \in \mathcal{A}_e = [f_{e,l}, f_{e,u}]$ (the horizontal gray line is the f -axis). The dashed magenta line represents the true volume fraction $f^{(1)}$. The parameters used to create this figure are the same as those in Figure 2.3. In this case we only recover the elementary bounds $0.794 \leq f^{(1)} \leq 0.808$.

Note that $\partial\mathcal{E}_f^{(1)}$ is tangent to the vertical segments of the black box and $\partial\mathcal{E}_f^{(2)}$ is tangent to the horizontal segments, as remarked after Lemma 2.3. In particular, at $f = f_{e,l}$ (Figure 2.4(a)), $\mathcal{E}_{f_{e,l}}^{(1)}$ is a point (represented by the red dot); at $f = f_{e,u}$ (Figure 2.4(h)), $\mathcal{E}_{f_{e,u}}^{(2)}$ is a point (represented by the blue dot). In Figure 2.4(i) we plot Δ_f (solid black line), $p_f^{(1)}(\mathbf{r}^{(2)})$ (red dashed line), and $p_f^{(2)}(\mathbf{r}^{(1)})$ (blue dash-dotted line) over the interval \mathcal{A}_e . The true volume fraction is represented by the magenta dashed line and the horizontal gray line represents the f -axis. Figure 2.4(i) shows that each $f \in \mathcal{A}_e$ is admissible; when $\Delta_f < 0$, we have either $p^{(2)}(\mathbf{r}^{(1)}) \geq 0$ and $p^{(1)}(\mathbf{r}^{(2)}) < 0$ (so $\mathcal{E}_f^{(1)} \subset \mathcal{E}_f^{(2)}$) or $p^{(1)}(\mathbf{r}^{(2)}) \geq 0$ and $p^{(2)}(\mathbf{r}^{(1)}) < 0$ (so $\mathcal{E}_f^{(2)} \subset \mathcal{E}_f^{(1)}$). Thus for each $f \in \mathcal{A}_e$ the set $\mathcal{F}_f = \mathcal{E}_f$ is nonempty and we conclude that $\mathcal{A} = \mathcal{A}_e$; in this example the bounds computed using the ellipses are no better than the elementary bounds. In the next section, we utilize two additional null Lagrangians to derive improved elementary bounds that hold in 2-D. We also develop similar “more sophisticated” bounds using elliptic disks; for the geometry sketched in Figure 2.3, these “more sophisticated” bounds are indeed stronger than the improved elementary bounds.

2.6 Additional Null Lagrangians in 2-D

In two dimensions we can include information from the additional null Lagrangians $\langle \mathbf{E}_1 \cdot R_\perp \mathbf{E}_2 \rangle$ and $\langle \mathbf{J}_1 \cdot R_\perp \mathbf{J}_2 \rangle$ — see (2.13). The details presented below are similar in nature to those in the previous two sections.

2.6.1 Improved Elementary Bounds

For arbitrary vectors $\mathbf{c}^{(\alpha)}, \mathbf{d}^{(\alpha)}$ in \mathbb{R}^2 and for $\alpha = 1, 2$ we define

$$\begin{aligned} \mathbf{h}^{(\alpha)}(\mathbf{x}; \mathbf{c}^{(\alpha)}, \mathbf{d}^{(\alpha)}) \equiv & \sum_{m=1}^2 c_m^{(\alpha)} \left[\mathbf{E}_m^{(\alpha)}(\mathbf{x}) - \frac{\chi^{(\alpha)}(\mathbf{x})}{f^{(\alpha)}} \langle \mathbf{E}_m^{(\alpha)} \rangle \right] \\ & + \sum_{n=1}^2 d_n^{(\alpha)} \left[R_\perp \mathbf{E}_n^{(\alpha)}(\mathbf{x}) - \frac{\chi^{(\alpha)}(\mathbf{x})}{f^{(\alpha)}} \langle R_\perp \mathbf{E}_n^{(\alpha)} \rangle \right]. \end{aligned} \quad (2.56)$$

For $\alpha = 1, 2$, and up to the constants $c_m^{(\alpha)}$ and $d_n^{(\alpha)}$, the field $\mathbf{h}^{(\alpha)}$ measures how the real and imaginary parts of the fields \mathbf{E} and $R_\perp \mathbf{E}$ vary around their average values over phase α . (The proof of this statement is exactly the same as that in the paragraph following (2.23).)

Note that $\langle \mathbf{h}^{(\alpha)} \rangle = 0$ (the proof is the same as the proof of the statement $\langle \mathbf{g}^{(\alpha)} \rangle = 0$ given in Section 2.3.2). We must have $\langle \mathbf{h}^{(\alpha)} \cdot \mathbf{h}^{(\alpha)} \rangle \geq 0$ for all $\mathbf{c}^{(\alpha)}, \mathbf{d}^{(\alpha)} \in \mathbb{R}^2$. Using computations similar to those in Section 2.3.2, one can show this is equivalent to

$$\mathbf{C}^{(\alpha)} \cdot M^{(\alpha)} \mathbf{C}^{(\alpha)} \geq 0, \quad (2.57)$$

where we have written

$$\mathbf{C}^{(\alpha)} \equiv \begin{bmatrix} \mathbf{c}^{(\alpha)} \\ \mathbf{d}^{(\alpha)} \end{bmatrix}$$

for arbitrary $\mathbf{c}^{(\alpha)}$ and $\mathbf{d}^{(\alpha)} \in \mathbb{R}^2$. For $\alpha = 1, 2$ the 4×4 matrix $M^{(\alpha)}$ is

$$M^{(\alpha)} \equiv \begin{bmatrix} S^{(\alpha)} & T^{(\alpha)} \\ -T^{(\alpha)} & S^{(\alpha)} \end{bmatrix},$$

where

$$T^{(\alpha)} \equiv \begin{bmatrix} B_{11}^{(\alpha)} - \frac{1}{f^{(\alpha)}} \langle \mathbf{E}_1^{(\alpha)} \rangle \cdot R_{\perp} \langle \mathbf{E}_1^{(\alpha)} \rangle & B_{12}^{(\alpha)} - \frac{1}{f^{(\alpha)}} \langle \mathbf{E}_1^{(\alpha)} \rangle \cdot R_{\perp} \langle \mathbf{E}_2^{(\alpha)} \rangle \\ B_{21}^{(\alpha)} - \frac{1}{f^{(\alpha)}} \langle \mathbf{E}_2^{(\alpha)} \rangle \cdot R_{\perp} \langle \mathbf{E}_1^{(\alpha)} \rangle & B_{22}^{(\alpha)} - \frac{1}{f^{(\alpha)}} \langle \mathbf{E}_2^{(\alpha)} \rangle \cdot R_{\perp} \langle \mathbf{E}_2^{(\alpha)} \rangle \end{bmatrix},$$

$$B_{mn}^{(\alpha)} \equiv \langle \chi^{(\alpha)} \mathbf{E}_m \cdot R_{\perp} \mathbf{E}_n \rangle = \langle \mathbf{E}_m^{(\alpha)} \cdot R_{\perp} \mathbf{E}_n^{(\alpha)} \rangle \quad (\text{for } m, n = 1, 2), \quad (2.58)$$

and R_{\perp} and $S^{(\alpha)}$ are as before (see (2.14) and (2.27), respectively). In particular, since $\langle \mathbf{h}^{(\alpha)} \cdot \mathbf{h}^{(\alpha)} \rangle \geq 0$ (2.57) implies

$$\mathbf{C}^{(\alpha)} \cdot M^{(\alpha)} \mathbf{C}^{(\alpha)} \geq 0 \quad \text{for all } \mathbf{C}^{(\alpha)} \in \mathbb{R}^4. \quad (2.59)$$

Because $\mathbf{w} \cdot R_{\perp} \mathbf{w} = 0$ for any vector $\mathbf{w} \in \mathbb{R}^2$, we have, for $m, \alpha = 1, 2$, that

$$T_{mm}^{(\alpha)} = \langle \mathbf{E}_m^{(\alpha)} \cdot R_{\perp} \mathbf{E}_m^{(\alpha)} \rangle - \frac{1}{f^{(\alpha)}} \langle \mathbf{E}_m^{(\alpha)} \rangle \cdot R_{\perp} \langle \mathbf{E}_m^{(\alpha)} \rangle = 0;$$

also, since $R_{\perp}^T = -R_{\perp}$ we have

$$\begin{aligned} T_{12}^{(\alpha)} &= B_{12}^{(\alpha)} - \frac{1}{f^{(\alpha)}} \langle \mathbf{E}_1^{(\alpha)} \rangle \cdot R_{\perp} \langle \mathbf{E}_2^{(\alpha)} \rangle \\ &= \langle \mathbf{E}_1^{(\alpha)} \cdot R_{\perp} \mathbf{E}_2^{(\alpha)} \rangle - \frac{1}{f^{(\alpha)}} \langle \mathbf{E}_1^{(\alpha)} \rangle \cdot R_{\perp} \langle \mathbf{E}_2^{(\alpha)} \rangle \\ &= -\langle R_{\perp} \mathbf{E}_1^{(\alpha)} \cdot \mathbf{E}_2^{(\alpha)} \rangle + \frac{1}{f^{(\alpha)}} R_{\perp} \langle \mathbf{E}_1^{(\alpha)} \rangle \cdot \langle \mathbf{E}_2^{(\alpha)} \rangle \\ &= -\left[B_{21}^{(\alpha)} - \frac{1}{f^{(\alpha)}} \langle \mathbf{E}_2^{(\alpha)} \rangle \cdot R_{\perp} \langle \mathbf{E}_1^{(\alpha)} \rangle \right] \\ &= -T_{21}^{(\alpha)}. \end{aligned}$$

Therefore $T^{(\alpha)}$ is antisymmetric for $\alpha = 1, 2$.

For $f \in \mathcal{A}_e$ we define

$$M_f^{(\alpha)}(x, y) \equiv \begin{bmatrix} S_f^{(\alpha)}(x, y) & T_f^{(\alpha)} \\ -T_f^{(\alpha)} & S_f^{(\alpha)}(x, y) \end{bmatrix}, \quad (2.60)$$

where $S_f^{(\alpha)}(x, y)$ is defined in (2.35),

$$T_f^{(\alpha)} = -[T_f^{(\alpha)}]^T = \begin{bmatrix} 0 & \sqrt{\tau_f^{(\alpha)}} \\ -\sqrt{\tau_f^{(\alpha)}} & 0 \end{bmatrix}$$

where

$$\tau_f^{(\alpha)} \equiv \det T_f^{(\alpha)} = \left[B_{12}^{(\alpha)} - \frac{1}{f_*} \langle \mathbf{E}_1^{(\alpha)} \rangle \cdot R_{\perp} \langle \mathbf{E}_2^{(\alpha)} \rangle \right]^2 \geq 0, \quad (2.61)$$

and f_* is defined in (2.50). Since $S_f^{(\alpha)}$ is symmetric for all $(x, y) \in \mathbb{R}^2$ and all $f \in (0, 1)$ and $T_f^{(\alpha)}$ is antisymmetric, $M_f^{(\alpha)}(x, y)$ is symmetric for $f \in \mathcal{A}_e$ and all $(x, y) \in \mathbb{R}^2$.

Next we apply the splitting method to $\langle \mathbf{E}_1 \cdot R_{\perp} \mathbf{E}_2 \rangle$ and $\langle \mathbf{J}_1 \cdot R_{\perp} \mathbf{J}_2 \rangle$ (see (2.30)).

This gives

$$\langle \mathbf{E}_1 \cdot R_{\perp} \mathbf{E}_2 \rangle = \langle \mathbf{E}_1^{(1)} \cdot R_{\perp} \mathbf{E}_2^{(1)} \rangle + \langle \mathbf{E}_1^{(2)} \cdot R_{\perp} \mathbf{E}_2^{(2)} \rangle = B_{12}^{(1)} + B_{12}^{(2)} \quad (2.62)$$

and

$$\begin{aligned} \langle \mathbf{J}_1 \cdot R_{\perp} \mathbf{J}_2 \rangle &= \langle \mathbf{J}_1^{(1)} \cdot R_{\perp} \mathbf{J}_2^{(1)} \rangle + \langle \mathbf{J}_1^{(2)} \cdot R_{\perp} \mathbf{J}_2^{(2)} \rangle \\ &= \sum_{\alpha=1}^2 \left\{ \left\langle \left[\sigma_1^{(\alpha)} \mathbf{E}_1^{(\alpha)} - \sigma_2^{(\alpha)} \mathbf{E}_2^{(\alpha)} \right] \cdot R_{\perp} \left[\sigma_2^{(\alpha)} \mathbf{E}_1^{(\alpha)} + \sigma_1^{(\alpha)} \mathbf{E}_2^{(\alpha)} \right] \right\rangle \right\} \\ &= \sum_{\alpha=1}^2 \left\{ \sigma_1^{(\alpha)} \sigma_2^{(\alpha)} \langle \mathbf{E}_1^{(\alpha)} \cdot R_{\perp} \mathbf{E}_1^{(\alpha)} \rangle + [\sigma_1^{(\alpha)}]^2 \langle \mathbf{E}_1^{(\alpha)} \cdot R_{\perp} \mathbf{E}_2^{(\alpha)} \rangle \right. \\ &\quad \left. - [\sigma_2^{(\alpha)}]^2 \langle \mathbf{E}_2^{(\alpha)} \cdot R_{\perp} \mathbf{E}_1^{(\alpha)} \rangle - \sigma_2^{(\alpha)} \sigma_1^{(\alpha)} \langle \mathbf{E}_2^{(\alpha)} \cdot R_{\perp} \mathbf{E}_2^{(\alpha)} \rangle \right\} \\ &= \sum_{\alpha=1}^2 \left\{ [\sigma_1^{(\alpha)}]^2 \langle \mathbf{E}_1^{(\alpha)} \cdot R_{\perp} \mathbf{E}_2^{(\alpha)} \rangle + [\sigma_2^{(\alpha)}]^2 \langle R_{\perp} \mathbf{E}_2^{(\alpha)} \cdot \mathbf{E}_1^{(\alpha)} \rangle \right\} \\ &= \sum_{\alpha=1}^2 \left\{ [\sigma_1^{(\alpha)}]^2 + [\sigma_2^{(\alpha)}]^2 \right\} \langle \mathbf{E}_1^{(\alpha)} \cdot R_{\perp} \mathbf{E}_2^{(\alpha)} \rangle \\ &= |\sigma^{(1)}|^2 B_{12}^{(1)} + |\sigma^{(2)}|^2 B_{12}^{(2)}. \end{aligned} \quad (2.63)$$

Combining (2.62) and (2.63) gives the system

$$\begin{bmatrix} 1 & 1 \\ |\sigma^{(1)}|^2 & |\sigma^{(2)}|^2 \end{bmatrix} \begin{bmatrix} B_{12}^{(1)} \\ B_{12}^{(2)} \end{bmatrix} = \begin{bmatrix} \langle \mathbf{E}_1 \cdot R_{\perp} \mathbf{E}_2 \rangle \\ \langle \mathbf{J}_1 \cdot R_{\perp} \mathbf{J}_2 \rangle \end{bmatrix}.$$

As long as $|\sigma^{(1)}| \neq |\sigma^{(2)}|$, we can solve this system for $B_{12}^{(1)}$ and $B_{12}^{(2)}$; in that case

$$\begin{bmatrix} B_{12}^{(1)} \\ B_{12}^{(2)} \end{bmatrix} = \frac{1}{|\sigma^{(2)}|^2 - |\sigma^{(1)}|^2} \begin{bmatrix} |\sigma^{(2)}|^2 \langle \mathbf{E}_1 \cdot R_{\perp} \mathbf{E}_2 \rangle - \langle \mathbf{J}_1 \cdot R_{\perp} \mathbf{J}_2 \rangle \\ -|\sigma^{(1)}|^2 \langle \mathbf{E}_1 \cdot R_{\perp} \mathbf{E}_2 \rangle + \langle \mathbf{J}_1 \cdot R_{\perp} \mathbf{J}_2 \rangle \end{bmatrix} \quad (2.64)$$

and $B_{12}^{(1)}$ and $B_{12}^{(2)}$ (hence $T_f^{(1)}$ and $T_f^{(2)}$) are known.

Definition 2.4 For $f \in \mathcal{A}_e$ we set

$$\widetilde{\mathcal{F}}_f^{(\alpha)} \equiv \{(x, y) \in \mathbb{R}^2 : M_f^{(\alpha)}(x, y) \text{ is positive-semidefinite}\}.$$

Then the set $\widetilde{\mathcal{F}}_f \equiv \widetilde{\mathcal{F}}_f^{(1)} \cap \widetilde{\mathcal{F}}_f^{(2)}$ is called the restricted feasible region associated with f . In addition, the set $\widetilde{\mathcal{A}} \equiv \{f \in \mathcal{A}_e : \widetilde{\mathcal{F}}_f \neq \emptyset\}$ is called the restricted set of admissible test values.

To find the set $\widetilde{\mathcal{A}}$, we need to find the values of $f \in \mathcal{A}_e$ such that there is at least one point $(x, y) \in \mathbb{R}^2$ at which both $M_f^{(1)}(x, y)$ and $M_f^{(2)}(x, y)$ are simultaneously positive-semidefinite. We will see that $\widetilde{\mathcal{A}} \subseteq \mathcal{A}$, so the bounds in this section are in general tighter than those in the previous sections.

Lemma 2.5 Assume $\beta \neq 0$, $\eta^{(\alpha)} \neq 0$ for $\alpha = 1, 2$, $f_{e,l} \neq 0$, $f_{e,u} \neq 1$, and $|\sigma^{(1)}| \neq |\sigma^{(2)}|$. Then for $f \in \mathcal{A}_e$ and $\alpha = 1, 2$, the matrix $M_f^{(\alpha)}(x, y)$ defined in (2.60) is positive-semidefinite if and only if $p_f^{(\alpha)}(x, y) = \det S_f^{(\alpha)}(x, y) \geq \tau_f^{(\alpha)}$, where $\tau_f^{(\alpha)}$ is defined in (2.61).

Proof of Lemma 2.5: Recall that a symmetric matrix is positive-semidefinite if and only if all of its eigenvalues are nonnegative. For $\alpha = 1, 2$ the eigenvalues of $M_f^{(\alpha)}$, each with algebraic multiplicity 2, are

$$\lambda_{f,\pm}^{(\alpha)}(x, y) = \frac{1}{2} \left\{ \text{Tr } S_f^{(\alpha)} \pm \sqrt{[\text{Tr } S_f^{(\alpha)}]^2 - 4[\det S_f^{(\alpha)} - \det T_f^{(\alpha)}]} \right\}. \quad (2.65)$$

(We have suppressed the dependence on x and y on the right-hand side for clarity.)

By (2.35) and (2.41),

$$\text{Tr } S_f^{(\alpha)}(x, y) = \eta^{(\alpha)} - \frac{\|\mathbf{E}_1^{(\alpha)}\|^2 + \|\mathbf{E}_2^{(\alpha)}\|^2}{f_*}$$

is independent of x and y and is nonnegative if and only if $f \in \mathcal{A}_e$. We note that the expression under the square root in (2.65) must be nonnegative for all points $(x, y) \in \mathbb{R}^2$ and all $f \in \mathcal{A}_e$ since $M_f^{(\alpha)}(x, y)$ is symmetric for all such values of x, y , and f .

The previous paragraph implies that the eigenvalues $\lambda_{f,\pm}^{(\alpha)}(x, y)$ will be nonnegative for those points $(x, y) \in \mathbb{R}^2$ and those values of $f \in \mathcal{A}_e$ for which

$$4 \left[\det S_f^{(\alpha)}(x, y) - \det T_f^{(\alpha)} \right] \geq 0 \Leftrightarrow \det S_f^{(\alpha)}(x, y) \geq \tau_f^{(\alpha)}.$$

This completes the proof.

Now $p_f^{(\alpha)} \geq \tau_f^{(\alpha)}$ if and only if $\tilde{p}_f^{(\alpha)} \geq 0$, where $\tilde{p}_f^{(\alpha)} \equiv p_f^{(\alpha)} - \tau_f^{(\alpha)}$. Using calculus (i.e., setting the gradient of $\tilde{p}_f^{(\alpha)}(x, y)$ equal to 0 and solving for (x, y)) we find that

$$\begin{aligned} \tilde{p}_{f,\max}^{(\alpha)} &\equiv \max_{(x,y) \in \mathbb{R}^2} \tilde{p}_f^{(\alpha)}(x, y) \\ &= \tilde{p}_f^{(\alpha)}(\bar{x}_f^{(\alpha)}, \bar{y}_f^{(\alpha)}) \\ &= \frac{1}{4f_*^2} \left[\langle \|\mathbf{v}_+^{(\alpha)}\|^2 \rangle f_* - \|\langle \mathbf{v}_+^{(\alpha)} \rangle\|^2 \right] \left[\langle \|\mathbf{v}_-^{(\alpha)}\|^2 \rangle f_* - \|\langle \mathbf{v}_-^{(\alpha)} \rangle\|^2 \right], \end{aligned} \quad (2.66)$$

where f_* is defined in (2.50), the point $(\bar{x}_f^{(\alpha)}, \bar{y}_f^{(\alpha)})$ is defined in (2.48), and

$$\mathbf{v}_{\pm}^{(\alpha)} \equiv \chi^{(\alpha)} (\mathbf{E}_1 \pm R_{\perp} \mathbf{E}_2) = \mathbf{E}_1^{(\alpha)} \pm R_{\perp} \mathbf{E}_2^{(\alpha)}.$$

Note that $\langle \mathbf{v}_{\pm}^{(\alpha)} \rangle = \langle \mathbf{E}_1^{(\alpha)} \rangle \pm R_{\perp} \langle \mathbf{E}_2^{(\alpha)} \rangle$ is known (by the statement following (2.31)).

Also, by (2.37) and the fact that R_{\perp} is unitary (so it preserves lengths), the quantity

$$\begin{aligned} \langle \|\mathbf{v}_{\pm}^{(\alpha)}\|^2 \rangle &= \langle \mathbf{v}_{\pm}^{(\alpha)} \cdot \mathbf{v}_{\pm}^{(\alpha)} \rangle \\ &= \langle \mathbf{E}_1^{(\alpha)} \cdot \mathbf{E}_1^{(\alpha)} \rangle \pm \langle \mathbf{E}_1^{(\alpha)} \cdot R_{\perp} \mathbf{E}_2^{(\alpha)} \rangle \pm \langle R_{\perp} \mathbf{E}_2^{(\alpha)} \cdot \mathbf{E}_1^{(\alpha)} \rangle + \langle R_{\perp} \mathbf{E}_2^{(\alpha)} \cdot R_{\perp} \mathbf{E}_2^{(\alpha)} \rangle \\ &= \langle \|\mathbf{E}_1^{(\alpha)}\|^2 \rangle \pm 2 \langle \mathbf{E}_1^{(\alpha)} \cdot R_{\perp} \mathbf{E}_2^{(\alpha)} \rangle + \langle \|\mathbf{E}_2^{(\alpha)}\|^2 \rangle \\ &= \langle \|\mathbf{E}_1^{(\alpha)}\|^2 \rangle + \langle \|\mathbf{E}_2^{(\alpha)}\|^2 \rangle \pm 2B_{12}^{(\alpha)} \\ &= \eta^{(\alpha)} \pm 2B_{12}^{(\alpha)} \end{aligned}$$

is known if and only if $|\sigma^{(1)}| \neq |\sigma^{(2)}|$ (by (2.36) and (2.64)). For now we assume that $\mathbf{v}_{\pm}^{(\alpha)} \not\equiv 0$ and $\eta^{(\alpha)} \neq 0$ (physically, this means that we assume that the real

and imaginary parts of the electric field are nonperpendicular and nonzero in both phases). Also notice that

$$\begin{aligned}
\|\langle \mathbf{v}_{\pm}^{(\alpha)} \rangle\|^2 &= [\langle \mathbf{E}_1^{(\alpha)} \rangle \pm R_{\perp} \langle \mathbf{E}_2^{(\alpha)} \rangle] \cdot [\langle \mathbf{E}_1^{(\alpha)} \rangle \pm R_{\perp} \langle \mathbf{E}_2^{(\alpha)} \rangle] \\
&= \|\langle \mathbf{E}_1^{(\alpha)} \rangle\|^2 \pm [\langle \mathbf{E}_1^{(\alpha)} \rangle \cdot R_{\perp} \langle \mathbf{E}_2^{(\alpha)} \rangle] \pm [R_{\perp} \langle \mathbf{E}_2^{(\alpha)} \rangle \cdot \langle \mathbf{E}_1^{(\alpha)} \rangle] + \|R_{\perp} \langle \mathbf{E}_2^{(\alpha)} \rangle\|^2 \\
&= \|\langle \mathbf{E}_1^{(\alpha)} \rangle\|^2 + \|\langle \mathbf{E}_2^{(\alpha)} \rangle\|^2 \pm 2[\langle \mathbf{E}_1^{(\alpha)} \rangle \cdot R_{\perp} \langle \mathbf{E}_2^{(\alpha)} \rangle].
\end{aligned}$$

This and (2.42) and (2.58) imply that

$$\begin{cases} \eta^{(1)} f_{e,l} \pm 2\langle \mathbf{E}_1^{(1)} \rangle \cdot R_{\perp} \langle \mathbf{E}_2^{(1)} \rangle & \text{if } \alpha = 1, \\ \eta^{(2)} (1 - f_{e,u}) \pm 2\langle \mathbf{E}_1^{(2)} \rangle \cdot R_{\perp} \langle \mathbf{E}_2^{(2)} \rangle & \text{if } \alpha = 2. \end{cases}$$

We now show that $\tilde{p}_{f,\max}^{(\alpha)} < 0$ on a subset of \mathcal{A}_e ; such values of f are not admissible by Lemma 2.5. Due to (2.66), $\tilde{p}_{f,\max}^{(1)} \geq 0$ if and only if

$$\begin{aligned}
\langle \|\mathbf{v}_+^{(1)}\|^2 \rangle f - \|\langle \mathbf{v}_+^{(1)} \rangle\|^2 &\geq 0 \quad \text{and} \quad \langle \|\mathbf{v}_-^{(1)}\|^2 \rangle f - \|\langle \mathbf{v}_-^{(1)} \rangle\|^2 \geq 0 \\
\Leftrightarrow f &\geq \frac{\|\langle \mathbf{v}_+^{(1)} \rangle\|^2}{\langle \|\mathbf{v}_+^{(1)}\|^2 \rangle} \quad \text{and} \quad f \geq \frac{\|\langle \mathbf{v}_-^{(1)} \rangle\|^2}{\langle \|\mathbf{v}_-^{(1)}\|^2 \rangle} \\
\Leftrightarrow f &\geq \tilde{f}_{e,l} \equiv \max \left\{ \frac{\|\langle \mathbf{v}_+^{(1)} \rangle\|^2}{\langle \|\mathbf{v}_+^{(1)}\|^2 \rangle}, \frac{\|\langle \mathbf{v}_-^{(1)} \rangle\|^2}{\langle \|\mathbf{v}_-^{(1)}\|^2 \rangle} \right\}, \tag{2.67}
\end{aligned}$$

or

$$\begin{aligned}
\langle \|\mathbf{v}_+^{(1)}\|^2 \rangle f - \|\langle \mathbf{v}_+^{(1)} \rangle\|^2 &\leq 0 \quad \text{and} \quad \langle \|\mathbf{v}_-^{(1)}\|^2 \rangle f - \|\langle \mathbf{v}_-^{(1)} \rangle\|^2 \leq 0 \\
\Leftrightarrow f &\leq \frac{\|\langle \mathbf{v}_+^{(1)} \rangle\|^2}{\langle \|\mathbf{v}_+^{(1)}\|^2 \rangle} \quad \text{and} \quad f \leq \frac{\|\langle \mathbf{v}_-^{(1)} \rangle\|^2}{\langle \|\mathbf{v}_-^{(1)}\|^2 \rangle} \\
\Leftrightarrow f &\leq Q^{(1)} \equiv \min \left\{ \frac{\|\langle \mathbf{v}_+^{(1)} \rangle\|^2}{\langle \|\mathbf{v}_+^{(1)}\|^2 \rangle}, \frac{\|\langle \mathbf{v}_-^{(1)} \rangle\|^2}{\langle \|\mathbf{v}_-^{(1)}\|^2 \rangle} \right\}. \tag{2.68}
\end{aligned}$$

The denominators in (2.67) and (2.68) are positive since we are assuming $\mathbf{v}_{\pm}^{(1)} \neq 0$, which implies $\langle \|\mathbf{v}_{\pm}^{(1)}\|^2 \rangle \neq 0$. We explicitly compute $Q^{(1)}$ and $\tilde{f}_{e,l}$ in the following lemma.

Lemma 2.6 Suppose $\beta \neq 0$, $\eta^{(\alpha)} \neq 0$ for $\alpha = 1, 2$, $f_{e,l} \neq 0$, $f_{e,u} \neq 1$, $|\sigma^{(1)}| \neq |\sigma^{(2)}|$, and $\mathbf{v}_{\pm}^{(\alpha)} \neq 0$ for $\alpha = 1, 2$. Then $Q^{(1)} \leq f_{e,l} \leq \tilde{f}_{e,l}$,

$$\tilde{f}_{e,l} = \begin{cases} \frac{\|\langle \mathbf{v}_+^{(1)} \rangle\|^2}{\langle \|\mathbf{v}_+^{(1)}\|^2 \rangle} & \text{if } \langle \mathbf{E}_1^{(1)} \rangle \cdot R_{\perp} \langle \mathbf{E}_2^{(1)} \rangle > B_{12}^{(1)} f_{e,l}, \\ \frac{\|\langle \mathbf{v}_-^{(1)} \rangle\|^2}{\langle \|\mathbf{v}_-^{(1)}\|^2 \rangle} & \text{if } \langle \mathbf{E}_1^{(1)} \rangle \cdot R_{\perp} \langle \mathbf{E}_2^{(1)} \rangle < B_{12}^{(1)} f_{e,l}, \\ \frac{\|\langle \mathbf{v}_+^{(1)} \rangle\|^2}{\langle \|\mathbf{v}_+^{(1)}\|^2 \rangle} = \frac{\|\langle \mathbf{v}_-^{(1)} \rangle\|^2}{\langle \|\mathbf{v}_-^{(1)}\|^2 \rangle} & \text{if } \langle \mathbf{E}_1^{(1)} \rangle \cdot R_{\perp} \langle \mathbf{E}_2^{(1)} \rangle = B_{12}^{(1)} f_{e,l}, \end{cases} \quad (2.69)$$

and

$$Q^{(1)} = \begin{cases} \frac{\|\langle \mathbf{v}_-^{(1)} \rangle\|^2}{\langle \|\mathbf{v}_-^{(1)}\|^2 \rangle} & \text{if } \langle \mathbf{E}_1^{(1)} \rangle \cdot R_{\perp} \langle \mathbf{E}_2^{(1)} \rangle > B_{12}^{(1)} f_{e,l}, \\ \frac{\|\langle \mathbf{v}_+^{(1)} \rangle\|^2}{\langle \|\mathbf{v}_+^{(1)}\|^2 \rangle} & \text{if } \langle \mathbf{E}_1^{(1)} \rangle \cdot R_{\perp} \langle \mathbf{E}_2^{(1)} \rangle < B_{12}^{(1)} f_{e,l}, \\ \frac{\|\langle \mathbf{v}_+^{(1)} \rangle\|^2}{\langle \|\mathbf{v}_+^{(1)}\|^2 \rangle} = \frac{\|\langle \mathbf{v}_-^{(1)} \rangle\|^2}{\langle \|\mathbf{v}_-^{(1)}\|^2 \rangle} & \text{if } \langle \mathbf{E}_1^{(1)} \rangle \cdot R_{\perp} \langle \mathbf{E}_2^{(1)} \rangle = B_{12}^{(1)} f_{e,l}. \end{cases} \quad (2.70)$$

Proof of Lemma 2.6: We have the following inequalities:

$$\begin{aligned} \frac{\|\langle \mathbf{v}_+^{(1)} \rangle\|^2}{\langle \|\mathbf{v}_+^{(1)}\|^2 \rangle} &= \frac{\eta^{(1)} f_{e,l} + 2 \langle \mathbf{E}_1^{(1)} \rangle \cdot R_{\perp} \langle \mathbf{E}_2^{(1)} \rangle}{\eta^{(1)} + 2B_{12}^{(1)}} \geq f_{e,l} \\ &\Leftrightarrow \langle \mathbf{E}_1^{(1)} \rangle \cdot R_{\perp} \langle \mathbf{E}_2^{(1)} \rangle \geq B_{12}^{(1)} f_{e,l}; \end{aligned} \quad (2.71a)$$

$$\begin{aligned} \frac{\|\langle \mathbf{v}_-^{(1)} \rangle\|^2}{\langle \|\mathbf{v}_-^{(1)}\|^2 \rangle} &= \frac{\eta^{(1)} f_{e,l} - 2 \langle \mathbf{E}_1^{(1)} \rangle \cdot R_{\perp} \langle \mathbf{E}_2^{(1)} \rangle}{\eta^{(1)} - 2B_{12}^{(1)}} \leq f_{e,l} \\ &\Leftrightarrow \langle \mathbf{E}_1^{(1)} \rangle \cdot R_{\perp} \langle \mathbf{E}_2^{(1)} \rangle \geq B_{12}^{(1)} f_{e,l}. \end{aligned} \quad (2.71b)$$

Taking (2.67) and (2.68) into account, (2.71) implies $Q^{(1)} \leq f_{e,l} \leq \tilde{f}_{e,l}$ with equality in both inequalities if and only if $\langle \mathbf{E}_1^{(1)} \rangle \cdot R_{\perp} \langle \mathbf{E}_2^{(1)} \rangle = B_{12}^{(1)} f_{e,l}$. In addition, (2.69) and (2.70) follow from the inequalities (2.71) in combination with (2.67) and (2.68). This completes the proof.

Since $Q^{(1)} \leq f_{e,l} \leq \tilde{f}_{e,l}$, the inequality in (2.68) will not be satisfied for all $f \geq f_{e,l}$ and can safely be ignored. Moreover, we will have the chain of equalities $Q^{(1)} = f_{e,l} = \tilde{f}_{e,l}$ if and only if

$$\langle \mathbf{E}_1^{(1)} \rangle \cdot R_{\perp} \langle \mathbf{E}_2^{(1)} \rangle = B_{12}^{(1)} f_{e,l}. \quad (2.72)$$

If $\mathbf{E}^{(1)}$ is a (nonzero) constant such that $\mathbf{E}_1^{(1)} \cdot R_\perp \mathbf{E}_2^{(1)} \neq 0$, then (2.72) becomes $f_{e,l} = f^{(1)}$, which is consistent with our work in Section 2.4. To see this, note that if $\mathbf{E}^{(1)}$ is a constant then the left-hand side of (2.72) is

$$\begin{aligned} \langle \mathbf{E}_1^{(1)} \rangle \cdot R_\perp \langle \mathbf{E}_2^{(1)} \rangle &= \left[\frac{1}{|\Omega|} \int_\Omega \chi^{(1)}(\mathbf{x}) \mathbf{E}_1 d\mathbf{x} \right] \cdot R_\perp \left[\frac{1}{|\Omega|} \int_\Omega \chi^{(1)}(\mathbf{x}) \mathbf{E}_2 d\mathbf{x} \right] \\ &= [\langle \chi^{(1)} \rangle]^2 [\mathbf{E}_1^{(1)} \cdot R_\perp \mathbf{E}_2^{(1)}] \\ &= [f^{(1)}]^2 [\mathbf{E}_1^{(1)} \cdot R_\perp \mathbf{E}_2^{(1)}], \end{aligned} \quad (2.73)$$

while the right-hand side of (2.72) is

$$\begin{aligned} B_{12}^{(1)} f_{e,l} &= \langle \chi^{(1)} \mathbf{E}_1 \cdot R_\perp \mathbf{E}_2 \rangle f_{e,l} \\ &= f_{e,l} \langle \chi^{(1)} \rangle [\mathbf{E}_1^{(1)} \cdot R_\perp \mathbf{E}_2^{(1)}] \\ &= f_{e,l} f^{(1)} [\mathbf{E}_1^{(1)} \cdot R_\perp \mathbf{E}_2^{(1)}]. \end{aligned} \quad (2.74)$$

As long as $\mathbf{E}_1^{(1)} \cdot R_\perp \mathbf{E}_2^{(1)} \neq 0$, the desired result follows by comparing (2.73) and (2.74).

The above computations are summarized in Figure 2.5, which is a plot of the functions $\tilde{p}_{f,\max}^{(\alpha)}$ as a function of f . The function $\tilde{p}_{f,\max}^{(1)}$ is plotted as a red solid curve. If (2.72) does not hold, its zeros $Q^{(1)}$ and $\tilde{f}_{e,l}$ are below and above the elementary lower bound $f_{e,l}$, respectively. Thus all values of $f \in [f_{e,l}, \tilde{f}_{e,l})$ are not admissible, giving us the improved elementary lower bound $\tilde{f}_{e,l} \leq f^{(1)}$. If (2.72) holds, then $Q^{(1)} = \tilde{f}_{e,l} = f_{e,l}$, and we do not obtain an improved elementary lower bound. In Figure 2.5, $f_{e,l}$ is indicated with the left gray vertical line while $\tilde{f}_{e,l}$ is indicated by the left black vertical line.

Due to (2.66), $\tilde{p}_{f,\max}^{(2)} \geq 0$ if and only if

$$\begin{aligned} \langle \|\mathbf{v}_+^{(2)}\|^2 \rangle (1-f) - \langle \mathbf{v}_+^{(2)} \rangle \|^2 &\geq 0 \quad \text{and} \quad \langle \|\mathbf{v}_-^{(2)}\|^2 \rangle (1-f) - \langle \mathbf{v}_-^{(2)} \rangle \|^2 \geq 0 \\ \Leftrightarrow \quad f &\leq 1 - \frac{\langle \langle \mathbf{v}_+^{(2)} \rangle \rangle^2}{\langle \|\mathbf{v}_+^{(2)}\|^2 \rangle} \quad \text{and} \quad f \leq 1 - \frac{\langle \langle \mathbf{v}_-^{(2)} \rangle \rangle^2}{\langle \|\mathbf{v}_-^{(2)}\|^2 \rangle} \\ \Leftrightarrow \quad f &\leq \tilde{f}_{e,u} \equiv \min \left\{ 1 - \frac{\langle \langle \mathbf{v}_+^{(2)} \rangle \rangle^2}{\langle \|\mathbf{v}_+^{(2)}\|^2 \rangle}, 1 - \frac{\langle \langle \mathbf{v}_-^{(2)} \rangle \rangle^2}{\langle \|\mathbf{v}_-^{(2)}\|^2 \rangle} \right\} \end{aligned} \quad (2.75)$$

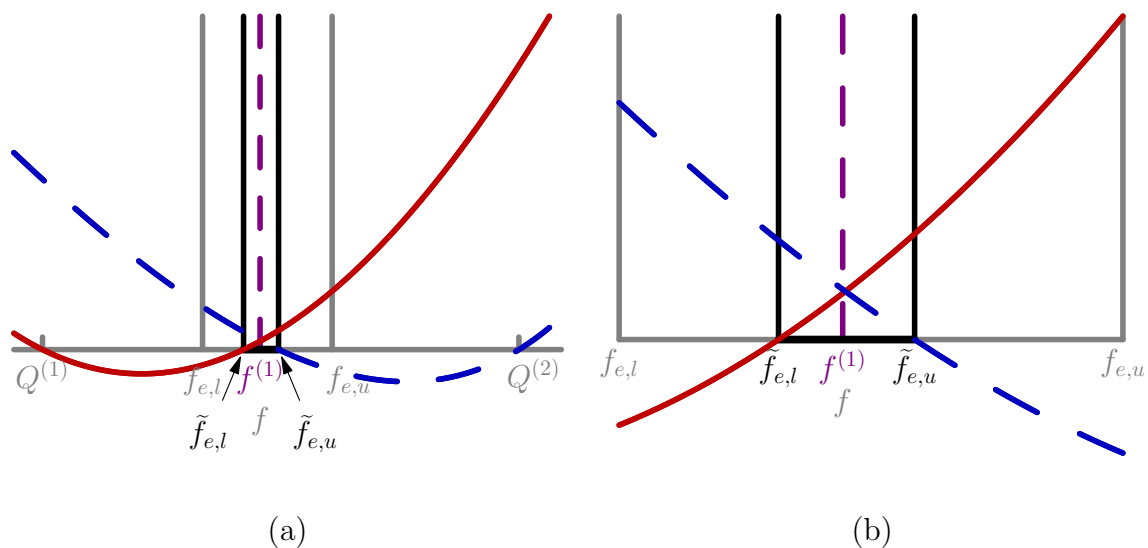


Figure 2.5. These are plots of the improved elementary bounds in 2-D. (a) A plot of $\tilde{p}_{f,\max}^{(1)}$ (red solid curve) and $\tilde{p}_{f,\max}^{(2)}$ (blue dashed curve) — the horizontal gray line represents the f -axis. The geometry and parameters used to create these plots are the same as those used to create Figure 2.3. (b) A zoomed-in version of (a) — here we plot the functions over the interval $[f_{e,l}, f_{e,u}]$. In both figures the set $\tilde{A}_e = [\tilde{f}_{e,l}, \tilde{f}_{e,u}]$ is highlighted by the darkened interval. Some relevant numbers are $f_{e,l} \approx 0.794$, $f_{e,u} \approx 0.808$, $\tilde{f}_{e,l} \approx 0.798$, $\tilde{f}_{e,u} \approx 0.802$, $Q^{(1)} \approx 0.776$, $Q^{(2)} \approx 0.828$, and $f^{(1)} = 0.8$. So we obtain the better bounds $0.798 \leq f^{(1)} \leq 0.802$.

or

$$\begin{aligned}
& \langle \|\mathbf{v}_+^{(2)}\|^2 \rangle (1-f) - \|\langle \mathbf{v}_+^{(2)} \rangle\|^2 \leq 0 \quad \text{and} \quad \langle \|\mathbf{v}_-^{(2)}\|^2 \rangle (1-f) - \|\langle \mathbf{v}_-^{(2)} \rangle\|^2 \leq 0 \\
& \Leftrightarrow \quad f \geq 1 - \frac{\|\langle \mathbf{v}_+^{(2)} \rangle\|^2}{\langle \|\mathbf{v}_+^{(2)}\|^2 \rangle} \quad \text{and} \quad f \geq 1 - \frac{\|\langle \mathbf{v}_-^{(2)} \rangle\|^2}{\langle \|\mathbf{v}_-^{(2)}\|^2 \rangle} \\
& \Leftrightarrow \quad f \geq Q^{(2)} \equiv \max \left\{ 1 - \frac{\|\langle \mathbf{v}_+^{(2)} \rangle\|^2}{\langle \|\mathbf{v}_+^{(2)}\|^2 \rangle}, 1 - \frac{\|\langle \mathbf{v}_-^{(2)} \rangle\|^2}{\langle \|\mathbf{v}_-^{(2)}\|^2 \rangle} \right\}. \quad (2.76)
\end{aligned}$$

Since we are assuming $\mathbf{v}_\pm^{(2)} \neq 0$, $\langle \|\mathbf{v}_\pm^{(2)}\|^2 \rangle \neq 0$; thus the denominators in (2.75) and (2.76) are positive. We explicitly compute $Q^{(2)}$ and $\tilde{f}_{e,u}$ in the following lemma.

Lemma 2.7 *Suppose $\beta \neq 0$, $\eta^{(\alpha)} \neq 0$ for $\alpha = 1, 2$, $f_{e,l} \neq 0$, $f_{e,u} \neq 1$, $|\sigma^{(1)}| \neq |\sigma^{(2)}|$, and $\mathbf{v}_\pm^{(\alpha)} \neq 0$ for $\alpha = 1, 2$. Then $\tilde{f}_{e,u} \leq f_{e,u} \leq Q^{(2)}$,*

$$\tilde{f}_{e,u} = \begin{cases} 1 - \frac{\|\langle \mathbf{v}_+^{(2)} \rangle\|^2}{\langle \|\mathbf{v}_+^{(2)}\|^2 \rangle} & \text{if } \langle \mathbf{E}_1^{(2)} \rangle \cdot R_\perp \langle \mathbf{E}_2^{(2)} \rangle > B_{12}^{(2)}(1 - f_{e,u}), \\ 1 - \frac{\|\langle \mathbf{v}_-^{(2)} \rangle\|^2}{\langle \|\mathbf{v}_-^{(2)}\|^2 \rangle} & \text{if } \langle \mathbf{E}_1^{(2)} \rangle \cdot R_\perp \langle \mathbf{E}_2^{(2)} \rangle < B_{12}^{(2)}(1 - f_{e,u}), \\ 1 - \frac{\|\langle \mathbf{v}_+^{(2)} \rangle\|^2}{\langle \|\mathbf{v}_+^{(2)}\|^2 \rangle} = 1 - \frac{\|\langle \mathbf{v}_-^{(2)} \rangle\|^2}{\langle \|\mathbf{v}_-^{(2)}\|^2 \rangle} & \text{if } \langle \mathbf{E}_1^{(2)} \rangle \cdot R_\perp \langle \mathbf{E}_2^{(2)} \rangle = B_{12}^{(2)}(1 - f_{e,u}), \end{cases} \quad (2.77)$$

and

$$Q^{(2)} = \begin{cases} 1 - \frac{\|\langle \mathbf{v}_-^{(2)} \rangle\|^2}{\langle \|\mathbf{v}_-^{(2)}\|^2 \rangle} & \text{if } \langle \mathbf{E}_1^{(2)} \rangle \cdot R_\perp \langle \mathbf{E}_2^{(2)} \rangle > B_{12}^{(2)}(1 - f_{e,u}), \\ 1 - \frac{\|\langle \mathbf{v}_+^{(2)} \rangle\|^2}{\langle \|\mathbf{v}_+^{(2)}\|^2 \rangle} & \text{if } \langle \mathbf{E}_1^{(2)} \rangle \cdot R_\perp \langle \mathbf{E}_2^{(2)} \rangle < B_{12}^{(2)}(1 - f_{e,u}), \\ 1 - \frac{\|\langle \mathbf{v}_+^{(2)} \rangle\|^2}{\langle \|\mathbf{v}_+^{(2)}\|^2 \rangle} = 1 - \frac{\|\langle \mathbf{v}_-^{(2)} \rangle\|^2}{\langle \|\mathbf{v}_-^{(2)}\|^2 \rangle} & \text{if } \langle \mathbf{E}_1^{(2)} \rangle \cdot R_\perp \langle \mathbf{E}_2^{(2)} \rangle = B_{12}^{(2)}(1 - f_{e,u}). \end{cases} \quad (2.78)$$

Proof of Lemma 2.7: The proof of Lemma 2.7 is similar to the proof of Lemma 2.6.

This completes the proof.

Since $\tilde{f}_{e,u} \leq f_{e,u} \leq Q^{(2)}$, the inequality in (2.76) will not be satisfied for $f \leq f_{e,u}$ so it can be ignored. We will have the chain of equalities $\tilde{f}_{e,u} = f_{e,u} = Q^{(2)}$ if and only if

$$\langle \mathbf{E}_1^{(2)} \rangle \cdot R_\perp \langle \mathbf{E}_2^{(2)} \rangle = B_{12}^{(2)}(1 - f_{e,u}). \quad (2.79)$$

If $\mathbf{E}^{(2)}$ is a (nonzero) constant such that $\mathbf{E}_1^{(2)} \cdot R_\perp \mathbf{E}_2^{(2)} \neq 0$, then (2.79) becomes $f_{e,u} = f^{(1)}$, which is consistent with our work in Section 2.4. To see this, note that if $\mathbf{E}^{(2)}$ is a constant then the left-hand side of (2.79) is

$$\begin{aligned} \langle \mathbf{E}_1^{(2)} \rangle \cdot R_\perp \langle \mathbf{E}_2^{(2)} \rangle &= \left[\frac{1}{|\Omega|} \int_\Omega \chi^{(2)}(\mathbf{x}) \mathbf{E}_1 d\mathbf{x} \right] \cdot R_\perp \left[\frac{1}{|\Omega|} \int_\Omega \chi^{(2)}(\mathbf{x}) \mathbf{E}_2 d\mathbf{x} \right] \\ &= [\langle \chi^{(2)} \rangle]^2 [\mathbf{E}_1^{(2)} \cdot R_\perp \mathbf{E}_2^{(2)}] \\ &= [1 - f^{(1)}]^2 [\mathbf{E}_1^{(2)} \cdot R_\perp \mathbf{E}_2^{(2)}], \end{aligned}$$

while the right-hand side of (2.79) is

$$\begin{aligned} B_{12}^{(2)}(1 - f_{e,u}) &= \langle \chi^{(2)} \mathbf{E}_1 \cdot R_\perp \mathbf{E}_2 \rangle (1 - f_{e,u}) \\ &= (1 - f_{e,u}) \langle \chi^{(2)} \rangle [\mathbf{E}_1^{(2)} \cdot R_\perp \mathbf{E}_2^{(2)}] \\ &= (1 - f_{e,u})(1 - f^{(1)}) [\mathbf{E}_1^{(2)} \cdot R_\perp \mathbf{E}_2^{(2)}], \end{aligned}$$

which, if $\mathbf{E}_1^{(2)} \cdot R_\perp \mathbf{E}_2^{(2)} \neq 0$, implies $1 - f_{e,u} = 1 - f^{(1)} \Leftrightarrow f_{e,u} = f^{(1)}$.

The function $\tilde{p}_{f,\max}^{(2)}$ is plotted as a blue dashed curve in Figure 2.5. If (2.79) does not hold, the values of $f \in (\tilde{f}_{e,u}, f_{e,u}]$ are not admissible so we obtain the improved elementary upper bound $f \leq \tilde{f}_{e,u}$; if (2.79) holds then $Q^{(2)} = \tilde{f}_{e,u} = f_{e,u}$ and we do not obtain an improved elementary upper bound. In Figure 2.5, $\tilde{f}_{e,u}$ and $f_{e,u}$ are indicated by the right black and gray vertical lines, respectively.

Finally, we can show that $\tilde{f}_{e,l} \leq \tilde{f}_{e,u}$ and provide a much simpler derivation of the improved elementary bounds as follows. We begin by noting that

$$\left\langle \left\| \mathbf{v}_\pm^{(\alpha)} - \frac{\chi^{(\alpha)}}{f^{(\alpha)}} \langle \mathbf{v}_\pm^{(\alpha)} \rangle \right\|^2 \right\rangle \geq 0.$$

Since $\|\mathbf{u}\|^2 = \mathbf{u} \cdot \mathbf{u}$ for any vector \mathbf{u} , this is equivalent to

$$\begin{aligned} \langle \mathbf{v}_\pm^{(\alpha)} \cdot \mathbf{v}_\pm^{(\alpha)} \rangle - \frac{2}{f^{(\alpha)}} \langle \chi^{(\alpha)} \mathbf{v}_\pm^{(\alpha)} \rangle \cdot \langle \mathbf{v}_\pm^{(\alpha)} \rangle + \frac{\langle [\chi^{(\alpha)}]^2 \rangle}{[f^{(\alpha)}]^2} \langle \mathbf{v}_\pm^{(\alpha)} \rangle \cdot \langle \mathbf{v}_\pm^{(\alpha)} \rangle &\geq 0 \\ \Leftrightarrow \langle \|\mathbf{v}_\pm^{(\alpha)}\|^2 \rangle - \frac{1}{f^{(\alpha)}} \|\langle \mathbf{v}_\pm^{(\alpha)} \rangle\|^2 &\geq 0 \\ \Leftrightarrow \frac{\|\langle \mathbf{v}_\pm^{(\alpha)} \rangle\|^2}{\langle \|\mathbf{v}_\pm^{(\alpha)}\|^2 \rangle} &\leq f^{(\alpha)}, \end{aligned} \tag{2.80}$$

with equality if and only if $\mathbf{v}_{\pm}^{(\alpha)}$ is a (nonzero) constant, i.e., if and only if $\mathbf{v}_{\pm}^{(\alpha)} \equiv \langle \mathbf{v}_{\pm}^{(\alpha)} \rangle / f^{(\alpha)}$. Then, in combination with (2.80), (2.67) and (2.75) imply that

$$\tilde{f}_{e,l} \leq f^{(1)} \quad \text{and} \quad \tilde{f}_{e,u} \geq 1 - f^{(2)} = f^{(1)},$$

respectively. The first inequality above will be satisfied as an equality if and only if $\mathbf{v}_+^{(1)}$ or $\mathbf{v}_-^{(1)}$ is a (nonzero) constant; the second inequality above will be satisfied as an equality if and only if $\mathbf{v}_+^{(2)}$ or $\mathbf{v}_-^{(2)}$ is a (nonzero) constant.

Definition 2.5 *The set $\tilde{\mathcal{A}}_e \equiv \{f \in \mathcal{A}_e : \tilde{f}_{e,l} \leq f \leq \tilde{f}_{e,u}\}$ is called the restricted elementary set of admissible test values.*

We have thus proven the following theorem.

Theorem 2.3 *Suppose $\beta \neq 0$, $\eta^{(\alpha)} \neq 0$ for $\alpha = 1, 2$, $f_{e,l} \neq 0$, $f_{e,u} \neq 1$, $|\sigma^{(1)}| \neq |\sigma^{(2)}|$, and $\mathbf{v}_{\pm}^{(\alpha)} \neq 0$ for $\alpha = 1, 2$. Then the volume fraction $f^{(1)} = \langle \chi^{(1)} \rangle$ satisfies the bounds $\tilde{f}_{e,l} \leq f^{(1)} \leq \tilde{f}_{e,u}$ where $\tilde{f}_{e,l}$ and $\tilde{f}_{e,u}$ are defined in (2.67) and (2.75), respectively (also see (2.69) and (2.77)). Moreover, the lower bound is satisfied as an equality (i.e., $\tilde{f}_{e,l} = f^{(1)}$) if and only if $\mathbf{v}_+^{(1)}$ or $\mathbf{v}_-^{(1)}$ is a nonzero constant while the upper bound is satisfied as an equality (i.e., $\tilde{f}_{e,u} = f^{(1)}$) if and only if $\mathbf{v}_+^{(2)}$ or $\mathbf{v}_-^{(2)}$ is a nonzero constant. Finally, these are tighter bounds than those discussed in Theorem 2.1, i.e., $f_{e,l} \leq \tilde{f}_{e,l}$ with equality if and only if (2.72) holds and $\tilde{f}_{e,u} \leq f_{e,u}$ with equality if and only if (2.79) holds.*

2.6.2 Attainment of the Improved Elementary Bounds

We now consider a configuration of concentric disks for which the improved elementary lower bound from Section 2.6.1 gives the exact volume fraction while the original elementary lower bound from Section 2.4 only gives a lower bound on the volume fraction. Thus for this example we will see that

$$f_{e,l} < \tilde{f}_{e,l} = f^{(1)} < \tilde{f}_{e,u} < f_{e,u}.$$

We denote the radii and conductivities of the inner disk (core) and outer annulus (shell) by R_1 and R_2 and $\sigma^{(1)}$ and $\sigma^{(2)}$, respectively. Throughout this section we take $z = x + iy = re^{i\theta}$; the complex conjugate of z is denoted by \bar{z} and is given by

$\bar{z} = x - iy = re^{-i\theta}$. We note that the condition $\mathbf{v}_+^{(\alpha)}$ being constant is equivalent to the potential in phase α being the sum of function linear in z plus a function $g(\bar{z})$, or conversely, $\mathbf{v}_-^{(\alpha)}$ being constant is equivalent to the potential in phase α being a function linear in \bar{z} plus a function $g(z)$. We prove this statement for $\mathbf{v}_+^{(\alpha)}$ — the proof for $\mathbf{v}_-^{(\alpha)}$ is similar.

First, suppose that $\mathbf{v}_+^{(\alpha)} \equiv \mathbf{C} = [C_1, C_2]^T \in \mathbb{R}^2$ in phase α , which we assume to be connected. We claim that this implies $V^{(\alpha)} = V_1^{(\alpha)} + iV_2^{(\alpha)} = \tilde{C}z + g(\bar{z})$ where g is a holomorphic function of \bar{z} , $z = x + iy$, $\bar{z} = x - iy$, and $\tilde{C} \equiv \frac{1}{2}(-C_1 + iC_2)$ is a constant. (If phase α is not connected, the constant C and the function g will be different in each connected component of phase α .) Now,

$$\mathbf{v}_+^{(\alpha)} = \mathbf{E}_1^{(\alpha)} + R_\perp \mathbf{E}_2^{(\alpha)} = -\nabla V_1^{(\alpha)} - R_\perp \nabla V_2^{(\alpha)} = \begin{bmatrix} -\frac{\partial V_1^{(\alpha)}}{\partial x} \\ -\frac{\partial V_1^{(\alpha)}}{\partial y} \end{bmatrix} - \begin{bmatrix} \frac{\partial V_2^{(\alpha)}}{\partial y} \\ -\frac{\partial V_2^{(\alpha)}}{\partial x} \end{bmatrix}.$$

Since $\mathbf{v}_+^{(\alpha)} = \mathbf{C}$, this implies

$$\frac{\partial V_1^{(\alpha)}}{\partial x} = -\frac{\partial V_2^{(\alpha)}}{\partial y} - C_1 \quad (2.81a)$$

$$\frac{\partial V_1^{(\alpha)}}{\partial y} = \frac{\partial V_2^{(\alpha)}}{\partial x} - C_2 \quad (2.81b)$$

for all points z in phase α . Notice that if $C_1 = C_2 = 0$, then (2.81) are the Cauchy–Riemann Equations up to a negative sign.

Next, using the Chain rule we have

$$\frac{\partial V_1^{(\alpha)}}{\partial x} + i\frac{\partial V_2^{(\alpha)}}{\partial x} = \frac{\partial V^{(\alpha)}}{\partial x} = \frac{\partial V^{(\alpha)}}{\partial z} + \frac{\partial V^{(\alpha)}}{\partial \bar{z}}, \quad (2.82a)$$

$$\frac{\partial V_1^{(\alpha)}}{\partial y} + i\frac{\partial V_2^{(\alpha)}}{\partial y} = \frac{\partial V^{(\alpha)}}{\partial y} = i\frac{\partial V^{(\alpha)}}{\partial z} - i\frac{\partial V^{(\alpha)}}{\partial \bar{z}}. \quad (2.82b)$$

We now insert (2.81) into (2.82b) and multiply the result by $-i$; then (2.82) becomes

$$\begin{aligned} \frac{\partial V_1^{(\alpha)}}{\partial x} + i\frac{\partial V_2^{(\alpha)}}{\partial x} &= \frac{\partial V^{(\alpha)}}{\partial z} + \frac{\partial V^{(\alpha)}}{\partial \bar{z}} \\ -i\frac{\partial V_2^{(\alpha)}}{\partial x} + iC_2 - \frac{\partial V_1^{(\alpha)}}{\partial x} - C_1 &= \frac{\partial V^{(\alpha)}}{\partial z} - \frac{\partial V^{(\alpha)}}{\partial \bar{z}}. \end{aligned}$$

Adding the two above equations and dividing by 2 gives

$$\frac{\partial V^{(\alpha)}}{\partial z} = \frac{1}{2}(-C_1 + iC_2) = \tilde{C}. \quad (2.83)$$

This implies that $V^{(\alpha)} = \tilde{C}z + g(\bar{z})$, where g is a holomorphic function of \bar{z} . To see this, we define

$$\tilde{V}^{(\alpha)} \equiv V^{(\alpha)} - \tilde{C}z. \quad (2.84)$$

Then, by (2.83),

$$\frac{\partial \tilde{V}^{(\alpha)}}{\partial z} = \frac{\partial V^{(\alpha)}}{\partial z} - \tilde{C} = 0;$$

in other words,

$$\frac{\partial \tilde{V}_1^{(\alpha)}}{\partial x} = -\frac{\partial \tilde{V}_2^{(\alpha)}}{\partial y} \quad \text{and} \quad \frac{\partial \tilde{V}_1^{(\alpha)}}{\partial y} = \frac{\partial \tilde{V}_2^{(\alpha)}}{\partial x}. \quad (2.85)$$

Since $\tilde{V}_1^{(\alpha)}$ and $\tilde{V}_2^{(\alpha)}$ are differentiable (in fact, they are infinitely differentiable since they are harmonic — see Section 2.2), we must have $\tilde{V}^{(\alpha)} = g(\bar{z})$ for some holomorphic function g (this follows from Theorem 11.2 in the book by Rudin [113] — since our function satisfies (2.85), the Cauchy–Riemann Equations up to a minus sign, it will be a holomorphic function of \bar{z} rather than z). Then (2.84) gives $V^{(\alpha)} = \tilde{C}z + g(\bar{z})$.

Conversely, since $g(\bar{z}) = g'(x, y) + ig''(x, y)$ is a holomorphic function of $\bar{z} = x - iy$, by the Cauchy–Riemann Equations we have

$$\frac{\partial g'}{\partial x}(x, y) = -\frac{\partial g''}{\partial y}(x, y) \quad \text{and} \quad \frac{\partial g'}{\partial y}(x, y) = \frac{\partial g''}{\partial x}(x, y) \quad (2.86)$$

for all (x, y) in phase α . Then, since $V^{(\alpha)}(z) = \tilde{C}z + g(\bar{z}) = \frac{1}{2}(-C_1 + iC_2)z + g(\bar{z})$, we have

$$V_1^{(\alpha)}(x, y) + iV_2^{(\alpha)}(x, y) = -\frac{1}{2}C_1x - \frac{1}{2}C_2y + g'(x, y) + i \left[\frac{1}{2}C_2x - \frac{1}{2}C_1y + g''(x, y) \right].$$

From this we have

$$\frac{\partial V_1^{(\alpha)}}{\partial x} + \frac{\partial V_2^{(\alpha)}}{\partial y} = -\frac{1}{2}C_1 + \frac{\partial g'}{\partial x}(x, y) - \frac{1}{2}C_1 + \frac{\partial g''}{\partial y}(x, y) = -C_1,$$

where the last equality follows from the first equation in (2.86); this is (2.81a). We also have

$$\frac{\partial V_1^{(\alpha)}}{\partial y} - \frac{\partial V_2^{(\alpha)}}{\partial x} = -\frac{1}{2}C_2 + \frac{\partial g'}{\partial y}(x, y) - \frac{1}{2}C_2 - \frac{\partial g''}{\partial x}(x, y) = -C_2,$$

where the last equality follows from the second equation in (2.86); this is (2.81b).

The proof of the fact that $\mathbf{v}_-^{(\alpha)}$ is a constant in phase α if and only if the potential in phase α is a linear function of \bar{z} plus a holomorphic function $h(z)$ is similar.

We take the Dirichlet Boundary Condition

$$V(R_2, \theta) \equiv V_0(\theta) \equiv \left(aR_2 + \frac{b}{R_2} \right) e^{i\theta} + \left(cR_2^2 + \frac{d}{R_2^2} \right) e^{-2i\theta},$$

where

$$\begin{aligned} a &= \frac{\sigma^{(1)} + \sigma^{(2)}}{2\sigma^{(2)}}, & b &= -\frac{R_1^2[\sigma^{(1)} + \sigma^{(2)}]}{2\sigma^{(2)}}, \\ c &= \frac{k[\sigma^{(1)} + \sigma^{(2)}]}{2\sigma^{(2)}}, & d &= -\frac{kR_1^4[\sigma^{(1)} - \sigma^{(2)}]}{2\sigma^{(2)}}, \end{aligned} \tag{2.87}$$

and $k \in \mathbb{R}$ (entering (2.87)) is a given constant. The potential in the core (for $0 < r < R_1$) is then given by

$$V^{(1)}(z, \bar{z}) = z + k(\bar{z})^2.$$

The potential in the shell ($R_1 < r < R_2$) can be found by using the continuity of the potential V and the current flux $-\sigma \nabla V \cdot \mathbf{n}$ across the boundary at $r = R_1$; in particular we find

$$V^{(2)}(z, \bar{z}) = az + \frac{b}{\bar{z}} + c(\bar{z})^2 + \frac{d}{z^2},$$

where a, b, c , and d are given in (2.87).

Let

$$\hat{\mathbf{x}} = \begin{bmatrix} 1 \\ 0 \end{bmatrix} \quad \text{and} \quad \hat{\mathbf{y}} = \begin{bmatrix} 0 \\ 1 \end{bmatrix}$$

be the standard orthonormal basis for \mathbb{R}^2 . Then, since $\mathbf{E} = -\nabla V$, the electric field in each phase is given by

$$\begin{aligned} \mathbf{E}^{(1)} &= -(1 + 2k\bar{z})\hat{\mathbf{x}} - i(1 - 2k\bar{z})\hat{\mathbf{y}} \\ \mathbf{E}^{(2)} &= -\left[a - \frac{b}{(\bar{z})^2} + 2c\bar{z} - \frac{2d}{z^3} \right] \hat{\mathbf{x}} - i\left[a + \frac{b}{(\bar{z})^2} - 2c\bar{z} - \frac{2d}{z^3} \right] \hat{\mathbf{y}}. \end{aligned} \tag{2.88}$$

We emphasize that neither of these fields is constant; therefore Theorem 2.1 implies

$$f_{e,l} < f^{(1)} < f_{e,u}.$$

In particular

$$f_{e,l} = \left(\frac{1}{1 + 2k^2 R_1^2} \right) \frac{R_1^2}{R_2^2}. \tag{2.89}$$

For $k \neq 0$ this is strictly less than $f^{(1)} = (R_1/R_2)^2$.

Recall that $\mathbf{v}_{\pm}^{(\alpha)} = \mathbf{E}_1^{(\alpha)} \pm R_{\perp} \mathbf{E}_2^{(\alpha)}$. We can compute

$$\mathbf{v}_+^{(1)} = -2\hat{\mathbf{x}} \quad \text{and} \quad \mathbf{v}_-^{(1)} = 4k(-x\hat{\mathbf{x}} + y\hat{\mathbf{y}}); \quad (2.90)$$

thus $\mathbf{v}_+^{(1)}$ is a constant. We note that both fields $\mathbf{v}_{\pm}^{(2)}$ are not uniform. Theorem 2.3 thus implies that $\tilde{f}_{e,l} = f^{(1)}$ and $f^{(1)} < \tilde{f}_{e,u}$.

Finally, if $k = 0$ note that (2.88) implies that $\mathbf{E}^{(1)} = -\hat{\mathbf{x}} - i\hat{\mathbf{y}}$ is a constant. Thus Theorem 2.1 implies that $f_{e,l} = f^{(1)}$, which is verified by (2.89). Additionally (2.90) implies that $\mathbf{v}_-^{(1)} \equiv 0$, so Theorem 2.3 implies that $\tilde{f}_{e,l} = f_{e,l}$.

2.7 More Sophisticated Bounds in 2-D

We now proceed to find improved bounds; the method is very similar to that in Section 2.5.

Definition 2.6 For $\alpha = 1, 2$ and for $f \in \tilde{\mathcal{A}}_e$ we define

$$\tilde{\mathcal{E}}_f^{(\alpha)} \equiv \{(x, y) \in \mathbb{R}^2 : p_f^{(\alpha)}(x, y) \geq \tau_f^{(\alpha)}\} \quad \text{and} \quad \tilde{\mathcal{E}}_f \equiv \tilde{\mathcal{E}}_f^{(1)} \cap \tilde{\mathcal{E}}_f^{(2)}.$$

Since $\tau_f^{(\alpha)} \geq 0$ (see (2.61)), Lemma 2.5 implies that $\tilde{\mathcal{E}}_f^{(\alpha)} \subseteq \mathcal{E}_f^{(\alpha)}$; that is, the elliptic disks in this case are smaller than those in Section 2.5 (which can be obtained by taking $\tau_f^{(\alpha)} \equiv 0$). For each $f \in \tilde{\mathcal{A}}_e$ we check to see whether or not $\tilde{\mathcal{E}}_f$ is empty. If $\tilde{\mathcal{E}}_f \neq \emptyset$, then $f \in \tilde{\mathcal{A}}$; if $\tilde{\mathcal{E}}_f = \emptyset$, then $f \notin \tilde{\mathcal{A}}$. As in Section 2.5, we cannot work through everything explicitly due to the complexity of the expressions involved. However, Lemmas 2.2–2.4 (and therefore Theorem 2.2) extend immediately; we present their extensions here for completeness.

Lemma 2.8 Assume that $\beta \neq 0$, $\eta^{(\alpha)} \neq 0$ for $\alpha = 1, 2$, $f_{e,l} \neq 0$, $f_{e,u} \neq 1$, $|\sigma^{(1)}| \neq |\sigma^{(2)}|$, and $\mathbf{v}_{\pm}^{(\alpha)} \neq \mathbf{0}$ for $\alpha = 1, 2$. Then the following properties hold.

- (1) For $f \in (\tilde{f}_{e,l}, \tilde{f}_{e,u})$ and $\alpha = 1, 2$, $\tilde{\mathcal{E}}_f^{(\alpha)}$ is a closed elliptic disk; its boundary is the ellipse $\partial\tilde{\mathcal{E}}_f^{(\alpha)} = \{(x, y) \in \mathbb{R}^2 : \tilde{p}_f^{(\alpha)}(x, y) = 0\}$;
- (2) $\tilde{\mathcal{E}}_{f_{e,l}}^{(1)}$ is a point and $\tilde{\mathcal{E}}_{f_{e,l}}^{(2)}$ is a closed elliptic disk;
- (3) $\tilde{\mathcal{E}}_{f_{e,u}}^{(1)}$ is a closed elliptic disk and $\tilde{\mathcal{E}}_{f_{e,u}}^{(2)}$ is a point.

Proof of Lemma 2.8: We simply apply the proof of Lemma 2.2 to $\tilde{p}_f^{(\alpha)}$. This completes the proof.

Lemma 2.9 *Assume that $\beta \neq 0$, $\eta^{(\alpha)} \neq 0$ for $\alpha = 1, 2$, $f_{e,l} \neq 0$, $f_{e,u} \neq 1$, $|\sigma^{(1)}| \neq |\sigma^{(2)}|$, and $\mathbf{v}_{\pm}^{(\alpha)} \neq 0$ for $\alpha = 1, 2$. Then for each $f \in \tilde{\mathcal{A}}_e, \tilde{\mathcal{E}}_f \subseteq \mathcal{F}_{f,e}$.*

Proof of Lemma 2.9: For each $f \in \tilde{\mathcal{A}}_e, \tilde{\mathcal{E}}_f \subseteq \mathcal{E}_f$ by Lemma 2.5; since $\mathcal{E}_f \subseteq \mathcal{F}_{f,e}$ for each $f \in \mathcal{A}_e \supseteq \tilde{\mathcal{A}}_e$ by Lemma 2.3, $\tilde{\mathcal{E}}_f \subseteq \mathcal{F}_{f,e}$ for each $f \in \tilde{\mathcal{A}}_e$. This completes the proof.

Lemma 2.10 *Assume that $\beta \neq 0$, $\eta^{(\alpha)} \neq 0$ for $\alpha = 1, 2$, $f_{e,l} \neq 0$, $f_{e,u} \neq 1$, $|\sigma^{(1)}| \neq |\sigma^{(2)}|$, and $\mathbf{v}_{\pm}^{(\alpha)} \neq 0$ for $\alpha = 1, 2$. Then for each $f \in \tilde{\mathcal{A}}_e$ the set $\partial\tilde{\mathcal{E}}_f^{(1)} \cap \partial\tilde{\mathcal{E}}_f^{(2)}$ contains at most two points.*

Proof of Lemma 2.10: The proof is a word-for-word repeat of the proof of Lemma 2.4 applied to $\tilde{p}_f^{(\alpha)}$. This completes the proof.

Therefore we can numerically search for tighter bounds as follows. For each $f \in \tilde{\mathcal{A}}_e$, if $\tilde{\Delta}_f \geq 0$ then $f \in \tilde{\mathcal{A}}$, where $\tilde{\Delta}_f$ is the same as Δ_f (defined in (2.55)) but with $a_6^{(\alpha)}$ replaced by $\tilde{a}_6^{(\alpha)} \equiv a_6^{(\alpha)} - \tau_f^{(\alpha)}$. If $\tilde{\Delta}_f < 0$, then $f \notin \tilde{\mathcal{A}}$ if and only if $\tilde{p}_f^{(1)}(\mathbf{r}^{(2)}) < 0$ and $\tilde{p}_f^{(2)}(\mathbf{r}^{(1)}) < 0$, where $\mathbf{r}^{(1)}$ and $\mathbf{r}^{(2)}$ are defined in (2.48). Combining this analysis with Lemmas 2.8–2.10 proves the following theorem.

Theorem 2.4 *Assume that $\beta \neq 0$, $\eta^{(\alpha)} \neq 0$ for $\alpha = 1, 2$, $f_{e,l} \neq 0$, $f_{e,u} \neq 1$, $|\sigma^{(1)}| \neq |\sigma^{(2)}|$, and $\mathbf{v}_{\pm}^{(\alpha)} \neq 0$ for $\alpha = 1, 2$. Then for $f \in \tilde{\mathcal{A}}_e (= [\tilde{f}_{e,l}, \tilde{f}_{e,u}])$, if $\tilde{\Delta}_f \geq 0$, then $f \in \tilde{\mathcal{A}}$ where $\tilde{\Delta}_f$ is defined in (2.55) by replacing $a_6^{(\alpha)}$ by $\tilde{a}_6^{(\alpha)} \equiv a_6^{(\alpha)} - \tau_f^{(\alpha)}$. If $\tilde{\Delta}_f < 0$, then $f \notin \tilde{\mathcal{A}}$ if and only if $\tilde{p}_f^{(1)}(\mathbf{r}^{(2)}) < 0$ and $\tilde{p}_f^{(2)}(\mathbf{r}^{(1)}) < 0$, where $\tilde{p}_f^{(\alpha)}$ is defined in (2.45) by replacing $a_6^{(\alpha)}$ by $\tilde{a}_6^{(\alpha)}$ and $\mathbf{r}^{(\alpha)}$ is defined in (2.48).*

The numerically computed bounds may or may not be tighter than the improved elementary bounds, depending on the problem under consideration — see the last paragraph in Section 2.4, in which we discussed this issue in the context of the bounds from that section. If we consider concentric disks in which the inner disk is labeled as phase 1, then the improved elementary lower bound will be exactly equal to the volume fraction, i.e., $\tilde{f}_{e,l} = f^{(1)}$. In this case the field inside the inner disk is constant, so $\mathbf{v}_+^{(1)}$ and $\mathbf{v}_-^{(1)}$ are both constants as well. This example is somewhat trivial in the

sense that the original elementary lower bound is also equal to the volume fraction, i.e., $f_{e,l} = f^{(1)}$ (see the last paragraph in Section 2.4). In the case of a two-phase simple laminate we find that $f_{e,l} = \tilde{f}_{e,l} = \tilde{f}_{e,u} = f_{e,u} = f^{(1)}$ since the electric field is constant in both phases. In Section 2.6.2 we gave an example of a geometry and boundary conditions in which the improved elementary lower bound $\tilde{f}_{e,l}$ is equal to the true volume fraction $f^{(1)}$ but the elementary lower bound $f_{e,l}$ is strictly less than the volume fraction.

In Figures 2.6(a)–2.6(h) we plot the sets $\tilde{\mathcal{E}}_f^{(1)}$ (red) and $\tilde{\mathcal{E}}_f^{(2)}$ (blue) at various values of $f \in \tilde{\mathcal{A}}_e = [\tilde{f}_{e,l}, \tilde{f}_{e,u}]$; the centers of each ellipse are indicated by a dot while the black box is the boundary of the set $\mathcal{F}_{f,e}$ (defined in Definition 2.2). For comparison we plot $\mathcal{E}_f^{(1)}$ (red dashed ellipse) and $\mathcal{E}_f^{(2)}$ (blue dashed ellipse). Note that $\mathcal{E}_f \neq \emptyset$ in Figures 2.6(a)–2.6(h) but that $\tilde{\mathcal{E}}_f \neq \emptyset$ only in Figures 2.6(c)–2.6(f). In Figure 2.6(i) we plot $\tilde{\Delta}_f$ (solid black line), $\tilde{p}_f^{(1)}(\mathbf{r}^{(2)})$ (red dashed line), and $\tilde{p}_f^{(2)}(\mathbf{r}^{(1)})$ (blue dash-dotted line) over the interval $\tilde{\mathcal{A}}_e$. The true volume fraction is represented by the magenta dashed line and the horizontal gray line represents the f -axis. In addition, the set $\tilde{\mathcal{A}}$ is indicated by the darkened interval. In this case $\tilde{\mathcal{A}} \subset \tilde{\mathcal{A}}_e$ (which is in contrast to the example in Figure 2.4 where $\mathcal{A} = \mathcal{A}_e$), so the bounds computed using the ellipses are better than the improved elementary bounds. Since $\tilde{p}_f^{(1)}(\mathbf{r}^{(2)})$ and $\tilde{p}_f^{(2)}(\mathbf{r}^{(1)})$ are both negative for all $f \in \tilde{\mathcal{A}}_e$, the set $\tilde{\mathcal{A}}$ is simply the set on which $\tilde{\Delta}_f \geq 0$.

To search for geometries for which these more sophisticated bounds are attained, one could look for geometries such that for some choice of real vectors $\mathbf{c}^{(1)}, \mathbf{d}^{(1)}$ (that are not both zero) and $\mathbf{c}^{(2)}, \mathbf{d}^{(2)}$ (that are not both zero) we have

$$\begin{cases} \mathbf{h}^{(1)}(\mathbf{x}; \mathbf{c}^{(1)}, \mathbf{d}^{(1)}) \equiv 0 & \text{for } \mathbf{x} \in \text{phase 1,} \\ \mathbf{h}^{(2)}(\mathbf{x}; \mathbf{c}^{(2)}, \mathbf{d}^{(2)}) \equiv 0 & \text{for } \mathbf{x} \in \text{phase 2.} \end{cases} \quad (2.91)$$

In this case $\tilde{p}_f^{(1)}$ and $\tilde{p}_f^{(2)}$ will both be zero and (x, y) must be at an intersection point of the boundary of the elliptic disk $\tilde{\mathcal{E}}_f^{(1)}$ and the boundary of the elliptic disk $\tilde{\mathcal{E}}_f^{(2)}$. Conversely, if (x, y) is at such an intersection point then (2.91) must hold. Additionally we require that the two ellipses only touch at one point and the meaning of this condition in terms of fields is not so clear. Therefore (2.91) is a necessary, but not sufficient, condition for attainability of the bounds. A similar remark applies to the attainability of the “more sophisticated” bounds derived in Section 2.5.

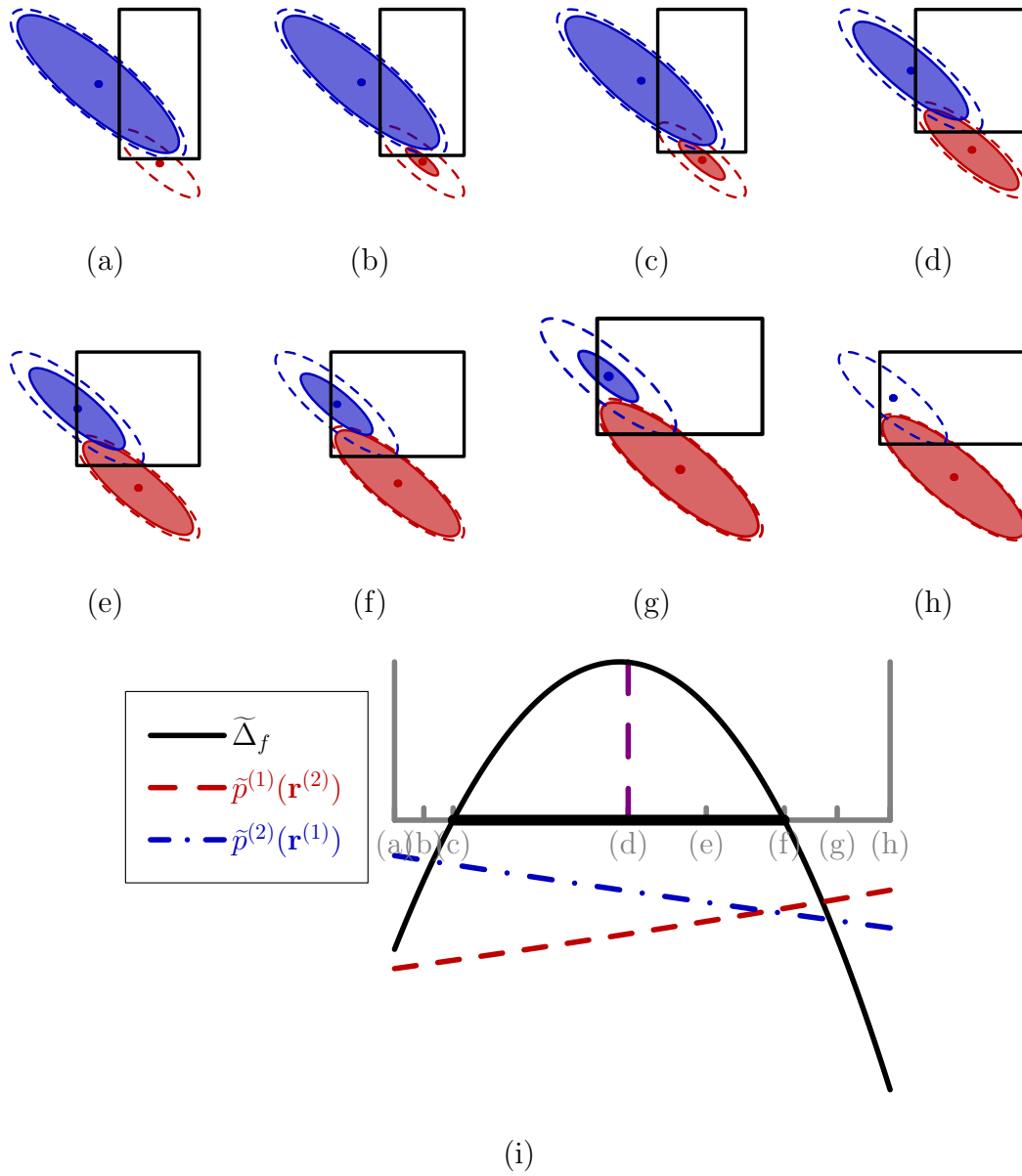


Figure 2.6. The rectangle $\mathcal{F}_{f,e}$ (outlined in black) and the sets $\tilde{\mathcal{E}}_f^{(1)}$ (red) and $\tilde{\mathcal{E}}_f^{(2)}$ (blue) are drawn for several test values. We took: (a) $f = \tilde{f}_{e,l} \approx 0.7982$; (b) $f \approx 0.7984$; (c) $f \approx 0.7987$ (where $\tilde{\Delta}_f = 0$); (d) $f = f^{(1)} = 0.80$; (e) $f \approx 0.8006$; (f) $f \approx 0.8012$ (where $\tilde{\Delta}_f = 0$); (g) $f \approx 0.8016$; (h) $f = \tilde{f}_{e,u} \approx 0.8020$. The red (blue) dashed ellipse is the boundary of $\mathcal{E}_f^{(1)}$ ($\mathcal{E}_f^{(2)}$). (i) This is a plot of $\tilde{\Delta}_f$ (black solid line), $\frac{1}{5}\tilde{p}_f^{(1)}(\mathbf{r}^{(2)})$ (red dashed line), and $\frac{1}{5}\tilde{p}_f^{(2)}(\mathbf{r}^{(1)})$ (blue dash-dotted line) for $f \in \tilde{\mathcal{A}}_e = [\tilde{f}_{e,l}, \tilde{f}_{e,u}]$. The parameters used to create this figure are the same as those in Figure 2.3. Thus, we obtain the bounds $0.7987 \leq f^{(1)} \leq 0.8012$, which are better than the improved elementary bounds from Section 2.6.1 and Figure 2.5.

2.7.1 Degenerate Cases

In this section we briefly discuss the degenerate cases. If $\mathbf{v}_+^{(1)}$ or $\mathbf{v}_-^{(1)} \equiv 0$ ($\mathbf{v}_+^{(2)}$ or $\mathbf{v}_-^{(2)} \equiv 0$), then $\tilde{p}_{f,\max}^{(1)} \equiv 0$ ($\tilde{p}_{f,\max}^{(2)} \equiv 0$) for all $f \in \mathcal{A}_e$ by (2.66), so we are unable to derive a tighter lower (upper) elementary bound. If $\mathbf{v}_\pm^{(\alpha)} = 0$ for $\alpha = 1, 2$ we again have $\tilde{\mathcal{A}}_e = \mathcal{A}_e$. In summary we construct Table 2.1 for the restricted elementary set of admissible volume fractions, $\tilde{\mathcal{A}}_e$, assuming $\eta^{(\alpha)} \neq 0$ for $\alpha = 1, 2$. As the table shows, if $\mathbf{v}_\pm^{(\alpha)} = 0$ we have $\tilde{\mathcal{A}}_e = \mathcal{A}_e = [f_{e,l}, f_{e,u}]$. One can apply the procedure discussed in the paragraph preceding Theorem 2.4 to try to improve these elementary bounds.

2.8 Numerical Example

In this section we present the results of several numerical experiments. We used the 2-D configuration and boundary conditions from Figure 2.3 to create the plots in Figure 2.7. In each subplot $\sigma^{(1)}$ is fixed and $\sigma^{(2)} = 1$; we varied the volume fraction by fixing $R_1 = 0.45$ and $R_3 = 5$ while varying R_2 between approximately 0.6727 and 4.995.

Each subplot contains the following data scaled by $f^{(1)}$: $f_{e,l}$ (red stars); $\inf \mathcal{A}$ (red circles); $\tilde{f}_{e,l}$ (red crosses); $\inf \tilde{\mathcal{A}}$ (red squares); $f_{e,u}$ (blue stars); $\sup \mathcal{A}$ (blue circles); $\tilde{f}_{e,u}$ (blue crosses); $\sup \tilde{\mathcal{A}}$ (blue squares). In all of the plots, $f_{e,l}/f^{(1)} = \inf \mathcal{A}/f^{(1)}$ and $f_{e,u}/f^{(1)} = \sup \mathcal{A}/f^{(1)}$, so the bounds obtained by using the elliptic disks $\mathcal{E}_f^{(1)}$ and $\mathcal{E}_f^{(2)}$ from Section 2.5 (namely $\inf \mathcal{A}$ and $\sup \mathcal{A}$) are simply the elementary bounds $f_{e,l}$ and $f_{e,u}$ from Section 2.4.

For many cases in this 2-D example the bounds obtained by using the elliptic disks $\tilde{\mathcal{E}}_f^{(1)}$ and $\tilde{\mathcal{E}}_f^{(2)}$ from Section 2.7 (namely $\inf \tilde{\mathcal{A}}$ and $\sup \tilde{\mathcal{A}}$) are substantially better than the improved elementary bounds $\tilde{f}_{e,l}$ and $\tilde{f}_{e,u}$ from Section 2.6.1. In particular,

Table 2.1. This table provides a summary of our elementary bounds on the volume fraction.

	$\mathbf{v}_\pm^{(1)} \neq 0$ and $\mathbf{v}_\pm^{(2)} \neq 0$	$\mathbf{v}_+^{(1)}$ or $\mathbf{v}_-^{(1)} \equiv 0$ and $\mathbf{v}_\pm^{(2)} \neq 0$	$\mathbf{v}_+^{(2)}$ or $\mathbf{v}_-^{(2)} \equiv 0$ and $\mathbf{v}_\pm^{(1)} \neq 0$	$\mathbf{v}_\pm^{(1)} \equiv 0$ and $\mathbf{v}_\pm^{(2)} \equiv 0$
$\tilde{\mathcal{A}}_e$	$[\tilde{f}_{e,l}, \tilde{f}_{e,u}]$	$[f_{e,l}, \tilde{f}_{e,u}]$	$[\tilde{f}_{e,l}, f_{e,u}]$	$[f_{e,l}, f_{e,u}] = \mathcal{A}_e$

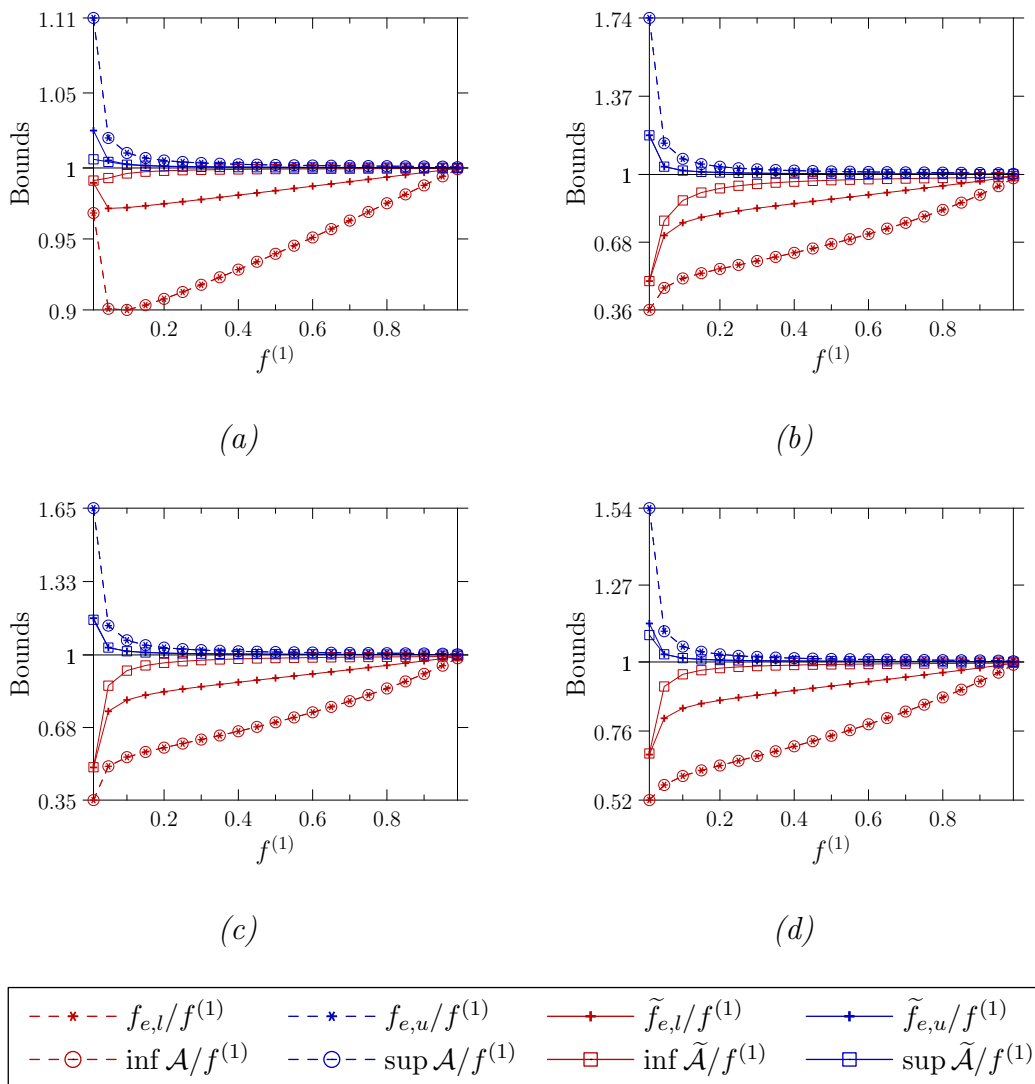


Figure 2.7. These are plots of the bounds in the case of an annulus (see Figure 2.3(a)) for several volume fractions ranging from $f^{(1)} = 0.01$ to $f^{(1)} = 0.99$. In each subfigure the conductivity of the annular ring is $\sigma^{(2)} = 1$ while the conductivity of the surrounding medium in each subfigure is: (a) $\sigma^{(1)} = 2 + 0.5i$; (b) $\sigma^{(1)} = 2 + 10i$; (c) $\sigma^{(1)} = 10 + 10i$; (d) $\sigma^{(1)} = 10 + 0.5i$. The legend at the bottom indicates the symbol used to represent each bound; in particular we used the following labels: red circles: elementary lower bound ($f_{e,l}$: see Section 2.4); red stars: “sophisticated” lower bound (see Section 2.5); red crosses: improved elementary lower bound ($\tilde{f}_{e,l}$: see Section 2.6.1); red squares: improved “sophisticated” lower bound (see Section 2.7); blue circles: elementary upper bound ($f_{e,u}$: see Section 2.4); blue stars: “sophisticated” upper bound (see Section 2.5); blue crosses: improved elementary upper bound ($\tilde{f}_{e,u}$: see Section 2.6.1); blue squares: improved “sophisticated” upper bound (see Section 2.7).

the extra information from the elliptic disks $\tilde{\mathcal{E}}^{(1)}$ and $\tilde{\mathcal{E}}^{(2)}$ gives us lower bounds that, most of the time, are better than the improved elementary bounds $\tilde{f}_{e,l}$ and $\tilde{f}_{e,u}$; this extra information does not seem to improve the upper bound in most cases, however. A summary of our results for this example is included in Table 2.2. The elementary and ellipse bounds do quite well; also note how tight the improved elementary and ellipse bounds are for this example.

Table 2.2. This table gives a summary of our bounds corresponding to the test problem described in Figure 2.3.

true volume fraction $f^{(1)}$	0.8
elementary bounds ($f_{e,l} \leq f^{(1)} \leq f_{e,u}$)	$0.794 \leq f^{(1)} \leq 0.808$
ellipse bounds ($\inf \mathcal{A} \leq f^{(1)} \leq \sup \mathcal{A}$)	$0.794 \leq f^{(1)} \leq 0.808$
improved elementary bounds ($\tilde{f}_{e,l} \leq f^{(1)} \leq \tilde{f}_{e,u}$)	$0.7982 \leq f^{(1)} \leq 0.8020$
improved ellipse bounds ($\inf \tilde{\mathcal{A}} \leq f^{(1)} \leq \sup \tilde{\mathcal{A}}$)	$0.7987 \leq f^{(1)} \leq 0.8012$

CHAPTER 3

EXACT DETERMINATION OF THE VOLUME OF AN INCLUSION IN A BODY HAVING CONSTANT SHEAR MODULUS

In this chapter, we utilize a single measurement of the displacement and normal stress around the boundary of a body to derive an exact formula for the volume of an inclusion in the body.

3.1 Introduction

A fundamental and interesting problem in the study of materials is the estimation of the volume fraction occupied by an inclusion D in a body Ω . Although the volume fraction could be determined by weighing the body, the densities of the materials may be close or unknown or weighing the body may be impractical. Because of this, many methods have been developed which utilize measurements of certain fields around $\partial\Omega$ to derive bounds on the volume fraction $|D|/|\Omega|$ (where $|U|$ is the Lebesgue measure of the set U) [2–4, 7, 14, 25, 26, 29, 62, 64–68, 85, 86, 89, 90, 96, 111, 112, 120]; also see Chapter 2. In this chapter, we show that under certain circumstances the volume fraction $|D|/|\Omega|$ can be computed exactly from a single appropriate boundary measurement around $\partial\Omega$. We note that many of the results in the literature (and our results in this chapter) can also be applied when Ω contains a two-phase composite with microstructure much smaller than the dimensions of Ω .

We consider an inclusion D in a body Ω (or a two-phase composite inside Ω), where Ω is a subset of \mathbb{R}^d ($d = 2$ or 3). In Chapter 2, we utilized an electrical measurement around $\partial\Omega$ to derive bounds on the volume fraction of the inclusion; in this chapter we utilize a linearly elastic boundary measurement to exactly determine the volume fraction of the inclusion. We assume that the inclusion and body are

filled with linearly elastic materials with the same shear modulus μ and Lamé Moduli λ_1 and λ_2 , respectively. Our goal is to determine the volume fraction occupied by the inclusion, namely $|D|/|\Omega|$, in terms of a measurement of the displacement and traction around $\partial\Omega$. The boundary conditions around $\partial\Omega$ are taken to be such that they mimic the body Ω being placed in an infinite medium with a suitable field at infinity. The starting point for our result is based on an exact relation due to Hill [60], which we now describe.

One of the most important problems in the study of composite materials is the determination of effective moduli given information about the local moduli — see the work by Hashin [54] and the book by Milton [88] (Chapters 1 and 2 in particular). In general, it is extremely difficult (if not impossible) to determine effective parameters exactly, even if the microgeometry of the composite is known and relatively uncomplicated. However, many useful approximation techniques and bounds on effective properties of composites have been derived in the literature — see the book by Milton [88] and the references therein for a vast collection of such results. Surprisingly, there are several circumstances in which exact links between effective moduli (or exact formulas for the moduli themselves) can be derived regardless of the complexity of the microstructure; such links are known as *exact relations*.

Exact relations exist for a variety of problems including elasticity and coupled problems such as thermoelasticity, thermoelectricity, piezoelectricity, thermo-piezoelectricity and others — see the review article by Milton [87], the work by Grabovsky, Milton, and Sage [42], and the works by Hegg [56, 57] for summaries of numerous previous and current results on exact relations.

Perhaps even more surprising than the existence of exact relations is the existence of a general mathematical theory of exact relations, developed by Grabovsky, Milton, and Sage [39–43], that allows us to determine all of the above mentioned exact relations and many more. For example, Hegg [56, 57] applied this general theory to the study of fiber-reinforced elastic composites.

Rather than study the general theory, we focus on a specific exact relation derived by Hill [60, 61]. In particular, Hill considered a two-phase composite material consisting of two homogeneous and isotropic phases with the same shear modulus μ

but different Lamé Moduli λ_1 and λ_2 . Hill proved that such a composite is macroscopically elastically isotropic with shear modulus μ and effective Lamé Modulus λ_* ; he also derived an exact formula for λ_* that holds regardless of the complexity of the microgeometry — see (3.13). Hill's [60, 61] derivation of this formula provides the starting point of our work in this paper.

We begin by assuming that the body Ω is embedded in an infinite medium with Lamé Modulus λ_E and shear modulus μ (we take $\lambda_E = \lambda_2$ for simplicity) and that a displacement $\mathbf{u} = \nabla g$ is applied at infinity. Using a method similar to Hill's derivation of λ_* , we derive a formula for $|D|/|\Omega|$ in terms of a measurement of the displacement around $\partial\Omega$, the (known) parameters λ_1, λ_2 , and μ , and the (known) function g . In order to make the situation more practical, we derive a certain nonlocal boundary condition that can be applied to $\partial\Omega$ that forces the body to behave as if it actually were embedded in an infinite medium with Lamé Modulus λ_2 , shear modulus μ , and an applied displacement $\mathbf{u} = \nabla g$ at infinity. This nonlocal boundary condition couples the measurements of the traction and displacement around $\partial\Omega$.

Nonlocal boundary conditions which mimic infinite media similar to the one mentioned above are common tools used in the numerical solution of PDEs and ordinary differential equations (ODEs) in infinite domains — see the review article by Givoli [38] for examples specific to scattering problems, the work by Han and Wu on the Laplace and elasticity equations [52, 53], and the work by Lee, Caffisch, and Lee [76] on the elasticity equations.

To illustrate the idea, consider an open, bounded set $U \subset \mathbb{R}^d$ containing the origin, and suppose $\mathbb{R}^d \setminus \bar{U}$ contains a linearly elastic, homogeneous, and isotropic material with Lamé Modulus λ and shear modulus μ . Suppose also that we are interested in solving the linear elasticity problem

$$\begin{cases} -(\lambda + \mu)\nabla(\nabla \cdot \mathbf{u}) - \mu\Delta\mathbf{u} = 0 & \text{in } \mathbb{R}^d \setminus \bar{U}, \\ \mathbf{u} = \mathbf{u}_0 \text{ or } \boldsymbol{\sigma} \cdot \mathbf{n} = \mathbf{t}_0 & \text{on } \partial U, \\ \mathbf{u} \rightarrow 0 & \text{as } |\mathbf{x}| \rightarrow \infty, \end{cases} \quad (3.1)$$

where \mathbf{u} is the displacement, $\boldsymbol{\sigma}$ is the Cauchy stress tensor, \mathbf{n} is the outward unit normal vector to ∂U , and \mathbf{u}_0 or \mathbf{t}_0 are a given displacement or traction around ∂U , respectively. Issues arise when one attempts to solve (3.1) using the finite

element method, for example, since (3.1) is posed on an unbounded domain [52, 53]. Several approximate and exact resolutions to this problem have been proposed in the literature.

For example, one can set up an artificial boundary (usually a circle or sphere of radius R where R is large enough to contain the domain U) and solve the problem

$$\begin{cases} -(\lambda + \mu)\nabla(\nabla \cdot \mathbf{u}') - \mu\Delta\mathbf{u}' = 0 & \text{in } B_R \setminus \bar{U}, \\ \mathbf{u}' = \mathbf{u}_0 \text{ or } \boldsymbol{\sigma}' \cdot \mathbf{n} = \mathbf{t}_0 & \text{on } \partial U, \\ \text{appropriate boundary condition} & \text{on } \partial B_R \end{cases} \quad (3.2)$$

on the finite domain $B_R \setminus \bar{U}$ instead, where B_R denotes the ball of radius R centered at the origin. There remains the important question of what boundary condition to apply on ∂B_R . One possibility would be to apply the homogeneous Dirichlet Boundary Condition $\mathbf{u}' = 0$ on ∂B_R , but such a boundary condition is only approximate and may introduce large numerical errors in the solution [52, 53, 76]. To avoid such excessive errors in this case, one has to take R to be very large; this makes the numerical solution computationally expensive due to the large region of interest under consideration, namely $B_R \setminus \bar{U}$ — see the work by Lee et al. [76] for more on this.

A second option is to use boundary conditions on ∂B_R that are more accurate than the homogeneous Dirichlet Condition $\mathbf{u}' = 0$ — see the work by Han and Bao [51] and Bonnaillie-Noël, Dambrine, Hérau, and Vial [17, 18]. For example, Bonnaillie-Noël et al. [18] derived Ventcel-Type Boundary Conditions (which involve the Laplace-Beltrami Operator) on ∂B_R [17, 18]. (These same authors derived analogous boundary conditions for the Laplace Equation in their earlier work [17].) Although such boundary conditions are still approximate, they provide a better approximation to the true problem than the homogeneous Dirichlet boundary condition. Bonnaillie-Noël et al. [18] showed that the error in the solution was $O(R^{-2})$ for the Ventcel Boundary Conditions on ∂B_R while it was only $O(R^{-1})$ for the Dirichlet Boundary Condition on ∂B_R — in particular they discussed this statement when the Neumann Boundary Condition $\boldsymbol{\sigma}' \cdot \mathbf{n}$ is imposed on ∂U and U is a smooth perturbation of a disk.

The Dirichlet and Ventcel-Type Boundary Conditions on ∂B_R are local boundary conditions since they only depend on the displacement and its tangential derivatives on ∂B_R . Han and Wu [52, 53] derived a nonlocal boundary condition on ∂B_R with

the following property: if this boundary condition is applied on ∂B_R , then, in $B_R \setminus U$, the solution \mathbf{u}' to (3.2) will be exactly the same as the restriction to $B_R \setminus U$ of the solution \mathbf{u} to the infinite domain problem (3.1). In other words, $\mathbf{u}' = \mathbf{u}|_{B_R \setminus U}$.

As discussed above, our formula for the volume fraction $|D|/|\Omega|$ holds as long as the body Ω is embedded in an infinite medium with an applied displacement $\mathbf{u} = \nabla g$ at infinity. In Section 3.5 we derive a nonlocal boundary condition such that if this boundary condition is applied to $\partial\Omega$ the solution inside Ω will be equal to the restriction to Ω of the solution to the infinite problem. In other words, when these boundary conditions are applied, the body Ω will behave as if it actually were embedded in an infinite medium with shear modulus μ . Our boundary condition depends on the function g and on the Exterior Dirichlet-to-Neumann Map on $\partial\Omega$ (which, when the body Ω is absent, maps the displacement on $\partial\Omega$ to the traction on $\partial\Omega$ when no fields are applied at infinity). Thus it is closely related to the boundary condition of Han and Wu [52, 53] and Bonnaillie-Noël et al. [18] — see Section 3.5 for complete details.

The rest of this chapter is organized as follows. In Section 3.2 we briefly review the linear elasticity equations and relevant results from homogenization theory. In Section 3.3 we summarize a selection of uniform field relations that lead to exact relations for the effective elasticity tensors of certain composites. Next, in Section 3.4 we derive a formula that gives the exact volume fraction of an inclusion in a body when the inclusion and the body have the same shear modulus μ and the body is embedded in an infinite medium with shear modulus μ . We discuss the nonlocal boundary condition relevant to our problem in Section 3.5 so we can focus on a (more realistic) finite domain. Finally, in Section 3.6 we present the analytical expression of the nonlocal boundary condition in the particular case when Ω is a disk in \mathbb{R}^2 — this expression was first derived by Han and Wu [52, 53]. A complete derivation of our nonlocal boundary condition is given in Section B.2 of Appendix B.

3.2 Elasticity

In this section we briefly recall some important facts from tensor algebra, linear elasticity, and homogenization theory.

3.2.1 Tensor Algebra

We begin by recalling a few definitions given by Hegg [56, 57]. Let $d = 2$ or 3 be the dimension under consideration; then $\text{Sym}(\mathbb{R}^d)$ is the set of all symmetric linear mappings from \mathbb{R}^d to itself, i.e.,

$$\text{Sym}(\mathbb{R}^d) \equiv \{\mathbf{B} \in \mathbb{R}^d \otimes \mathbb{R}^d : \mathbf{B} = \mathbf{B}^T\}.$$

The *contraction* between two elements $\mathbf{B}, \mathbf{B}' \in \text{Sym}(\mathbb{R}^d)$ is defined by

$$\mathbf{B} : \mathbf{B}' \equiv B_{ij}B'_{ij},$$

where here and throughout this chapter we use the Einstein summation convention that repeated indices are summed from 1 to d . We define an inner product on $\text{Sym}(\mathbb{R}^d)$ by

$$\langle \mathbf{B}, \mathbf{B}' \rangle \equiv \frac{1}{2} \mathbf{B} : \mathbf{B}' = \frac{1}{2} \text{Tr}(\mathbf{B}\mathbf{B}') \quad (3.3)$$

for $\mathbf{B}, \mathbf{B}' \in \text{Sym}(\mathbb{R}^d)$ and where $\text{Tr}(\mathbf{B}) = B_{ii}$ is the trace of \mathbf{B} . The norm induced by the inner product (3.3) is

$$\|\mathbf{B}\|^2 = \frac{1}{2} \mathbf{B} : \mathbf{B}.$$

The set $\text{Sym}(\text{Sym}(\mathbb{R}^d))$ is defined as the set of symmetric linear mappings from $\text{Sym}(\mathbb{R}^d)$ to itself. If $\mathbb{A} \in \text{Sym}(\text{Sym}(\mathbb{R}^d))$ and $\mathbf{B} \in \text{Sym}(\mathbb{R}^d)$, then $\mathbb{A} : \mathbf{B} \in \text{Sym}(\mathbb{R}^d)$ with elements

$$(\mathbb{A} : \mathbf{B})_{ij} = A_{ijkl}B_{kl}. \quad (3.4)$$

We note that if $\mathbb{A} \in \text{Sym}(\text{Sym}(\mathbb{R}^d))$, then the elements of \mathbb{A} satisfy the major symmetries $A_{ijkl} = A_{klij}$ (since $\mathbb{A} = \mathbb{A}^T$) and the minor symmetries $A_{ijkl} = A_{jikl} = A_{ijlk}$ for $i, j, k, l = 1, \dots, d$ (the minor symmetries are due to (3.4) and the fact that $\mathbb{A} : \mathbf{B} \in \text{Sym}(\mathbb{R}^d)$).

The symbol \otimes denotes the *tensor product*. The tensor product of two vectors $\mathbf{q}, \mathbf{q}' \in \mathbb{R}^d$ is in $\mathbb{R}^d \otimes \mathbb{R}^d$ and has elements

$$(\mathbf{q} \otimes \mathbf{q}')_{ij} = q_i q'_j$$

for $i, j = 1, \dots, d$; similarly, the tensor product of two tensors $\mathbf{Q}, \mathbf{Q}' \in \mathbb{R}^d \otimes \mathbb{R}^d$ is in $\mathbb{R}^d \otimes \mathbb{R}^d \otimes \mathbb{R}^d \otimes \mathbb{R}^d$ and has elements

$$(\mathbf{Q} \otimes \mathbf{Q}')_{ijkl} = Q_{ij}Q'_{kl}$$

for $i, j, k, l = 1, \dots, d$.

3.2.2 Linear Elasticity

For more details on the topics in this section, see the book by Atkin and Fox [13]. Consider a linearly elastic body which is either a periodic composite material with unit cell $\Omega \subset \mathbb{R}^d$ or which occupies an open, bounded set $\Omega \subset \mathbb{R}^d$. Let $\mathbf{u}(\mathbf{x})$, $\boldsymbol{\varepsilon}(\mathbf{x})$, and $\boldsymbol{\sigma}(\mathbf{x})$ denote the displacement, linearized strain tensor, and Cauchy stress tensor, respectively, at the point $\mathbf{x} \in \Omega$. Then $\mathbf{u} \in \mathbb{R}^d$ while $\boldsymbol{\varepsilon}$ and $\boldsymbol{\sigma}$ belong to $\text{Sym}(\mathbb{R}^d)$ for all $\mathbf{x} \in \Omega$. By Hooke's Law, the stress and strain tensor are related through the linear constitutive relation

$$\boldsymbol{\sigma}(\mathbf{x}) = \mathbb{C}(\mathbf{x}) : \boldsymbol{\varepsilon}(\mathbf{x}), \quad (3.5)$$

where $\mathbb{C} \in \text{Sym}(\text{Sym}(\mathbb{R}^d))$ is the elasticity (or stiffness) tensor. We also assume \mathbb{C} is elliptic for all $\mathbf{x} \in \Omega$, i.e., there are positive constants a and b such that

$$\mathbf{B} : (\mathbb{C}(\mathbf{x}) : \mathbf{B}') \leq a \|\mathbf{B}\| \|\mathbf{B}'\| \quad \text{and} \quad \mathbf{B} : (\mathbb{C}(\mathbf{x}) : \mathbf{B}) \geq b \|\mathbf{B}\|^2$$

for all $\mathbf{B}, \mathbf{B}' \in \text{Sym}(\mathbb{R}^d)$. If there are no body forces present, then at equilibrium the elasticity equations are

$$\nabla \cdot \boldsymbol{\sigma}(\mathbf{x}) = 0, \quad \boldsymbol{\varepsilon}(\mathbf{x}) = \frac{1}{2} (\nabla \mathbf{u}(\mathbf{x}) + \nabla \mathbf{u}(\mathbf{x})^T), \quad \text{and} \quad \boldsymbol{\varepsilon}(\mathbf{x}) = \mathbb{C}(\mathbf{x}) : \boldsymbol{\sigma}(\mathbf{x}); \quad (3.6)$$

see the book by Milton [88, Chapter 2]. (Analogously to Chapters 2 and 4, these may also be considered as the quasistatic approximation to the time-harmonic dynamic elasticity equations if the wavelengths and attenuation lengths of the relevant displacement, strain, and stress fields are much larger than the dimensions of the body under consideration.)

If the composite is locally isotropic (so its material parameters are independent of direction), then the local elasticity tensor takes the form

$$\mathbb{C}(\mathbf{x}) = \lambda(\mathbf{x}) \mathbf{I} \otimes \mathbf{I} + 2\mu(\mathbf{x}) \mathbb{I},$$

where λ is the Lamé Modulus, μ is the shear modulus, $\mathbf{I} \in \text{Sym}(\mathbb{R}^d)$ is the second-order identity tensor with elements $I_{ij} = \delta_{ij}$ (where δ_{ij} is the Kronecker delta which is 1 if $i = j$ and 0 otherwise), and $\mathbb{I} \in \text{Sym}(\text{Sym}(\mathbb{R}^d))$ is the fourth-order identity tensor which maps an element in $\text{Sym}(\mathbb{R}^d)$ to itself under contraction, i.e., $\mathbb{I} : \mathbf{B} = \mathbf{B}$ for all $\mathbf{B} \in \text{Sym}(\mathbb{R}^d)$ [88].

In this case, Hooke's Law (3.5) reduces to

$$\mathcal{S}\mathbf{u}(\mathbf{x}) \equiv \boldsymbol{\sigma}(\mathbf{x}) = \lambda(\mathbf{x}) \operatorname{Tr}(\boldsymbol{\varepsilon}(\mathbf{x})) \mathbf{I} + 2\mu(\mathbf{x})\boldsymbol{\varepsilon}(\mathbf{x}) \quad (3.7)$$

$$= \lambda(\mathbf{x}) (\nabla \cdot \mathbf{u}(\mathbf{x})) \mathbf{I} + \mu(\mathbf{x}) (\nabla \mathbf{u}(\mathbf{x}) + \nabla \mathbf{u}(\mathbf{x})^T), \quad (3.8)$$

where $\mathcal{S} : \mathbb{R}^d \rightarrow \operatorname{Sym}(\mathbb{R}^d)$ is the linear stress operator that maps the displacement \mathbf{u} to the stress $\boldsymbol{\sigma}$ (note that \mathcal{S} itself depends on \mathbf{x} through $\lambda(\mathbf{x})$ and $\mu(\mathbf{x})$). We provide a more complete derivation of (3.7) and (3.8) in Section B.1 of Appendix B.

The bulk modulus, Young's Modulus, and the Poisson Ratio are related to λ and μ by

$$\kappa = \lambda + \frac{2\mu}{d}, \quad E = \frac{2\mu(d\lambda + 2\mu)}{(d-1)\lambda + 2\mu}, \quad \text{and} \quad \nu = \frac{\lambda}{(d-1)\lambda + 2\mu},$$

respectively [88, Chapter 2]. As was done by Ammari and Kang [11], throughout this chapter we assume

$$\mu(\mathbf{x}) > 0 \quad \text{and} \quad d\lambda(\mathbf{x}) + 2\mu(\mathbf{x}) > 0. \quad (3.9)$$

3.2.3 The Effective Elasticity Tensor

As in Chapter 2, we define the average of a tensor-valued function $\mathbf{M}(\mathbf{x})$ over a set $\mathcal{M} \subset \mathbb{R}^d$ by

$$\langle \mathbf{M} \rangle_{\mathcal{M}} \equiv \frac{1}{|\mathcal{M}|} \int_{\mathcal{M}} \mathbf{M}(\mathbf{x}) \, d\mathbf{x}, \quad (3.10)$$

where $|\mathcal{M}|$ denotes the Lebesgue measure of the set \mathcal{M} . The effective elasticity tensor \mathbb{C}_* is defined at sample points $\mathbf{x} \in \Omega$ through

$$\langle \boldsymbol{\sigma} \rangle_{\Omega'(\mathbf{x})} = \mathbb{C}_*(\mathbf{x}) \langle \boldsymbol{\varepsilon} \rangle_{\Omega'(\mathbf{x})}, \quad (3.11)$$

where $\Omega'(\mathbf{x})$ is a suitably chosen representative volume element centered at \mathbf{x} . When the composite is periodic, $\Omega'(\mathbf{x})$ is typically chosen to be the unit cell Ω ; when the composite fills an open bounded set $\Omega \subset \mathbb{R}^d$, $\Omega'(\mathbf{x})$ is typically a cube centered at \mathbf{x} that is small compared to Ω but large enough to ensure that the sample of the composite contained within $\Omega'(\mathbf{x})$ is representative of the composite as a whole. The effective tensor can then be defined for the remaining points in the composite by interpolation — see the review article by Hashin [54] and the book by Milton [88, Chapter 1] for brief introductions to homogenization theory and the references therein for more thorough treatments.

3.3 Uniform Field Relations

In this section we briefly summarize uniform field relations in the context of linear elasticity. These ideas were first introduced by Hill [58, 60, 61]. The main idea is contained in the following lemma, which in particular is due to Lurie, Cherkaev, and Federov [82, 83].

Lemma 3.1 *Let $\mathbf{V}, \mathbf{W} \in \text{Sym}(\mathbb{R}^d)$ be constant and let $\mathbb{C} \in \text{Sym}(\text{Sym}(\mathbb{R}^d))$ be the elasticity tensor of a linearly elastic material in Ω such that $\mathbb{C}(\mathbf{x}) : \mathbf{V} = \mathbf{W}$ for all $\mathbf{x} \in \Omega$. Then $\mathbb{C}_* : \mathbf{V} = \mathbf{W}$ as well.*

Proof of Lemma 3.1: Let $\mathbf{u}(\mathbf{x}) = \mathbf{V}\mathbf{x} + \mathbf{u}_0$, where $\mathbf{u}_0 \in \mathbb{R}^d$ is an arbitrary constant. Then, since $\mathbf{V} = \mathbf{V}^T$,

$$\boldsymbol{\varepsilon}(\mathbf{x}) = \frac{1}{2} (\nabla \mathbf{u}(\mathbf{x}) + \nabla \mathbf{u}(\mathbf{x})^T) = \frac{1}{2} (\mathbf{V} + \mathbf{V}^T) = \mathbf{V}$$

for all $\mathbf{x} \in \Omega$. If we set $\boldsymbol{\sigma}(\mathbf{x}) \equiv \mathbf{W}$, then $\nabla \cdot \boldsymbol{\sigma}(\mathbf{x}) = \nabla \cdot \mathbf{W} = 0$ and $\boldsymbol{\sigma}(\mathbf{x}) = \mathbf{W} = \mathbb{C}(\mathbf{x}) : \mathbf{V} = \mathbb{C}(\mathbf{x}) : \boldsymbol{\varepsilon}(\mathbf{x})$ for all $\mathbf{x} \in \Omega$. Thus $\boldsymbol{\varepsilon}(\mathbf{x}) = \mathbf{V}$ and $\boldsymbol{\sigma}(\mathbf{x}) = \mathbf{W}$ satisfy the elasticity equations (3.6) in Ω .

Since $\boldsymbol{\varepsilon}$ and $\boldsymbol{\sigma}$ are constant, they satisfy $\langle \boldsymbol{\varepsilon} \rangle_{\Omega'(\mathbf{x})} = \mathbf{V}$ and $\langle \boldsymbol{\sigma} \rangle_{\Omega'(\mathbf{x})} = \mathbf{W}$ for any set $\Omega'(\mathbf{x}) \subset \Omega$, particularly if $\Omega'(\mathbf{x})$ is a representative volume element centered at the sample point \mathbf{x} . Therefore

$$\mathbf{W} = \langle \boldsymbol{\sigma} \rangle_{\Omega'(\mathbf{x})} = \mathbb{C}_*(\mathbf{x}) : \langle \boldsymbol{\varepsilon} \rangle_{\Omega'(\mathbf{x})} = \mathbb{C}_*(\mathbf{x}) : \mathbf{V},$$

where the second equality holds by the definition of the effective elasticity tensor in (3.11). This completes the proof.

We now consider n -phase composites consisting of n isotropic and homogeneous materials with Lamé Moduli $\lambda_1, \dots, \lambda_n$ and shear modulus μ (Hill [60, 61] considered the case $n = 2$, although his results directly generalize to n -phase composites [88, Chapter 5]). The local elasticity tensor of such a material is

$$\mathbb{C}(\mathbf{x}) = \lambda(\mathbf{x})\mathbf{I} \otimes \mathbf{I} + 2\mu\mathbb{I}, \tag{3.12}$$

where $\lambda(\mathbf{x}) = \lambda_j \chi_j(\mathbf{x})$ and χ_j is the characteristic function of phase j , namely

$$\chi_j(\mathbf{x}) = \begin{cases} 1 & \text{if } \mathbf{x} \in \text{phase } j, \\ 0 & \text{otherwise.} \end{cases}$$

To see that a uniform field relation holds for this material, let $\mathbf{V} \in \text{Sym}(\mathbb{R}^d)$ be constant and orthogonal to \mathbf{I} , i.e., $\langle \mathbf{V}, \mathbf{I} \rangle = \frac{1}{2} \mathbf{V} : \mathbf{I} = \frac{1}{2} \text{Tr}(\mathbf{V}) = 0$. Then, by (3.12) (see also (3.7)),

$$\mathbb{C}(\mathbf{x}) : \mathbf{V} = \lambda(\mathbf{x}) \text{Tr}(\mathbf{V}) \mathbf{I} + 2\mu \mathbf{V} = 2\mu \mathbf{V},$$

which is constant. Lemma 3.1 then implies

$$\mathbb{C}_* : \mathbf{V} = 2\mu \mathbf{V} \Leftrightarrow (\mathbb{C}_* - 2\mu \mathbb{I}) : \mathbf{V} = 0$$

for all $\mathbf{V} \in \text{Sym}(\mathbb{R}^d)$ orthogonal to \mathbf{I} . This implies that the nullspace of $\mathbb{C}_* - 2\mu \mathbb{I}$ at least contains all tensors $\mathbf{V} \in \text{Sym}(\mathbb{R}^d)$ orthogonal to \mathbf{I} .

It is well known that if the local elasticity tensor \mathbb{C} is symmetric, then the effective elasticity tensor \mathbb{C}_* is symmetric as well [88, Section 12.10]. Thus $\mathbb{C}_* - 2\mu \mathbb{I}$ is symmetric. The Fredholm Alternative Theorem states that the nullspace and range of a tensor $\mathbb{D} \in \text{Sym}(\text{Sym}(\mathbb{R}^d))$ orthogonally decompose $\mathbb{R}^d \otimes \mathbb{R}^d$; in other words, any element $\mathbf{B} \in \text{Sym}(\mathbb{R}^d)$ can be written as $\mathbf{B}_r + \mathbf{B}_n$, where \mathbf{B}_r is in the range of \mathbb{D} and \mathbf{B}_n is in the nullspace of \mathbb{D} . Since the nullspace of the symmetric tensor $\mathbb{C}_* - 2\mu \mathbb{I}$ contains at least all $\mathbf{V} \in \text{Sym}(\mathbb{R}^d)$ orthogonal to $\mathbf{I} \in \text{Sym}(\mathbb{R}^d)$, by the Fredholm Alternative Theorem the range of $\mathbb{C}_* - 2\mu \mathbb{I}$ contains at most all tensors in $\text{Sym}(\mathbb{R}^d)$ parallel to \mathbf{I} . In other words, $\mathbb{C}_* - 2\mu \mathbb{I}$ is rank-one of the form

$$\mathbb{C}_* - 2\mu \mathbb{I} = \lambda_* \mathbf{I} \otimes \mathbf{I} \Leftrightarrow \mathbb{C}_* = \lambda_* \mathbf{I} \otimes \mathbf{I} + 2\mu \mathbb{I},$$

where λ_* is the effective Lamé Modulus. Therefore, the effective medium with elasticity tensor \mathbb{C}_* is elastically isotropic with shear modulus μ regardless of the microstructural complexity (which is encoded in the functions χ_j) — this was first recognized by Hill [61] in the two-phase composite case. See the review article of Milton [87], the work by Grabovsky et al. [42], the book by Milton [88, Chapter 5], and the thesis by Hegg [56] for collections of additional exact relations derived from uniform field relations.

Using techniques similar to those outlined in Section 3.4, Hill [60, 61] also showed that the effective Lamé Modulus λ_* is given by the exact formula

$$(\lambda_*(\mathbf{x}) + 2\mu)^{-1} = \langle (\lambda + 2\mu)^{-1} \rangle_{\Omega'(\mathbf{x})}, \quad (3.13)$$

where $\Omega'(\mathbf{x})$ is a suitably chosen representative volume element centered at the sample point $\mathbf{x} \in \Omega$ (although Hill [60, 61] only directly worked with the case $n = 2$, the formula (3.13) holds for all integers $n > 2$ as well [88, Chapter 5]).

We note that if the composite is a two-phase periodic or statistically homogeneous material, then the left- and right-hand sides of (3.13) are independent of \mathbf{x} and reduce to

$$\begin{aligned}
(\lambda_* + 2\mu)^{-1} &= \langle (\lambda + 2\mu)^{-1} \rangle_{\Omega'} \\
&= \frac{1}{|\Omega'|} \int_{\Omega'} (\lambda(\mathbf{x}) + 2\mu)^{-1} d\mathbf{x} \\
&= \frac{1}{|\Omega'|} \int_{\Omega'} (\lambda_1 + 2\mu)^{-1} \chi_1(\mathbf{x}) d\mathbf{x} + \frac{1}{|\Omega'|} \int_{\Omega'} (\lambda_2 + 2\mu)^{-1} \chi_2(\mathbf{x}) d\mathbf{x} \\
&= (\lambda_1 + 2\mu)^{-1} \langle \chi_1 \rangle_{\Omega'} + (\lambda_2 + 2\mu)^{-1} \langle \chi_2 \rangle_{\Omega'} \\
&= (\lambda_1 + 2\mu)^{-1} \theta_1 + (\lambda_2 + 2\mu)^{-1} \theta_2, \tag{3.14}
\end{aligned}$$

where, for $j = 1, 2$, $\theta_j \equiv \langle \chi_j \rangle_{\Omega'}$ is the volume fraction of phase j ; note that $\theta_1 + \theta_2 = 1$. Therefore, if λ_* is known (through an experimental measurement, for example), then the volume fraction of phase 1 is given exactly by

$$\theta_1 = \frac{(\lambda_2 - \lambda_*)(\lambda_1 + 2\mu)}{(\lambda_2 - \lambda_1)(\lambda_* + 2\mu)} \tag{3.15}$$

(where we have used the fact that $\theta_2 = 1 - \theta_1$ in (3.14)). In the n -phase case, (3.15) would be an exact relation between the volume fractions $\theta_1, \theta_2, \dots, \theta_n$ rather than an exact formula for θ_1 . For example, if $n = 3$, (3.13) gives the relationship

$$\theta_1 = \frac{(\lambda_1 + 2\mu)[(\lambda_2 + 2\mu)(\lambda_3 - \lambda_*) + \theta_2(\lambda_* + 2\mu)(\lambda_2 - \lambda_3)]}{(\lambda_* + 2\mu)(\lambda_2 + 2\mu)(\lambda_3 - \lambda_1)}$$

between θ_1 and θ_2 , where we have also used the relationship $\theta_1 + \theta_2 + \theta_3 = 1$. If, in addition, the individual densities ρ_1, ρ_2 , and ρ_3 are known and the overall density $\rho_* = \rho_1\theta_1 + \rho_2\theta_2 + \rho_3\theta_3$ has been measured, then the volume fractions θ_1, θ_2 , and θ_3 can all be determined exactly, at least in the generic case.

3.4 Exact Volume Fraction

In this section we derive a formula that gives the exact volume fraction occupied by an inclusion in a body, where our formula depends on a boundary measurement

of the displacement rather than on a measurement of λ_* as in (3.15). Let D and Ω be open, bounded sets in \mathbb{R}^d with $D \subset \Omega$. Suppose \mathbb{R}^d is filled with a linearly elastic, locally isotropic material with constant shear modulus μ and Lamé Modulus

$$\lambda(\mathbf{x}) = \lambda_1 \chi_D(\mathbf{x}) + \lambda_2 \chi_{\mathbb{R}^d \setminus \overline{D}}(\mathbf{x}). \quad (3.16)$$

Since the material is locally isotropic, the elasticity tensor is

$$\mathbb{C}(\mathbf{x}) = \lambda(\mathbf{x}) \mathbf{I} \otimes \mathbf{I} + 2\mu \mathbb{I}. \quad (3.17)$$

We can write $\mathcal{S}\mathbf{u}(\mathbf{x})$ from (3.8) as

$$\mathcal{S}\mathbf{u}(\mathbf{x}) = \begin{cases} \mathcal{S}_1 \mathbf{u}(\mathbf{x}) \equiv \lambda_1 (\nabla \cdot \mathbf{u}(\mathbf{x})) \mathbf{I} + \mu (\nabla \mathbf{u}(\mathbf{x}) + \nabla \mathbf{u}(\mathbf{x})^T) & \text{for } \mathbf{x} \in D, \\ \mathcal{S}_2 \mathbf{u}(\mathbf{x}) \equiv \lambda_2 (\nabla \cdot \mathbf{u}(\mathbf{x})) \mathbf{I} + \mu (\nabla \mathbf{u}(\mathbf{x}) + \nabla \mathbf{u}(\mathbf{x})^T) & \text{for } \mathbf{x} \in \mathbb{R}^d \setminus \overline{D}. \end{cases} \quad (3.18)$$

According to the elasticity equations in (3.6), the displacement \mathbf{u} satisfies

$$\begin{cases} \mathcal{L}_1 \mathbf{u} = 0 & \text{in } D, \\ \mathcal{L}_2 \mathbf{u} = 0 & \text{in } \mathbb{R}^d \setminus \overline{D}, \\ \mathbf{u}, \boldsymbol{\sigma} \cdot \mathbf{n}_D = (\mathcal{S}\mathbf{u}) \cdot \mathbf{n}_D & \text{continuous across } \partial D, \\ \mathbf{u} - \mathbf{f} = \mathcal{O}(|\mathbf{x}|^{1-d}) & \text{as } |\mathbf{x}| \rightarrow \infty, \end{cases} \quad (3.19)$$

where $\mathcal{L}_j \mathbf{u} = -(\lambda_j + \mu) \nabla (\nabla \cdot \mathbf{u}) - \mu \Delta \mathbf{u}$ (for $j = 1, 2$) is the Lamé Operator, \mathbf{n}_D is the outward unit normal vector to ∂D , $\boldsymbol{\sigma} = \mathcal{S}\mathbf{u}$ is the stress tensor associated with \mathbf{u} , and the function $\mathbf{f} = \nabla g$ is given and satisfies $\mathcal{L}_2 \mathbf{f} = \mathcal{L}_2 \nabla g = 0$ for all $\mathbf{x} \in \mathbb{R}^d$. To avoid possible technical complications we assume that g is at least three times continuously differentiable in \mathbb{R}^d . The function \mathbf{f} represents the “displacement at infinity”; perhaps the simplest example of such a function is $\mathbf{f}(\mathbf{x}) = \mathbf{x}$, in which case $g = \frac{1}{2}(\mathbf{x} \cdot \mathbf{x}) + \text{constant}$. As shown by Ammari and Kang [11, Chapters 9 and 10], there exists a unique solution \mathbf{u} to (3.19) if D is a Lipschitz Domain. For a derivation of (3.19) from (3.6), see Section B.1 in Appendix B.

Following Hill’s work [60, 61], we assume there is a continuously differentiable potential ϕ such that $\mathbf{u} = \nabla \phi$. In particular, we assume ϕ and $\nabla \phi$ are continuous across ∂D (by (3.19), $\mathbf{u} = \nabla \phi$ must be continuous across ∂D). Also, for $i, j = 1, \dots, d$, we have

$$(\nabla \nabla \phi)_{ij} = \frac{\partial^2 \phi}{\partial x_i \partial x_j}; \quad (3.20)$$

note that the matrix $\nabla\nabla\phi$ is symmetric in each phase. We only assume that ϕ and $\nabla\phi$ are continuous across ∂D (indeed, as shown by Hill [59], $\frac{\partial^2\phi}{\partial x_i\partial x_j}$ is discontinuous across ∂D). Then from (3.6) we have

$$\boldsymbol{\varepsilon} = \frac{1}{2}(\nabla\mathbf{u} + \nabla\mathbf{u}^T) = \frac{1}{2}(\nabla\nabla\phi + (\nabla\nabla\phi)^T) = \nabla\nabla\phi. \quad (3.21)$$

From (3.20) and (3.21) we have $\text{Tr}(\boldsymbol{\varepsilon}) = \text{Tr}(\nabla\nabla\phi) = \Delta\phi$, where $\Delta = \nabla \cdot \nabla = \frac{\partial^2}{\partial x_i\partial x_i}$ is the Laplacian. Then (3.7) and (3.21) imply

$$\boldsymbol{\sigma}(\mathbf{x}) = \mathbb{C}(\mathbf{x}) : \boldsymbol{\varepsilon}(\mathbf{x}) = \lambda(\mathbf{x})\Delta\phi\mathbf{I} + 2\mu\nabla\nabla\phi. \quad (3.22)$$

Finally, for $j = 1$ and $j = 2$ we have

$$\begin{aligned} \mathcal{L}_j\mathbf{u} &= -(\lambda_j + \mu)\nabla(\nabla \cdot \nabla\phi) - \mu\Delta(\nabla\phi) \\ &= -(\lambda_j + \mu)\nabla(\Delta\phi) - \mu\nabla(\Delta\phi) \\ &= -(\lambda_j + 2\mu)\nabla(\Delta\phi). \end{aligned} \quad (3.23)$$

By assumption, we have

$$0 = \mathcal{L}_2\mathbf{f} = -(\lambda_2 + 2\mu)\nabla(\Delta g)$$

for all $x \in \mathbb{R}^d$, so $\nabla(\Delta g) = 0$ for all $\mathbf{x} \in \mathbb{R}^d$. Then we must have $\Delta g = C_g \neq 0$ for all $\mathbf{x} \in \mathbb{R}^d$, where C_g is a constant. (The constant C_g is known since g is known; later we discuss why we must take $C_g \neq 0$.) Thus the function g must be chosen so that $g = \frac{C_g}{2}\mathbf{x} \cdot \mathbf{x} + g_h$, where g_h is harmonic in \mathbb{R}^d . This implies that g is infinitely differentiable in \mathbb{R}^d [32, Chapter 2].

Recalling that $\mathbf{u} = \nabla\phi$ and $\mathbf{f} = \nabla g$, we see that (3.23) implies that (3.19) becomes

$$\begin{cases} \nabla(\Delta\phi) = 0 & \text{in } D \text{ and } \mathbb{R}^d \setminus \overline{D}, \\ \nabla\phi, \boldsymbol{\sigma} \cdot \mathbf{n}_D = (\mathcal{S}\nabla\phi) \cdot \mathbf{n}_D & \text{continuous across } \partial D, \\ \nabla\phi - \nabla g = \mathcal{O}(|x|^{1-d}) & \text{as } |\mathbf{x}| \rightarrow \infty, \end{cases} \quad (3.24)$$

where $\boldsymbol{\sigma} = \mathcal{S}\nabla\phi$ is given in (3.22).

3.4.1 Behavior of $\Delta\phi$

In this section we study the behavior of $\Delta\phi$. Recall that we assume ϕ to be at least continuously differentiable in \mathbb{R}^d ; this implies that ϕ and $\mathbf{u} = \nabla\phi$ are continuous

across ∂D (see (3.24)). According to Ammari and Kang [11, equation (10.2)], if \mathbf{f} is smooth the solution \mathbf{u} to (3.19) is smooth in $\mathbb{R}^d \setminus \overline{D}$ and in D (although it is only continuous across ∂D).

Since ϕ is smooth in D and $\mathbb{R}^d \setminus \overline{D}$, (3.24) implies that $\Delta\phi$ is constant in each phase, i.e.,

$$\Delta\phi = \begin{cases} C_1 & \text{in } D, \\ C_2 & \text{in } \mathbb{R}^d \setminus \overline{D}. \end{cases} \quad (3.25)$$

Recall from (3.6) that $\nabla \cdot \boldsymbol{\sigma} = 0$ in \mathbb{R}^d . By (3.22), this becomes

$$\begin{aligned} 0 &= \nabla \cdot \boldsymbol{\sigma}(\mathbf{x}) \\ &= \nabla \cdot (\lambda(\mathbf{x})\Delta\phi(\mathbf{x})\mathbf{I} + 2\mu\nabla\nabla\phi(\mathbf{x})) \\ &= \nabla(\lambda(\mathbf{x})\Delta\phi(\mathbf{x})) + 2\mu\nabla \cdot \nabla\nabla\phi(\mathbf{x}) \\ &= \nabla(\lambda(\mathbf{x})\Delta\phi(\mathbf{x})) + 2\mu\Delta(\nabla\phi(\mathbf{x})) \\ &= \nabla((\lambda(\mathbf{x}) + 2\mu)\Delta\phi(\mathbf{x})). \end{aligned} \quad (3.26)$$

This implies that

$$(\lambda(\mathbf{x}) + 2\mu)\Delta\phi(\mathbf{x}) = C \quad \Leftrightarrow \quad \Delta\phi(\mathbf{x}) = \frac{C}{\lambda(\mathbf{x}) + 2\mu} \quad (3.27)$$

almost everywhere in \mathbb{R}^d , where C is a constant — see the book by Evans and Gariepy [33, Section 5.6.1]. Then, due to (3.25) and (3.27), we have

$$\Delta\phi = \begin{cases} C_1 = \frac{C}{\lambda_1 + 2\mu} & \text{in } D, \\ C_2 = \frac{C}{\lambda_2 + 2\mu} & \text{in } \mathbb{R}^d \setminus \overline{D}. \end{cases} \quad (3.28)$$

By (3.24), we have $\nabla\phi - \nabla g \rightarrow 0$ as $|\mathbf{x}| \rightarrow \infty$; thus $\Delta\phi - \Delta g \rightarrow 0$ as $|\mathbf{x}| \rightarrow \infty$. Since $\Delta g = C_g$, $\Delta\phi \rightarrow C_g$ as $|\mathbf{x}| \rightarrow \infty$. Since $\lambda(\mathbf{x}) = \lambda_2$ for large enough \mathbf{x} , we take the limit of (3.27) and find that

$$C = \lim_{|\mathbf{x}| \rightarrow \infty} ((\lambda(\mathbf{x}) + 2\mu)\Delta\phi(\mathbf{x})) = (\lambda_2 + 2\mu)C_g. \quad (3.29)$$

Finally, (3.16), (3.27), and (3.29) imply that

$$\Delta\phi = \nabla \cdot \mathbf{u} = \begin{cases} C_1 = \left(\frac{\lambda_2 + 2\mu}{\lambda_1 + 2\mu}\right) C_g & \text{in } D, \\ C_g & \text{in } \mathbb{R}^d \setminus \overline{D}. \end{cases} \quad (3.30)$$

3.4.2 Main Result

The divergence theorem and (3.30) imply

$$\begin{aligned}
\int_{\partial\Omega} \mathbf{u} \cdot \mathbf{n}_\Omega \, dS &= \int_{\Omega} \nabla \cdot \mathbf{u} \, d\mathbf{x} \\
&= \int_D \nabla \cdot \mathbf{u} \, d\mathbf{x} + \int_{\Omega \setminus \overline{D}} \nabla \cdot \mathbf{u} \, d\mathbf{x} \\
&= C_1 |D| + C_2 |\Omega \setminus \overline{D}| \\
&= C_1 |D| + C_2 (|\Omega| - |D|) \\
&= (C_1 - C_2) |D| + C_2 |\Omega|.
\end{aligned}$$

Therefore the volume fraction of the inclusion is given by the formula

$$\frac{|D|}{|\Omega|} = \frac{1}{C_1 - C_2} \left(\frac{1}{|\Omega|} \int_{\partial\Omega} \mathbf{u} \cdot \mathbf{n}_\Omega \, dS - C_2 \right), \quad (3.31)$$

where C_1 and C_2 are related to C_g by (3.30), respectively. Since we are assuming we have complete knowledge of \mathbf{u} around $\partial\Omega$ from our measurement, and since $C_g = \Delta g$ is given, (3.31) allows us to exactly determine $|D|/|\Omega|$. Note also that we must take $C_g \neq 0$. If $C_g = 0$, then (3.30) implies that $C_1 = C_2 = 0$, which makes the formula in (3.31) undefined. We have thus proved the following theorem.

Theorem 3.1 *Let D and Ω be open, bounded sets in \mathbb{R}^d ($d = 2$ or 3) such that $D \subset \Omega$ and $\partial D, \partial\Omega$ are smooth. Suppose \mathbb{R}^d is filled with a material described by the local elasticity tensor given by (3.17) and (3.16). Also suppose $\mathbf{f} = \nabla g$ is given and $\mathcal{L}_2 \mathbf{f} = -(\lambda_2 + \mu) \nabla(\nabla \cdot \mathbf{f}) - \mu \Delta \mathbf{f} = 0$ ($\Leftrightarrow \Delta g = C_g \neq 0$) for all $\mathbf{x} \in \mathbb{R}^d$. Assume that $\mathbf{u} \cdot \mathbf{n}_\Omega$ is known around $\partial\Omega$. Then the volume fraction of the inclusion D is given by (3.31).*

3.5 Finite Medium

Consider again the linear elasticity problem from Section 3.4, namely that of an inclusion D in a body Ω which in turn is embedded in an infinite medium $\mathbb{R}^d \setminus \overline{\Omega}$. The isotropic and homogeneous materials in D and $\mathbb{R}^d \setminus \overline{D}$ have Lamé Moduli λ_1 and λ_2 , respectively; we also assume that both materials have the same shear modulus μ . If a displacement $\mathbf{f} = \nabla g$ is applied at infinity, then the displacement $\mathbf{u} = \nabla \phi$ satisfies (3.19) (so ϕ satisfies (3.24)). Recall that we require $\mathcal{L}_2 \mathbf{f} = 0$ in \mathbb{R}^d , which implies $\Delta g = C_g$ in \mathbb{R}^d . Since g and $\mathbf{f} = \nabla g$ are smooth in \mathbb{R}^d , g , \mathbf{f} , and $\mathcal{S}_2 \mathbf{f}$ are continuous

up to ∂D from outside D ; in other words the limits $g|_{\partial D^+}$, $\mathbf{f}|_{\partial D^+}$, and $(\mathcal{S}_2\mathbf{f})|_{\partial D^+}$ exist and are finite at each point of ∂D , where $h|_{\partial D^+}$ and $h|_{\partial D^-}$ denote the restriction of the function h to ∂D from outside and inside D , respectively.

We now derive a boundary condition \mathbf{P} so that the solution \mathbf{u}' to

$$\begin{cases} \mathcal{L}_1\mathbf{u}' = 0 & \text{for } \mathbf{x} \in D, \\ \mathcal{L}_2\mathbf{u}' = 0 & \text{for } \mathbf{x} \in \Omega \setminus \overline{D}, \\ \mathbf{u}', \boldsymbol{\sigma}' \cdot \mathbf{n}_D = (\mathcal{S}\mathbf{u}') \cdot \mathbf{n}_D & \text{continuous across } \partial D, \\ \mathbf{P}(\mathbf{u}'_0, \mathbf{t}'_0, \mathbf{f}_0, \mathbf{F}_0) = 0 & \text{on } \partial\Omega \end{cases} \quad (3.32)$$

is equal to the solution \mathbf{u} to (3.19) restricted to $\overline{\Omega}$, i.e., $\mathbf{u}' = \mathbf{u}|_{\overline{\Omega}}$; we have defined

$$\mathbf{u}'_0 \equiv \mathbf{u}'|_{\partial\Omega^-}, \quad \mathbf{t}'_0 \equiv (\boldsymbol{\sigma}'|_{\partial\Omega^-}) \cdot \mathbf{n}_\Omega, \quad \mathbf{f}_0 \equiv \mathbf{f}|_{\partial\Omega^+}, \quad \text{and} \quad \mathbf{F}_0 \equiv ((\mathcal{S}_2\mathbf{f})|_{\partial\Omega^+}) \cdot \mathbf{n}_\Omega. \quad (3.33)$$

This allows us to apply our formula (3.31) to the problem (3.32), which is posed on the finite domain Ω . For details on a related problem (including proofs of the well-posedness of problems similar to (3.32)), see Han and Wu's work [52, 53].

To derive the boundary condition \mathbf{P} , we begin by considering the following exterior problem:

$$\begin{cases} \mathcal{L}_E\tilde{\mathbf{u}}_E = 0 & \text{for } \mathbf{x} \in \mathbb{R}^d \setminus \overline{\Omega}, \\ \tilde{\mathbf{u}}_E = \tilde{\mathbf{u}} & \text{on } \partial\Omega, \\ \tilde{\mathbf{u}}_E \rightarrow 0 & \text{as } |\mathbf{x}| \rightarrow \infty, \end{cases} \quad (3.34)$$

where $\mathcal{L}_E\mathbf{u} = -(\lambda_E + \mu)\nabla(\nabla \cdot \mathbf{u}) - \mu\Delta\mathbf{u}$, $\lambda_E = \lambda_2$, and $\tilde{\mathbf{u}}$ is a given displacement on $\partial\Omega$. Ultimately we wish to find the normal stress distribution $(\tilde{\boldsymbol{\sigma}}_E|_{\partial\Omega^+}) \cdot \mathbf{n}_\Omega$ around $\partial\Omega$ given $\tilde{\mathbf{u}}$ — this mapping from the displacement on the boundary to the traction on the boundary is defined as the Exterior Dirichlet-to-Neumann Map.

Definition 3.1 *The Exterior Dirichlet-to-Neumann (DtN) Map Λ_E is defined by*

$$\Lambda_E(\tilde{\mathbf{u}}_E|_{\partial\Omega^+}) = \Lambda_E(\tilde{\mathbf{u}}) \equiv (\tilde{\boldsymbol{\sigma}}_E|_{\partial\Omega^+}) \cdot \mathbf{n}_\Omega = ((\mathcal{S}\tilde{\mathbf{u}}_E)|_{\partial\Omega^+}) \cdot \mathbf{n}_\Omega, \quad (3.35)$$

where $\tilde{\mathbf{u}}_E$ solves (3.34) and $\tilde{\boldsymbol{\sigma}}_E$ and $\mathcal{S}\tilde{\mathbf{u}}_E$ are given by (3.8) (with $\lambda(\mathbf{x}) = \lambda_E$).

3.5.1 Equivalent Boundary Value Problems

We now return to the problem (3.19), which has a unique solution \mathbf{u} . We introduce exterior fields

$$\mathbf{u}_E(\mathbf{x}) \equiv \mathbf{u}|_{\mathbb{R}^d \setminus \Omega} \quad \text{and} \quad \boldsymbol{\sigma}_E(\mathbf{x}) \equiv \boldsymbol{\sigma}|_{\mathbb{R}^d \setminus \Omega}; \quad (3.36)$$

we also introduce interior fields

$$\mathbf{u}_I(\mathbf{x}) \equiv \mathbf{u}|_{\bar{\Omega}} \quad \text{and} \quad \boldsymbol{\sigma}_I(\mathbf{x}) \equiv \boldsymbol{\sigma}|_{\bar{\Omega}}. \quad (3.37)$$

Recall that $\lambda_E = \lambda_2$.

Lemma 3.2 *Define $\tilde{\mathbf{u}}_E \equiv \mathbf{u}_E - \mathbf{f}$ where \mathbf{u}_E is defined in (3.36) and $\mathbf{f} = \nabla g$ satisfies $\mathcal{L}_E \mathbf{f} = 0$ in \mathbb{R}^d . Then $\tilde{\mathbf{u}}_E$ solves (3.34) with $\tilde{\mathbf{u}} = (\mathbf{u}_I|_{\partial\Omega^-}) - \mathbf{f}_0$, where $\mathbf{f}_0 = \mathbf{f}|_{\partial\Omega^+}$ is defined in (3.33).*

Proof of Lemma 3.2: First, since $\mathcal{L}_E \mathbf{u}_E = 0$ in $\mathbb{R}^d \setminus \bar{\Omega}$ (by (3.19)) and $\mathcal{L}_E \mathbf{f} = 0$ in $\mathbb{R}^d \setminus \bar{\Omega}$, we have

$$\mathcal{L}_E \tilde{\mathbf{u}}_E = \mathcal{L}_E(\mathbf{u}_E - \mathbf{f}) = \mathcal{L}_E \mathbf{u}_E - \mathcal{L}_E \mathbf{f} = 0$$

in $\mathbb{R}^d \setminus \bar{\Omega}$ as well. Second, recall from (3.34) that $\tilde{\mathbf{u}} \equiv \tilde{\mathbf{u}}_E|_{\partial\Omega^+} \equiv (\mathbf{u}_E|_{\partial\Omega^+}) - \mathbf{f}_0$. Since $\lambda_E = \lambda_2$, \mathbf{u} must be continuous across $\partial\Omega$, i.e., $\mathbf{u}_E|_{\partial\Omega^+} = \mathbf{u}_I|_{\partial\Omega^-}$. Hence $\tilde{\mathbf{u}} = (\mathbf{u}_I|_{\partial\Omega^-}) - \mathbf{f}_0$. Finally, $\tilde{\mathbf{u}}_E = \mathbf{u}_E - \mathbf{f} \rightarrow 0$ as $|\mathbf{x}| \rightarrow \infty$ by (3.19). Thus $\tilde{\mathbf{u}}_E$ solves (3.34) with $\tilde{\mathbf{u}} = (\mathbf{u}_I|_{\partial\Omega^-}) - \mathbf{f}_0$. This completes the proof.

Theorem 3.2 *Suppose \mathbf{u} solves (3.19) with $\mathbf{f} = \nabla g$ and $g = \frac{C_g}{2} \mathbf{x} \cdot \mathbf{x} + g_h$ where $C_g \neq 0$ is an arbitrary constant and $\Delta g_h = 0$ in \mathbb{R}^d . Define \mathbf{u}_E , $\boldsymbol{\sigma}_E$ and \mathbf{u}_I , $\boldsymbol{\sigma}_I$ as in (3.36) and (3.37), respectively. Finally, define $\tilde{\mathbf{u}}_E = \mathbf{u}_E - \mathbf{f}$. Then \mathbf{u}_I satisfies*

$$\begin{cases} \mathcal{L}_1 \mathbf{u}_I = 0 & \text{in } D, \\ \mathcal{L}_2 \mathbf{u}_I = 0 & \text{in } \Omega \setminus \bar{D}, \\ \mathbf{u}_I, \boldsymbol{\sigma}_I \cdot \mathbf{n}_D = (\mathcal{S} \mathbf{u}_I) \cdot \mathbf{n}_D & \text{continuous across } \partial D, \\ \mathbf{P}(\mathbf{u}_I|_{\partial\Omega^-}, (\boldsymbol{\sigma}_I|_{\partial\Omega^-}) \cdot \mathbf{n}_\Omega, \mathbf{f}_0, \mathbf{F}_0) = 0 & \text{on } \partial\Omega, \end{cases} \quad (3.38)$$

where

$$\mathbf{P}(\mathbf{u}_I|_{\partial\Omega^-}, (\boldsymbol{\sigma}_I|_{\partial\Omega^-}) \cdot \mathbf{n}_\Omega, \mathbf{f}_0, \mathbf{F}_0) \equiv (\boldsymbol{\sigma}_I|_{\partial\Omega^-}) \cdot \mathbf{n}_\Omega - \Lambda_E((\mathbf{u}_I|_{\partial\Omega^-}) - \mathbf{f}_0) - \mathbf{F}_0 \quad (3.39)$$

and \mathbf{f}_0 and \mathbf{F}_0 are defined in (3.33).

Proof of Theorem 3.2: By definition (see (3.19) and (3.37)), \mathbf{u}_I satisfies the differential equations and continuity conditions in (3.38). By Lemma 3.2, $\tilde{\mathbf{u}}_E = \mathbf{u}_E - \mathbf{f}$ solves (3.34) with $\tilde{\mathbf{u}} = (\mathbf{u}_I|_{\partial\Omega^-}) - \mathbf{f}|_{\partial\Omega^+}$. By (3.35), then, we have

$$(\tilde{\boldsymbol{\sigma}}_E|_{\partial\Omega^+}) \cdot \mathbf{n}_\Omega = \Lambda_E(\tilde{\mathbf{u}}) = \Lambda_E((\mathbf{u}_I|_{\partial\Omega^-}) - \mathbf{f}_0). \quad (3.40)$$

Since \mathcal{S}_E is linear, we have

$$(\tilde{\boldsymbol{\sigma}}_E|_{\partial\Omega^+}) \cdot \mathbf{n}_\Omega = ((\mathcal{S}_E \tilde{\mathbf{u}}_E)|_{\partial\Omega^+}) \cdot \mathbf{n}_\Omega = ((\mathcal{S}_E \mathbf{u}_E)|_{\partial\Omega^+}) \cdot \mathbf{n}_\Omega - \mathbf{F}_0. \quad (3.41)$$

Then (3.40) and (3.41) imply

$$((\mathcal{S}_E \mathbf{u}_E)|_{\partial\Omega^+}) \cdot \mathbf{n}_\Omega = \Lambda_E((\mathbf{u}_I|_{\partial\Omega^-}) - \mathbf{f}_0) + \mathbf{F}_0. \quad (3.42)$$

Since $\lambda_E = \lambda_2$, the traction across $\partial\Omega$ must be continuous, i.e.,

$$((\mathcal{S}_E \mathbf{u}_E)|_{\partial\Omega^+}) \cdot \mathbf{n}_\Omega = (\boldsymbol{\sigma}_E|_{\partial\Omega^+}) \cdot \mathbf{n}_\Omega = (\boldsymbol{\sigma}_I|_{\partial\Omega^-}) \cdot \mathbf{n}_\Omega.$$

Inserting this into (3.42) gives

$$\Lambda_E((\mathbf{u}_I|_{\partial\Omega^-}) - \mathbf{f}_0) + \mathbf{F}_0 = (\boldsymbol{\sigma}_I|_{\partial\Omega^-}) \cdot \mathbf{n}_\Omega. \quad (3.43)$$

We define $\mathbf{P}(\mathbf{u}_I|_{\partial\Omega^-}, (\boldsymbol{\sigma}_I|_{\partial\Omega^-}) \cdot \mathbf{n}_\Omega, \mathbf{f}_0, \mathbf{F}_0)$ as in (3.39). Then, due to (3.43), the interior part of the solution \mathbf{u} , namely \mathbf{u}_I , satisfies (3.38). This completes the proof.

We can thus identify the solution \mathbf{u}' of (3.32) with \mathbf{u}_I which solves (3.38), i.e., $\mathbf{u}' = \mathbf{u}_I = \mathbf{u}|_{\overline{\Omega}}$. In other words, the solution to (3.32) in the finite domain Ω will be exactly the same as if Ω were placed in an infinite medium with Lamé Parameters λ_E and μ and a displacement ∇g were applied at infinity. Therefore, if we apply the boundary condition

$$\mathbf{P}(\mathbf{u}'_0, \mathbf{t}'_0, \mathbf{f}_0, \mathbf{F}_0) = \mathbf{t}'_0 - \Lambda_E(\mathbf{u}'_0 - \mathbf{f}_0) - \mathbf{F}_0 = 0 \quad (3.44)$$

on $\partial\Omega$, where \mathbf{u}'_0 , \mathbf{t}'_0 , \mathbf{f}_0 , and \mathbf{F}_0 are defined in (3.33), we can use the measurement of $\mathbf{u}' \cdot \mathbf{n}_\Omega$ around $\partial\Omega$ (i.e., $\mathbf{u}'_0 \cdot \mathbf{n}_\Omega$) along with (3.31) (with \mathbf{u} replaced by \mathbf{u}') to find the volume fraction occupied by D .

Remark 3.1 *Since the geometry inside the body Ω is unknown, we cannot write $\boldsymbol{\sigma}' \cdot \mathbf{n}_\Omega$ in terms of \mathbf{u}' (since we would not know whether or not to use λ_1 or λ_2 in (3.8)). Practically, we would typically apply a displacement \mathbf{u}'_0 around $\partial\Omega$ with a known \mathbf{f} and measure the resulting traction \mathbf{t}'_0 around $\partial\Omega$. The displacement \mathbf{u}'_0 and traction \mathbf{t}'_0 around $\partial\Omega$ must be tailored so that $\mathbf{P}(\mathbf{u}'_0, \mathbf{t}'_0, \mathbf{f}_0, \mathbf{F}_0) = 0$ — see (3.44).*

3.6 2-D Example

The results presented here were first derived in a slightly different form by Han and Wu [52, 53]. We consider the case when $d = 2$ and Ω is a disk of radius R centered at the origin, denoted B_R . In this geometry, it is possible to determine Λ_E exactly by first solving (3.34) for the displacement $\tilde{\mathbf{u}}_E$ in terms of $\tilde{\mathbf{u}} = \tilde{\mathbf{u}}_E|_{\partial B_R}$ and then computing the corresponding traction around ∂B_R , namely

$$(\tilde{\boldsymbol{\sigma}}_E|_{\partial B_R^+}) \cdot \mathbf{n}_{B_R} = \left(\tilde{\boldsymbol{\sigma}}_E \cdot \frac{\mathbf{x}}{R} \right) \Big|_{\partial B_R^+} = \left(\mathcal{S}_E(\tilde{\mathbf{u}}_E) \cdot \frac{\mathbf{x}}{R} \right) \Big|_{\partial B_R^+}.$$

We state the main results here and defer the calculations to Section B.2 in Appendix B. For more general regions, Λ_E may have to be computed numerically.

3.6.1 Exterior Dirichlet-to-Neumann Map

We denote the polar components of $\tilde{\mathbf{u}}_E$ by $\tilde{u}_{E,r}$ and $\tilde{u}_{E,\theta}$. It is convenient to write

$$\tilde{\mathbf{u}}_E(r, \theta) = \tilde{u}_{E,r}(r, \theta) + i\tilde{u}_{E,\theta}(r, \theta),$$

where $i = \sqrt{-1}$; see Section B.2 in Appendix B and the books by Muskhelishvili [99] and England [30] for more details.

We begin by expanding $\tilde{\mathbf{u}}(\theta) = \tilde{u}_r(\theta) + i\tilde{u}_\theta(\theta)$ in a Fourier Series, namely

$$\tilde{u}_r(\theta) + i\tilde{u}_\theta(\theta) = \sum_{n=-\infty}^{\infty} \tilde{u}_n e^{in\theta}, \quad \text{where} \quad \tilde{u}_n = \frac{1}{2\pi} \int_0^{2\pi} (\tilde{u}_r(\theta') + i\tilde{u}_\theta(\theta')) e^{-in\theta'} d\theta', \quad (3.45)$$

for $n \in \mathbb{Z}$. Then it can be shown that

$$\begin{aligned} & \tilde{u}_{E,r}(r, \theta) + i\tilde{u}_{E,\theta}(r, \theta) \\ &= \tilde{u}_0 R r^{-1} + \sum_{n=1}^{\infty} \tilde{u}_{-n} R^{n-1} r^{-(n-1)} e^{-in\theta} \\ & \quad + \sum_{n=1}^{\infty} \left(\tilde{u}_n R^{n+1} r^{-(n+1)} + \left(\frac{n-1}{\rho_E} \right) \overline{\tilde{u}_{-n}} R^{n-1} r^{-(n+1)} (r^2 - R^2) \right) e^{in\theta} \end{aligned} \quad (3.46)$$

for $r \geq R$ and where $\rho_E \equiv (\lambda_E + 3\mu)/(\lambda + \mu)$ — see Appendix B.

Next we recall from (3.35) that $\Lambda_E(\tilde{\mathbf{u}}) = (\tilde{\boldsymbol{\sigma}}_E|_{\partial B_R^+}) \cdot \mathbf{n}_{B_R}$. In polar coordinates, the components of the traction around the boundary of the disk of radius $r \geq R$ are $\tilde{\sigma}_{E,rr}(r, \theta) + i\tilde{\sigma}_{E,r\theta}(r, \theta)$ (where $\tilde{\sigma}_{E,rr}$ is the radial component of the traction and $\tilde{\sigma}_{E,r\theta}$

is the angular component of the traction). In particular, the traction around ∂B_R is given by

$$\tilde{\sigma}_{E,rr}(R^+, \theta) + i\tilde{\sigma}_{E,r\theta}(R^+, \theta) = \Lambda_E(\tilde{\mathbf{u}}) = \sum_{n=-\infty}^{\infty} \tilde{\sigma}_n e^{in\theta}, \quad (3.47)$$

where $\tilde{\sigma}_{E,rr}(R^+, \theta) + i\tilde{\sigma}_{E,r\theta}(R^+, \theta) = (\tilde{\sigma}_{E,rr} + i\tilde{\sigma}_{E,r\theta})|_{\partial B_R^+}$,

$$\begin{cases} \tilde{\sigma}_n = -\frac{2\mu}{R}(n+1)\tilde{u}_n & (n \geq 0), \\ \tilde{\sigma}_{-n} = -\frac{2\mu}{R\rho_E}(n-1)\tilde{u}_{-n} & (n \geq 1), \end{cases} \quad (3.48)$$

and the coefficients \tilde{u}_n are defined in (3.45).

3.6.2 Nonlocal Boundary Condition

Next, we derive an expression for the boundary condition $\mathbf{P}(\mathbf{u}'_0, \mathbf{t}'_0, \mathbf{f}_0, \mathbf{F}_0) = 0$, where \mathbf{P} is defined in (3.44). We begin by expanding \mathbf{f}_0 in a Fourier Series around ∂B_R ; we have

$$(f_r + if_\theta)|_{\partial B_R^+} = f_r(R^+, \theta) + if_\theta(R^+, \theta) = f_{0,r}(\theta) + if_{0,\theta}(\theta) = \sum_{n=-\infty}^{\infty} f_{0,n} e^{in\theta}, \quad (3.49)$$

where

$$f_{0,n} = \frac{1}{2\pi} \int_0^{2\pi} (f_{0,r}(\theta') + if_{0,\theta}(\theta')) e^{-in\theta'} d\theta'.$$

Next we define

$$\mathbf{F} \equiv \mathcal{S}_E \mathbf{f} = \mathcal{S}_E \nabla g = \lambda_E \Delta g \mathbf{I} + 2\mu \nabla \nabla g,$$

where the last equality holds by (3.18). Recall from (3.33) that $\mathbf{F}_0 = (\mathbf{F}|_{\partial B_R^+}) \cdot \mathbf{n}_{B_R}$. In complex notation, the normal components of \mathbf{F} around the boundary of a disk of radius $r \geq R$ are given by $F_{rr}(r, \theta) + iF_{r\theta}(r, \theta)$, where F_{rr} is the radial component and $F_{r\theta}$ is the angular component. We can expand $(F_{rr} + iF_{r\theta})|_{\partial B_R^+}$ in a Fourier Series as

$$(F_{rr} + iF_{r\theta})|_{\partial B_R^+} = F_{rr}(R^+, \theta) + iF_{r\theta}(R^+, \theta) = F_{0,r}(\theta) + iF_{0,\theta}(\theta) = \sum_{n=-\infty}^{\infty} F_{0,n} e^{in\theta}, \quad (3.50)$$

where

$$F_{0,n} = \frac{1}{2\pi} \int_0^{2\pi} (F_{0,r}(\theta') + iF_{0,\theta}(\theta')) e^{-in\theta'} d\theta'.$$

Next we expand g in a Fourier Series around the disk of radius $r \geq R$ as

$$g(r, \theta) = \sum_{n=-\infty}^{\infty} g_n(r) e^{in\theta}, \quad \text{where} \quad g_n(r) = \frac{1}{2\pi} \int_0^{2\pi} g(r, \theta') e^{-in\theta'} d\theta'.$$

We can write the Fourier Coefficients $F_{0,n}$ in terms of the coefficients g_n as

$$\begin{aligned} F_{0,n} = & (\lambda_E + 2\mu) \frac{\partial^2 g_n(r)}{\partial r^2} \Big|_{r \rightarrow R^+} + \lambda_E \left(\frac{1}{R} \frac{\partial g_n(r)}{\partial r} \Big|_{r \rightarrow R^+} - \frac{n^2}{R^2} g_n(R^+) \right) \\ & + 2\mu \left(-\frac{n}{R} \frac{\partial g_n(r)}{\partial r} \Big|_{r \rightarrow R^+} + \frac{n}{R^2} g_n(R^+) \right). \end{aligned} \quad (3.51)$$

Returning to (3.39), recall that $(\mathbf{u}'|_{\partial B_R^-}) - \mathbf{f}|_{\partial B_R^+} = \mathbf{u}'_0 - \mathbf{f}_0 = \tilde{\mathbf{u}}$, where \mathbf{u}' solves (3.32). Thus if we write

$$(u'_r + iu'_\theta)|_{\partial B_R^-} = u'_r(R^-, \theta) + iu'_\theta(R^-, \theta) = u'_{0,r}(\theta) + iu'_{0,\theta}(\theta) = \sum_{n=-\infty}^{\infty} u'_{0,n} e^{in\theta},$$

where

$$u'_{0,n} = \frac{1}{2\pi} \int_0^{2\pi} (u'_{0,r}(\theta') + iu'_{0,\theta}(\theta')) e^{in\theta'} d\theta',$$

then $u'_{0,n} - f_{0,n} = \tilde{u}_n$ — see (3.45). The components of the traction $(\boldsymbol{\sigma}'|_{\partial B_R^-}) \cdot \mathbf{n}_{B_R} = \mathbf{t}'_0$ can be written in polar coordinates as $t'_{0,r}(\theta) + it'_{0,\theta}(\theta)$. This can be expanded in a Fourier Series as well, namely

$$(\sigma'_{rr} + i\sigma'_{r\theta})|_{\partial B_R^-} = \sigma'_{rr}(R^-, \theta) + i\sigma'_{r\theta}(R^-, \theta) = t'_{0,r}(\theta) + it'_{0,\theta}(\theta) = \sum_{n=-\infty}^{\infty} t'_{0,n} e^{in\theta},$$

where

$$t'_{0,n} = \frac{1}{2\pi} \int_0^{2\pi} (t'_{0,r}(\theta') + it'_{0,\theta}(\theta')) e^{-in\theta'} d\theta'.$$

Recalling the Fourier Expansions of \mathbf{f}_0 given in (3.49), \mathbf{F}_0 given in (3.50) (and (3.51)), and $\Lambda_E(\tilde{\mathbf{u}}) = \Lambda_E(\mathbf{u}'_0 - \mathbf{f}_0)$ given in (3.47)–(3.48), the boundary condition $\mathbf{P}(\mathbf{u}'_0, \mathbf{t}'_0, \mathbf{f}_0, \mathbf{F}_0) = 0$ is equivalent to

$$\begin{aligned} \mathbf{t}'_0 - \mathbf{F}_0 - \Lambda_E(\mathbf{u}'_0 - \mathbf{f}_0) &= 0 \\ \Leftrightarrow \sum_{n=-1}^{\infty} \left(t'_{0,n} - F_{0,n} + \frac{2\mu}{R}(n+1)(u'_{0,n} - f_{0,n}) \right) e^{in\theta} \\ &+ \sum_{n=2}^{\infty} \left(t'_{0,-n} - F_{0,-n} + \frac{2\mu}{R\rho_E}(n-1)(u'_{-n} - f_{0,-n}) \right) e^{-in\theta} = 0. \end{aligned} \quad (3.52)$$

Therefore we have the following relationships between the Fourier Coefficients of the polar components of the displacement, traction, and applied stress around ∂B_R :

$$\left\{ \begin{array}{l} t'_{0,n} - F_{0,n} + \frac{2\mu}{R}(n+1)(u'_{0,n} - f_{0,n}) = 0 \quad (n \geq -1), \\ t'_{0,-n} - F_{0,-n} + \frac{2\mu}{R\rho_E}(n-1)(u'_{-n} - f_{0,-n}) = 0 \quad (n \geq 2). \end{array} \right. \quad (3.53)$$

Remark 3.2 Recall from (3.32) that \mathbf{t}'_0 is the traction around ∂B_R due to the applied displacement \mathbf{u}'_0 . In practice, one could consider applying a displacement \mathbf{u}'_0 around $\partial\Omega$ with a known \mathbf{f} and then measuring \mathbf{t}'_0 around ∂B_R . The applied displacement \mathbf{u}'_0 and measured traction \mathbf{t}'_0 have to be such that (3.52) (and, hence, (3.53)) holds.

3.6.3 Previous Results

Previously, Han and Wu [52, 53] also derived an expression for the Exterior DtN Map $\Lambda_E(\tilde{\mathbf{u}})$. They found the solution $\tilde{\mathbf{u}}_E$ to (3.34) by a method slightly different from the one we used; they then computed the Cartesian Components of the traction $\tilde{\boldsymbol{\sigma}}_E \cdot \mathbf{n}_\Omega$ around ∂B_R . In particular, if we denote the Cartesian Components of $\tilde{\mathbf{u}}_E$ by \tilde{u}_E and \tilde{v}_E , the Cartesian Components of $\tilde{\mathbf{u}}_E|_{\partial B_R^+} = \tilde{\mathbf{u}}$ by \tilde{u} and \tilde{v} , and the Cartesian Components of the traction $(\tilde{\boldsymbol{\sigma}}_E|_{\partial B_R^+}) \cdot \mathbf{n}_{B_R}$ by \tilde{X} and \tilde{Y} , then $\Lambda_E(\tilde{\mathbf{u}}) = \Lambda_E(\tilde{u} + i\tilde{v}) = \tilde{X} + i\tilde{Y}$. In particular, Han and Wu [53, equations (29) and (30)] showed that

$$\begin{aligned} \tilde{X} &= \frac{2 + 2\eta}{1 + 2\eta} \frac{\mu}{\pi R} \sum_{n=1}^{\infty} \int_0^{2\pi} \frac{d^2 \tilde{u}(\theta')}{d\theta'^2} \frac{\cos n(\theta - \theta')}{n} d\theta' \\ &\quad - \frac{2\eta}{1 + 2\eta} \frac{\mu}{\pi R} \sum_{n=1}^{\infty} \int_0^{2\pi} \frac{d^2 \tilde{v}(\theta')}{d\theta'^2} \frac{\sin n(\theta - \theta')}{n} d\theta'; \\ \tilde{Y} &= \frac{2 + 2\eta}{1 + 2\eta} \frac{\mu}{\pi R} \sum_{n=1}^{\infty} \int_0^{2\pi} \frac{d^2 \tilde{v}(\theta')}{d\theta'^2} \frac{\cos n(\theta - \theta')}{n} d\theta' \\ &\quad + \frac{2\eta}{1 + 2\eta} \frac{\mu}{\pi R} \sum_{n=1}^{\infty} \int_0^{2\pi} \frac{d^2 \tilde{u}(\theta')}{d\theta'^2} \frac{\sin n(\theta - \theta')}{n} d\theta' \end{aligned} \tag{3.54}$$

where $\tilde{u}(\theta') = \tilde{u}_E(R^+, \theta')$, $\tilde{v}(\theta') = \tilde{v}_E(R^+, \theta')$, and $\eta = \mu/(\lambda_E + \mu)$. Also see the books by Muskhelishvili [99, Section 83] and England [30, Section 4.2] for solutions to problems related to (3.34) based on potential formulations. In Section B.3 Appendix B we show that our formulas (3.47)–(3.48) agree with (3.54) as long as $\tilde{\mathbf{u}}$ is smooth enough.

CHAPTER 4

SENSITIVITY OF ANOMALOUS LOCALIZED RESONANCE PHENOMENA TO DISSIPATION

In this chapter we study the effects of placing charge density distributions in the vicinity of a superlens, which, roughly speaking, is a slab of material with a negative index of refraction. We will see that the electrical power dissipated in the lens has quite interesting behavior.

4.1 Introduction

No matter how well a conventional lens is constructed, it cannot focus light to an arbitrarily small point; in particular, the best resolution one can expect from even a perfectly constructed lens is on the order of $\lambda/2$, where λ is the wavelength of the light being used to image the object [37, 109]. In general there are two types of waves present when an object is illuminated: propagating waves and evanescent waves. Propagating waves can be collected and focused by conventional lenses, but evanescent waves, which contain information about the finest details of the object to be imaged, decay exponentially in amplitude away from the object and thus cannot be focused by a conventional lens [37, 95, 109]. Pendry [109] pointed out that this limitation of lenses to focus light to an arbitrarily small point is a physical restriction that cannot be reduced by using a larger aperture or by constructing a perfect lens.

For example, in vacuum green light has a wavelength of about 500 nanometers. Thus if one uses green light to illuminate an object and a conventional lens for imaging, the best resolution one can expect is approximately 250 nanometers; in other words, the smallest objects that could be distinguished in this setup are on the order of 250 nanometers in size. Many objects of biological interest, such as DNA and proteins,

are smaller than this (many proteins can fit in a sphere with a radius on the order of a few tens of nanometers [31]), so an improvement in the resolving power of lenses would be welcomed by many people.

Pendry [109] suggested that certain materials, known as negative index materials (due to their negative index of refraction), could be used to construct *superlenses* with perfect resolving power; such lenses would be able to image arbitrarily small objects perfectly, with no limitation on the resolution. Pendry claimed that such a lens would operate by collecting and focusing both propagating waves and evanescent waves. In particular, he argued that a superlens would amplify the evanescent waves (in contrast to conventional lenses, in which evanescent waves decay), thus allowing the finest details of the object to be imaged. Pendry also noted that this amplification does not violate conservation of energy since evanescent waves do not transport any energy.

The superlens discussed by Pendry [109] was in fact first formally studied by Veselago in 1967 [121]. The geometry Veselago studied is illustrated in Figure 4.1. It consists of a slab of material with dielectric constant (relative permittivity) ε and relative permeability μ inserted in vacuum (which has dielectric constant 1 and relative permeability 1). In the surrounding medium (vacuum), the index of refraction is $n_0 = 1$; the index of refraction in the slab is $n = \pm\sqrt{\varepsilon\mu}$. As discussed by Veselago, if ε and μ are both positive, then the positive sign must be chosen for n to ensure causality; on the other hand, if ε and μ are both negative, then the negative sign must be chosen for n to preserve causality. Veselago showed that materials with $\varepsilon = \mu = -1$ (hence with $n = -1$) have quite interesting behavior.

For example, consider Figure 4.1. We have a slab of material located in the region $0 \leq x \leq d$ with index of refraction n surrounded by vacuum; there is a point source located at the point $(-l, 0)$. In Figure 4.1(a), we trace the trajectories of four light rays as they pass through a slab with index of refraction $n = 2$. Even though there is a slight bending of the rays at the interfaces of the lens due to Snell's Law, the rays move farther apart as they travel from left to right. In particular, the rays on each side of an interface are on opposite sides of the normal to that interface. In Figure 4.1(b), we trace the trajectories of four rays in the case when the slab has an

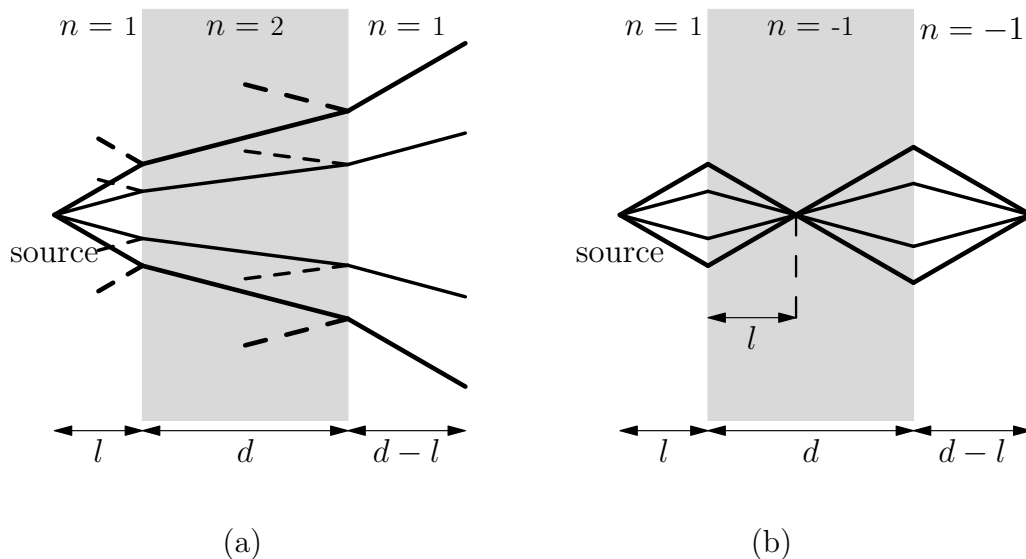


Figure 4.1. In this figure, we illustrate the behavior of light rays as they pass through a conventional (positive-index) slab lens and a slab superlens (with a negative index of refraction). (a) This is a plot of a slab with index of refraction $n = 2$ inserted in vacuum (with index of refraction 1). The rays are traced using Snell’s Law and the geometric optics approximation. Reflected waves are shown as dashed lines. (b) This is the same plot as (a) but now the slab has an index of refraction $n = -1$. Note that there are no reflected waves in this case.

index of refraction $n = -1$. Veselago showed that Snell’s Law still holds in this case, so that the rays on each side of an interface appear on the same side of the normal to the interface. Also, the rays focus at the points $(l, 0)$ and $(2d - l, 0)$. This slab is impedance matched with vacuum, so there are no reflected waves [109, 121].

Veselago deemed materials with negative ε and μ left-handed materials since the electric field, magnetic field, and wave vector form a left-handed set in these materials (they form a right-handed set in materials with a positive index of refraction). He also showed that the phase velocity is negative in the slab (i.e., from right to left in Figure 4.1(b)) but that the Poynting Vector, which gives the direction of energy transport, points from left to right in Figure 4.1(b). In other words, for a monochromatic wave in such a material the phase velocity is in the direction opposite to the direction of energy flow. The Doppler Effect is reversed in left-handed materials, and such materials also have several other interesting properties [121].

Pendry’s [109] suggestion that a slab like that in Figure 4.1(b) could amplify evanescent waves and produce images with superresolution created quite a controversy

— see the article by Minkel [95]. Garcia and Nieto-Vesperinas [37] showed that there were mistakes in Pendry’s work, such as an inconsistent choice of the sign of the wavenumber. However, there is an even more fundamental issue, discovered by Nicorovici, McPhedran, and Milton in 1994 [104].

From now on we follow Nicorovici et al. [104] and Milton, Nicorovici, McPhedran, and Podolskiy [94] and consider a cylindrical superlens in the quasistatic regime, in which the wavelengths and attenuation lengths of the electric and magnetic fields are much larger than relevant dimensions of the body (we review the results for the Veselago Slab Lens later in this section). See Chapter 2 for more on the quasistatic approximation.

The geometry of the problem is illustrated in Figure 4.2. In particular, Nicorovici et al. [104] and Milton et al. [94] considered a core of radius r_c with dielectric constant ε_c surrounded by a shell of inner radius r_c and outer radius r_s with dielectric constant ε_s ; this in turn was embedded in a medium with dielectric constant ε_m which extended out to r_m . If $\varepsilon_c = \varepsilon_m = 1$ and $\varepsilon_s = -1$, this situation is analogous to the Veselago Lens mentioned above. (Milton, Nicorovici, McPhedran, and Podolskiy [94] also studied the slab lens — we review their results for that case, which are very similar to their results for the cylindrical case, later in this section.) As pointed out by Nicorovici et al. [104] and Milton et al. [94], the above choice of parameters is not feasible since the quasistatic equations (discussed below — see (4.2)) do not have a solution unless the lens in the annulus (or the slab) has some loss. Loss is typically represented by a small positive imaginary part in the dielectric constant.

In particular, the dielectric constant is given by

$$\varepsilon(r) = \begin{cases} \varepsilon_c & \text{for } 0 \leq r < r_c, \\ \varepsilon_s & \text{for } r_c \leq r \leq r_s, \\ \varepsilon_m & \text{for } r_s < r \leq r_m. \end{cases}$$

We take ε_s to be of the form $\varepsilon_s = -1 + i\delta$, where $\delta > 0$ represents the loss in the lens. In the quasistatic regime, the complex potential V satisfies

$$-\nabla \cdot [\varepsilon(r)\nabla V(r, \theta)] = \rho, \quad (4.1)$$

where ρ represents a charge density distribution. Similar to Chapter 2, the electric field is given by $\mathbf{E} = -\nabla V$ and the displacement field is given by $\mathbf{D} = \varepsilon\mathbf{E}$. The

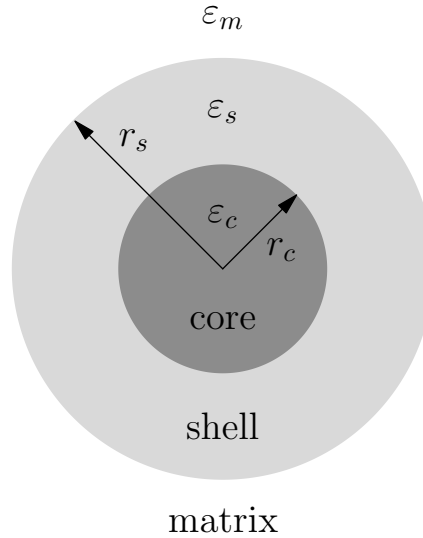


Figure 4.2. This is a sketch of the cylindrical superlens. The core is a cylinder of radius r_c containing a material with dielectric constant ϵ_c ; the shell or superlens is contained within the annulus $r_c < r < r_s$ and has a dielectric constant of $\epsilon_s = -1 + i\delta$ where $\delta > 0$ is small; the matrix extends out to r_m (which we generally take to be quite large) and has a dielectric constant of ϵ_m .

complex permittivity ϵ is related to the complex conductivity σ from Chapter 2 by $\epsilon = (i/\omega)\sigma$. See Section C.1 in Appendix C for more on this.

Following Nicorovici et al. [104] (also see the work by Milton et al. [94]), we take ρ to be a dipole located at a distance r_0 from the origin with $r_s < r_0 < r_m$. Although Nicorovici et al. [104] and Milton et al. [94] presented numerous interesting results, we present only a selection of them here. We should also point out that the paper by Nicorovici et al. [104] contains a minor error, but it was later corrected by Milton et al. [94]; however, the results of Nicorovici et al. [104] still hold.

Nicorovici, McPhedran, and Milton assumed that ρ was a dipole scaled in such a way that the potential due to ρ was given by $1/(z - r_0)$, where $z = re^{i\theta} = x + iy$ is a complex variable and the dipole was located at the point $(r_0, 0)$. They then used separation of variables and the requirements that the potential V and the normal displacement $-\epsilon \frac{\partial V}{\partial r}$ must be continuous across material boundaries to derive the solution for the potential in the core, shell, and matrix.

Their first result is as follows. Define $r_* \equiv r_s^2/r_c > r_s$, and suppose that $r_0 > r_*$. Then the response of the coated cylinder (the core/shell configuration) to this

applied (quasistatic) dipole field will be exactly the same as if the coated cylinder were replaced by a solid cylinder of radius r_* with dielectric constant ε_c [94, 104]. In particular, if $\varepsilon_c = \varepsilon_m$, then the annulus in $r_c < r < r_s$ will be completely invisible to external observers. We note that this result holds for any applied quasistatic field with sources outside the radius r_* , not just dipole sources. In Figure 4.3(a) we provide a contour plot of the real part of V in the case when $\varepsilon_c = 4$, $\varepsilon_m = 1$, and $\varepsilon_s = -1 + i10^{-12}$. Figure 4.3(b) is a contour plot of the real part of the potential in the case when only a solid cylinder of radius r_* and dielectric constant ε_c is present. Note the similarity between Figures 4.3(a) and (b) outside of the radius r_* . Note also the similarity between the potential in the core in Figure 4.3(a) and the potential in the solid cylinder in Figure 4.3(b). Figure 4.4 is the same as Figure 4.3, except in this case we take $\varepsilon_c = \varepsilon_m = 1$. Notice that the annular lens is essentially invisible to an external observer in this case, and that the potentials in Figures 4.4(a) and (b) are the same all the way up to the radius r_s . Finally, note the similarity of the potential inside the radius r_c in Figure 4.4(a) with the potential inside the radius r_* in Figure 4.4(b). Figures 4.3 and 4.4 were created using equations (2.1), (2.3), (2.17), and (3.7) from the work by Milton et al. [94] (we cut off the sums at $N = 100$).

The potential due to a dipole located at $(r_0, 0)$ with a solid cylinder of radius r_* and dielectric constant ε_c centered at the origin can be solved using the method of images [63, Chapter 4], which can be described as follows. If the dipole is located at the point $(r_0, 0)$, consider an image dipole located at the point $(r_i, 0)$, where $(r_i, 0) = (r_*^2/r_0, 0)$ is the image of the point $(r_0, 0)$ under reflection through the circle of radius r_* centered at the origin. (One must also take into account the reflection of the dipole moment through the circle of radius r_* , but for our purposes the location of the image dipole is sufficient.) Figure 4.5 provides an illustration of the method of images.

What Nicorovici et al. [104] noticed was that the image dipole, located at $(r_i, 0) = (r_*^2/r_0, 0)$, was inside the shell if and only if $r_0 > r_{\text{crit}} \equiv r_s^3/r_c^2$. To see this, note that

$$r_i = \frac{r_*^2}{r_0} = \frac{r_s^4}{r_0 r_c^2} = \left(\frac{r_{\text{crit}}}{r_0} \right) r_s,$$

so $r_i < r_s$ if and only if $r_0 > r_{\text{crit}}$. If $r_i > r_s$, the image dipole would be located in the matrix in the physical configuration (the core surrounded by the shell). In other words, the potential would have a singularity at $(r_i, 0)$ in the matrix in addition to the

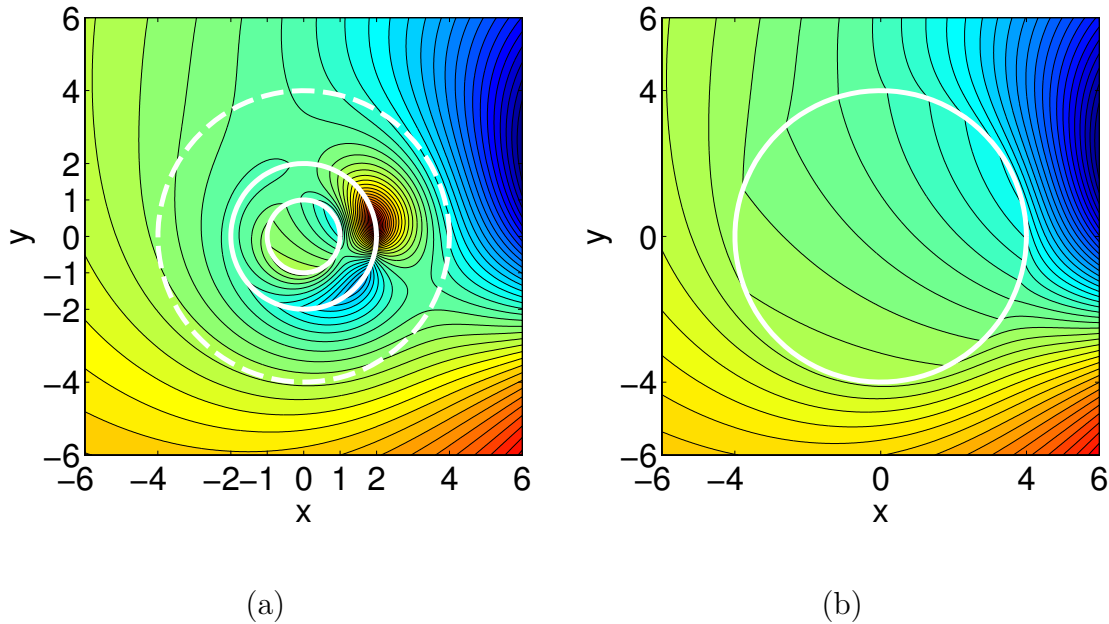


Figure 4.3. We illustrate the nonresonant potential in the case when the core and the surrounding medium have different dielectric constants. (a) We plot the real part of the potential V when the superlens is present. The dipole is located at the point $(r_0, 0)$, where $r_0 > r_{\text{crit}}$. The boundaries of the core and shell are illustrated by the inner and outer solid white circles, respectively; the dashed circle at the radius r_* is drawn for reference. (b) The corresponding plot of the real part of the potential V when a solid cylinder of radius $r_* = r_s^2/r_c$ with dielectric constant $\varepsilon_c = 4$ is present. Note that both figures are the same outside the radius r_* (shown by the dashed line in (a) and the solid line in (b)). The relevant parameters are: $r_c = 1$, $r_s = 2$, $r_* = 4$, $r_{\text{crit}} = 8$, $r_0 = 12$, $\varepsilon_c = 4$, $\varepsilon_s = -1 + i10^{-12}$, and $\varepsilon_m = 1$. The values of the potential range from -0.1008 (blue) to 0.1051 (red).

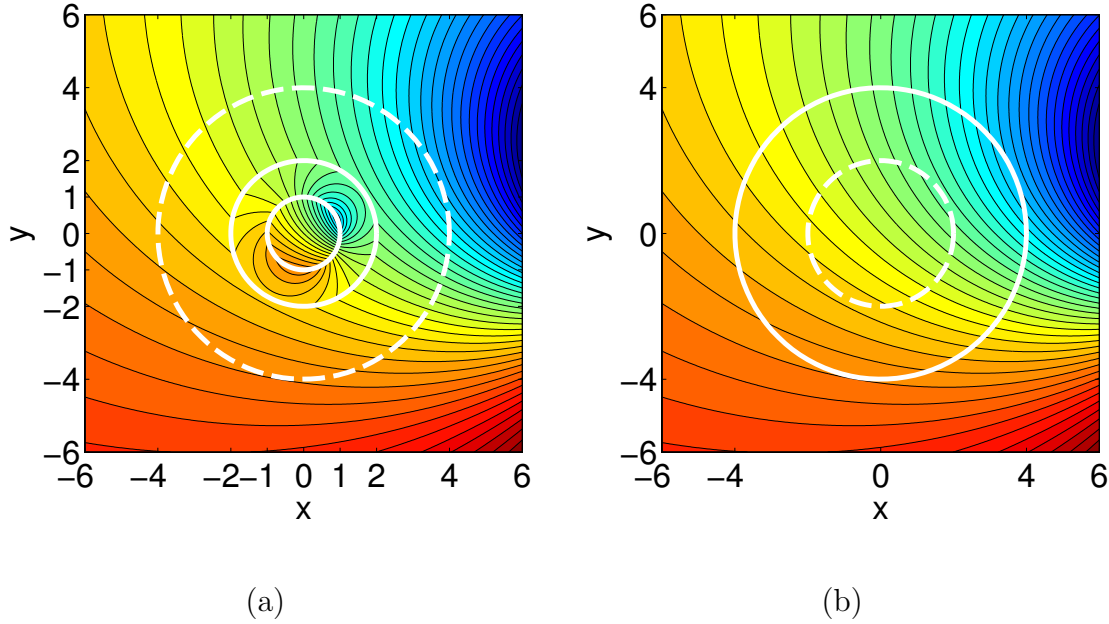


Figure 4.4. This figure is the same as Figure 4.3, except now we have taken $\varepsilon_c = \varepsilon_m = 1$. The values of the potential are between -0.1179 (blue) and 0.0833 (red). In (b) we plot a circle of radius r_s (white dashed curve) for reference.

physical singularity at $(r_0, 0)$. This leads to a contradiction [94, 104]. In particular, suppose $r_s < r_i < \tilde{r} < r_* < r_0$. Then, since there are no physical sources in the annulus $r_s < r < \tilde{r}$ and the real and imaginary parts of the potential are harmonic there due to (4.1), the maximum principle implies that the real and imaginary parts of the potential must attain their maximum values on the boundary of this annulus, namely at $r = r_s$ or $r = \tilde{r}$ [32, Chapter 2]. If the real or imaginary part of the potential diverges at $r = r_i$ in the limit as $\delta \rightarrow 0^+$, then the maximum of the real or imaginary part of the potential (which occurs at $r = r_s$ or $r = \tilde{r}$) must diverge in this limit as well. In other words, there cannot be an isolated singularity at the point $(r_i, 0)$. Finally, note that this image dipole is only used to solve for the potential in the matrix; thus if the image dipole is in the shell or core so that $r_i < r_s$ there is no problem — the shell potential does not contain this singularity.

This is what leads to the phenomenon of anomalous localized resonance: as $\delta \rightarrow 0^+$, the potential diverges in regions with sharp boundaries not defined by physical boundaries between different media; outside these regions the potential converges to a smooth potential (we discuss this more below). A dramatic illustration of this is given

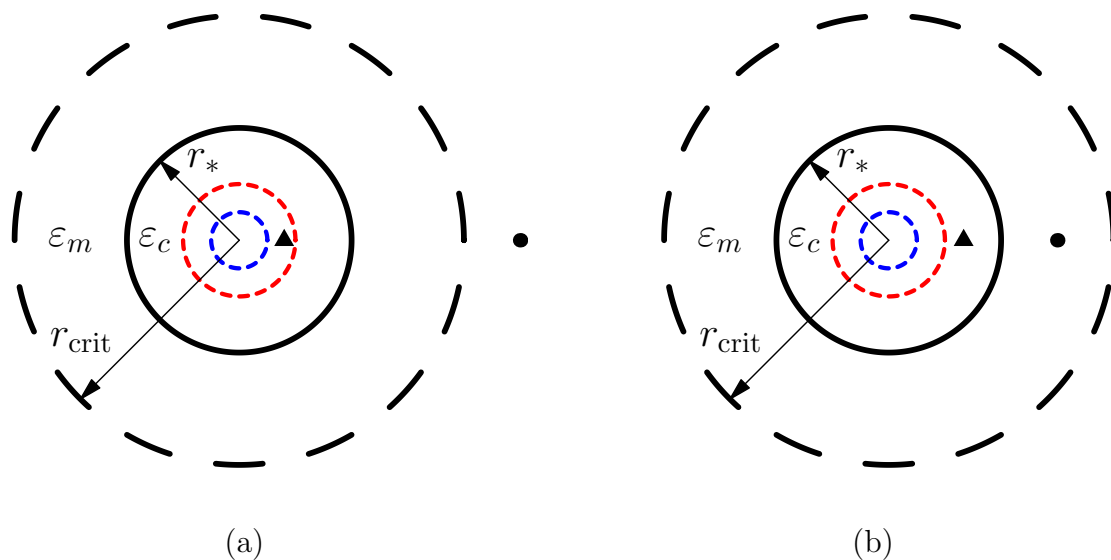


Figure 4.5. This figure illustrates the method of images. The source (black dot), located at the point $(r_0, 0)$, is reflected through the circle of radius r_* (solid circle) to obtain an image source (black triangle) inside the circle of radius r_* . The circle of radius r_{crit} is drawn as a black dashed curve. The outer and inner boundaries of the shell (at r_s and r_c , respectively) are drawn as red and blue dashed curves, respectively, for reference. (a) Here the source is located beyond the critical radius, so $r_0 > r_{\text{crit}}$. Thus the image dipole is located inside the shell (i.e., $r_i < r_s$). (b) The source is located within the critical radius (but outside the radius r_*), so $r_s < r_0 < r_{\text{crit}}$. The image dipole is therefore located outside of the shell (i.e., $r_i > r_s$).

in Figure 4.6, which is based on Figure 4 in the work of Milton et al. [94]. Figure 4.6(a) is a plot of the real part of the potential when $r_s < r_0 < r_{\text{crit}}$ and $\varepsilon_c \neq \varepsilon_m$. Note that the resonance is localized to an annular region around the boundary of the shell. Outside of this resonant region the potential is smooth — in particular, for $r > r_*$, the potential in Figures 4.6(a) and (b) is the same in the limit $\delta \rightarrow 0^+$. Also, near the boundaries of the resonant region, the potential looks suspiciously like a reflected version of the dipole source (it can be rigorously shown that the potential does indeed converge to a reflected version of the dipole — see below for more on this). This was discovered in 1994 by Nicorovici et al. [104], and, as mentioned by Milton et al. [94], it may have been the first observation of perfect imaging of a point source.

Finally, note that r_* takes the place of r_{crit} when $\varepsilon_c = \varepsilon_m$ since there is no image dipole in that case (the equivalent cylinder with dielectric constant $\varepsilon_c = \varepsilon_m$ is really just part of the matrix in that case). In Figure 4.7 we plot the (a) real and (b) imaginary parts of the potential in the case when $\varepsilon_c = \varepsilon_m = 1$ and $r_s < r_0 < r_*$.

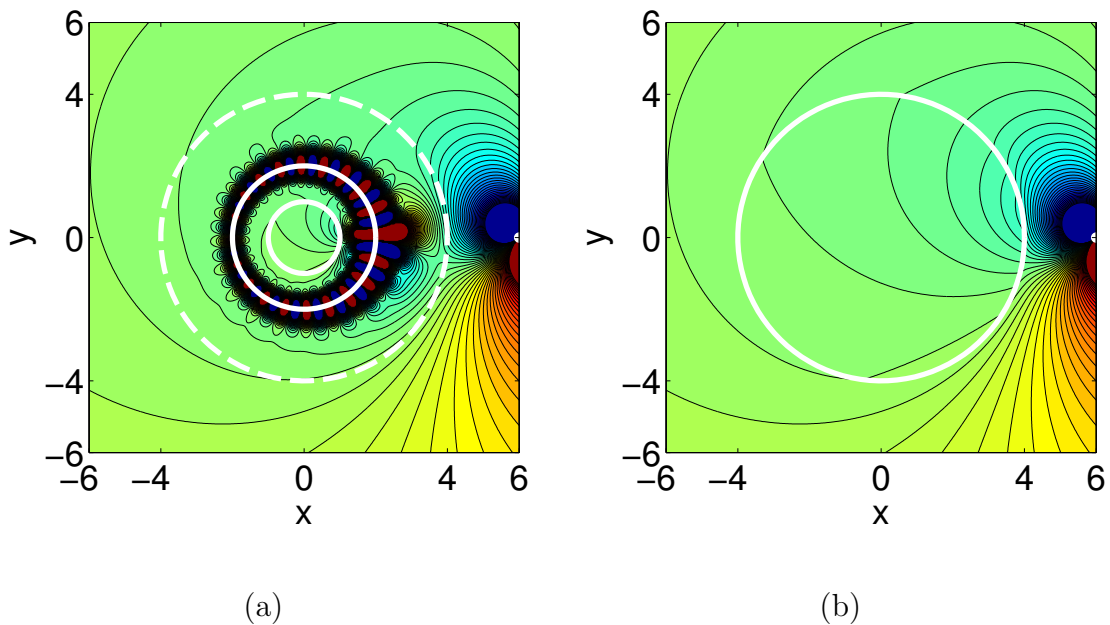


Figure 4.6. This figure is the same as Figure 4.3, except now the dipole is located within the critical radius, i.e., $r_s < r_0 < r_{\text{crit}}$. In particular, we took $r_0 = 6$ and $r_{\text{crit}} = 8$. The values of the potential in $[-1, 1]$ are displayed on a color scale going from dark blue ($V \leq -1$) to dark red ($V \geq 1$). The white dot represents the location of the dipole at the point $(r_0, 0)$.

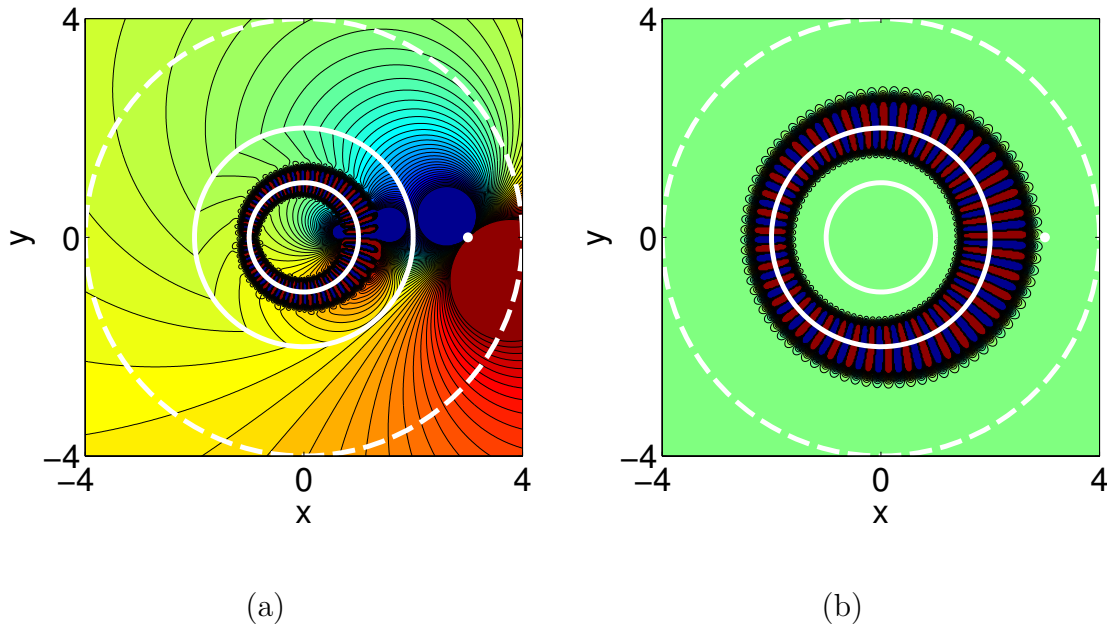


Figure 4.7. The parameters used in this figure are exactly the same as those in Figure 4.4, except now the dipole is located within the critical radius, i.e., $r_s < r_0 < r_*$ (since $\varepsilon_c = \varepsilon_m = 1$, the critical radius is now r_*). In particular, we took $r_0 = 3$ and $r_* = 4$. The values of the potential in $[-1, 1]$ are displayed on a color scale going from dark blue ($V \leq -1$) to dark red ($V \geq 1$). The white dot represents the location of the dipole at the point $(r_0, 0)$. (a) The real part of the potential — note the resonant annulus around the boundary of the core and the (nearly) perfect and magnified image dipoles near the boundaries of the resonant layer. (b) The imaginary part of the potential — note that the resonant annulus surrounds the boundary of the shell.

Figure 4.7 is also based on Figure 4 from the work of Milton et al. [94]. Notice that there are resonant annuli around the boundary of the shell and around the boundary of the core. In the case $\varepsilon_c \neq \varepsilon_m$ there is no resonant region around the core. Figures 4.6 and 4.7 were created using equations (2.1), (2.3), (2.17), and (3.7) from the work by Milton et al. [94] (we cut off the sums at $N = 100$).

As shown by Milton and Nicorovici [91], perhaps the most surprising result is that a polarizable dipole (one whose dipole moment depends on the external field acting on the dipole) becomes cloaked in the limit as $\delta \rightarrow 0^+$ if it is close enough to the lens. In particular, suppose an external field with sources located only outside of the radius r_{crit} is applied. Then, if $\varepsilon_c = \varepsilon_m = 1$ the polarizable dipole (and any finite collection of polarizable dipoles) will be cloaked in the limit $\delta \rightarrow 0^+$ as long as it is located within the annulus $r_s < r < \sqrt{r_s^3/r_c}$. See the works by Milton and Nicorovici [91] and Nicorovici, McPhedran, Botten, and Milton [108] for numerical illustrations of cloaking due to anomalous localized resonance.

4.1.1 Our Results

In this chapter, we discuss anomalous localized resonance phenomena observed at the interface between positive index and negative index materials. Such phenomena have been at the center of an interesting cloaking strategy [8–10, 15, 20, 23, 72, 91–94, 104–108, 122].

As illustrated in Figure 4.8, the (2-D) geometry we consider consists of a central layer in $\mathcal{S} \equiv [0, a] \times (-\infty, \infty)$ bordered by a layer to the left in $\mathcal{C} \equiv (-\infty, 0) \times (-\infty, \infty)$ and a layer to the right in $\mathcal{M} \equiv (a, +\infty) \times (-\infty, \infty)$. We work in the nonmagnetic quasistatic regime, i.e., the regime in which the magnetic permeability equals 1 and relevant wavelengths and attenuation lengths are much larger than other dimensions in the problem (such as a , the thickness of the slab \mathcal{S}). In this regime the complex electric potential V satisfies the Laplace equation

$$-\nabla \cdot [\varepsilon(x, y) \nabla V(x, y)] = \rho \quad \text{in } \mathbb{R}^2, \quad (4.2)$$

where V is also subject to certain continuity conditions and conditions at infinity (these are discussed in more detail in Section 4.2), ε is the dielectric constant (relative

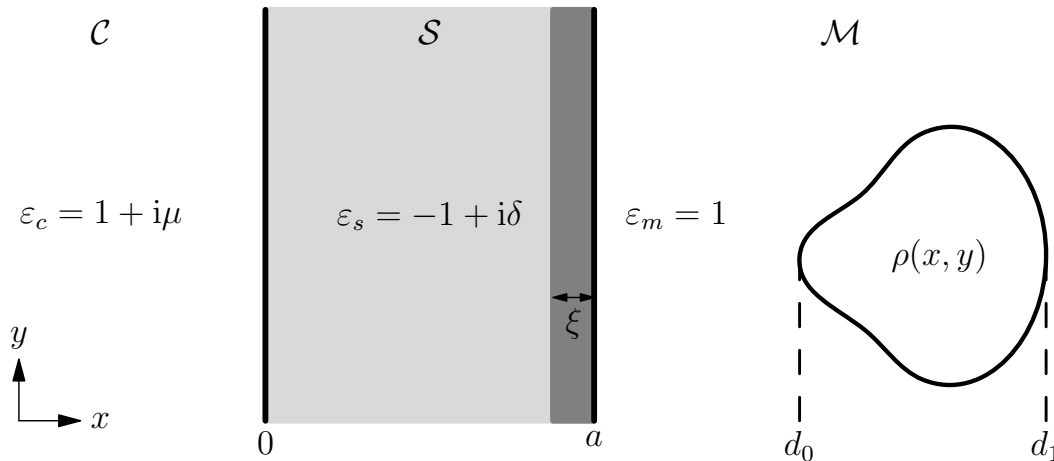


Figure 4.8. We consider a slab geometry with a dielectric constant as illustrated in the figure. The slab (shaded light gray) is in the region $\mathcal{S} = [0, a] \times (-\infty, \infty)$. The charge density ρ has compact support in the region $x > a$. For certain charge densities ρ that are close enough to a , the energy dissipation in the slab (in particular in the darkly shaded region $a - \xi < x < a$) tends to infinity as a sequence δ_j tends to 0.

permittivity), and ρ is a given charge density distribution. We assume that ρ is real-valued and that $\rho \in \mathcal{P}$, where

$$\mathcal{P} \equiv \{\rho \in L^2(\mathcal{M}) \cap L^\infty(\mathcal{M}) : \rho \text{ has compact support in } \mathcal{M}\}. \quad (4.3)$$

Throughout this chapter, we also assume that

$$0 < |\text{supp } \rho| < \infty, \quad (4.4)$$

where $\text{supp } \rho$ is the smallest compact subset of \mathcal{M} such that $\rho = 0$ almost everywhere outside of $\text{supp } \rho$ and $|\text{supp } \rho|$ denotes the Lebesgue Measure of $\text{supp } \rho$. Note that the conditions we impose on ρ in (4.3) and (4.4) exclude the case when ρ is a dipole. For a brief derivation of (4.2), see Section C.1 in Appendix C.

For the purposes of the current chapter we assume the layers are occupied by three different materials such that the imaginary parts of their dielectric constants are small (corresponding to small losses) and the real parts of their dielectric constants are equal but with opposite signs. In particular we take the dielectric constant $\varepsilon(x, y)$ to be

$$\varepsilon(x, y) \equiv \begin{cases} \varepsilon_c = 1 + i\mu & \text{if } x < 0, \\ \varepsilon_s = -1 + i\delta & \text{if } 0 \leq x \leq a, \\ \varepsilon_m = 1 & \text{if } x > a, \end{cases} \quad (4.5)$$

where $0 < \delta < 1$ and $\mu = \delta + \lambda\delta^\beta$ for some constants $\lambda \in \mathbb{R}$ and $\beta > 0$. In the limit $\delta \rightarrow 0^+$ the moduli (4.5) are that of a quasistatic 2-D superlens (“poor man’s superlens”). The question we address in this chapter is to determine those ρ for which the power dissipation in this superlens blows up as $\delta \rightarrow 0^+$. As we shall explain shortly this is closely tied with cloaking due to anomalous resonance. Curiously we will see that the answer depends on the value of β , thus showing the sensitivity of the energy dissipation rate to perturbations.

We say that λ is *feasible* if

$$\lambda > 0 \quad \text{for } 0 < \beta < 1, \quad \lambda \geq -1 \quad \text{for } \beta = 1, \quad \text{or } \lambda \neq 0 \quad \text{for } \beta > 1. \quad (4.6)$$

We define $0 < \delta_\mu(\beta, \lambda) < 1$ such that $\mu \geq 0$ for $0 < \delta \leq \delta_\mu$ (which is required physically — the restrictions we placed on λ ensure that such a δ_μ exists).

Given a charge density $\rho(x, y) \in \mathcal{P}$, we define

$$d_0 \equiv \min\{x : (x, y) \in \text{supp}(\rho)\} \quad \text{and} \quad d_1 \equiv \max\{x : (x, y) \in \text{supp}(\rho)\} \quad (4.7)$$

(see Figure 4.8). Since ρ has compact support in \mathcal{M} , we have

$$\text{supp } \rho \subseteq [d_0, d_1] \times [h_0, h_1] \quad (4.8)$$

for some (finite) constants $h_0 < h_1$. The physical charge density is $\Re(\rho e^{-i\omega t})$ and the physical time-harmonic electric field is given by $\mathbf{E} = \Re(-\nabla V e^{-i\omega t})$. In order to enforce charge conservation, we require

$$\int_{d_0}^{d_1} \int_{-\infty}^{\infty} \rho(x, y) dy dx = \int_{d_0}^{d_1} \int_{h_0}^{h_1} \rho(x, y) dy dx = 0. \quad (4.9)$$

To see why (4.9) must hold, suppose that ρ is positive over its entire support. Then the time-harmonic charge density is $\Re(\rho e^{-i\omega t}) = \rho \cos(\omega t)$. At time $t = 0$, the charge density is positive, but at time $t = \pi/\omega$ the charge density is negative, which violates conservation of charge since the charge is assumed to be confined to the support of ρ .

We say anomalous localized resonance (ALR) occurs if the following two properties hold as $\delta \rightarrow 0^+$ [94]:

1. $|V| \rightarrow \infty$ in certain localized regions with boundaries that are not defined by discontinuities in the relative permittivity and
2. V approaches a smooth limit outside these localized regions.

For example, when ρ is a dipole, $\varepsilon_c = \varepsilon_m = 1$, and when ALR occurs, as the loss in the lens (represented by δ) tends to zero the potential diverges and oscillates wildly in regions that contain the boundaries of the lens. It is important to note that the boundaries of the resonant regions move as the dipole is moved. Outside the resonant regions the potential converges to what we expect from perfect lensing [109, 110]. This behavior and its relation to sub-wavelength resolution in imaging (superlensing) were first discovered by Nicorovici et al. [104] and were analyzed in more depth by Milton et al. [94].

Milton et al. [94] showed that if ρ is a dipole and $\varepsilon_c = \varepsilon_m = 1$, then ALR occurs if $a < d_0 < 2a$, where d_0 is the location of the dipole. In this case there are two locally resonant strips — one centered on each face of the slab. As mentioned above, outside these regions the potential converges to a smooth function that satisfies mirroring properties of a perfect lens. In particular, to an observer far enough to the right of the lens it will appear only as if there is a dipole at d_0 ; to an observer far enough to the left of the lens it will appear only as if there is a dipole located at $-d_0$ [94]. In neither case can the observer determine whether or not a lens is present. (However, if either observer is close to the lens, the presence of the lens will be obvious due to the resonance.) If $d_0 > 2a$, then there is no resonance and again the potential converges to a smooth function that satisfies the mirroring properties expected of a perfect lens. That is, to an observer far enough to the right of the lens (beyond the dipole) it will appear as if there is a dipole at d_0 and no lens, while to an observer to the left of the lens it will appear as if there is a dipole at $d_0 - a$ and no lens [94, 109, 124].

Cloaking due to ALR (CALR) can be understood from an energetic perspective. First, consider the quantity

$$E(\delta) \equiv \delta \int_0^a \int_{-\infty}^{\infty} |\nabla V|^2 dy dx; \quad (4.10)$$

$E(\delta)$ is proportional to the time-averaged electrical power dissipated in the slab [91]. Suppose ρ is independent of δ such that, in the limit $\delta \rightarrow 0^+$, we have $E(\delta) \rightarrow \infty$

and $|V| \leq C$ for some constant C for all $(x, y) \in \mathbb{R}^2$ with $|x| > b$ for some $b > 0$. This blow-up in the power dissipation is not physical, as it implies the fixed source ρ must produce an infinite amount of power in the limit $\delta \rightarrow 0^+$ [9, 91]. The power dissipation was proved to blow up as $\delta \rightarrow 0^+$ for finite collections of dipole sources close enough to the lens by Milton et al. [91, 94]; also see Bergman's work [15].

To make sense out of this we rescale the source ρ by defining $\rho_r \equiv \rho/\sqrt{E(\delta)}$. Since (4.2) is linear, the associated potential will be $V_r \equiv V/\sqrt{E(\delta)}$ and thanks to (4.10) the rescaled time-averaged electrical power dissipation will be

$$E_r(\delta) \equiv \delta \int_0^a \int_{-\infty}^{\infty} |\nabla V_r|^2 dy dx = \delta \int_0^a \int_{-\infty}^{\infty} \frac{|\nabla V|^2}{E(\delta)} dy dx = 1.$$

Thus the source ρ_r produces constant power independent of δ . Also, the rescaled potential satisfies $|V_r| = |V|/\sqrt{E(\delta)} \rightarrow 0$ as $\delta \rightarrow 0^+$ for $|x| > b$, implying that the source ρ_r becomes invisible in this limit to observers beyond $|x| = b$. This idea was introduced by Milton and Nicorovici [91]; also see the works by Kohn, Lu, Schweizer, and Weinstein [72] and Ammari, Ciraolo, Kang, Lee, and Milton [9, 10].

Cloaking due to anomalous localized resonance in the quasistatic regime was first analyzed by Milton and Nicorovici [91]. Milton and Nicorovici used separation of variables and rigorous analytic estimates to prove that if $\varepsilon_c = \varepsilon_m = 1$ and a fixed field is applied to the system (e.g., a uniform field at infinity), then a polarizable dipole located in the region $a < d_0 < 3a/2$ causes anomalous localized resonance and is cloaked in the limit $\delta \rightarrow 0^+$; if $\varepsilon_c \neq \varepsilon_m = 1$ (here ε_c has no relation to the value we chose in (4.5)), then the cloaking region becomes $a < d_0 < 2a$.

Milton and Nicorovici [91] also derived analogous results for circular cylindrical lenses, some of which we discussed previously. In that case they assumed the relative permittivity was ε_c for $0 \leq r < r_c$, $\varepsilon_s = -1 + i\delta$ for $r_c < r < r_s$, and $\varepsilon_m = 1$ for $r_s < r$. With r_0 denoting the distance of the polarizable dipole from the origin, the cloaking region was found to be $r_s < r_0 < r_* = r_s^2/r_c$ if $\varepsilon_c \neq \varepsilon_m$ and $r_s < r_0 < r_{\#} = \sqrt{r_s^3/r_c}$ if $\varepsilon_c = \varepsilon_m$. In particular they proved that an arbitrary number of polarizable dipoles within the cloaking region will be cloaked — see the work by Nicorovici et al. [108] for numerical verification of this result. Milton and Nicorovici [91] also extended their results to the finite-frequency and three-dimensional cases for the Veselago Slab Lens [121] (where $\varepsilon_c = \varepsilon_m = 1$).

To summarize, suppose $\varepsilon_c = \varepsilon_m = 1$ and the polarizable dipole is absent and a uniform electric field at infinity is applied to the slab lens configuration. The lens will not perturb this external field in the limit $\delta \rightarrow 0^+$, and, hence, is invisible to external observers [94, 104]. When the polarizable dipole is placed in this uniform field but outside of the cloaking region (so $d_0 > 3a/2$), it will become polarized and create a dipole field of its own which interacts with the lens. If $d_0 > 2a$ as well there will be no resonance in the limit $\delta \rightarrow 0^+$; to an external observer, the lens will be invisible but the dipole will be clearly visible in this limit. If $3a/2 < d_0 < 2a$, resonance will occur as $\delta \rightarrow 0^+$ but it will be localized to strips around the boundaries of the lens — in particular the resonant fields will not interact with the dipole. The dipole will still be visible in this limit but to an observer outside of the resonance region (and outside the lens) the lens will be invisible. Finally, if $a < d_0 < 3a/2$ (so the polarizable dipole is within the cloaking region), the resonant field will interact with the polarizable dipole and effectively cancel the effect of the external field on it. In other words, the net field at the location of the polarizable dipole will be zero, and, hence, its induced dipole moment will be zero (in the limit as $\delta \rightarrow 0^+$) — both the lens and the dipole will be invisible to external observers. See Figure 3 in the work by Milton and Nicorovici [91] and the figures in the work by Nicorovici et al. [108] for dramatic illustrations of this in the circular cylindrical case.

Nicorovici, McPhedran, Enoch, and Tayeb [107] studied CALR for the circular cylindrical superlens in the finite-frequency case. For physically plausible values of δ they discovered that the cloaking device (the superlens) can effectively cloak a tiny cylindrical inclusion located within the cloaking region but that the superlens does not necessarily cloak itself — they deemed this phenomenon the “ostrich effect.” In the quasistatic (long-wavelength) limit, however, the lens can effectively cloak both the inclusion and itself even at rather large values of δ , which was also pointed out in the case of a polarizable dipole by Milton and Nicorovici [91].

Bouchitté and Schweizer [20] considered an annular lens with inner and outer radii of 1 and R , respectively, and relative permittivity $\varepsilon_s = -1 + i\delta$ embedded in vacuum. They proved that a small circular inclusion of radius $\gamma(\delta)$ (with $\gamma(\delta) \rightarrow 0$ as $\delta \rightarrow 0^+$) is cloaked in the limit $\delta \rightarrow 0^+$ if it is located within the annulus $R < |x_0| < R_* = R^{3/2}$,

where x_0 is the position of the circular source. If $|x_0| > R_*$, then the source is visible but the annular superlens is not. Both of these results are consistent with the previous results of Milton and Nicorovici [91]. Bruno and Lintner [23] considered a similar scenario and showed numerically that a small dielectric disk is not perfectly cloaked. They verified (numerically) that an annular superlens embedded in vacuum by itself is invisible to an external applied field in the zero loss limit (assuming the source is at a position farther than R_* from the origin) — a fact that was first shown analytically by Nicorovici et al. [104]; however, Bruno and Lintner also showed that elliptical superlenses can cloak polarizable dipoles that are near enough to the lens but that such lenses are not invisible themselves. That is, the polarizable dipole is cloaked but it is obvious to external observers that something is being hidden — this is another example of the “ostrich effect” [107].

Kohn et al. [72] used variational principles to derive resonance results in the quasistatic regime in core/shell geometries (where the superlens resides in the shell) that are not necessarily radial. They assumed the source was supported on the boundary of a disk in \mathbb{R}^2 ; they obtained results similar to those described above.

Ammari et al. [9, 10] used properties of certain Neumann-Poincaré Operators to prove results analogous to those of Milton and Nicorovici [91]. The most general results they derived hold for very general core/shell geometries and charge density distributions ρ with compact support in the quasistatic regime. In the circular cylindrical case their requirements are more explicit and involve gap conditions on the Fourier Coefficients of the Newtonian Potential of ρ . Although these gap conditions may be difficult to deal with for a given source, they verified that their results are consistent with those of Milton and Nicorovici [91] when ρ is a dipole or quadrupole. Their results can be summarized as follows. First, if the support of ρ is completely contained within the cloaking region ($r_s < r_0 < r_*$ if $\varepsilon_c \neq \varepsilon_m = 1$ and $r_s < r_0 < r_\#$ if $\varepsilon_c = \varepsilon_m = 1$), and if ρ satisfies the gap property, then CALR occurs. Second, weak CALR (defined by $\limsup_{\delta \rightarrow 0^+} E(\delta) = \infty$ and $|V| < C$ for all δ where $C > 0$ is independent of δ) occurs if the support of ρ is completely inside the cloaking region and the Newtonian Potential does not extend harmonically to all of \mathbb{R}^2 . Third, if $\Re(\varepsilon_s) \neq -1$, then CALR does not occur. Fourth, CALR does not occur for any

isotropic constant values of ε_c and ε_s when the core and shell are concentric spheres in \mathbb{R}^3 . Using a folded geometry approach (extending that of Leonhardt and Philbin [77] and Leonhardt and Tyc [78]), Ammari, Ciraolo, Kang, Lee, and Milton [8] proved that CALR can occur in 3-D when the core and shell are concentric spheres and the shell has a certain anisotropic relative permittivity — see the work by Milton, Nicorovici, McPhedran, Cherednichenko, and Jacob [93] for the analogous problem in 2-D.

Nicorovici, McPhedran, Botten, and Milton [106] asked whether or not one can enlarge the cloaking region by spatially overlapping the cloaking regions of identical circular cylindrical superlenses. Curiously they found that doing so *reduces* the cloaking effect (at least in the quasistatic regime). The cloaking region can be extended by arranging the disks in such a way that their corresponding cloaking regions just touch.

Milton and Nicorovici [92] utilized a correspondence (first discovered although not fully exploited in the work of Yaghjian and Hansen [123]) between the perfect Veselago Lens at a fixed frequency in the long-time limit and the lossy Veselago Lens in the quasistatic limit to show that transverse magnetic dipole sources that generate bounded power eventually become cloaked if they are within the cloaking region ($a < d_0 < 3a/2$). Xiao, Huang, Dong, and Chan [122] obtained similar results in the case when both the permittivity and permeability of the Veselago Lens had a positive imaginary part.

Finally, Nguyen [103] proved that arbitrary inhomogeneous objects are magnified by properly constructed superlenses in both the quasistatic and finite-frequency regimes in 2-D and 3-D.

In this chapter we consider the scenario sketched in Figure 4.8 and described by (4.2)–(4.9). We study the behavior of

$$E_\xi(\delta) \equiv \delta \int_{a-\xi}^a \int_{-\infty}^{\infty} |\nabla V|^2 dy dx, \quad (4.11)$$

where $0 < \xi < a$ is a small parameter. The quantity $E_\xi(\delta)$ is proportional to the time-averaged electrical power dissipated in the strip $R_\xi \equiv \{(x, y) \in \mathbb{R}^2 : a - \xi < x < a\}$, illustrated by the darkened strip in Figure 4.8; $E_\xi(\delta)$ is also a lower bound on the

quantity defined in (4.10). In particular, we derive conditions on ρ that determine whether or not $\limsup_{\delta \rightarrow 0^+} E_\xi(\delta) = \infty$ (*weak* CALR), $\lim_{\delta \rightarrow 0^+} E_\xi(\delta) = \infty$ (*strong* CALR), or $E_\xi(\delta) < C$ for a constant $C > 0$ as $\delta \rightarrow 0^+$ (no CALR).

In order to do this, we begin by taking the Fourier Transform of (4.2) in the y -variable and calculating $E_\xi(\delta)$ explicitly in terms of $\hat{\rho}(x, k)$ (the Fourier Transform of ρ in the y -variable). We then derive upper and lower bounds on $E_\xi(\delta)$ to obtain our results. The result for unbounded energy is contained in Corollary 4.1. Essentially, if there is a $d_* \in [d_0, d_1]$ such that

$$\limsup_{k \rightarrow \infty} \left| e^{d_* k} \int_{d_0}^{d_1} \hat{\rho}(x, k) e^{-kx} dx \right| > 0$$

and $a < d_* < \tau(\beta)a$ where

$$\tau(\beta) = \begin{cases} \frac{\beta + 2}{\beta + 1} & \text{for } 0 < \beta < 1, \\ \frac{3}{2} & \text{for } \beta \geq 1, \end{cases}$$

then $\limsup_{\delta \rightarrow 0^+} E_\xi(\delta) = \infty$. As far as we are aware, there are two novelties to our result. First, the blow-up in energy occurs only if ρ is within a critical distance of the slab that depends nontrivially on β . Second, unlike in Theorem 5.3 of Ammari et al. [9] and Theorem 4.1 of Ammari et al. [10], we do not assume that the support of ρ is completely contained within the critical distance. In fact, there are examples of charge density distributions ρ that cause a blow-up in energy if only part of the support of ρ is within the critical distance — see Sections 4.6.1.1 and 4.6.1.2. (As discussed by Ammari et al. [9, 10], it seems like their results would hold even if only part of the support of ρ is within the critical distance to the lens.) In Theorem 4.4 we show that $\lim_{\delta \rightarrow 0^+} E_\xi(\delta) = 0$ if ρ is supported outside the critical distance.

The remainder of this chapter is organized as follows. In Section 4.2 we derive an expression for the potential in Fourier Space. In Section 4.4 we compute some useful formulas. We derive the expression for $E_\xi(\delta)$ in Section 4.5. In Section 4.6 we derive some lower bounds that are used to prove our result about the blow-up of $E_\xi(\delta)$ as $\delta \rightarrow 0^+$. We then analytically and numerically illustrate our results for two charge density distributions. In Section 4.7 we prove that $E_\xi(\delta)$ remains bounded (and, in fact, goes to 0) as $\delta \rightarrow 0^+$ if ρ is outside of the critical distance. Finally, in

Section 4.8, we prove that the potential remains bounded far enough away from the slab regardless of the position of charge density distribution ρ .

4.2 Derivation of the Potential

In the quasistatic regime the potential $V \in L^2_{\text{loc}}(\mathbb{R}^2)$ solves the following problem:

$$\left\{ \begin{array}{l} -\nabla \cdot [\varepsilon(x, y)\nabla V(x, y)] = \rho(x, y) \text{ in } \mathbb{R}^2, \\ V(x, y), \varepsilon \frac{\partial V}{\partial x}(x, y) \text{ continuous across } x = 0, a \text{ for almost every } y \in \mathbb{R}, \\ \frac{\partial V}{\partial x}(x, y) \rightarrow 0 \text{ as } |x| \rightarrow \infty \text{ for almost every } y \in \mathbb{R}, \\ V(x, \cdot) \in H^1(\mathbb{R}) \text{ for almost every } x \in \mathbb{R}, \\ \frac{\partial V}{\partial x}(x, \cdot) \in L^2(\mathbb{R}) \text{ for almost every } x \in \mathbb{R}, \end{array} \right. \quad (4.12)$$

where ε is given in (4.5). In this section, we take the Fourier Transform with respect to the y -variable of the problem (4.12). Since $V \in L^2_{\text{loc}}(\mathbb{R}^2)$, the PDE (4.12) can be understood in a distributional sense (since L^2_{loc} functions are distributions [36]). The continuity conditions in (4.12) ensure continuity of the potential and the normal component of the electric displacement field $\mathbf{D} = -\varepsilon\nabla V$ across the left and right edges of the slab (since the normal vector to the edges of the slab is in the negative x -direction at $x = 0$, the normal component of \mathbf{D} along the edge at $x = 0$ is $\mathbf{D} \cdot \mathbf{n} = \varepsilon \frac{\partial V}{\partial x}$; at the edge along $x = a$, the normal vector is in the positive x -direction, so $\mathbf{D} \cdot \mathbf{n} = -\varepsilon \frac{\partial V}{\partial x}$ there). The continuity conditions on the potential and normal component of the displacement field are typical in quasistatic problems — see the works by Griffiths [45, Section 4.4.2] and Milton et al. [94]. The condition at infinity in (4.12) ensures that the x -component of the electric field, namely $-\frac{\partial V}{\partial x}$, vanishes as $x \rightarrow -\infty$ and $x \rightarrow \infty$. It turns out that this condition is sufficient for our purposes (for the problem stated in (4.12) one can show that the y -component of the electric field, namely $-\frac{\partial V}{\partial y}$, goes to 0 as $|x| \rightarrow \infty$ as well). We only consider $|x| \rightarrow \infty$ since the slab extends infinitely in the y -direction. The last two requirements are regularity results that we impose to ensure that we can perform the computations in this section. In Sections C.3–C.6 in Appendix C we prove that the solutions we

derive in this section satisfy (4.12) (also see Section C.3.4 in Appendix C for more about the Sobolev space $H^1(\mathbb{R})$).

We recall the following definitions:

$$\begin{cases} \mathcal{C} \equiv \{(x, y) \in \mathbb{R}^2 : x < 0\}; \\ \mathring{\mathcal{S}} \equiv \{(x, y) \in \mathbb{R}^2 : 0 < x < a\}; \\ \mathcal{M} \equiv \{(x, y) \in \mathbb{R}^2 : a < x\}. \end{cases} \quad (4.13)$$

We then define

$$\begin{aligned} V_c(x, y) &\equiv \chi_{\mathcal{C}}(x, y)V(x, y), \\ V_s(x, y) &\equiv \chi_{\mathring{\mathcal{S}}}(x, y)V(x, y), \\ \text{and } V_m(x, y) &\equiv \chi_{\mathcal{M}}(x, y)V(x, y), \end{aligned} \quad (4.14)$$

where

$$\chi_U(x, y) = \begin{cases} 1 & \text{if } (x, y) \in U, \\ 0 & \text{if } (x, y) \notin U, \end{cases} \quad (4.15)$$

is the characteristic function of the set $U \subset \mathbb{R}^2$. We use the convention that the Fourier Transform of a function $f(x, y)$ with respect to the variable y is defined by

$$\widehat{f}(x, k) \equiv \int_{-\infty}^{\infty} f(x, y)e^{-iky} dy. \quad (4.16)$$

Now $\frac{\partial V}{\partial x}(x, \cdot) \in L^2(\mathbb{R})$ and $\frac{\partial V}{\partial y}(x, \cdot) \in L^2(\mathbb{R})$ for almost every $x \in \mathbb{R}$ thanks to (4.12).

Thus for almost every $x \in \mathbb{R}$ we have

$$\widehat{\frac{\partial V}{\partial x}}(x, k) = \frac{\partial \widehat{V}}{\partial x}(x, k) \quad \text{and} \quad \widehat{\frac{\partial V}{\partial y}}(x, k) = ik\widehat{V}(x, k) \quad (4.17)$$

for almost every $x \in \mathbb{R}$ — see Section C.7 in Appendix C. We mention here that we take $k \in \mathbb{R}$ throughout this chapter. We also let $|z| = \sqrt{(z')^2 + (z'')^2}$ denote the modulus of the complex number $z = z' + iz''$.

4.2.1 The Solution in the Set \mathcal{C}

Due to (4.5) and (4.12), in the set \mathcal{C} the potential satisfies

$$\begin{cases} \Delta V_c(x, y) = 0 & \text{for } x < 0, \\ \frac{\partial V_c}{\partial x}(x, y) \rightarrow 0 & \text{as } x \rightarrow -\infty. \end{cases} \quad (4.18)$$

(There are also continuity conditions at the boundary $x = 0$, but deal with these in Section 4.2.2.) We take the Fourier Transform of (4.18) and recall the properties of \widehat{V}_c from (4.17) to find that \widehat{V}_c satisfies

$$\begin{cases} \frac{\partial^2 \widehat{V}_c}{\partial x^2}(x, k) - k^2 \widehat{V}_c(x, k) = 0 & \text{for } x < 0, \\ \frac{\partial \widehat{V}_c}{\partial x}(x, k) \rightarrow 0 & \text{as } x \rightarrow -\infty. \end{cases} \quad (4.19)$$

Since k is real, the general solution to (4.19) is

$$\widehat{V}_c(x, k) = A_k e^{|k|x} + B_k e^{-|k|x}.$$

We have

$$\lim_{x \rightarrow -\infty} \frac{\partial \widehat{V}_c}{\partial x}(x, k) = \lim_{x \rightarrow -\infty} (|k|A_k e^{|k|x} - |k|B_k e^{-|k|x}).$$

In order to force this limit to be 0 we take $B_k = 0$ (for $k \neq 0$ — B_0 is arbitrary). Thus the general form of the Fourier Transform of $\widehat{V}_c(x, k)$ is

$$\widehat{V}_c(x, k) = A_k e^{|k|x} \quad (4.20)$$

for arbitrary constants A_k .

4.2.2 The Solution in the Set \mathring{S}

Due to (4.5) and (4.12), in the set \mathring{S} the potential satisfies

$$\begin{cases} \Delta V_s(x, y) = 0 & \text{for } 0 < x < a, \\ \lim_{x \rightarrow 0^+} V_s(x, y) = \lim_{x \rightarrow 0^-} V_c(x, y), \\ \lim_{x \rightarrow 0^+} \varepsilon_s \frac{\partial V_s}{\partial x}(x, y) = \lim_{x \rightarrow 0^-} \varepsilon_c \frac{\partial V_c}{\partial x}(x, y). \end{cases} \quad (4.21)$$

(There are analogous continuity conditions at the boundary $x = a$, but we deal with these in Section 4.2.3.) Taking the Fourier Transform of (4.21) gives us the following equation for $\widehat{V}_s(x, k)$:

$$\begin{cases} \frac{\partial^2 \widehat{V}_s}{\partial x^2}(x, k) - k^2 \widehat{V}_s(x, k) = 0 & \text{for } 0 < x < a, \\ \lim_{x \rightarrow 0^+} \widehat{V}_s(x, k) = \lim_{x \rightarrow 0^-} \widehat{V}_c(x, k), \\ \lim_{x \rightarrow 0^+} \varepsilon_s \frac{\partial \widehat{V}_s}{\partial x}(x, k) = \lim_{x \rightarrow 0^-} \varepsilon_c \frac{\partial \widehat{V}_c}{\partial x}(x, k). \end{cases} \quad (4.22)$$

Again since k is real, the general solution to (4.22) is

$$\widehat{V}_s(x, k) = C_k e^{|k|x} + D_k e^{-|k|x}. \quad (4.23)$$

Next we enforce the continuity conditions on the Fourier Transform of the potential across the left boundary of the slab. First, by (4.20) and (4.23) we have

$$\lim_{x \rightarrow 0^+} \widehat{V}_s(x, k) = \lim_{x \rightarrow 0^-} \widehat{V}_c(x, k) \Leftrightarrow C_k + D_k = A_k. \quad (4.24)$$

Similarly, for $k \neq 0$, the continuity condition on the derivative of \widehat{V}_s is

$$\lim_{x \rightarrow 0^+} \varepsilon_s \frac{\partial \widehat{V}_s}{\partial x}(x, k) = \lim_{x \rightarrow 0^-} \varepsilon_c \frac{\partial \widehat{V}_c}{\partial x}(x, k) \Leftrightarrow C_k - D_k = \chi_c A_k, \quad (4.25)$$

where

$$\chi_c \equiv \varepsilon_s / \varepsilon_c. \quad (4.26)$$

(Note that the derivative condition (4.25) is automatically satisfied when $k = 0$.)

Solving (4.24) and (4.25) for C_k and D_k gives

$$\widehat{V}_s(x, k) = \frac{A_k}{2\chi_c} [(\chi_c + 1)e^{|k|x} + (\chi_c - 1)e^{-|k|x}]. \quad (4.27)$$

4.2.3 The Solution in the Set \mathcal{M}

Next we show the details of the derivation for the solution in the third layer, \mathcal{M} .

From (4.5) and (4.12) we note that in the set \mathcal{M} the potential satisfies

$$\left\{ \begin{array}{ll} \Delta V_m(x, y) = -\rho(x, y) & \text{for } x > a, \\ \lim_{x \rightarrow a^+} V_m(x, y) = \lim_{x \rightarrow a^-} V_s(x, y), \\ \lim_{x \rightarrow a^+} \varepsilon_m \frac{\partial V_m}{\partial x}(x, y) = \lim_{x \rightarrow a^-} \varepsilon_s \frac{\partial V_s}{\partial x}(x, y), \\ \frac{\partial V_m}{\partial x}(x, y) \rightarrow 0 & \text{as } x \rightarrow \infty. \end{array} \right.$$

After taking the Fourier Transform with respect to y we find that $\widehat{V}_m(x, k)$ satisfies

$$\left\{ \begin{array}{ll} \frac{\partial^2 \widehat{V}_m}{\partial x^2}(x, k) - k^2 \widehat{V}_m(x, k) = -\widehat{\rho}(x, k) & \text{for } x > a, \\ \lim_{x \rightarrow a^+} \widehat{V}_m(x, k) = \lim_{x \rightarrow a^-} \widehat{V}_s(x, k), \\ \lim_{x \rightarrow a^+} \varepsilon_m \frac{\partial \widehat{V}_m}{\partial x}(x, k) = \lim_{x \rightarrow a^-} \varepsilon_s \frac{\partial \widehat{V}_s}{\partial x}(x, k), \\ \frac{\partial \widehat{V}_m}{\partial x}(x, k) \rightarrow 0 & \text{as } x \rightarrow \infty. \end{array} \right. \quad (4.28)$$

We make the change of variables $z = x - a$ so that (4.28) becomes

$$\begin{cases} \frac{\partial^2 \widehat{V}_m}{\partial z^2}(z, k) - k^2 \widehat{V}_m(z, k) = -\widehat{\rho}(z, k) & \text{for } z > 0, \\ \lim_{z \rightarrow 0^+} \widehat{V}_m(z, k) = \lim_{z \rightarrow 0^-} \widehat{V}_s(z, k) = A_k \psi_k^+, \\ \lim_{z \rightarrow 0^+} \frac{\partial \widehat{V}_m}{\partial z}(z, k) = \lim_{z \rightarrow 0^-} \chi_m \frac{\partial \widehat{V}_s}{\partial z}(z, k) = A_k \psi_k^-, \end{cases} \quad (4.29)$$

where $\widehat{\rho}(x, k) = \underline{\widehat{\rho}}(x - a, k)$, $\widehat{V}_j(x, k) = \underline{\widehat{V}}_j(x - a, k)$ for $j = m, s$,

$$\psi_k^+ = \frac{1}{2\chi_c} [(\chi_c + 1) e^{|k|a} + (\chi_c - 1) e^{-|k|a}], \quad (4.30)$$

$$\psi_k^- = \frac{|k|\chi_m}{2\chi_c} [(\chi_c + 1) e^{|k|a} - (\chi_c - 1) e^{-|k|a}], \quad (4.31)$$

$$\text{and } \chi_m = \varepsilon_s / \varepsilon_m. \quad (4.32)$$

(We have eliminated the condition at infinity for now — we will return to it later.) In addition, we have used (4.27) to simplify the limits in (4.29).

We define Laplace Transform of $\underline{\widehat{V}}_m(z, k)$ to be

$$u(s, k) \equiv \int_0^\infty \underline{\widehat{V}}_m(z, k) e^{-sz} dz$$

(since $\frac{\partial \widehat{V}_m}{\partial x} \rightarrow 0$ as $x \rightarrow \infty$, the function $u(s, k)$ is well defined — the potential $\widehat{V}_m(x, k)$ cannot grow exponentially for large x). We use the notation $\mathcal{L}\{g\}$ to denote the Laplace Transform of the function g . Recall that the Laplace Transform satisfies

$$\mathcal{L}\left\{\frac{dg}{dx}\right\}(s) = s\mathcal{L}\{g\}(s) - g(0);$$

see the book by Schiff [114, Section 2.3]. We need to solve the ODE in (4.29) for the cases $k = 0$ and $k \neq 0$ separately.

Case I: $k = 0$

Here the Laplace-Transformed version of (4.29) is

$$s^2 u(s, 0) - s A_0 \psi_0^+ - A_0 \psi_0^- = -\mathcal{L}\{\widehat{\rho}(z, 0)\}(s, 0),$$

Thus

$$u(s, 0) = \frac{A_0}{s} - [\mathcal{L}\{\widehat{\rho}(z, 0)\}(s, 0)] \cdot \frac{1}{s^2},$$

where we have used (4.30) and (4.31) to simplify the expression for $u(s, 0)$. Since $\widehat{V}_m = 0$ for $z < 0$ (see (4.13)–(4.15)), we can use the convolution theorem for Laplace Transforms to find

$$\widehat{V}_m(z, 0) = A_0 - \int_0^z (z - z') \widehat{\rho}(z', 0) dz' \Rightarrow \widehat{V}_m(x, 0) = A_0 - \int_0^{x-a} (x - a - z') \widehat{\rho}(z', 0) dz'.$$

Next we make the change of variables $z' = x' - a$ in the above integral to find

$$\widehat{V}_m(x, 0) = A_0 - \int_a^x (x - x') \widehat{\rho}(x' - a, 0) dx' = A_0 + \int_a^x (x' - x) \widehat{\rho}(x', 0) dx'.$$

We now impose the condition as $x \rightarrow \infty$ — see (4.28). We require

$$\lim_{x \rightarrow \infty} \frac{\partial \widehat{V}_m}{\partial x}(x, 0) = \lim_{x \rightarrow \infty} \left\{ \frac{\partial}{\partial x} \left[A_0 + \int_a^x (s - x) \widehat{\rho}(s, 0) ds \right] \right\} = 0.$$

By the Leibniz Rule (see Section C.2 in Appendix C), this is equivalent to the requirement

$$\lim_{x \rightarrow \infty} \left[- \int_a^x \widehat{\rho}(s, 0) ds \right] = 0.$$

For $x > d_1$, (4.9) implies

$$\int_a^x \widehat{\rho}(s, 0) ds = \int_{d_0}^{d_1} \widehat{\rho}(s, 0) ds = \int_{d_0}^{d_1} \int_{h_0}^{h_1} \rho(s, y) dy ds = 0.$$

Thus the condition at infinity is automatically satisfied for any choice of A_0 .

Case 2: $k \neq 0$

Here the Laplace-Transformed version of (4.29) is

$$s^2 u(s, k) - s A_k \psi_k^+ - A_k \psi_k^- - k^2 u(s, k) = -\mathcal{L} \{ \widehat{\rho}(z, k) \} (s, k).$$

Therefore

$$u(s, k) = A_k \psi_k^+ \frac{s}{s^2 - k^2} + A_k \psi_k^- \frac{1}{s^2 - k^2} - \frac{\mathcal{L} \{ \widehat{\rho}(z, k) \} (s, k)}{s^2 - k^2}.$$

Recalling that $\widehat{V}_m(z, k) = 0$ for $z < 0$ (see (4.13)–(4.15)), by the convolution theorem for Laplace Transforms we have

$$\begin{aligned} \widehat{V}_m(z, k) &= A_k \psi_k^+ \cosh(|k|z) + A_k \psi_k^- \frac{\sinh(|k|z)}{|k|} \\ &\quad - \int_0^z \frac{\sinh[|k|(z - z')]}{|k|} \widehat{\rho}(z', k) dz' \end{aligned}$$

$$\Leftrightarrow \widehat{V}_m(x, k) = A_k \psi_k^+ \cosh [|k|(x - a)] + A_k \psi_k^- \frac{\sinh [|k|(x - a)]}{|k|} - \int_0^{x-a} \frac{\sinh [|k|(x - a - z')]}{|k|} \widehat{\rho}(z', k) dz'.$$

We make the change of variables $z' = x' - a$ in the above integral to find

$$\begin{aligned} \widehat{V}_m(x, k) &= A_k \psi_k^+ \cosh [|k|(x - a)] + \frac{A_k \psi_k^-}{|k|} \sinh [|k|(x - a)] \\ &+ \frac{1}{|k|} \int_a^x \sinh [|k|(x' - x)] \widehat{\rho}(x', k) dx', \end{aligned} \quad (4.33)$$

where we have used the fact that $\widehat{\rho}(x - a, k) = \widehat{\rho}(x, k)$.

We now impose the limit conditions at infinity from (4.28). We use the Leibniz Rule (see Section C.2 in Appendix C) to find

$$\begin{aligned} &\lim_{x \rightarrow \infty} \frac{\partial \widehat{V}_m}{\partial x}(x, k) \\ &= \lim_{x \rightarrow \infty} \left(A_k \left\{ |k| \psi_k^+ \sinh [|k|(x - a)] + \psi_k^- \cosh [|k|(x - a)] \right\} \right. \\ &\quad \left. - \int_a^x \widehat{\rho}(x', k) \cosh [|k|(x' - x)] dx' \right) \\ &= \lim_{x \rightarrow \infty} \left\{ |k| e^{|k|x} \left[\frac{A_k \psi_k^+ e^{-|k|a}}{2} + \frac{A_k \psi_k^- e^{-|k|a}}{2|k|} - \frac{1}{2|k|} \int_{d_0}^{d_1} \widehat{\rho}(s, k) e^{-|k|s} ds \right] \right. \\ &\quad \left. + \underbrace{|k| e^{-|k|x} \left[-\frac{A_k \psi_k^+ e^{|k|a}}{2} + \frac{A_k \psi_k^- e^{|k|a}}{2|k|} - \frac{1}{2|k|} \int_{d_0}^{d_1} \widehat{\rho}(s, k) e^{|k|s} ds \right]}_{\rightarrow 0 \text{ as } x \rightarrow \infty} \right\} \\ &= \lim_{x \rightarrow \infty} \left\{ |k| e^{|k|x} \left[\frac{A_k e^{-|k|a}}{2|k|} (|k| \psi_k^+ + \psi_k^-) - \frac{1}{2|k|} \int_{d_0}^{d_1} \widehat{\rho}(s, k) e^{-|k|s} ds \right] \right\}. \end{aligned}$$

This limit is 0 if and only if we choose

$$A_k \equiv \frac{I_k}{e^{-|k|a} (|k| \psi_k^+ + \psi_k^-)}, \quad (4.34)$$

where

$$I_k \equiv \int_{d_0}^{d_1} \widehat{\rho}(s, k) e^{-|k|s} ds. \quad (4.35)$$

By (4.5) and (4.26) we have

$$\frac{\chi_c - 1}{\chi_c + 1} = \frac{2i + \delta - \mu}{\delta + \mu},$$

so by (4.27) the potential in the set $\mathring{\mathcal{S}}$ is

$$\widehat{V}_s(x, k) = \begin{cases} A_0 & \text{if } k = 0, \\ \frac{I_k}{|k|g} \left[e^{|k|x} + \left(\frac{2i - \lambda\delta^\beta}{2\delta + \lambda\delta^\beta} \right) e^{-|k|x} \right] & \text{if } k \neq 0, \end{cases} \quad (4.36)$$

where

$$g \equiv \frac{2\chi_c e^{-|k|a} \left(\psi_k^+ + \frac{1}{|k|} \psi_k^- \right)}{\chi_c + 1} = i\delta \left[1 - \frac{(\delta + 2i)(2i - \lambda\delta^\beta)}{\delta(2\delta + \lambda\delta^\beta)} e^{-2|k|a} \right] \quad (4.37)$$

and A_0 is an arbitrary complex constant.

4.3 Some Properties of I_k

In this section we study some of the properties of I_k , which is defined in (4.35). Recall that $\rho \in \mathcal{P}$ where \mathcal{P} is defined in (4.3). Since $\rho \in L^2(\mathcal{M})$, we have $\rho \in L^1(\mathcal{M})$ as well: by the Cauchy–Schwarz Inequality and (4.4),

$$\begin{aligned} \int_{\mathcal{M}} |\rho| \, d\mathbf{x} &= \int_{\text{supp}(\rho)} |\rho| \, d\mathbf{x} \\ &\leq \left(\int_{\text{supp}(\rho)} |\rho|^2 \, d\mathbf{x} \right)^{\frac{1}{2}} \left(\int_{\text{supp}(\rho)} d\mathbf{x} \right)^{\frac{1}{2}} \\ &= \|\rho\|_{L^2(\mathcal{M})} |\text{supp}(\rho)|^{\frac{1}{2}}. \end{aligned}$$

We will need the following theorems [71, Section 6.3], which we reproduce here in a form suited to our needs. In fact, in the book by Klenke [71], the theorems were stated for functions $f : \mathbb{R} \rightarrow \mathbb{R}$ (they are Theorems 6.27 and 6.28, respectively); however, they also hold for functions $f : \mathbb{R} \rightarrow \mathbb{C}$ as can be seen by applying the original theorems to the real and imaginary parts of f separately.

Theorem 4.1 *Let $k_0 \in \mathbb{R}$ and let $f : [d_0, d_1] \times \mathbb{R} \rightarrow \mathbb{C}$ be a map with the following properties.*

(i) *For any $k \in \mathbb{R}$, the map $s \mapsto f(s, k)$ is in $L^1([d_0, d_1])$.*

(ii) *For almost all $s \in [d_0, d_1]$, the map $k \mapsto f(s, k)$ is continuous at the point k_0 .*

(iii) The map $h : s \mapsto \sup_{k \in \mathbb{R}} |f(s, k)|$ is in $L^1([d_0, d_1])$.

Then the map $F : \mathbb{R} \rightarrow \mathbb{C}$, $k \mapsto \int_{d_0}^{d_1} f(s, k) ds$ is continuous at k_0 .

Theorem 4.2 *Let $K \subset \mathbb{R}$ be a nontrivial open interval and let $f : [d_0, d_1] \times K \rightarrow \mathbb{C}$ be a map with the following properties.*

(i) *For any $k \in K$, the map $s \mapsto f(s, k)$ is in $L^1([d_0, d_1])$.*

(ii) *For almost all $s \in [d_0, d_1]$, the map $K \rightarrow \mathbb{C}$, $k \mapsto f(s, k)$ is differentiable with derivative $\frac{\partial f}{\partial k}$.*

(iii) $h \equiv \sup_{k \in K} |\frac{\partial f}{\partial k}(\cdot, k)| \in L^1([d_0, d_1])$.

Then, for any $k \in K$, $\frac{\partial f}{\partial k}(\cdot, k) \in L^1([d_0, d_1])$ and the function $F : k \mapsto \int_{d_0}^{d_1} f(s, k) ds$ is differentiable with derivative

$$F'(k) = \int_{d_0}^{d_1} \frac{\partial f}{\partial k}(s, k) ds.$$

In the following lemma, we collect a summary of important properties of I_k that are used throughout the remainder of this chapter.

Lemma 4.1 *Suppose $\rho \in \mathcal{P}$ (where \mathcal{P} is defined in (4.3)) and that I_k is defined as in (4.35). Then*

1. *for almost every $s \in [d_0, d_1]$, $\hat{\rho}(s, k)$ is infinitely continuously differentiable as a function of k for all $k \in \mathbb{R}$;*

2. *for each $k \in \mathbb{R}$,*

$$|I_k|^2 \leq (d_1 - d_0) \|\rho\|_{L^2(\mathcal{M})}^2 e^{-2|k|d_0};$$

3. *if ρ is real-valued, then $I_{-k} = \overline{I_k}$; this implies that $|I_k|^2$ is an even function of k for $k \in \mathbb{R}$;*

4. *the function I_k is continuous at k for each $k \in \mathbb{R}$;*

5. $\lim_{k \rightarrow 0} I_k = I_0 = 0$;

6. $\lim_{k \rightarrow 0} (|I_k|/|k|) = |C_0| < \infty$, where C_0 is defined in (4.41) and (4.42); moreover, there is a positive constant C_I such that $|I_k|/|k| \leq C_I$ for all $k \in \mathbb{R}$.

Proof of Lemma 4.1:

1. For almost every $x \in [d_0, d_1]$ and for each nonnegative integer n , the function $(-iy)^n \rho(x, y)$ is in $L^1(\mathbb{R})$ as a function of y since ρ has compact support and is in $L^\infty(\mathcal{M})$; in particular, for almost every $x \in [d_0, d_1]$ we have

$$\int_{-\infty}^{\infty} |(-iy)^n \rho(x, y)| dy = \int_{h_0}^{h_1} |y|^n |\rho(x, y)| dy \leq \|\rho\|_{L^\infty(\mathcal{M})} C_h^n (h_1 - h_0) < \infty,$$

where $C_h \equiv \max\{|h_0|, |h_1|\}$. This implies that $\hat{\rho}$ satisfies some very useful properties.

First, by the Riemann–Lebesgue Lemma (see Theorem 1.7 in Chapter VI of the book by Katznelson [70]),

$$\lim_{|k| \rightarrow \infty} \hat{\rho}(x, k) = 0$$

for almost every $x \in [d_0, d_1]$. Second, by Theorem 1.2 in Chapter VI of the book by Katznelson [70], $\hat{\rho}(x, k)$ is uniformly continuous in k for all $k \in \mathbb{R}$ and for almost every $x \in [d_0, d_1]$. Third, since $-iy\rho(x, y) \in L^1(\mathbb{R})$, Theorem 1.6 in Chapter VI of the book by Katznelson [70] implies that $\hat{\rho}(x, k)$ is differentiable with respect to k for almost all $x \in [d_0, d_1]$ and that

$$\frac{\partial \hat{\rho}}{\partial k}(x, k) = \widehat{(-iy\rho)}(x, k)$$

for almost every $x \in [d_0, d_1]$. Using induction on this third property in combination with the fact that $(-iy)^n \rho(x, y) \in L^1(\mathbb{R})$ as a function of y for almost every $x \in [d_0, d_1]$ implies that $\hat{\rho}(x, k)$ is infinitely differentiable as a function of k ; in particular

$$\frac{\partial^n \hat{\rho}}{\partial k^n}(x, k) = \widehat{((-iy)^n \rho)}(x, k)$$

for almost every $x \in [d_0, d_1]$, for all $k \in \mathbb{R}$, and for all nonnegative integers n .

2. For $k \in \mathbb{R}$ we have

$$\begin{aligned} |I_k|^2 &= \left| \int_{d_0}^{d_1} \hat{\rho}(s, k) e^{-|k|s} ds \right|^2 \\ &\leq \left[\int_{d_0}^{d_1} |\hat{\rho}(s, k)|^2 ds \right] \left(\int_{d_0}^{d_1} e^{-2|k|s} ds \right) \end{aligned}$$

$$\begin{aligned}
&= \left[\int_{d_0}^{d_1} \left| \int_{-\infty}^{\infty} \rho(s, y) e^{-iky} dy \right|^2 ds \right] \left(\int_{d_0}^{d_1} e^{-2|k|s} ds \right) \\
&\leq \left\{ \int_{d_0}^{d_1} \left[\int_{h_0}^{h_1} |\rho(s, y)|^2 dy \right] ds \right\} \left(\int_{d_0}^{d_1} e^{-2|k|s} ds \right) \\
&= \left[\int_a^{\infty} \int_{h_0}^{h_1} |\rho(s, y)|^2 dy ds \right] \left(\int_{d_0}^{d_1} e^{-2|k|s} ds \right) \\
&= \|\rho\|_{L^2(\mathcal{M})}^2 \int_{d_0}^{d_1} e^{-2|k|s} ds \\
&\leq (d_1 - d_0) \|\rho\|_{L^2(\mathcal{M})}^2 e^{-2|k|d_0}.
\end{aligned}$$

3. First we note that I_k is well defined for each $k \in \mathbb{R}$ (by part (2) of this lemma).

Then, since ρ is real-valued, for each $k \in \mathbb{R}$ we have

$$\begin{aligned}
I_{-k} &= \int_{d_0}^{d_1} \widehat{\rho}(s, -k) e^{-|-k|s} ds \\
&= \int_{d_0}^{d_1} \int_{-\infty}^{\infty} \rho(s, y) e^{iky} dy e^{-|k|s} ds \\
&= \overline{\int_{d_0}^{d_1} \int_{-\infty}^{\infty} \rho(s, y) e^{-iky} dy e^{-|k|s} ds} \\
&= \overline{I_k}.
\end{aligned}$$

Then $|I_{-k}|^2 = I_{-k} \overline{I_{-k}} = \overline{I_k} I_k = |I_k|^2$.

4. The proof of this part of the lemma is based on Theorem 4.1. In particular, we define $f : [d_0, d_1] \times \mathbb{R}$ by

$$f(s, k) \equiv \widehat{\rho}(s, k) e^{-|k|s}.$$

Then the function f satisfies the hypotheses of Theorem 4.1.

(i) For each $k \in \mathbb{R}$, the map $s \mapsto f(s, k) = \widehat{\rho}(s, k) e^{-|k|s} \in L^1([d_0, d_1])$ since

$$\int_{d_0}^{d_1} |\widehat{\rho}(s, k)| e^{-|k|s} ds \leq \int_{d_0}^{d_1} \int_{-\infty}^{\infty} |\rho(s, y) e^{-iky}| dy ds = \|\rho\|_{L^1(\mathcal{M})} < \infty.$$

(ii) Part (1) of this lemma implies that for almost all $s \in [d_0, d_1]$, $\widehat{\rho}(s, k)$ is (uniformly) continuous as a function of k for each $k \in \mathbb{R}$. Since $e^{-|k|s}$ is

continuous in \mathbb{R} as a function of k for each $s \in [d_0, d_1]$, $f(s, k)$ is continuous on \mathbb{R} as a function of k for almost every $s \in [d_0, d_1]$.

(iii) For almost every $s \in [d_0, d_1]$ and every $k \in \mathbb{R}$ we have

$$|\widehat{\rho}(s, k)e^{-|k|s}| \leq \int_{h_0}^{h_1} |\rho(s, y)e^{-iky}| dy \leq \|\rho\|_{L^\infty(\mathcal{M})}(h_1 - h_0),$$

where h_0 and h_1 are defined in (4.8). Since ρ has compact support, $h_1 - h_0$ is finite. Thus

$$\begin{aligned} \int_{d_0}^{d_1} \sup_{k \in \mathbb{R}} |\widehat{\rho}(s, k)e^{-|k|s}| ds &\leq \int_{d_0}^{d_1} (h_1 - h_0) \|\rho\|_{L^\infty(\mathcal{M})} ds \\ &\leq \|\rho\|_{L^\infty(\mathcal{M})}(d_1 - d_0)(h_1 - h_0), \end{aligned} \quad (4.38)$$

and this is less than infinity. Thus the map $h : s \mapsto \sup_{k \in \mathbb{R}} |f(s, k)|$ is in $L^1([d_0, d_1])$.

Therefore Theorem 4.1 implies that the function I_k is continuous at k_0 for each $k_0 \in \mathbb{R}$.

5. Since I_k is continuous at each $k \in \mathbb{R}$, we have

$$\lim_{k \rightarrow 0} I_k = I_0 = \int_{d_0}^{d_1} \widehat{\rho}(s, 0) ds = \int_{d_0}^{d_1} \int_{-\infty}^{\infty} \rho(s, y) dy ds = 0$$

by (4.9).

6. Since $I_k \rightarrow 0$ as $k \rightarrow 0^+$ by part (5) of this lemma,

$$\lim_{k \rightarrow 0^+} \frac{I_k}{k}$$

is an indeterminate form of type 0/0. We now prove that I_k is differentiable for $k > 0$ using Theorem 4.2. In this case we take the interval K from the theorem to be $K = (0, \infty)$. Note that, since $k > 0$, we have $I_k = \int_{d_0}^{d_1} \widehat{\rho}(s, k)e^{-ks} ds$.

(i) The proof of this is exactly the same as the proof of (i) in part (4) of this lemma.

(ii) Part (1) of this lemma implies that, for almost every $s \in [d_0, d_1]$, $\widehat{\rho}(s, k)$ is infinitely differentiable as a function of k for all $k \in K$. Since e^{-ks}

is infinitely differentiable as a function of k for all $k \in K$ and for all $s \in [d_0, d_1]$, the function $\widehat{\rho}(s, k)e^{-ks}$ is infinitely differentiable as a function of k for all $k \in K$ and for almost every $s \in [d_0, d_1]$.

(iii) For almost every $s \in [d_0, d_1]$ and by part (1) of this lemma we have, for each $k \in K$, that

$$\begin{aligned} \left| \frac{\partial}{\partial k} [\widehat{\rho}(s, k)e^{-ks}] \right| &= \left| \frac{\partial \widehat{\rho}}{\partial k}(s, k)e^{-ks} - \widehat{\rho}(s, k)se^{-ks} \right| \\ &\leq \left[|(-iy\rho)(s, k)| + |\widehat{\rho}(s, k)||s| \right] e^{-ks} \\ &\leq e^{-ks} \left[\int_{h_0}^{h_1} |y||\rho(s, y)| dy + |s| \int_{h_0}^{h_1} |\rho(s, y)| dy \right] \\ &\leq e^{-ks} \|\rho\|_{L^\infty(\mathcal{M})} (C_h + |s|) (h_1 - h_0) \\ &\leq \|\rho\|_{L^\infty(\mathcal{M})} (C_h + |s|) (h_1 - h_0). \end{aligned} \quad (4.39)$$

Then (4.39) implies

$$\begin{aligned} \int_{d_0}^{d_1} \sup_{k \in K} \left| \frac{\partial f}{\partial k}(s, k) \right| ds &\leq \|\rho\|_{L^\infty(\mathcal{M})} (h_1 - h_0) \int_{d_0}^{d_1} (C_h + |s|) ds \\ &\leq \|\rho\|_{L^\infty(\mathcal{M})} (C_h + d_1) (d_1 - d_0) (h_1 - h_0). \end{aligned}$$

Therefore Theorem 4.2 implies that

$$\begin{aligned} \frac{\partial I_k}{\partial k} &= \int_{d_0}^{d_1} \frac{\partial}{\partial k} [\widehat{\rho}(s, k)e^{-ks}] ds \\ &= \int_{d_0}^{d_1} -s\widehat{\rho}(s, k)e^{-ks} ds + \int_{d_0}^{d_1} \frac{\partial \widehat{\rho}}{\partial k}(s, k)e^{-ks} ds \\ &= - \int_{d_0}^{d_1} \int_{h_0}^{h_1} s\rho(s, y)e^{-iky}e^{-ks} dy ds - \int_{d_0}^{d_1} \int_{h_0}^{h_1} iy\rho(s, y)e^{-iky}e^{-ks} dy ds \end{aligned} \quad (4.40)$$

for $k > 0$. Note that the expression in (4.40) is well defined and continuous for all $k \in \mathbb{R}$ by an argument similar to that given in items (1) and (4) (applied to $-s\widehat{\rho}(s, k)$ and $\frac{\partial \widehat{\rho}}{\partial k}(s, k)$). In particular we have

$$\begin{aligned} \lim_{k \rightarrow 0^+} \frac{\partial I_k}{\partial k} &= \lim_{k \rightarrow 0^+} \left[\int_{d_0}^{d_1} -s\widehat{\rho}(s, k)e^{-ks} ds + \int_{d_0}^{d_1} \frac{\partial \widehat{\rho}}{\partial k}(s, k)e^{-ks} ds \right] \\ &= \int_{d_0}^{d_1} -s\widehat{\rho}(s, 0) ds + \int_{d_0}^{d_1} \frac{\partial \widehat{\rho}}{\partial k}(s, 0) ds \end{aligned} \quad (4.41)$$

$$\begin{aligned} &= - \int_{d_0}^{d_1} \int_{h_0}^{h_1} s\rho(s, y) dy ds - \int_{d_0}^{d_1} \int_{h_0}^{h_1} iy\rho(s, y) dy ds \\ &\equiv C_0, \end{aligned} \quad (4.42)$$

which is well defined since $\rho \in L^1(\mathcal{M})$ (we note that one can also justify passing the limit inside the integrals using the Lebesgue Dominated Convergence Theorem — see Theorem 1.34 and Remark 9.3(a) in the book by Rudin [113]).

Then the l'Hospital Rule and the fact that the function $|\cdot|$ is continuous imply that

$$\lim_{k \rightarrow 0^+} \frac{|I_k|}{|k|} = \left| \lim_{k \rightarrow 0^+} \frac{I_k}{k} \right| = \left| \lim_{k \rightarrow 0^+} \frac{\partial I_k}{\partial k} \right| = |C_0|.$$

Since $|I_k|$ and $|k|$ are even functions of k by item (3) of this lemma, we also have $\lim_{k \rightarrow 0^-} |I_k|/|k| = |C_0|$. Therefore $\lim_{k \rightarrow 0} |I_k|/|k| = |C_0|$.

Finally, since $|I_k|/|k|$ is continuous for all $k \in \mathbb{R}$ (if we define it to be equal to $|C_0|$ when $k = 0$) and since $\lim_{k \rightarrow \pm\infty} |I_k|/|k| = 0$ by item (2) of this lemma, we must have $|I_k|/|k| \leq C_I$ for some positive constant C_I .

This completes the proof.

4.4 Some Useful Computations

In this section we perform some useful calculations that are used frequently in the remainder of this chapter.

Lemma 4.2 *Let ψ_k^+ and ψ_k^- be defined as in (4.30) and (4.31), respectively. Then for each $k \in \mathbb{R}$,*

$$\begin{aligned} ||k|\psi_k^+ + \psi_k^-|^2 &= \frac{|k|^2}{4(1 + \delta^2)} \left[\delta^2(\delta + \mu)^2 e^{2|k|a} + 2\delta(\delta + \mu)(4 + \delta(\mu - \delta)) \right. \\ &\quad \left. + (4 + (\mu - \delta)^2)(4 + \delta^2)e^{-2|k|a} \right]. \end{aligned} \quad (4.43)$$

Proof of Lemma 4.2: From (4.30) and (4.31) we have

$$\begin{aligned} ||k|\psi_k^+ + \psi_k^-|^2 &= \left| \frac{|k|}{2\chi_c} [(\chi_c + 1)e^{|k|a} + (\chi_c - 1)e^{-|k|a}] \right. \\ &\quad \left. + \frac{|k|\chi_m}{2\chi_c} [(\chi_c + 1)e^{|k|a} - (\chi_c - 1)e^{-|k|a}] \right|^2 \\ &= \frac{|k|^2}{4} \left| \frac{(\chi_c + 1)(\chi_m + 1)}{\chi_c} e^{|k|a} + \frac{(\chi_c - 1)(1 - \chi_m)}{\chi_c} e^{-|k|a} \right|^2. \end{aligned} \quad (4.44)$$

From (4.5), (4.26), and (4.32) we have

$$\frac{(\chi_c + 1)(\chi_m + 1)}{\chi_c} = \frac{(\varepsilon_s/\varepsilon_c + 1)(\varepsilon_s/\varepsilon_m + 1)}{\varepsilon_s/\varepsilon_c}$$

$$\begin{aligned}
&= \frac{(\varepsilon_s + \varepsilon_c)(\varepsilon_s + \varepsilon_m)}{\varepsilon_s \varepsilon_m} \\
&= \frac{(-1 + i\delta + 1 + i\mu)(-1 + i\delta + 1)}{(-1 + i\delta)} \\
&= \frac{i(\delta + \mu)(i\delta)}{(-1 + i\delta)} \\
&= \frac{\delta(\delta + \mu)}{1 - i\delta}
\end{aligned} \tag{4.45}$$

and

$$\begin{aligned}
\frac{(\chi_c - 1)(1 - \chi_m)}{\chi_c} &= \frac{(\varepsilon_s/\varepsilon_c - 1)(1 - \varepsilon_s/\varepsilon_m)}{\varepsilon_s/\varepsilon_c} \\
&= \frac{(\varepsilon_s - \varepsilon_c)(\varepsilon_m - \varepsilon_s)}{\varepsilon_s \varepsilon_m} \\
&= \frac{(-1 + i\delta - (1 + i\mu))(1 - (-1 + i\delta))}{-1 + i\delta} \\
&= \frac{(2 + i(\mu - \delta))(2 - i\delta)}{1 - i\delta}.
\end{aligned} \tag{4.46}$$

Inserting (4.45) and (4.46) into (4.44) gives

$$\begin{aligned}
||k|\psi_k^+ + \psi_k^-|^2 &= \frac{|k|^2}{4} \left| \frac{\delta(\delta + \mu)}{1 - i\delta} e^{|k|a} + \frac{(2 + i(\mu - \delta))(2 - i\delta)}{1 - i\delta} e^{-|k|a} \right|^2 \\
&= \frac{|k|^2}{4(1 + \delta^2)} \left[\delta(\delta + \mu)e^{|k|a} + (2 + i(\mu - \delta))(2 - i\delta)e^{-|k|a} \right] \\
&\quad \cdot \left[\delta(\delta + \mu)e^{|k|a} + (2 - i(\mu - \delta))(2 + i\delta)e^{-|k|a} \right] \\
&= \frac{|k|^2}{4(1 + \delta^2)} \left[\delta^2(\delta + \mu)^2 e^{2|k|a} + \delta(\delta + \mu)(2 - i(\mu - \delta))(2 + i\delta) \right. \\
&\quad \left. + \delta(\delta + \mu)(2 + i(\mu - \delta))(2 - i\delta) \right. \\
&\quad \left. + (2 + i(\mu - \delta))(2 - i\delta)(2 - i(\mu - \delta))(2 + i\delta)e^{-2|k|a} \right] \\
&= \frac{|k|^2}{4(1 + \delta^2)} \left[\delta^2(\delta + \mu)^2 e^{2|k|a} + 2\delta(\delta + \mu)(4 + \delta(\mu - \delta)) \right. \\
&\quad \left. + (4 + (\mu - \delta)^2)(4 + \delta^2)e^{-2|k|a} \right].
\end{aligned}$$

This completes the proof.

Lemma 4.3 *Let ψ_k^+ and ψ_k^- be defined as in (4.30) and (4.31), respectively. Then for each $k \in \mathbb{R}$,*

$$\begin{aligned} \left| \psi_k^+ - \frac{1}{|k|} \psi_k^- \right|^2 &= \frac{1}{4(1 + \delta^2)} [(\delta + \mu)^2(4 + \delta^2)e^{2|k|a} + 2\delta(\delta + \mu)(\delta(\mu - \delta) - 4) \\ &\quad + \delta^2(4 + (\mu - \delta)^2)e^{-2|k|a}]. \end{aligned} \quad (4.47)$$

Proof of Lemma 4.3: Performing calculations similar to those in Lemma 4.2 and using (4.30) and (4.31) gives the desired result. This completes the proof.

4.5 Power Dissipation

Using the definition in (4.11), we compute the power dissipation in the strip R_ξ as follows. First, note that the integral in (4.11) is well defined because $V \in H^1(\mathring{\mathcal{S}})$ (so, in particular, $\nabla V \in L^2(\mathring{\mathcal{S}})$); this is shown in Lemma C.9 in Appendix C. Note that for any function $f : \mathbb{R}^2 \rightarrow \mathbb{C}$ such that

$$\int_{-\infty}^{\infty} |f(x, y)|^2 dy < \infty \quad \text{or} \quad \int_{-\infty}^{\infty} |\widehat{f}(x, k)|^2 dk < \infty,$$

the Plancherel Theorem holds, namely

$$\int_{-\infty}^{\infty} |f(x, y)|^2 dy = \frac{1}{2\pi} \int_{-\infty}^{\infty} |\widehat{f}(x, k)|^2 dk. \quad (4.48)$$

Using (4.48) together with the properties of the Fourier Transform (given in (4.17)), we have

$$\begin{aligned} E_\xi(\delta) &= \delta \int_{a-\xi}^a \left[\int_{-\infty}^{\infty} \left| \frac{\partial V_s}{\partial x}(x, y) \right|^2 dy + \int_{-\infty}^{\infty} \left| \frac{\partial V_s}{\partial y}(x, y) \right|^2 dy \right] dx \\ &= \delta \int_{a-\xi}^a \left[\int_{-\infty}^{\infty} \left| \frac{\partial \widehat{V}_s}{\partial x}(x, k) \right|^2 dk + \int_{-\infty}^{\infty} \left| \frac{\partial \widehat{V}_s}{\partial y}(x, k) \right|^2 dk \right] dx \\ &= \frac{\delta}{2\pi} \int_{a-\xi}^a \left[\int_{-\infty}^{\infty} \left| \frac{\partial \widehat{V}_s}{\partial x}(x, k) \right|^2 dk + \int_{-\infty}^{\infty} |k|^2 |\widehat{V}_s(x, k)|^2 dk \right] dx. \end{aligned} \quad (4.49)$$

The first equality is a consequence of the Plancherel Theorem (4.48) and the fact that $\frac{\partial V}{\partial x}(x, \cdot)$ and $\frac{\partial V}{\partial y}(x, \cdot)$ are in $L^2(\mathbb{R})$ for every $0 \leq x \leq a$ — see Lemma C.2 and Lemma C.6 in Appendix C. Since $\widehat{V}_s(x, 0)$ and $\frac{\partial \widehat{V}_s}{\partial x}(x, 0)$ are finite for all $x \in [d_0, d_1]$ (see (4.36)), we can omit the point $k = 0$ from the integrals in (4.49) without changing

the value of $E_\xi(\delta)$. Inserting (4.36) into (4.49) gives (after some straightforward computations)

$$\begin{aligned}
E_\xi(\delta) &= \frac{2\delta}{2\pi} \int_{a-\xi}^a \left\{ \int_{k \neq 0} \frac{|I_k|^2}{|g|^2} \left[e^{2|k|x} + \frac{e^{-2|k|x} (\lambda^2 \delta^{2\beta} + 4)}{(2\delta + \lambda \delta^\beta)^2} \right] dk \right\} dx \\
&= \frac{\delta}{\pi} \int_{k \neq 0} \frac{|I_k|^2}{|g|^2} \left\{ \int_{a-\xi}^a \left[e^{2|k|x} + \frac{e^{-2|k|x} (\lambda^2 \delta^{2\beta} + 4)}{(2\delta + \lambda \delta^\beta)^2} \right] dx \right\} dk \\
&= \frac{\delta}{\pi} \int_{k \neq 0} \frac{|I_k|^2}{|g|^2} \left\{ \frac{e^{2|k|x}}{2|k|} \Big|_{x=a-\xi}^a + \frac{e^{-2|k|x} [\lambda^2 \delta^{2\beta} + 4]}{-2|k|(2\delta + \lambda \delta^\beta)^2} \Big|_{x=a-\xi}^a \right\} dk \\
&= \frac{\delta}{\pi} \int_{k \neq 0} \frac{|I_k|^2}{|g|^2} \cdot \left\{ \frac{e^{2|k|a} - e^{2|k|(a-\xi)}}{2|k|} + \frac{(e^{-2|k|(a-\xi)} - e^{-2|k|a}) [\lambda^2 \delta^{2\beta} + 4]}{2|k|(2\delta + \lambda \delta^\beta)^2} \right\} dk \\
&= \frac{\delta}{2\pi} \int_{k \neq 0} \frac{|I_k|^2}{|k||g|^2} \cdot \left\{ e^{2|k|a} (1 - e^{-2|k|\xi}) + \frac{[\lambda^2 \delta^{2\beta} + 4]}{(2\delta + \lambda \delta^\beta)^2} e^{-2|k|a} (e^{2|k|\xi} - 1) \right\} dk \\
&= \frac{\delta}{2\pi} \int_{k \neq 0} \frac{|I_k|^2}{|k||g|^2} e^{2|k|a} \cdot \left[(1 - e^{-2|k|\xi}) + \frac{(\lambda^2 \delta^{2\beta} + 4)}{(2\delta + \lambda \delta^\beta)^2} e^{-4|k|a} (e^{2|k|\xi} - 1) \right] dk \\
&= \frac{\delta}{\pi} \int_0^\infty \frac{|I_k|^2}{k|g|^2} e^{2ka} \cdot \left[(1 - e^{-2k\xi}) + \frac{(\lambda^2 \delta^{2\beta} + 4)}{(2\delta + \lambda \delta^\beta)^2} e^{-4ka} (e^{2k\xi} - 1) \right] dk \quad (4.50)
\end{aligned}$$

$$\geq \tilde{E}_\xi(\delta) \equiv \int_{\tilde{k}}^\infty F dk, \quad (4.51)$$

where $\tilde{k} > 0$ is arbitrary,

$$F \equiv \left(\frac{\delta |I_k|^2}{\pi k |g|^2} \right) e^{2ka} L, \quad (4.52)$$

$$L \equiv (1 - e^{-2k\xi}) + \frac{(\lambda^2 \delta^{2\beta} + 4)}{(2\delta + \lambda \delta^\beta)^2} e^{-4ka} (e^{2k\xi} - 1), \quad (4.53)$$

and (4.50) holds since $|I_k|^2$ is an even function of k (see Lemma 4.1).

4.6 Lower Bound on Power Dissipation

In this section we derive some asymptotic estimates on the function F defined in (4.52). From (4.37) we have

$$|g|^2 = \delta^2 \left\{ \left(1 + \frac{4 + \lambda \delta^{\beta+1}}{2\delta^2 + \lambda \delta^{\beta+1}} e^{-2ka} \right)^2 + \left[\frac{2(\delta - \lambda \delta^\beta)}{2\delta^2 + \lambda \delta^{\beta+1}} e^{-2ka} \right]^2 \right\}. \quad (4.54)$$

Upon inspection of (4.50) we see (heuristically) that if $|g|^2 = O(\delta^2)$ as $\delta \rightarrow 0^+$, we may be able to show that the power dissipation blows up as $\delta \rightarrow 0^+$. To this end we define

$$k_0(\delta) \equiv \frac{1}{2a} \ln \left(\frac{1}{\delta(\delta + \mu)} \right) = \frac{1}{2a} \ln \left(\frac{1}{2\delta^2 + \lambda\delta^{\beta+1}} \right). \quad (4.55)$$

Note that $k_0(\delta) \rightarrow \infty$ as $\delta \rightarrow 0^+$. From (4.51) and recalling (4.37) and (4.52)–(4.53) we see that

$$E_\xi(\delta) \geq \int_{k_0(\delta)}^{\infty} F dk \quad (4.56)$$

for all $0 < \delta \leq \delta_0(\beta, \lambda)$ where $0 < \delta_0 \leq \delta_\mu$ is such that $k_0(\delta) > 0$ for $0 < \delta \leq \delta_0$ (recall $\delta_\mu(\beta, \lambda)$ is defined so that $\mu = \delta + \lambda\delta^\beta \geq 0$ for all $\delta \leq \delta_\mu$).

Lemma 4.4 *Suppose $\beta > 0$, λ is feasible (see (4.6)), and $C_1 > 25$. Then there exists $0 < \delta_g(\beta, \lambda, C_1) \leq \delta_\mu(\beta, \lambda)$ such that if $0 < \delta \leq \delta_g$ and $k \geq k_0(\delta)$ then*

$$|g|^2 \leq C_1 \delta^2.$$

Proof of Lemma 4.4: Note that (4.54) is equivalent to

$$|g|^2 = \delta^2 \left[1 + \frac{2(4 + \lambda\delta^{\beta+1})}{2\delta^2 + \lambda\delta^{\beta+1}} e^{-2ka} + \frac{16 + 4\delta^2 + \lambda^2\delta^{2\beta}(4 + \delta^2)}{(2\delta^2 + \lambda\delta^{\beta+1})^2} e^{-4ka} \right].$$

All three terms in the above equation are positive for all $0 < \delta \leq \delta_\mu$. To see this, recall that, by definition, $\mu = \delta + \lambda\delta^\beta \geq 0$ if $\delta \leq \delta_\mu$. Hence the denominator in the second term, namely $2\delta^2 + \lambda\delta^{\beta+1} = \delta(\delta + \mu) \geq 0$ for $\delta \leq \delta_\mu$. Similarly, the numerator in the second term is nonnegative since $\mu \geq 0$ if and only if $\lambda\delta^\beta \geq -\delta \geq -1$ since δ_μ is assumed to be less than 1. Thus $4 + \lambda\delta^{\beta+1} \geq 4 - \delta \geq 3$.

Also, since $k \geq k_0(\delta)$, $e^{-2ka} \leq e^{-2k_0(\delta)a} = 2\delta^2 + \lambda\delta^{\beta+1}$. Then, for $0 < \delta \leq \delta_\mu$ we have

$$\begin{aligned} |g|^2 &\leq \delta^2 \left[1 + \frac{2(4 + \lambda\delta^{\beta+1})}{2\delta^2 + \lambda\delta^{\beta+1}} e^{-2k_0(\delta)a} + \frac{16 + 4\delta^2 + \lambda^2\delta^{2\beta}(4 + \delta^2)}{(2\delta^2 + \lambda\delta^{\beta+1})^2} e^{-4k_0(\delta)a} \right] \\ &\leq \delta^2 \left[25 + 2\lambda\delta^{\beta+1} + 4\delta^2 + \lambda^2\delta^{2\beta}(4 + \delta^2) \right]. \end{aligned}$$

We then choose $\delta_g(\beta, \lambda, C_1) \leq \delta_\mu(\beta, \lambda)$ small enough to ensure that the term in brackets is less than or equal to C_1 for all $0 < \delta \leq \delta_g$. This completes the proof.

Lemma 4.5 *Suppose $\beta > 0$, λ is feasible, $0 < \xi < a$, and let $0 < C_L < 1$ be a constant. Then there exists $0 < \delta_L(\beta, \lambda, \frac{\xi}{a}, C_L) \leq \delta_\mu(\beta, \lambda)$ such that if $0 < \delta \leq \delta_L$ and $k \geq k_0(\delta)$, then $L \geq C_L$.*

Proof of Lemma 4.5: From (4.53) we have

$$\begin{aligned} L &= (1 - e^{-2k\xi}) + \frac{\lambda^2 \delta^{2\beta} + 4}{(2\delta + \lambda \delta^\beta)^2} e^{-4ka} (e^{2k\xi} - 1) \\ &\geq 1 - e^{-2k\xi} \\ &\geq 1 - e^{-2k_0(\delta)\xi} \\ &= 1 - (2\delta^2 + \lambda \delta^{\beta+1})^{\frac{\xi}{a}} \\ &\geq C_L \end{aligned}$$

for $0 < \delta \leq \delta_L(\beta, \lambda, \frac{\xi}{a}, C_L)$, where $0 < \delta_L \leq \delta_\mu$ is such that $(2\delta^2 + \lambda \delta^{\beta+1})^{\frac{\xi}{a}} \leq 1 - C_L$ for $0 < \delta \leq \delta_L$. This completes the proof.

For $0 < \delta \leq \min\{\delta_0, \delta_g, \delta_L\}$ we apply the bounds from Lemmas 4.4 and 4.5 to (4.56) and, recalling (4.52)–(4.54), find

$$E_\xi(\delta) \geq \frac{C_L}{\pi C_1 \delta} \int_{k_0(\delta)}^{\infty} \frac{|I_k|^2}{k} e^{2ka} dk. \quad (4.57)$$

Note that this integral converges by Lemma 4.1; in particular, for $k \geq k_0(\delta) > 0$ we have $k^{-1}|I_k|^2 e^{2ka} \leq (d_1 - d_0) \|\rho\|_{L^2(\mathcal{M})}^2 k_0(\delta)^{-1} e^{-2k(d_0 - a)}$, which is integrable on $(k_0(\delta), \infty)$ because $d_0 > a$. Our goal is to show that $E_\xi(\delta)$ tends to infinity as a sequence δ_j tends to 0.

From (4.57) we have

$$E_\xi(\delta) \geq \frac{C_L}{\pi C_1 \delta} \int_{k_0(\delta)}^{k_0(\delta) + \frac{1}{\ln(\frac{e}{\delta})}} \frac{|I_k|^2}{k} e^{2ka} dk. \quad (4.58)$$

Since $0 < \delta < 1$, we have $\ln(\frac{e}{\delta}) \geq 1$; thus

$$k_0(\delta) + \frac{1}{\ln(\frac{e}{\delta})} \leq k_0(\delta) + 1.$$

This in combination with (4.58) implies

$$E_\xi(\delta) \geq \left(\frac{C_L}{\pi C_1} \right) \left(\frac{e^{2k_0(\delta)a}}{\delta [k_0(\delta) + 1]} \right) \int_{k_0(\delta)}^{k_0(\delta) + \frac{1}{\ln(\frac{e}{\delta})}} |I_k|^2 dk.$$

Since $|I_k|^2$ is a continuous function of k for $k > 0$ by Lemma 4.1, we may apply the mean value theorem for integrals to the expression above to obtain

$$E_\xi(\delta) \geq \left(\frac{C_L}{\pi C_1} \right) \left[\frac{e^{2k_0(\delta)a}}{\delta \ln \left(\frac{e}{\delta} \right) [k_0(\delta) + 1]} \right] |I_{k_0(\delta)+t(\delta)}|^2 \quad (4.59)$$

for some $0 \leq t(\delta) \leq \frac{1}{\ln(\frac{e}{\delta})} \leq 1$. Note that $t(\delta) \rightarrow 0$ as $\delta \rightarrow 0^+$. So now we must show that the lower bound (4.59) tends to infinity as a sequence δ_j tends to 0.

Theorem 4.3 *Let $\rho \in \mathcal{P}$, $\beta > 0$, and λ be feasible. Assume there exist constants $d_* \in [d_0, d_1]$ and $\Lambda \in (0, \infty]$ such that $\limsup_{k \rightarrow \infty} |I_k e^{kd_*}| = \Lambda$. Then there exists a sequence $\{\delta_j\}_{j=1}^\infty$ with $\delta_j \rightarrow 0^+$ as $j \rightarrow \infty$ and there exist positive constants $C' \equiv \frac{C_L e^{-2d_*}}{2\pi C_1}$, $C_2 \equiv \frac{C' a \Lambda^2 \lambda^{(d_*-a)/a}}{2}$, $C_3 \equiv \ln \lambda$, and $C_4 \equiv \frac{C' a \Lambda^2}{4}$ such that*

$$E_\xi(\delta_j) \geq \begin{cases} \frac{C_2 \delta_j^{(\beta+1)(\frac{d_*-a}{a})-1}}{(\ln \delta_j - 1) [C_3 + (\beta + 1) \ln \delta_j]} & \text{for } 0 < \beta < 1, \\ \frac{C_4 \delta_j^{2(\frac{d_*-a}{a})-1}}{(\ln \delta_j - 1) \ln \delta_j} & \text{for } \beta \geq 1. \end{cases} \quad (4.60)$$

(The constants C_2 and C_3 are well defined since $\lambda > 0$ if $0 < \beta < 1$ — see (4.6).)

Moreover, if $\lim_{k \rightarrow \infty} |I_k e^{kd_*}| = \Lambda$, then for δ small enough we have

$$E_\xi(\delta) \geq \begin{cases} \frac{C_2 \delta^{(\beta+1)(\frac{d_*-a}{a})-1}}{(\ln \delta - 1) [C_3 + (\beta + 1) \ln \delta]} & \text{for } 0 < \beta < 1, \\ \frac{C_4 \delta^{2(\frac{d_*-a}{a})-1}}{(\ln \delta - 1) \ln \delta} & \text{for } \beta \geq 1. \end{cases} \quad (4.61)$$

Proof of Theorem 4.3: If $0 < \delta \leq \min\{\delta_0, \delta_g, \delta_L\}$, then (4.59) holds. Since $0 \leq t(\delta) \leq 1$ and $k_0(\delta) + 1 \leq 2k_0(\delta)$ for δ small enough (equivalently $k_0(\delta)$ large enough), (4.59) implies

$$\begin{aligned} E_\xi(\delta) &\geq \left(\frac{C_L}{2\pi C_1} \right) \left[\frac{e^{2k_0(\delta)a}}{\delta \ln \left(\frac{e}{\delta} \right) k_0(\delta)} \right] \left| [I_{k_0(\delta)+t(\delta)}] e^{[k_0(\delta)+t(\delta)]d_*} \right|^2 e^{-2[k_0(\delta)+t(\delta)]d_*} \\ &= \left(\frac{C_L e^{-2t(\delta)d_*}}{2\pi C_1} \right) \frac{e^{-2k_0(\delta)(d_*-a)}}{\delta \ln \left(\frac{e}{\delta} \right) k_0(\delta)} \left| I_{k'(\delta)} e^{k'(\delta)d_*} \right|^2, \end{aligned} \quad (4.62)$$

where $k'(\delta) \equiv k_0(\delta) + t(\delta)$. Since $0 \leq t(\delta) \leq 1$, we have $0 \geq -2t(\delta)d_* \geq -2d_*$, which implies $1 \geq e^{-2t(\delta)d_*} \geq e^{-2d_*}$. Inserting this into (4.62) gives

$$E_\xi(\delta) \geq \frac{C' e^{-2k_0(\delta)(d_*-a)}}{\delta \ln\left(\frac{e}{\delta}\right) k_0(\delta)} \left| I_{k'(\delta)} e^{k'(\delta)d_*} \right|^2. \quad (4.63)$$

Since $\limsup_{k \rightarrow \infty} |I_k e^{kd_*}| = \Lambda$, there exists a sequence $\{k_j\}_{j=1}^\infty$ with $k_j \rightarrow \infty$ as $j \rightarrow \infty$ and

$$\lim_{j \rightarrow \infty} |I_{k_j} e^{k_j d_*}| = \Lambda. \quad (4.64)$$

We choose a sequence $\{\delta_j\}_{j=1}^\infty$ such that $\delta_j \rightarrow 0^+$ as $j \rightarrow \infty$ and $k_j = k_0(\delta_j)$ (where $k_0(\delta) = -\frac{1}{2a} \ln(2\delta^2 + \lambda\delta^{\beta+1})$ is defined in (4.55)).

We define $k'_j \equiv k'(\delta_j) = k_0(\delta_j) + t(\delta_j)$; note that $k'_j = k_j + t(\delta_j) \rightarrow \infty$ as $j \rightarrow \infty$ (i.e., as $\delta_j \rightarrow 0^+$). Also, $|k'_j - k_j| = |t(\delta_j)| \rightarrow 0$ as $j \rightarrow \infty$. Thus $|k'_j - k_j|$ can be made arbitrarily small by taking j large enough. Since $|I_k e^{kd_*}|$ is a continuous function of k , by taking j large enough we can ensure that $|I_{k'_j} e^{k'_j d_*} - I_{k_j} e^{k_j d_*}|$ is as small as we wish; this, in combination with (4.64), implies

$$\lim_{j \rightarrow \infty} |I_{k'_j} e^{k'_j d_*}| = \Lambda.$$

Thus, for j large enough (i.e., δ_j small enough), $|I_{k'_j} e^{k'_j d_*}| \geq \Lambda/2$ (if $\Lambda = \infty$ any positive number here will do in place of $\Lambda/2$). Hence for large enough j we have (from (4.63))

$$E_\xi(\delta_j) \geq \left(\frac{C' \Lambda^2}{4} \right) \frac{e^{-2k_0(\delta_j)(d_*-a)}}{\delta_j \ln\left(\frac{e}{\delta_j}\right) k_0(\delta_j)} = \left(\frac{C' \Lambda^2}{4} \right) \frac{(2\delta_j^2 + \lambda\delta_j^{\beta+1})^{(d_*-a)/a}}{\delta_j \ln\left(\frac{e}{\delta_j}\right) k_0(\delta_j)}. \quad (4.65)$$

With j large enough so that $\delta_j \leq \delta_\mu$ we have $\mu_j \equiv \delta_j + \lambda\delta_j^\beta \geq 0$. Thus if $\beta \geq 1$ and j is large enough so that $\mu_j \geq 0$, then $2\delta_j^2 + \lambda\delta_j^{\beta+1} = \delta_j(\delta_j + \mu_j) \geq \delta_j^2$. On the other hand, if $0 < \beta < 1$, then $\lambda > 0$ (by (4.6)) and so $2\delta_j^2 + \lambda\delta_j^{\beta+1} \geq \lambda\delta_j^{\beta+1}$. In summary, for j large enough so that $\delta_j \leq \delta_\mu$ we have the inequality

$$2\delta_j^2 + \lambda\delta_j^{\beta+1} \geq \begin{cases} \lambda\delta_j^{\beta+1} & \text{for } 0 < \beta < 1, \\ \delta_j^2 & \text{for } \beta \geq 1. \end{cases} \quad (4.66)$$

Recalling the definition of k_0 in (4.55), we note that (4.66) implies

$$k_0(\delta_j) = \frac{1}{2a} \ln \left(\frac{1}{2\delta_j^2 + \lambda\delta_j^{\beta+1}} \right)$$

$$\begin{aligned}
&= -\frac{1}{2a} \ln(2\delta_j^2 + \lambda\delta_j^{\beta+1}) \\
&\leq \begin{cases} -\frac{1}{2a} \ln(\lambda\delta_j^{\beta+1}) & \text{for } 0 < \beta < 1, \\ -\frac{1}{2a} \ln(\delta_j^2) & \text{for } \beta \geq 1. \end{cases} \tag{4.67}
\end{aligned}$$

To finish the proof, we apply the inequalities (4.66) to (4.65). In particular, if $0 < \beta < 1$, (4.67) implies

$$\begin{aligned}
E_\xi(\delta_j) &\geq \left(\frac{C'\Lambda^2}{4}\right) \frac{(\lambda\delta_j^{\beta+1})^{(d_*-a)/a}}{\delta_j \ln\left(\frac{e}{\delta_j}\right)} \cdot \left[-\frac{2a}{\ln(\lambda\delta_j^{\beta+1})}\right] \\
&= \left(\frac{C'a\Lambda^2\lambda^{(d_*-a)/a}}{2}\right) \frac{\delta_j^{(\beta+1)(\frac{d_*-a}{a})}}{\delta_j(\ln\delta_j - 1)[\ln\lambda + (\beta+1)\ln\delta_j]} \\
&= \frac{C_2\delta_j^{(\beta+1)(\frac{d_*-a}{a})-1}}{(\ln\delta_j - 1)[C_3 + (\beta+1)\ln\delta_j]}.
\end{aligned}$$

Similarly, if $\beta \geq 1$ then (4.65), (4.66)–(4.67) imply

$$\begin{aligned}
E_\xi(\delta) &\geq \left(\frac{C'\Lambda^2}{4}\right) \frac{(\delta_j^2)^{(d_*-a)/a}}{\delta_j \ln\left(\frac{e}{\delta_j}\right)} \cdot \left[-\frac{2a}{\ln(\delta_j^2)}\right] \\
&= \left(\frac{C'a\Lambda^2}{4}\right) \frac{\delta_j^{2(\frac{d_*-a}{a})}}{\delta_j(\ln\delta_j - 1)\ln\delta_j} \\
&= \frac{C_4\delta_j^{2(\frac{d_*-a}{a})-1}}{(\ln\delta_j - 1)\ln\delta_j}.
\end{aligned}$$

Similarly, if the stronger condition $\lim_{k \rightarrow \infty} |I_k e^{kd_*}| = \Lambda$ holds, since $k'(\delta) \rightarrow \infty$ as $\delta \rightarrow 0^+$ we have $|I_{k'(\delta)} e^{k'(\delta)d_*}| \geq \frac{\Lambda}{2}$ and

$$E_\xi(\delta) \geq \left(\frac{C'\Lambda^2}{4}\right) \frac{(2\delta^2 + \lambda\delta^{\beta+1})^{(d_*-a)/a}}{\delta \ln\left(\frac{e}{\delta}\right) k_0(\delta)} \tag{4.68}$$

for δ small enough; this is the continuous analog of (4.65) and is a consequence of (4.63). Finally, (4.61) is obtained by inserting the inequality

$$2\delta^2 + \lambda\delta^{\beta+1} \geq \begin{cases} \lambda\delta^{\beta+1} & \text{for } 0 < \beta < 1, \\ \delta^2 & \text{for } \beta \geq 1, \end{cases}$$

which holds for δ small enough, into (4.68). This completes the proof.

The next corollary follows from Theorem 4.3.

Corollary 4.1 *Let $\rho \in \mathcal{P}$, $\beta > 0$, and λ be feasible. Assume there exist constants $d_* \in [d_0, d_1]$ and $\Lambda \in (0, \infty]$ such that*

$$(a) \limsup_{k \rightarrow \infty} |I_k e^{kd_*}| = \Lambda; \text{ or}$$

$$(b) \lim_{k \rightarrow \infty} |I_k e^{kd_*}| = \Lambda.$$

If $d_* < \tau(\beta)a$, where τ is the continuous function

$$\tau(\beta) \equiv \begin{cases} \frac{\beta+2}{\beta+1} & \text{if } 0 < \beta < 1, \\ \frac{3}{2} & \text{if } \beta \geq 1, \end{cases} \quad (4.69)$$

then $\limsup_{\delta \rightarrow 0^+} E_\xi(\delta) = \infty$ if (a) holds (weak CALR) and $\lim_{\delta \rightarrow 0^+} E_\xi(\delta) = \infty$ if (b) holds (strong CALR).

Proof of Corollary 4.1: If $0 < \beta < 1$, then, since $\delta_j \rightarrow 0^+$ as $j \rightarrow \infty$, the l'Hospital Rule implies

$$\lim_{j \rightarrow \infty} \left\{ \frac{C_2 \delta_j^{(\beta+1)\left(\frac{d_*-a}{a}\right)-1}}{(\ln \delta_j - 1) [C_3 + (\beta+1) \ln \delta_j]} \right\} = \infty$$

if and only if

$$(\beta+1) \left(\frac{d_*-a}{a} \right) - 1 < 0 \quad \Leftrightarrow \quad d_* < a + \frac{a}{\beta+1} = \left(\frac{\beta+2}{\beta+1} \right) a. \quad (4.70)$$

Since

$$E_\xi(\delta_j) \geq \frac{C_2 \delta_j^{(\beta+1)\left(\frac{d_*-a}{a}\right)-1}}{(\ln \delta_j - 1) [C_3 + (\beta+1) \ln \delta_j]}$$

for j large enough by Theorem 4.3, $\lim_{j \rightarrow \infty} E_\xi(\delta_j) = \infty$ if and only if the condition (4.70) holds.

Similarly,

$$\lim_{j \rightarrow \infty} \left[\frac{C_4 \delta_j^{2\left(\frac{d_*-a}{a}\right)-1}}{(\ln \delta_j - 1) \ln \delta_j} \right] = \infty$$

if and only if

$$2 \left(\frac{d_*-a}{a} \right) - 1 < 0 \quad \Leftrightarrow \quad d_* < \frac{a}{2} + a = \frac{3}{2}a. \quad (4.71)$$

Since

$$E_\xi(\delta_j) \geq \frac{C_4 \delta_j^{2\left(\frac{d_*-a}{a}\right)-1}}{(\ln \delta_j - 1) \ln \delta_j}$$

for j large enough by Theorem 4.3, $\lim_{j \rightarrow \infty} E_\xi(\delta_j) = \infty$ if and only if the condition (4.71) holds.

The proof in the case where the hypothesis (b) holds is proved in the same way. This completes the proof.

Remark 4.1 *According to the previous corollary, the region of influence, i.e., the region in which the charge density ρ should be placed to cause the power dissipation blow-up near the inner right edge of the slab, is the interval $(a, \tau(\beta)a)$. In particular we can take $d_1 < \tau(\beta)a$ to guarantee that ρ is completely inside this region (assuming the support of ρ is small enough so that $d_0 > a$ as well). This region of influence is the same as that found in the cloaking paper by Milton and Nicorovici [91] and also in the superlensing paper by Milton et al. [94] in the particular case when ρ is a dipole source. Also see Bergman's work [15].*

4.6.1 Numerical Discussion

In this section, we study the behavior of two charge density distributions ρ . In particular, we show that they satisfy the conditions of Theorem 4.3 that lead to weak CALR, i.e., they satisfy $\limsup_{k \rightarrow \infty} |I_k e^{kd_*}| = \Lambda$. We also provide plots illustrating the blow-up of the dissipated electrical power as δ goes to 0^+ for these charge density distributions.

4.6.1.1 Rectangle

The first charge density distribution we consider has support in a rectangle centered at (x_0, y_0) . The left and right edges of the rectangle are at $d_0 = x_0 - d$ and $d_1 = x_0 + d$, respectively, where $d > 0$. The bottom and top edges are at $h_0 = y_0 - h$ and $h_1 = y_0 + h$, respectively, where $h > 0$. These parameters are chosen so $d_0 > a$. We define the charge density distribution as

$$\rho(x, y) = \begin{cases} Q & \text{for } (x, y) \in [d_0, d_1] \times (y_0, h_1], \\ -Q & \text{for } (x, y) \in [d_0, d_1] \times [h_0, y_0), \\ 0 & \text{otherwise,} \end{cases} \quad (4.72)$$

where $Q \neq 0$. Since $\rho \in L^1(\mathcal{M}) \cap L^2(\mathcal{M})$, we can use calculus, (4.16), and (4.35) to find

$$\widehat{\rho}(x, k) = -\frac{4Q}{k} [\sin(y_0 k) + i \cos(y_0 k)] \sin^2\left(\frac{hk}{2}\right) \quad (4.73)$$

and

$$|I_k| = \frac{4|Q|}{k^2} \sin^2\left(\frac{hk}{2}\right) e^{-d_0 k} (1 - e^{-2dk}) \quad (4.74)$$

for $k > 0$. If we take $k_j = \frac{(2j-1)\pi}{h}$ for $j = 1, 2, \dots$ and $d_* = d_0 + \alpha$ for $\alpha > 0$ we have

$$|I_{k_j} e^{d_* k_j}| = \frac{4|Q|}{k_j^2} e^{\alpha k_j} (1 - e^{-2d k_j}) \rightarrow \infty \quad \text{as } j \rightarrow \infty.$$

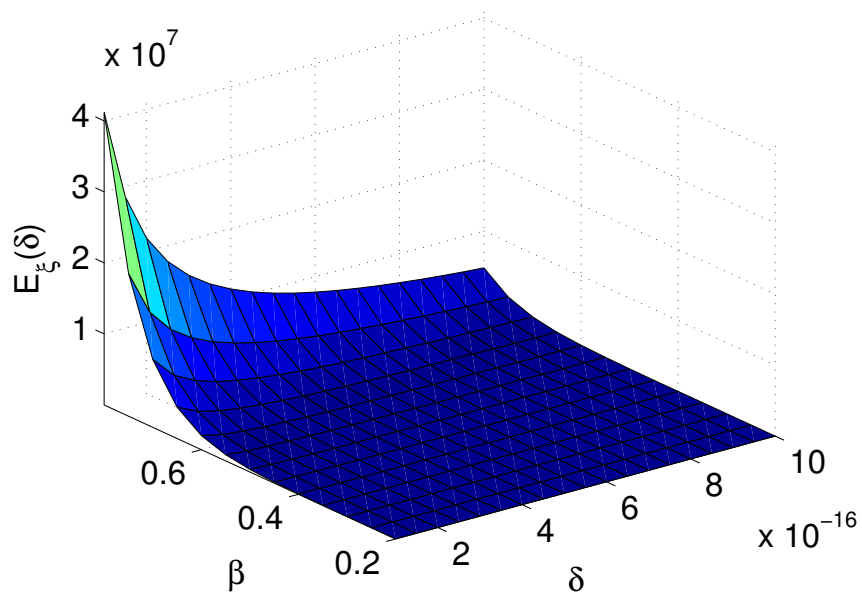
This implies $\limsup_{k \rightarrow \infty} |I_k e^{d_* k}| = \infty$, so ρ satisfies the conditions of Theorem 4.3. Thus there is a sequence $\delta_j \rightarrow 0^+$ as $j \rightarrow \infty$ such that $E_\xi(\delta_j) \rightarrow \infty$ as $j \rightarrow \infty$ if $d_0 + \alpha < \tau(\beta)a$; according to Theorem 4.4 in Section 4.7, if $d_0 > \tau(\beta)a$, then $E_\xi(\delta) \rightarrow 0$ as $\delta \rightarrow 0^+$.

Since $\alpha > 0$ is arbitrary, the limit superior of the power dissipation blows up as the dissipation in the lens tends to 0 as long as any part of the charge density distribution ρ is within the region of influence $(a, \tau(\beta)a)$.

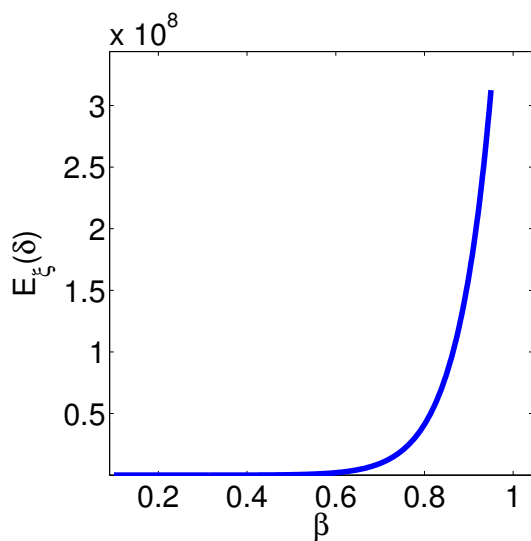
In Figure 4.9 we plot $E_\xi(\delta)$ for the rectangular charge density ρ studied above for various values of β and δ . The support of ρ is centered at $(6, 6)$, and has width and height 2; thus $d_0 = h_0 = 5$, $d_1 = h_1 = 7$, and $d = h = 1$. We take $0 < \beta < 1$ and $a = d_1/\tau(\beta) = d_1 \left(\frac{\beta+1}{\beta+2}\right)$, so the support of ρ is completely inside the region of influence (see (4.69) and Remark 4.1). Figure 4.9(a) is a plot of the power dissipation $E_\xi(\delta)$ as a function of β and δ . We observe the divergence of $E_\xi(\delta)$ as $\delta \rightarrow 0^+$ for $0 < \beta < 1$; in particular the divergence appears to be more severe for larger values of β . In Figure 4.9(b) we fix $\delta = 10^{-16}$ and plot $E_\xi(\delta)$ as a function of β . Note the strong dependence of the divergence of $E_\xi(\delta)$ on the relative dissipation parameter β . Finally, in Figure 4.9(c) we plot $E_\xi(\delta)$ as a function of δ for $\beta = 0.8$.

4.6.1.2 Circle

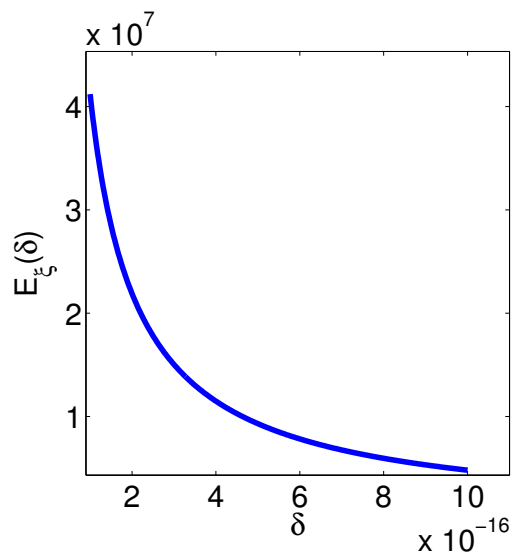
We now consider a charge density distribution with support in a circle of radius R centered at (x_0, y_0) . In this case we have $d_0 = x_0 - R$ and $d_1 = x_0 + R$. Again we



(a)



(b)



(c)

Figure 4.9. (Rectangular ρ) In all of these figures we take $a = d_1/\tau(\beta)$ so ρ is completely within the region of influence. (a) A plot of $E_{\xi}(\delta)$ versus β and δ — the z -axis scale is 10^7 ; (b) a plot of $E_{\xi}(\delta)$ for $\delta = 10^{-16}$ as a function of β — the y -axis scale is 10^8 ; (c) a plot of $E_{\xi}(\delta)$ for $\beta = 0.8$ as a function of δ — the y -axis scale is 10^7 .

choose the parameters so that $d_0 > a$. We define the charge density distribution as

$$\rho(x, y) = \begin{cases} Q & \text{for } d_0 \leq x \leq d_1, y_0 < y \leq h_1(x), \\ -Q & \text{for } d_0 \leq x \leq d_1, h_0(x) \leq y < y_0, \\ 0 & \text{otherwise,} \end{cases}$$

where $Q \neq 0$. Again, $\rho \in L^1(\mathcal{M}) \cap L^2(\mathcal{M})$, so (4.16) and (4.35) imply

$$\widehat{\rho}(x, k) = -\frac{4Q}{k} [\sin(y_0 k) + i \cos(y_0 k)] \sin^2 \left[\frac{k}{2} \sqrt{R^2 - (x - x_0^2)} \right]$$

and

$$|I_k| = \frac{4|Q|}{k} \int_{d_0}^{d_1} \sin^2 \left[\frac{k}{2} \sqrt{R^2 - (s - x_0^2)} \right] e^{-ks} ds$$

for $k > 0$.

Claim: If $d_* = x_0 + \alpha$ for $\alpha > 0$, then $\limsup_{k \rightarrow \infty} |I_k e^{d_* k}| = \infty$.

Proof of Claim: Let $\{k_j\}_{j=1}^{\infty}$ be the sequence whose j^{th} term is given by $k_j = \frac{2}{R} \left(\frac{\pi}{2} + 2\pi j \right)$. Then

$$|I_{k_j}| \geq \frac{4|Q|}{k_j} \int_{x_0}^{x_0 + \gamma_j} \sin^2 \left[\frac{k_j}{2} \sqrt{R^2 - (s - x_0^2)} \right] e^{-k_j s} dx, \quad (4.75)$$

where $\gamma_j = \frac{R}{j}$ for $j = 1, 2, \dots$

For $s \in [x_0, x_0 + \gamma_j]$ we have

$$\frac{k_j}{2} \sqrt{R^2 - \gamma_j^2} \leq \frac{k_j}{2} \sqrt{R^2 - (s - x_0)^2} \leq \frac{k_j R}{2}. \quad (4.76)$$

We also have

$$\frac{k_j}{2} \sqrt{R^2 - \gamma_j^2} = \left(\frac{\pi}{2} + 2\pi j \right) \sqrt{1 - \frac{1}{j^2}} = \frac{\pi}{2} - \zeta_j + 2\pi j, \quad (4.77)$$

where

$$\zeta_j \equiv \frac{\frac{\pi}{2} + 2\pi j}{j^2 \left(1 + \sqrt{1 - \frac{1}{j^2}} \right)} = \left(\frac{\pi}{2} + 2\pi j \right) \left(1 - \sqrt{1 - \frac{1}{j^2}} \right).$$

Note $\zeta_j \rightarrow 0^+$ as $j \rightarrow \infty$, so $0 < \zeta_j < \frac{\pi}{2}$ for j large enough. In combination with (4.76) and (4.77) this implies

$$2\pi j < \frac{\pi}{2} - \zeta_j + 2\pi j \leq \frac{k_j}{2} \sqrt{R^2 - (s - x_0)^2} \leq \frac{k_j R}{2} = \frac{\pi}{2} + 2\pi j \quad (4.78)$$

for j large enough. Since $\sin \theta$ is monotone increasing for $\theta \in (0, \frac{\pi}{2})$, (4.75) and (4.78)

imply

$$|I_{k_j}| \geq \frac{4|Q|}{k_j} \sin^2 \left(\frac{\pi}{2} - \zeta_j + 2\pi j \right) \int_{x_0}^{x_0 + \gamma_j} e^{-k_j s} ds$$

$$= \frac{4|Q|}{k_j^2} \sin^2\left(\frac{\pi}{2} - \zeta_j\right) e^{-k_j x_0} (1 - e^{-k_j \gamma_j}). \quad (4.79)$$

Now $k_j \gamma_j = \pi/j + 4\pi \geq 4\pi$ so $1 - e^{-k_j \gamma_j} \geq 1 - e^{-4\pi}$. Also, since $\zeta_j \rightarrow 0^+$ as $j \rightarrow \infty$, for j large enough we have $\sin(\pi/2 - \zeta_j) \geq 1/2$. Using the fact that $d_* = x_0 + \alpha$, we see that for j large enough (4.79) implies

$$\begin{aligned} |I_{k_j} e^{d_* k_j}| &\geq \frac{4|Q|}{k_j^2} \sin^2\left(\frac{\pi}{2} - \zeta_j\right) e^{\alpha k_j} (1 - e^{-k_j \gamma_j}) \\ &\geq |Q| (1 - e^{-4\pi}) \frac{e^{\alpha k_j}}{k_j^2} \rightarrow \infty \quad \text{as } j \rightarrow \infty. \end{aligned}$$

This implies that $\limsup_{k \rightarrow \infty} |I_k e^{d_* k}| = \infty$. This completes the proof of the claim.

Again we note that ρ need not be completely within the region of influence for the limit superior of the power dissipation to blow-up as the dissipation in the lens goes to 0. In particular, according to the above analysis, ρ only needs to be slightly more than halfway inside the region of influence for the blow-up to occur. However, numerical results seem to indicate that the power dissipation due to this charge density distribution blows up even if ρ is just inside the region of influence (as is the case for the rectangular charge density distribution analyzed in Section 4.6.1.1).

In Figure 4.10 we plot $E_\xi(\delta)$ as a function of β and δ for the circular charge distribution discussed above. We assume ρ is centered at $(6, 6)$ so $d_0 = 5$, $d_1 = 7$, and $d = 1$. as in the rectangular case. The only other difference between Figures 4.10 and 4.9 are the values of δ we used to construct the plots.

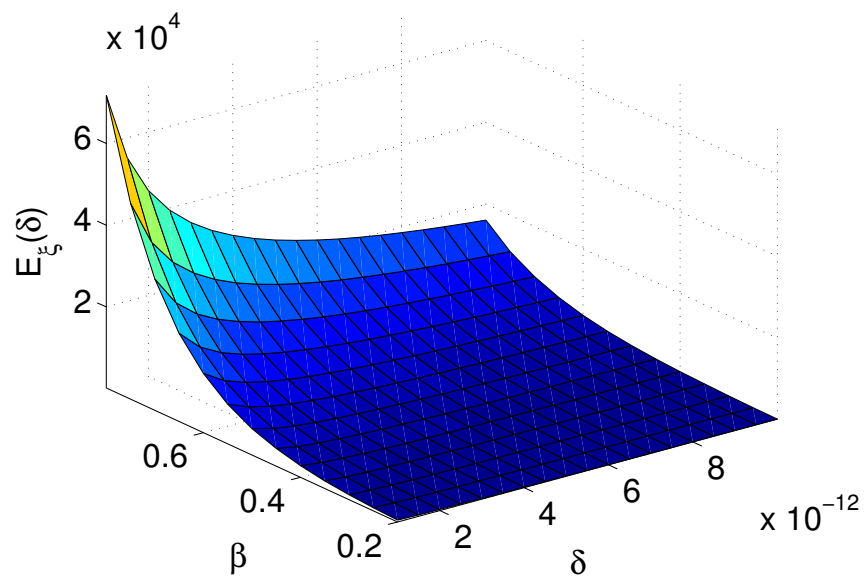
4.7 Upper Bound on Power Dissipation

In this section, we discuss what happens when $d_0 > \tau(\beta)a \geq \frac{3}{2}a$. Recall that ρ has compact support, so $\text{supp}(\rho) \subseteq [d_0, d_1] \times [h_0, h_1]$ for some constants $a < d_0 < d_1$ and $h_0 < h_1$.

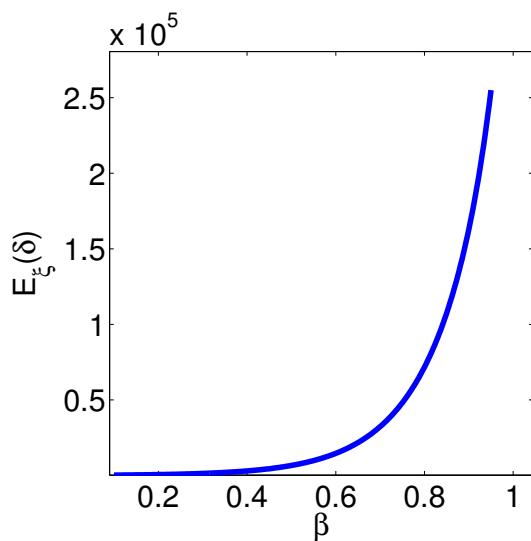
Recall that the power dissipation is given *exactly* by

$$E_\xi(\delta) = \int_0^\infty F dk;$$

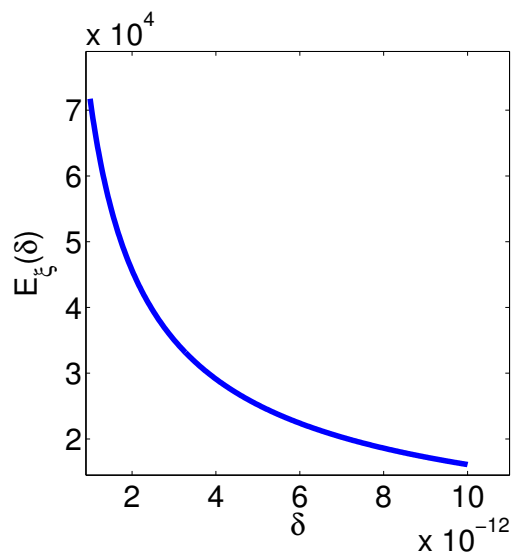
see (4.50) and (4.52)–(4.53). We now prove a series of lemmas that lead to an upper bound on $E_\xi(\delta)$. First we recall that $\delta_\mu < 1$ is such that $\mu = \delta + \lambda\delta^\beta \geq 0$ for $\delta \leq \delta_\mu$. Also, we note that $3/2 < \tau(\beta) < 2$ for $0 < \beta < 1$ due to (4.69).



(a)



(b)



(c)

Figure 4.10. (Circular ρ) In all of these figures we take $a = d_1/\tau(\beta)$ so ρ is completely within the region of influence. (a) A plot of $E_{\xi}(\delta)$ versus β and δ — the z -axis scale is 10^4 ; (b) a plot of $E_{\xi}(\delta)$ for $\delta = 10^{-12}$ as a function of β — the y -axis scale is 10^5 ; (c) a plot of $E_{\xi}(\delta)$ for $\beta = 0.8$ as a function of δ — the y -axis scale is 10^4 .

Lemma 4.6 Suppose $\beta > 0$ and λ is feasible, and let $k_0(\delta)$ be defined as in (4.55). Then for every $0 < \delta \leq \delta_0$

$$|g|^2 \geq \begin{cases} 9e^{-4ka} \frac{\delta^2}{(2\delta^2 + \lambda\delta^{\beta+1})^2} & \text{for } 0 \leq k \leq k_0(\delta), \\ e^{-ka} \frac{\delta^2}{(2\delta^2 + \lambda\delta^{\beta+1})^{\frac{1}{2}}} & \text{for } k \geq k_0(\delta). \end{cases}$$

Proof of Lemma 4.6: From (4.54) we have

$$\begin{aligned} |g|^2 &= \delta^2 \left\{ \left(1 + \frac{4 + \lambda\delta^{\beta+1}}{2\delta^2 + \lambda\delta^{\beta+1}} e^{-2ka} \right)^2 + \left[\frac{2(\delta - \lambda\delta^\beta)}{2\delta^2 + \lambda\delta^{\beta+1}} e^{-2ka} \right]^2 \right\} \\ &\geq \delta^2 \left(1 + \frac{4 + \lambda\delta^{\beta+1}}{2\delta^2 + \lambda\delta^{\beta+1}} e^{-2ka} \right)^2. \end{aligned} \quad (4.80)$$

For $0 < \delta \leq \delta_0 \leq \delta_\mu < 1$ (for which $\mu = \delta + \lambda\delta^\beta \geq 0$) we have $4 + \lambda\delta^{\beta+1} \geq 4 - \delta^2 \geq 4 - \delta_\mu^2 \geq 3$. Then, from (4.80), for fixed $\delta \leq \delta_0$ and for all $k \in \mathbb{R}$ we have

$$|g|^2 \geq \delta^2 \left(\frac{3}{2\delta^2 + \lambda\delta^{\beta+1}} e^{-2ka} \right)^2 = 9e^{-4ka} \frac{\delta^2}{(2\delta^2 + \lambda\delta^{\beta+1})^2}.$$

This bound holds for all k ; in particular it holds for $0 \leq k \leq k_0(\delta)$.

To prove the second part of the lemma we note that (4.80) implies that $|g|^2 \geq \delta^2$ when $0 < \delta \leq \delta_0 \leq \delta_\mu$ (since $4 + \lambda\delta^{\beta+1} \geq 3$ for $0 < \delta \leq \delta_\mu$ as above). If $k \geq k_0(\delta)$ holds as well we have

$$e^{-ka} \frac{\delta^2}{(2\delta^2 + \lambda\delta^{\beta+1})^{\frac{1}{2}}} \leq e^{-k_0(\delta)a} \frac{\delta^2}{(2\delta^2 + \lambda\delta^{\beta+1})^{\frac{1}{2}}} = \delta^2 \leq |g|^2.$$

This completes the proof.

Combining the computations from Lemmas 4.6 and 4.1 we find that (4.50) implies

$$\begin{aligned} E_\xi(\delta) &\leq \frac{\delta}{\pi} \int_0^{k_0(\delta)} \frac{(d_1 - d_0) \|\rho\|_{L^2(\mathcal{M})}^2 e^{-2kd_0} e^{4ka} (2\delta^2 + \lambda\delta^{\beta+1})^2}{9k\delta^2} e^{2ka} L dk \\ &\quad + \frac{\delta}{\pi} \int_{k_0(\delta)}^\infty \frac{(d_1 - d_0) \|\rho\|_{L^2(\mathcal{M})}^2 e^{-2kd_0} e^{ka} (2\delta^2 + \lambda\delta^{\beta+1})^{\frac{1}{2}}}{k\delta^2} \cdot e^{2ka} L dk \\ &= C_5 \delta \int_0^{k_0(\delta)} \frac{e^{-2k(d_0-3a)}}{k} (2\delta + \lambda\delta^\beta)^2 L dk \\ &\quad + 9C_5 \delta^{-\frac{1}{2}} \int_{k_0(\delta)}^\infty \frac{e^{-2k(d_0-\frac{3}{2}a)}}{k} (2\delta + \lambda\delta^\beta)^{\frac{1}{2}} L dk, \end{aligned}$$

where

$$C_5 \equiv \frac{(d_1 - d_0) \|\rho\|_{L^2(\mathcal{M})}^2}{9\pi}$$

and $0 < \delta \leq \delta_0$. Using (4.53) we can rewrite the above upper bound as

$$E_\xi(\delta) \leq T_1 + T_2 + T_3 + T_4, \quad (4.81)$$

where

$$T_1 \equiv C_5 \delta (2\delta + \lambda \delta^\beta)^2 \int_0^{k_0(\delta)} e^{-2k(d_0-3a)} \left(\frac{1 - e^{-2k\xi}}{k} \right) dk; \quad (4.82a)$$

$$T_2 \equiv C_5 \delta (\lambda^2 \delta^{2\beta} + 4) \int_0^{k_0(\delta)} e^{-2k(d_0-3a)} e^{-4ka} \left(\frac{e^{2k\xi} - 1}{k} \right) dk; \quad (4.82b)$$

$$T_3 \equiv 9C_5 \delta^{-\frac{1}{2}} (2\delta + \lambda \delta^\beta)^{\frac{1}{2}} \int_{k_0(\delta)}^\infty e^{-2k(d_0-\frac{3}{2}a)} \left(\frac{1 - e^{-2k\xi}}{k} \right) dk; \quad (4.82c)$$

$$T_4 \equiv 9C_5 \delta^{-\frac{1}{2}} (2\delta + \lambda \delta^\beta)^{-\frac{3}{2}} (\lambda^2 \delta^{2\beta} + 4) \int_{k_0(\delta)}^\infty e^{-2k(d_0-\frac{3}{2}a)} e^{-4ka} \left(\frac{e^{2k\xi} - 1}{k} \right) dk. \quad (4.82d)$$

We derive estimates of these integrals in the next four lemmas. Recall that $0 < \delta_0 \leq \delta_\mu$ is such that $k_0(\delta) > 0$ for $0 < \delta \leq \delta_0$. In the next four lemmas, we assume $0 < \delta \leq \delta_0$.

Lemma 4.7 *Suppose $\beta > 0$, λ is feasible, $0 < \xi < a$, $0 < \delta \leq \delta_0$, and $d_0 \geq \tau(\beta)a$.*

Then

$$\lim_{\delta \rightarrow 0^+} T_1 = \begin{cases} C_6 \lambda^{[2+(d_0-3a)/a]} & \text{if } 0 < \beta < 1 \text{ and } d_0 = \tau(\beta)a, \\ C_6 (2 + \lambda)^{[2+(d_0-3a)/a]} & \text{if } \beta = 1 \text{ and } d_0 = \tau(\beta)a, \\ C_6 2^{[2+(d_0-3a)/a]} & \text{if } \beta > 1 \text{ and } d_0 = \tau(\beta)a, \\ 0 & \text{if } d_0 > \tau(\beta)a, \end{cases}$$

where

$$C_6 = \frac{\xi C_5}{d_0 - 3a}.$$

Proof of Lemma 4.7: We begin by noting that (4.69) implies that $(3/2)a \leq \tau(\beta)a < 2a$ for all $\beta > 0$.

Next, the function $k^{-1}(1 - e^{-2k\xi})$ tends to 0 as k goes to infinity and is continuous and decreasing for $k \in [0, \infty)$ as long as we define it to be equal to 2ξ at $k = 0$. To see this, note that the l'Hospital Rule implies

$$\lim_{k \rightarrow 0} \frac{1 - e^{-2k\xi}}{k} = \lim_{k \rightarrow 0} 2\xi e^{-2k\xi} = 2\xi.$$

We also have

$$\frac{d}{dk} \left(\frac{1 - e^{-2k\xi}}{k} \right) = \frac{e^{-2k\xi}(2k\xi + 1) - 1}{k^2}. \quad (4.83)$$

The l'Hospital Rule implies that this function tends to $-2\xi^2$ as $k \rightarrow 0$.

For $k \neq 0$, the derivative in (4.83) is less than or equal to zero if and only if

$$e^{-2k\xi}(2k\xi + 1) - 1 \leq 0 \quad \Leftrightarrow \quad 2k\xi + 1 \leq e^{2k\xi}. \quad (4.84)$$

The line $2\xi k + 1$ is tangent to the function $e^{2k\xi}$ at the point $k = 0$. Since $e^{2\xi k}$ is convex for all k , the inequality (4.84) must hold for all $k \in \mathbb{R}$ and in particular for all $k \in (0, \infty)$ [21, Section 3.1.3]. Therefore $k^{-1}(1 - e^{-2k\xi}) \leq 2\xi$ for all $k \geq 0$. If $d_0 \neq 3a$, then in combination with (4.82a) this implies

$$T_1 \leq 2\xi C_5 \delta (2\delta + \lambda \delta^\beta)^2 \int_0^{k_0(\delta)} e^{-2k(d_0-3a)} dk \quad (4.85)$$

$$\begin{aligned} &= \frac{2\xi C_5}{2(d_0 - 3a)} \delta (2\delta + \lambda \delta^\beta)^2 [1 - e^{-2k_0(\delta)(d_0-3a)}] \\ &= C_6 \delta (2\delta + \lambda \delta^\beta)^2 - C_6 \delta (2\delta + \lambda \delta^\beta)^2 e^{-2k_0(\delta)(d_0-3a)}. \end{aligned} \quad (4.86)$$

The first term in (4.86) goes to 0 as $\delta \rightarrow 0^+$. The second term is equal to

$$-C_6 \delta (2\delta + \lambda \delta^\beta)^2 (2\delta^2 + \lambda \delta^{\beta+1})^{(d_0-3a)/a}. \quad (4.87)$$

If $0 < \beta < 1$ we rewrite this as

$$-C_6 (2\delta^{1-\beta} + \lambda)^2 [2\delta^{1-\beta} + \lambda]^{(d_0-3a)/a} \delta^{[1+2\beta+(\beta+1)(d_0-3a)/a]}.$$

This expression goes to 0 as $\delta \rightarrow 0^+$ if and only if

$$1 + 2\beta + (\beta + 1) \left(\frac{d_0 - 3a}{a} \right) > 0 \quad \Leftrightarrow \quad d_0 > \left(\frac{\beta + 2}{\beta + 1} \right) a = \tau(\beta)a,$$

and it goes to $C_6 \lambda^{[2+(d_0-3a)/a]}$ as $\delta \rightarrow 0^+$ if and only if $d_0 = \tau(\beta)a$.

If $\beta \geq 1$ we rewrite (4.87) as

$$-C_6(2 + \lambda\delta^{\beta-1})^2(2 + \lambda\delta^{\beta-1})^{(d_0-3a)/a}\delta^{[3+2(d_0-3a)/a]}.$$

This term goes to 0 as $\delta \rightarrow 0^+$ if and only if

$$3 + 2(d_0 - 3a)/a > 0 \quad \Leftrightarrow \quad d_0 > \frac{3}{2}a = \tau(\beta)a,$$

and if $d_0 = \tau(\beta)a$ it goes to $C_62^{[2+(d_0-3a)/a]}$ if $\beta > 1$ and $C_6(2 + \lambda)^{[2+(d_0-3a)/a]}$ if $\beta = 1$.

If $d_0 = 3a$, then from (4.85) we have

$$\begin{aligned} T_1 &\leq 2\xi C_5 \delta (2\delta + \lambda\delta^\beta)^2 k_0(\delta) \\ &= a^{-1} \xi C_5 \delta (2\delta + \lambda\delta^\beta)^2 \ln \left(\frac{1}{2\delta^2 + \lambda\delta^{\beta+1}} \right) \rightarrow 0 \quad \text{as } \delta \rightarrow 0^+ \end{aligned}$$

for all $\beta > 0$. This completes the proof.

Lemma 4.8 *Suppose $\beta > 0$, λ is feasible, $0 < \xi < \frac{a}{2}$, $0 < \delta \leq \delta_0$, and $d_0 \geq \tau(\beta)a$.*

Then

$$\lim_{\delta \rightarrow 0^+} T_2 = 0. \quad (4.88)$$

Proof of Lemma 4.8: We begin by noting that the function $k^{-1}(e^{2k\xi} - 1)$ is continuous for $k \in [0, \infty)$ if we define it to be equal to 2ξ at $k = 0$. Also, since $d_0 \geq \tau(\beta)a \geq 3a/2$, we have $d_0 - a \geq a/2$. This implies that $e^{-2k(d_0-3a)}e^{-4ka} = e^{-2k(d_0-a)} \leq e^{-ka}$ for all $k \geq 0$. Thus

$$\int_0^\infty e^{-2k(d_0-3a)}e^{-4ka} \left(\frac{e^{2k\xi} - 1}{k} \right) dk \leq \int_0^\infty \left(\frac{e^{2k(\xi-\frac{a}{2})} - e^{-ka}}{k} \right) dk;$$

The second integral (and, hence, the first integral) converges to a positive constant C as long as $0 < \xi < \frac{a}{2}$. Then, from (4.82b), $T_2 \leq CC_5\delta(\lambda^2\delta^{2\beta} + 4) \rightarrow 0$ as $\delta \rightarrow 0^+$. This completes the proof.

Lemma 4.9 *Suppose $\beta > 0$, λ is feasible, $0 < \xi < a$, $0 < \delta \leq \delta_0$, and $d_0 > \frac{3}{2}a$. Then*

$$\lim_{\delta \rightarrow 0^+} T_3 = \begin{cases} C_7 \lambda^{[\frac{1}{2}+(d_0-\frac{3}{2}a)/a]} & \text{if } 0 < \beta < 1 \text{ and } d_0 = \tau(\beta)a, \\ 0 & \text{if } d_0 > \tau(\beta)a, \end{cases}$$

where

$$C_7 = \frac{9C_5\xi}{d_0 - \frac{3}{2}a} > 0.$$

Proof of Lemma 4.9: As in the proof of Lemma 4.7 we have $k^{-1}(1 - e^{-2k\xi}) \leq 2\xi$ for all $k \geq 0$. Thus, from (4.82c),

$$\begin{aligned}
T_3 &\leq 18C_5\xi\delta^{-\frac{1}{2}}(2\delta + \lambda\delta^\beta)^{\frac{1}{2}} \int_{k_0(\delta)}^{\infty} e^{-2k(d_0 - \frac{3}{2}a)} dk \\
&= \frac{18C_5\xi}{2(d_0 - \frac{3}{2}a)} \delta^{-\frac{1}{2}}(2\delta + \lambda\delta^\beta)^{\frac{1}{2}} \left[-e^{-2k(d_0 - \frac{3}{2}a)} \Big|_{k_0(\delta)}^{\infty} \right] \\
&= C_7\delta^{-\frac{1}{2}}(2\delta + \lambda\delta^\beta)^{\frac{1}{2}} e^{-2k_0(\delta)(d_0 - \frac{3}{2}a)} \\
&= C_7\delta^{-\frac{1}{2}}(2\delta + \lambda\delta^\beta)^{\frac{1}{2}} (2\delta^2 + \lambda\delta^{\beta+1})^{(d_0 - \frac{3}{2}a)/a}. \tag{4.89}
\end{aligned}$$

If $0 < \beta < 1$, note that $\tau(\beta)a > \frac{3}{2}a$ — this implies that the above analysis holds as long as $d_0 \geq \tau(\beta)a$. We rewrite (4.89) as

$$C_7(2\delta^{1-\beta} + \lambda)^{\frac{1}{2}}(2\delta^{1-\beta} + \lambda)^{(d_0 - \frac{3}{2}a)/a} \delta^{[-\frac{1}{2} + \frac{\beta}{2} + (\beta+1)(d_0 - \frac{3}{2}a)/a]}.$$

This expression will go to 0 as $\delta \rightarrow 0^+$ if and only if

$$-\frac{1}{2} + \frac{\beta}{2} + (\beta+1) \left(\frac{d_0 - \frac{3}{2}a}{a} \right) > 0 \quad \Leftrightarrow \quad d_0 > \tau(\beta)a,$$

and if $d_0 = \tau(\beta)a$ it goes to $C_7\lambda^{[\frac{1}{2} + (d_0 - \frac{3}{2}a)/a]}$ as $\delta \rightarrow 0^+$.

If $\beta \geq 1$ we note that the analysis leading to (4.89) can only be applied if $d_0 > \tau(\beta)a = \frac{3}{2}a$. In this case we rewrite (4.89) as

$$C_7(2 + \lambda\delta^{\beta-1})^{\frac{1}{2}}(2 + \lambda\delta^{\beta-1})^{(d_0 - \frac{3}{2}a)/a} \delta^{2(d_0 - \frac{3}{2}a)/a},$$

which goes to 0 as δ goes to 0 if and only if $2(d_0 - \frac{3}{2}a)/a > 0 \Leftrightarrow d_0 > \tau(\beta)a = \frac{3}{2}a$.

This completes the proof.

Lemma 4.10 *Suppose $\beta > 0$, λ is feasible, $0 < \xi < a$, $0 < \delta \leq \delta_0$, and $d_0 \geq \tau(\beta)a$.*

Then

$$\lim_{\delta \rightarrow 0^+} T_4 = 0.$$

Proof of Lemma 4.10: From (4.82d) we have

$$T_4 = 9C_5\delta^{-\frac{1}{2}}(2\delta + \lambda\delta^\beta)^{-\frac{3}{2}}(\lambda^2\delta^{2\beta} + 4) \int_{k_0(\delta)}^{\infty} e^{-2k(d_0 - \frac{3}{2}a)} e^{-4ka} \left(\frac{e^{2k\xi} - 1}{k} \right) dk$$

$$\begin{aligned}
&= 9C_5 \delta^{-\frac{1}{2}} (2\delta + \lambda\delta^\beta)^{-\frac{3}{2}} (\lambda^2\delta^{2\beta} + 4) \int_{k_0(\delta)}^{\infty} e^{-k(2d_0+a)} \left(\frac{e^{2k\xi} - 1}{k} \right) dk \\
&\leq 9C_5 \frac{\delta^{-\frac{1}{2}} (2\delta + \lambda\delta^\beta)^{-\frac{3}{2}} (\lambda^2\delta^{2\beta} + 4)}{k_0(\delta)} \int_{k_0(\delta)}^{\infty} e^{-k(2d_0+a-2\xi)} dk \\
&= \left[\frac{9C_5 (\lambda^2\delta^{2\beta} + 4)}{2d_0 + a - 2\xi} \right] \left[\frac{\delta^{-\frac{1}{2}} (2\delta + \lambda\delta^\beta)^{-\frac{3}{2}} (\lambda^2\delta^{2\beta} + 4)}{k_0(\delta)} \right] e^{-k_0(\delta)(2d_0+a-2\xi)} \\
&= C_8 (\lambda^2\delta^{2\beta} + 4) \left[\frac{\delta^{-\frac{1}{2}} (2\delta + \lambda\delta^\beta)^{-\frac{3}{2}}}{k_0(\delta)} \right] (2\delta^2 + \lambda\delta^{\beta+1})^{(2d_0+a-2\xi)/(2a)}, \tag{4.90}
\end{aligned}$$

where

$$C_8 \equiv \frac{9C_5}{2d_0 + a - 2\xi} > 0.$$

If $0 < \beta < 1$ we rewrite (4.90) as

$$\left[\frac{C_8 (\lambda^2\delta^{2\beta} + 4)}{k_0(\delta)} \right] (2\delta^{1-\beta} + \lambda)^{-\frac{3}{2}} (2\delta^{1-\beta} + \lambda)^{(2d_0+a-2\xi)/(2a)} \delta^{[-\frac{1}{2} - \frac{3}{2}\beta + (\beta+1)(2d_0+a-2\xi)/(2a)]}.$$

This expression will go to 0 as $\delta \rightarrow 0^+$ if and only if

$$-\frac{1}{2} - \frac{3}{2}\beta + \frac{(\beta+1)(2d_0+a-2\xi)}{2a} \geq 0 \quad \Leftrightarrow \quad d_0 \geq \left(\frac{\beta}{\beta+1} \right) a + \xi.$$

Since $\xi < a$ and $0 < \beta < 1$ we have

$$\left(\frac{\beta}{\beta+1} \right) a + \xi < \left(\frac{\beta}{\beta+1} \right) a + a = \left(\frac{2\beta+1}{\beta+1} \right) a < \left(\frac{\beta+2}{\beta+1} \right) a = \tau(\beta)$$

Thus if $0 < \beta < 1$ and $d_0 \geq \tau(\beta)a$ we have $T_4 \rightarrow 0$ as $\delta \rightarrow 0^+$.

If $\beta \geq 1$ we rewrite (4.90) as

$$\left[\frac{C_8 (\lambda^2\delta^{2\beta} + 4)}{k_0(\delta)} \right] (2 + \lambda\delta^{\beta-1})^{-\frac{3}{2}} (2 + \lambda\delta^{\beta-1})^{(2d_0+a-2\xi)/(2a)} \delta^{[-2 + (2d_0+a-2\xi)/a]}.$$

This expression goes to 0 as $\delta \rightarrow 0^+$ if and only if

$$-2 + (2d_0 + a - 2\xi)/a \geq 0 \quad \Leftrightarrow \quad d_0 \geq \frac{a}{2} + \xi.$$

Since $\beta \geq 1$ and $0 < \xi < a$ we have $\frac{a}{2} + \xi < \frac{3}{2}a = \tau(\beta)a$; thus if $\beta \geq 1$ and $d_0 \geq \tau(\beta)a$ we have $T_4 \rightarrow 0$ as $\delta \rightarrow 0^+$. This completes the proof.

We summarize our result from this section in the following theorem.

Theorem 4.4 *Let $\beta > 0$ and λ feasible be fixed. Suppose also that $0 < \xi < \frac{a}{2}$ and $\rho \in \mathcal{P}$. If $d_0 > \tau(\beta)a$, then $\lim_{\delta \rightarrow 0^+} E_\xi(\delta) = 0$.*

Proof of Theorem 4.4: If the hypotheses of the theorem hold and if $\delta \leq \delta_0$, then (4.81) and Lemmas 4.6–4.10 imply

$$0 \leq E_\xi(\delta) \leq T_1 + T_2 + T_3 + T_4 \rightarrow 0 \quad \text{as } \delta \rightarrow 0^+.$$

This completes the proof.

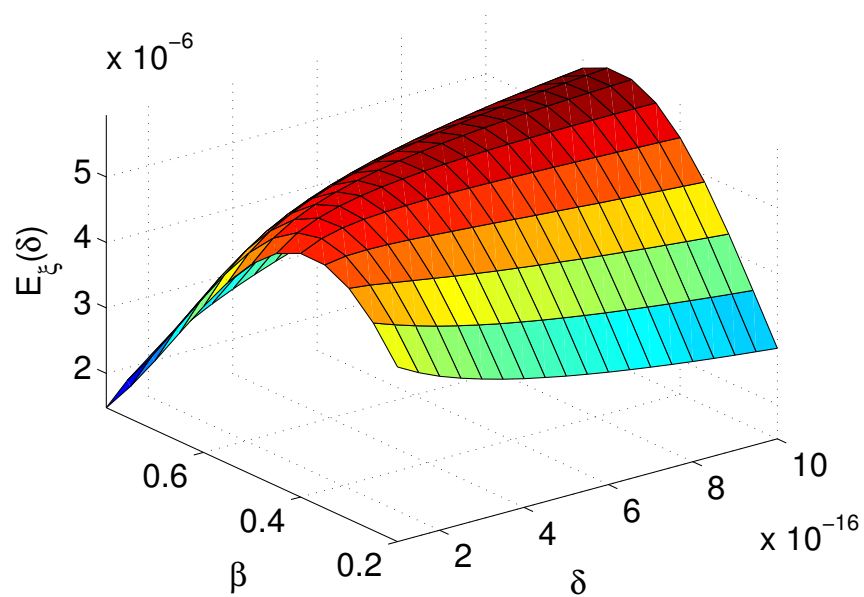
Remark 4.2 *Notice that (4.81) and Lemmas 4.6–4.10 imply that $E_\xi(\delta)$ remains bounded as $\delta \rightarrow 0^+$ if $0 < \beta < 1$ and $d_0 = \tau(\beta)$. Lemma 4.9 does not imply that T_3 remains bounded as $\delta \rightarrow 0^+$ if $\beta \geq 1$.*

Figures 4.11 and 4.12 are supporting numerical plots; they are the same as Figures 4.9 and 4.10, respectively, except in this case we have taken $a = d_0/\tau(\beta)$ so ρ just touches the region of influence (in order to accomplish this we have taken $\beta = 0.5$ in Figures 4.11(c) and 4.12(c) rather than $\beta = 0.8$ as in Figures 4.9(c) and 4.10(c)).

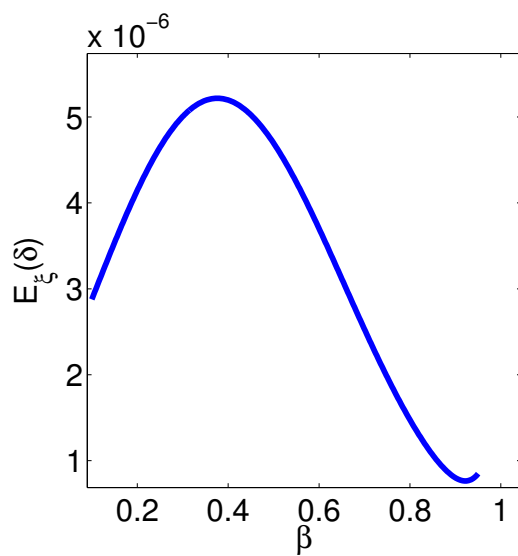
4.8 Boundedness of the Potential

In this section we derive bounds on the potential in regions far away from the slab. In particular, we prove that the potentials V_c and V_m to the left and right of the slab, respectively, are bounded by constants that are independent of δ (far enough away from the slab). As discussed in Section 4.1.1, this is the second requirement for cloaking by anomalous localized resonance to occur. At this point we do not address questions regarding which portions of the (rescaled) charge distribution $\rho/\sqrt{E_\xi(\delta)}$ will be cloaked. For example, if the (rescaled) rectangular charge distribution from Section 4.6.1.1 is halfway inside the cloaking region (so $x_0 = \tau(\beta)a$), we have not yet determined whether it will be completely cloaked or if only the leading half will be cloaked.

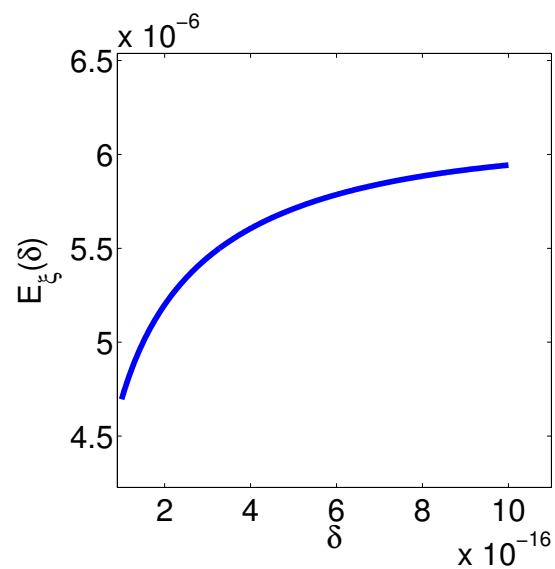
Recall from Section 4.2 (also see Theorem C.7 in Section C.6 in Appendix C) that $V \in L_{\text{loc}}^2(\mathbb{R}^2)$. The Cauchy–Schwarz Inequality implies that $V \in L_{\text{loc}}^1(\mathbb{R}^2)$ as well. To see this, let $B_r((x, y))$ denote the disk of radius $r > 0$ centered at the point $(x, y) \in \mathbb{R}^2$. Since $V \in L_{\text{loc}}^2(\mathbb{R}^2)$, we have



(a)

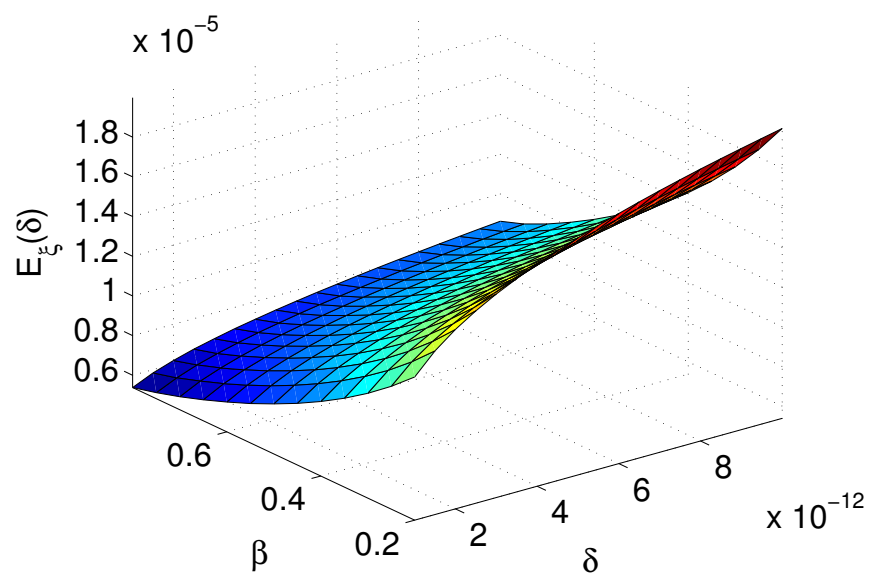


(b)

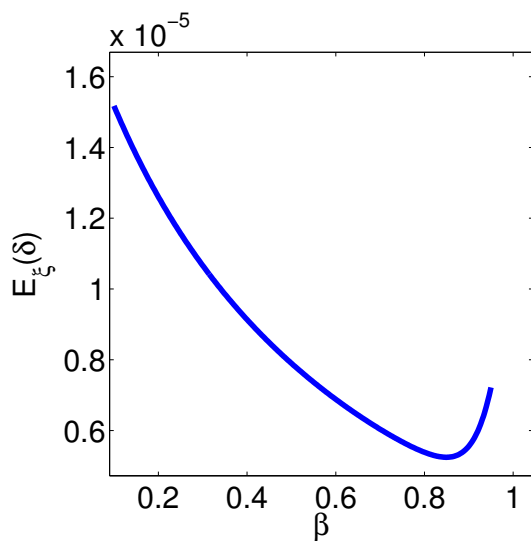


(c)

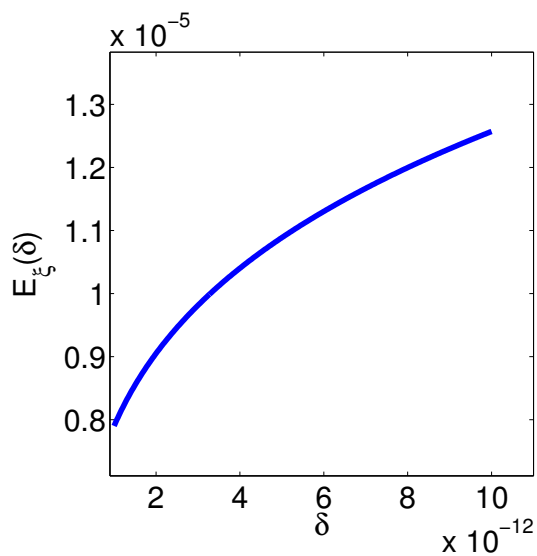
Figure 4.11. (Rectangular ρ) In all of these figures we take $a = d_0/\tau(\beta)$ so ρ is completely outside the region of influence. (a) A plot of $E_\xi(\delta)$ versus β and δ — the z -axis scale is 10^{-6} ; (b) a plot of $E_\xi(\delta)$ for $\delta = 10^{-16}$ as a function of β — the y -axis scale is 10^{-6} ; (c) a plot of $E_\xi(\delta)$ for $\beta = 0.5$ as a function of δ — the y -axis scale is 10^{-6} .



(a)



(b)



(c)

Figure 4.12. (Circular ρ) In all of these subfigures we take $a = d_0/\tau(\beta)$ so ρ is completely outside the region of influence. (a) A plot of $E_\xi(\delta)$ versus β and δ — the z -axis scale is 10^{-5} ; (b) a plot of $E_\xi(\delta)$ for $\delta = 10^{-12}$ as a function of β — the y -axis scale is 10^{-5} ; (c) a plot of $E_\xi(\delta)$ for $\beta = 0.5$ as a function of δ — the y -axis scale is 10^{-5} .

$$\|V\|_{L^2(B_r((x,y)))} = \left[\int_{B_r((x,y))} |V(x,y)|^2 dx dy \right]^{\frac{1}{2}} < \infty.$$

By the Cauchy–Schwarz Inequality we have

$$\begin{aligned} \|V\|_{L^1(B_r((x,y)))} &= \int_{B_r((x,y))} |V(x,y)| dx dy \\ &\leq \left[\int_{B_r((x,y))} |V(x,y)|^2 dx dy \right]^{\frac{1}{2}} \left[\int_{B_r((x,y))} dx dy \right]^{\frac{1}{2}} \\ &= \sqrt{\pi}r \left[\int_{B_r((x,y))} |V(x,y)|^2 dx dy \right]^{\frac{1}{2}} < \infty, \end{aligned}$$

so $V \in L^1_{\text{loc}}(\mathbb{R}^2)$.

Due to (4.12), V is harmonic on the set

$$\mathcal{G} \equiv \{(x,y) \in \mathbb{R}^2 : (x,y) \notin \text{supp } \rho \text{ and } x \neq 0 \text{ and } x \neq a\}.$$

In particular, if $B_r((x,y)) \subset \mathcal{G}$, then V is harmonic and locally integrable in $B_r(x,y)$. Then the Weyl Theorem [125, Theorem 18.G] implies that V is infinitely differentiable on $B_r((x,y))$ (after modification on a set of measure zero); hence V is infinitely differentiable in \mathcal{G} .

4.8.1 The Potential V_c

The next lemma states that, far enough away from the slab, the potential V_c is bounded for all $0 < \delta \leq \delta_\mu$.

Lemma 4.11 *Suppose $\rho \in \mathcal{P}$. Then there is a positive constant C_9 , independent of δ , such that $|V_c(x,y)| \leq C_9$ for all $x < -3a$ and all $0 < \delta \leq \delta_\mu$.*

Proof of Lemma 4.11: From (4.20) and (4.34) we have

$$|\widehat{V}_c(x,k)|^2 = |A_k|^2 e^{2|k|x} = \frac{|I_k|^2 e^{2|k|x}}{e^{-2|k|a} |k| |\psi_k^+ + \psi_k^-|^2}. \quad (4.91)$$

As in the proof of Lemma 4.6, $4 + \delta(\mu - \delta) = 4 + \lambda\delta^{\beta+1} \geq 3$ for $0 < \delta \leq \delta_\mu$. Then, for $0 < \delta \leq \delta_\mu < 1$, Lemma 4.2 implies that

$$|k| |\psi_k^+ + \psi_k^-|^2 \geq \frac{|k|^2}{4(1 + \delta^2)} (4 + (\mu - \delta)^2)(4 + \delta^2) e^{-2|k|a} \geq 2|k|^2 e^{-2|k|a} \quad (4.92)$$

for each $k \in \mathbb{R}$. In combination with (4.91), this implies that

$$|\widehat{V}_c(x,k)|^2 \leq \frac{|I_k|^2}{2|k|^2} e^{2|k|(x+2a)} \quad (4.93)$$

for $x < 0$, for all $k \in \mathbb{R}$, and for all $0 < \delta \leq \delta_\mu$. In particular, note that the expression in (4.93) is an even function of k if ρ is real-valued due to Lemma 4.1. Then for $x < 0$ (4.93) implies that

$$\begin{aligned}
\int_{-\infty}^{\infty} |\widehat{V}_c(x, k)|^2 dk &\leq \frac{1}{2} \int_{-\infty}^{\infty} \frac{|I_k|^2}{|k|^2} e^{2|k|(x+2a)} dk \\
&= \int_0^{\infty} \frac{|I_k|^2}{|k|^2} e^{2|k|(x+2a)} dk \\
&= \int_0^1 \frac{|I_k|^2}{k^2} e^{2k(x+2a)} dk + \int_1^{\infty} \frac{|I_k|^2}{k^2} e^{2k(x+2a)} dk \\
&= \int_0^1 \frac{|I_k|^2}{k^2} e^{2k(x+2a)} dk + (d_1 - d_0) \|\rho\|_{L^2(\mathcal{M})}^2 \int_1^{\infty} \frac{e^{2k(x+2a-d_0)}}{k^2} dk,
\end{aligned} \tag{4.94}$$

thanks to Lemma 4.1. Since

$$\frac{|I_k|^2}{k^2} \leq C_I^2$$

for $k \geq 0$ by Lemma 4.1, the first integral in (4.94) converges for any $x \in \mathbb{R}$. The second integral in (4.94) converges if and only if $x \leq d_0 - 2a$ (note that $d_0 - 2a > -a$ since $d_0 > a$). Then if $x < -2a$ we have, from (4.94), that

$$\begin{aligned}
\int_{-\infty}^{\infty} |\widehat{V}_c(x, k)|^2 dk &\leq \int_0^1 C_I^2 dk + (d_1 - d_0) \|\rho\|_{L^2(\mathcal{M})}^2 \int_1^{\infty} \frac{1}{k^2} dk \\
&= C_I^2 + (d_1 - d_0) \|\rho\|_{L^2(\mathcal{M})}^2.
\end{aligned}$$

Then the Plancherel Theorem (4.48) implies that for each $x < -2a$ we have

$$\int_{-\infty}^{\infty} |V_c(x, y)|^2 dy = \frac{1}{2\pi} \int_{-\infty}^{\infty} |\widehat{V}_c(x, k)|^2 dk \leq \frac{1}{2\pi} [C_I^2 + (d_1 - d_0) \|\rho\|_{L^2(\mathcal{M})}^2]. \tag{4.95}$$

Since $V_c(x, y)$ is harmonic for $x < -2a$, it satisfies the mean value property: for any point (x, y) with $x < -3a$ we have

$$V(x, y) = \frac{1}{|B_a((x, y))|} \int_{B_a((x, y))} V(x', y') dy' dx',$$

where $B_a((x, y))$ is the ball of radius a centered at the point (x, y) [32, Chapter 2]; note that all points $(x', y') \in B_a((x, y))$ satisfy $x' < -2a$ since $x < -3a$. Finally, by the Cauchy–Schwarz Inequality and (4.95) we have

$$|V_c(x, y)| = \frac{1}{|B_a((x, y))|} \left| \int_{B_a((x, y))} V(x', y') dy' dx' \right|$$

$$\begin{aligned}
&\leq \frac{1}{|B_a((x, y))|} \int_{B_a((x, y))} |V(x', y')| dy' dx' \\
&\leq \frac{1}{|B_a((x, y))|} \left[\int_{B_a((x, y))} |V(x', y')|^2 dy' dx' \right]^{\frac{1}{2}} \left[\int_{B_a((x, y))} dy' dx' \right]^{\frac{1}{2}} \\
&\leq \frac{1}{|B_a((x, y))|^{\frac{1}{2}}} \left[\int_{x-a}^{x+a} \int_{-\infty}^{\infty} |V(x', y')|^2 dy' dx' \right]^{\frac{1}{2}} \\
&\leq \int_{x-a}^{x+a} \frac{1}{2\pi^{3/2}a} [C_I^2 + (d_1 - d_0)\|\rho\|_{L^2(\mathcal{M})}^2] dx' \\
&= C_9,
\end{aligned}$$

where $C_9 = \pi^{-3/2} [C_I^2 + (d_1 - d_0)\|\rho\|_{L^2(\mathcal{M})}^2]$. This completes the proof.

4.8.2 The Potential V_m

We now show that $|V_m(x, y)|$ is bounded for x large enough. In particular, we at least assume that $x > d_1$. We begin with a lemma that is very similar to Lemma 4.1. For $x > d_1$ we define

$$J_k(x) \equiv \int_{d_0}^{d_1} \hat{\rho}(s, k) e^{-|k|(x-s)} ds. \quad (4.96)$$

Lemma 4.12 *Suppose $\rho \in \mathcal{P}$ (where \mathcal{P} is defined in (4.3)) and that, for $x > d_1$, $J_k(x)$ is defined as in (4.96). Then, for every $x > d_1$, $J_k(x)$ satisfies the following properties:*

1. for all $k \in \mathbb{R}$, $|J_k(x)|^2 \leq (d_1 - d_0)\|\rho\|_{L^2(\mathcal{M})}^2 e^{-2k(x-d_1)}$;
2. if ρ is real-valued, then $|J_k(x)|^2$ is an even function of k for $k \in \mathbb{R}$;
3. $J_k(x)$ is continuous at k for each $k \in \mathbb{R}$;
4. $\lim_{k \rightarrow 0} J_k(x) = J_0(x) = 0$;
5. for each $x > d_1$, $\lim_{k \rightarrow 0} (|J_k(x)|/|k|) = |C_0| < \infty$, where C_0 is defined in (4.41) and (4.42); moreover, there is a positive constant C_J , independent of x , such that $|J_k(x)|/|k| \leq C_J$ for all $x > d_1$ and all $k \in [0, 1]$.

Proof of Lemma 4.12: The proofs of items (1)–(4) are word-for-word repeats of the proofs of items (2)–(5) in Lemma 4.1. The proof of item (6) of Lemma 4.1 can

be extended to prove item (5) of this lemma. However, we need to be a bit more careful in deriving our bound on $J_k(x)/k$ near $k = 0$ in this case. We will again use Theorem 1.2.

We begin by defining $K \equiv (0, k_*)$, where $k_* > 0$ is arbitrary. We also define

$$f(s, k) \equiv \widehat{\rho}(s, k)e^{|k|s} \quad \text{and} \quad F(k) \equiv \int_{d_0}^{d_1} f(s, k) ds;$$

note that f is well defined for almost every $s \in [d_0, d_1]$ and for each $k \in K$. We now show that f satisfies items (i)–(iii) of Theorem 1.2. (In the proof of (i) that follows we show that F is well defined for each $k \in K$.)

(i) For any $k \in K$ we have

$$\begin{aligned} \int_{d_0}^{d_1} |f(s, k)| ds &= \int_{d_0}^{d_1} |\widehat{\rho}(s, k)e^{ks}| ds \\ &\leq e^{kd_1} \int_{d_0}^{d_1} \int_{h_0}^{h_1} |\rho(s, y)e^{-iky}| dy ds \\ &\leq e^{kd_1} \|\rho\|_{L^1(\mathcal{M})}, \end{aligned}$$

so the map $s \mapsto f(s, k)$ is in $L^1([d_0, d_1])$ and F is well defined for each $k \in K$.

(ii) For all $k \in K$, $\widehat{\rho}(s, k)$ is infinitely differentiable as a function of k for almost all $s \in [d_0, d_1]$ (by Lemma 4.1) and e^{ks} is infinitely differentiable for all $s \in [d_0, d_1]$. Hence $f(s, k)$ is infinitely differentiable as a function of k for almost every $s \in [d_0, d_1]$.

(iii) Following the steps leading up to (4.39) we find that

$$\left| \frac{\partial f}{\partial k} \right| \leq e^{kd_1} \|\rho\|_{L^\infty(\mathcal{M})} (C_h + |s|)(h_1 - h_0).$$

Thus

$$\begin{aligned} \int_{d_0}^{d_1} \sup_{k \in K} \left| \frac{\partial f}{\partial k}(s, k) \right| ds &\leq e^{k_* d_1} \|\rho\|_{L^\infty(\mathcal{M})} (h_1 - h_0) \int_{d_0}^{d_1} (C_h + |s|) ds \\ &\leq e^{k_* d_1} \|\rho\|_{L^\infty(\mathcal{M})} (C_h + d_1)(d_1 - d_0)(h_1 - h_0). \end{aligned}$$

Therefore Theorem 4.2 implies, for $k \in K$, that

$$\frac{\partial F}{\partial k} = \int_{d_0}^{d_1} \frac{\partial}{\partial k} [\widehat{\rho}(s, k)e^{ks}] ds$$

$$\begin{aligned}
&= \int_{d_0}^{d_1} s\widehat{\rho}(s, k)e^{ks} ds + \int_{d_0}^{d_1} \frac{\partial \widehat{\rho}}{\partial k}(s, k)e^{ks} ds \quad (4.97) \\
&= \int_{d_0}^{d_1} \int_{h_0}^{h_1} s\rho(s, y)e^{-iky}e^{ks} dy ds - \int_{d_0}^{d_1} \int_{h_0}^{h_1} iy\rho(s, y)e^{-iky}e^{ks} dy ds
\end{aligned}$$

for $0 < k < k_*$. Note that the expression in (4.97) is well defined and continuous for all $k \in (-k_*, k_*)$ by an argument similar to that given in items (1) and (4) of Lemma 4.1 (applied to $s\widehat{\rho}(s, k)e^{|k|s}$ and $\frac{\partial \widehat{\rho}}{\partial k}(s, k)e^{|k|s}$). In particular we have

$$\begin{aligned}
\lim_{k \rightarrow 0^+} \frac{\partial F}{\partial k} &= \lim_{k \rightarrow 0^+} \left[\int_{d_0}^{d_1} s\widehat{\rho}(s, k)e^{ks} ds + \int_{d_0}^{d_1} \frac{\partial \widehat{\rho}}{\partial k}(s, k)e^{ks} ds \right] \\
&= \int_{d_0}^{d_1} s\widehat{\rho}(s, 0) ds + \int_{d_0}^{d_1} \frac{\partial \widehat{\rho}}{\partial k}(s, 0) ds \\
&= \int_{d_0}^{d_1} \int_{h_0}^{h_1} s\rho(s, y) dy ds - \int_{d_0}^{d_1} \int_{h_0}^{h_1} iy\rho(s, y) dy ds \\
&= C_0,
\end{aligned}$$

which is well defined since $\rho \in L^1(\mathcal{M})$ (just as in the proof of item (6) of Lemma 4.1, the Lebesgue Dominated Convergence Theorem can also be used to justify passing the limit inside the integral). Then the l'Hospital Rule and the fact that the function $|\cdot|$ is continuous imply that

$$\lim_{k \rightarrow 0^+} \frac{|F(k)|}{|k|} = \left| \lim_{k \rightarrow 0^+} \frac{F(k)}{k} \right| = \left| \lim_{k \rightarrow 0^+} \frac{\partial F(k)}{\partial k} \right| = |C_{10}|.$$

Since $|F(k)|$ and $|k|$ are even functions of k , $\lim_{k \rightarrow 0^-} (|F(k)|/|k|) = |C_{10}|$ as well. Therefore

$$\lim_{k \rightarrow 0} \frac{|F(k)|}{|k|} = |C_{10}|.$$

Thanks to (4.96), this implies, for each $x > d_1$, that

$$\lim_{k \rightarrow 0} \frac{|J_k(x)|}{|k|} = \lim_{k \rightarrow 0} e^{-kx} \frac{|F(k)|}{|k|} = |C_{10}|.$$

Finally, since $|F(k)|/|k|$ is continuous for all $k \in (-k_*, k_*)$ (if we define it to be equal to $|C_{10}|$ when $k = 0$) and k_* is arbitrary, $|F(k)|/|k|$ is continuous for $k \in [0, 1]$; thus $|F(k)|/|k|$ attains its maximum value on $[0, 1]$. Then (4.96) implies, for $x > d_1$ and $k \in [0, 1]$, that

$$\frac{|J_k(x)|}{|k|} = e^{-|k|x} \frac{|F(k)|}{|k|} \leq \frac{|F(k)|}{|k|} \leq C_J,$$

where C_J is a positive constant.

This completes the proof.

Lemma 4.13 *Suppose $\rho \in \mathcal{P}$. Then there exists $0 < \delta_{\psi^-}(\beta, \lambda) \leq \delta_\mu$ and there exist positive constants $b > \max\{d_1, 4a\}$ and C_{11} such that $|V_m(x, y)| \leq C_{11}$ for all $x > b$ and for all $0 < \delta \leq \delta_{\psi^-}$.*

Proof of Lemma 4.13: We choose $0 < \delta_{\psi^-}(\beta, \lambda) \leq \delta_\mu$ such that $\delta(\mu - \delta) - 4 = \lambda\delta^{\beta+1} - 4 < 0$ and $4 + (\mu - \delta)^2 = 4 + \lambda^2\delta^{2\beta} \leq 5$ for all $0 < \delta \leq \delta_{\psi^-}$. Then, for $0 < \delta \leq \delta_{\psi^-}$, Lemma 4.3 implies that

$$\begin{aligned} \left| \psi_k^+ - \frac{1}{|k|} \psi_k^- \right|^2 &= \frac{1}{4(1 + \delta^2)} [(\delta + \mu)^2(4 + \delta^2)e^{2|k|a} + 2\delta(\delta + \mu)(\delta(\mu - \delta) - 4) \\ &\quad + \delta^2(4 + (\mu - \delta)^2)e^{-2|k|a}] \\ &\leq \frac{5}{4}(\delta + \mu)^2(e^{2|k|a} + e^{-2|k|a}) \\ &\leq \frac{5}{2}(\delta + \mu)^2e^{2|k|a} \end{aligned} \quad (4.98)$$

since $\mu \geq 0$ for $\delta \leq \delta_{\psi^-} \leq \delta_\mu$.

Based on our choice of A_k and I_k in (4.34) and (4.35), respectively, for $x > d_1$ we have

$$\widehat{V}_m(x, k) = e^{-|k|x} \left(\frac{A_k \psi_k^+ e^{|k|a}}{2} - \frac{A_k \psi_k^- e^{|k|a}}{2|k|} \right) + \frac{J_k(x)}{2|k|}; \quad (4.99)$$

see (4.33). Then (4.34), the triangle inequality, and the fact that $(p + q)^2 \leq 2p^2 + 2q^2$ for real numbers p and q (this inequality is equivalent to $(p - q)^2 \geq 0$) imply, for $x > d_1$, that

$$\begin{aligned} |\widehat{V}_m(x, k)|^2 &= \left| e^{-|k|x} \left(\frac{A_k \psi_k^+ e^{|k|a}}{2} - \frac{A_k \psi_k^- e^{|k|a}}{2|k|} \right) + \frac{J_k(x)}{2|k|} \right|^2 \\ &\leq \frac{e^{-2|k|(x-a)}}{2} |A_k|^2 \left| \psi_k^+ - \frac{1}{|k|} \psi_k^- \right|^2 + \frac{|J_k(x)|^2}{2|k|^2}. \end{aligned}$$

Then (4.91)–(4.92) and (4.98) imply, for $0 < \delta \leq \delta_{\psi^-}$, that

$$\begin{aligned} |\widehat{V}_m(x, k)|^2 &\leq \frac{e^{-2|k|(x-a)} |I_k|^2 e^{4|k|a}}{2|k|^2} \left| \psi_k^+ - \frac{1}{|k|} \psi_k^- \right|^2 + \frac{|J_k(x)|^2}{2|k|^2} \\ &\leq \frac{5e^{-2|k|(x-3a)} |I_k|^2}{8|k|^2} (\delta + \mu)^2 e^{2|k|a} + \frac{|J_k(x)|^2}{2|k|^2} \end{aligned}$$

$$\leq \frac{5}{8}(\delta + \mu)^2 \frac{|I_k|^2}{|k|^2} e^{-2|k|(x-4a)} + \frac{|J_k(x)|^2}{2|k|^2}. \quad (4.100)$$

Note that the expression in (4.100) is even as a function of k by Lemmas 4.1 and 4.12.

Then we have

$$\begin{aligned} \int_{-\infty}^{\infty} |\widehat{V}_m(x, k)|^2 dk &\leq \frac{5}{8}(\delta + \mu)^2 \int_{-\infty}^{\infty} \frac{|I_k|^2}{|k|^2} e^{-2|k|(x-4a)} dk + \int_{-\infty}^{\infty} \frac{|J_k(x)|^2}{2|k|^2} dk \\ &= \frac{5}{4}(\delta + \mu)^2 \left[\int_0^1 \frac{|I_k|^2}{k^2} e^{-2k(x-4a)} dk + \int_1^{\infty} \frac{|I_k|^2}{k^2} e^{-2k(x-4a)} dk \right] \\ &\quad + \int_0^1 \frac{|J_k(x)|^2}{k^2} dk + \int_1^{\infty} \frac{|J_k(x)|^2}{k^2} dk. \end{aligned}$$

Then Lemmas 4.1 and 4.12 imply

$$\begin{aligned} &\int_{-\infty}^{\infty} |\widehat{V}_m(x, k)|^2 dk \\ &\leq \frac{5}{4}(\delta + \mu)^2 C_0^2 \int_0^1 e^{-2k(x-4a)} dk + C_J^2 \\ &\quad + (d_1 - d_0) \|\rho\|_{L^2(\mathcal{M})}^2 \left[\frac{5}{4}(\delta + \mu)^2 \int_1^{\infty} \frac{e^{-2k(x-4a+d_0)}}{k^2} dk + \int_1^{\infty} \frac{e^{-2k(x-d_1)}}{k^2} dk \right]. \end{aligned} \quad (4.101)$$

If $x > \max\{d_1, 4a\}$, then all of the integrals in (4.101) converge. In particular, the integral from 0 to 1 and both of the integrals from 1 to ∞ converge to numbers less than or equal to 1 in that case. Therefore (4.101) becomes

$$\int_{-\infty}^{\infty} |\widehat{V}_m(x, k)|^2 dk \leq \frac{5}{4}(\delta + \mu)^2 C_0^2 + C_J^2 + (d_1 - d_0) \|\rho\|_{L^2(\mathcal{M})}^2 \left[\frac{5}{4}(\delta + \mu)^2 + 1 \right] \equiv \widetilde{C}_{11}.$$

If we define $b \equiv a + \max\{d_1, 4a\}$, for example, then for $x > b$ each point $(x', y') \in B_a((x, y))$ satisfies $x' > \max\{d_1, 4a\}$. Since V_m is harmonic in the region where $x' > d_1$, it satisfies the mean value property there. Using this in combination with the Plancherel Theorem (just as in the proof of Lemma 4.11) gives

$$|V_m(x, y)| \leq \int_{x-a}^{x+a} \frac{\widetilde{C}_{11}}{2\pi^{3/2}a} dx' \equiv C_{11},$$

where $C_{11} \equiv \pi^{-3/2} \widetilde{C}_{11}$. This completes the proof.

APPENDIX A

APPENDIX TO CHAPTER 2

In this appendix we provide a proof of Remark 2.5. The proof is also an alternative proof to Lemma 2.3. In particular, this proof shows that the set $\mathcal{E}_f \subset \mathcal{F}_{f,e}$ for all $f \in \mathcal{A}_e$; moreover, we prove that the ellipses $\partial\mathcal{E}_f^{(1)}$ and $\partial\mathcal{E}_f^{(2)}$ are tangent to the sets ∂X_f and ∂Y_f , respectively.

Proof of Remark 2.5: For $f \in \mathcal{A}_e$ and motivated by (2.40a) and (2.40b) we define the strips

$$X_f \equiv \left\{ (x, y) \in \mathbb{R}^2 : \frac{\|\langle \mathbf{E}_1^{(1)} \rangle\|^2}{f} \leq x \leq \eta^{(1)} - \frac{\|\langle \mathbf{E}_2^{(1)} \rangle\|^2}{f} \right\} \quad (\text{A.1a})$$

$$Y_f \equiv \left\{ (x, y) \in \mathbb{R}^2 : \frac{\|\langle \mathbf{E}_1^{(2)} \rangle\|^2}{1-f} \leq y \leq \eta^{(2)} - \frac{\|\langle \mathbf{E}_2^{(2)} \rangle\|^2}{1-f} \right\}. \quad (\text{A.1b})$$

Note that $\mathcal{F}_{f,e} = X_f \cap Y_f$. We now prove that $\mathcal{E}_f^{(1)} \subseteq X_f$ for all $f \in \mathcal{A}_e$.

Let $f = f_{e,l}$; then, by Lemma 2.2, $\mathcal{E}_{f_{e,l}}^{(1)}$ is the point $(\bar{x}_{f_{e,l}}^{(1)}, \bar{y}_{f_{e,l}}^{(1)})$, which is defined in (2.48). We note that, by (2.36), (2.42a), (2.46), and (2.48),

$$\bar{x}_{f_{e,l}}^{(1)} = \frac{\|\langle \mathbf{E}_1^{(1)} \rangle\|^2}{f_{e,l}} \quad \text{and} \quad X_{f_{e,l}} = \bar{x}_{f_{e,l}}^{(1)} \times (-\infty, \infty),$$

so $\mathcal{E}_{f_{e,l}}^{(1)} = (\bar{x}_{f_{e,l}}^{(1)}, \bar{y}_{f_{e,l}}^{(1)}) \subset X_{f_{e,l}}$.

If $f \in (f_{e,l}, f_{e,u}]$, Lemma 2.2 implies that $\mathcal{E}_f^{(1)}$ is a closed elliptic disk; its boundary is the ellipse described by the equation $p_f^{(1)}(x, y) = 0$. We define

$$x_{f,\min} \equiv \min \left\{ x \in \mathbb{R} : p_f^{(1)}(x, y) = 0 \right\} \quad \text{and} \quad x_{f,\max} \equiv \max \left\{ x \in \mathbb{R} : p_f^{(1)}(x, y) = 0 \right\}.$$

One may use the method of Lagrange Multipliers to find $x_{f,\min}$ and $x_{f,\max}$; however we use a slightly different (equivalent) approach keeping the geometry of our problem in mind.

We consider the equation $p^{(1)}(x, y) = 0$ as implicitly defining x as a function of y . Implicitly differentiating this equation, we find that

$$\frac{dx}{dy} = -\frac{a_2^{(1)}x + a_3^{(1)}y + a_5^{(1)}}{a_1^{(1)}x + a_2^{(1)}y + a_4^{(1)}}. \quad (\text{A.2})$$

The numerator of dx/dy is 0 if and only if

$$y = -\frac{a_2^{(1)}x + a_5^{(1)}}{a_3^{(1)}}. \quad (\text{A.3})$$

Note that $a_3^{(1)} \neq 0$ by (2.36) and (2.46). Inserting (A.3) into the equation $p^{(1)}(x, y) = 0$ we find that x must satisfy

$$(x - x_{f,\min})(x - x_{f,\max}) = 0$$

where

$$x_{f,\min} = \frac{\|\langle \mathbf{E}_1^{(1)} \rangle\|^2}{f} \quad \text{and} \quad x_{f,\max} = \eta^{(1)} - \frac{\|\langle \mathbf{E}_2^{(1)} \rangle\|^2}{f}.$$

Note that for $f \in \mathcal{A}_e$, $x_{f,\min} \leq x_{f,\max}$ (with equality if and only if $f = f_{e,l}$).

Finally, we note that the denominator in (A.2) is zero at $x_{f,\min}$ and $x_{f,\max}$ (where the corresponding value of y is given by (A.3)) if and only if $f = f_{e,l}$. Thus, for $f \in (f_{e,l}, f_{e,u}]$, the ellipse $\partial\mathcal{E}_f^{(1)} \subset X_f$ and so $\mathcal{E}_f^{(1)} \subset X_f$.

A similar proof shows that $\mathcal{E}_f^{(2)} \subseteq Y_f$ for all $f \in \mathcal{A}_e$. Therefore, for each $f \in \mathcal{A}_e$, $\mathcal{E}_f = [\mathcal{E}_f^{(1)} \cap \mathcal{E}_f^{(2)}] \subseteq (X_f \cap Y_f) = \mathcal{F}_{f,e}$. This completes the proof.

APPENDIX B

APPENDIX TO CHAPTER 3

In this appendix we provide a derivation of (3.19) (in Section B.1). In Section B.2, we derive the nonlocal boundary condition discussed in Section 3.6.2 when $\Omega \subset \mathbb{R}^2$ is a disk of radius R .

B.1 Derivation of Lamé Operator

In this section we present a derivation of (3.19) from (3.6). We begin by introducing some notation. The vectors $\mathbf{e}_i \in \mathbb{R}^d$ form an orthonormal basis of \mathbb{R}^d and contain a 1 in the i^{th} position and zeros elsewhere. In particular, note that $\mathbf{e}_i \cdot \mathbf{e}_j = \delta_{ij}$, where δ_{ij} is the Kronecker delta (which is 1 if $i = j$ and 0 if $i \neq j$). Following Nemat-Nasser and Hori [102], we also introduce the shorthand $\mathbf{e}_{ij} \equiv \mathbf{e}_i \otimes \mathbf{e}_j$; with this definition we have

$$\mathbf{e}_{ij} : \mathbf{e}_{kl} = \delta_{ik} \delta_{jl}. \quad (\text{B.1})$$

Finally, we also define $\partial_i \equiv \partial/\partial x_i$ for $i = 1, \dots, d$. Recall that we are using the Einstein summation convention so repeated indices are summed from $1, \dots, d$; for example the gradient operator can be written as $\mathbf{e}_i \partial_i = \mathbf{e}_1 \partial_1 + \mathbf{e}_2 \partial_2 + \mathbf{e}_3 \partial_3$ in the case $d = 3$.

B.1.1 Differential Constraints

We have

$$\nabla \mathbf{u} = \mathbf{e}_i \partial_i \otimes (u_j \mathbf{e}_j) = \partial_i u_j \mathbf{e}_{ij} \quad \text{and} \quad \nabla \mathbf{u}^T = \partial_j u_i \mathbf{e}_{ij} = \partial_i u_j \mathbf{e}_{ji}.$$

From (3.6) we then have

$$\boldsymbol{\varepsilon} = \frac{1}{2}(\nabla \mathbf{u} + \nabla \mathbf{u}^T) = \frac{1}{2}(\partial_i u_j \mathbf{e}_{ij} + \partial_i u_j \mathbf{e}_{ji}) = \frac{1}{2} \partial_i u_j (\mathbf{e}_{ij} + \mathbf{e}_{ji}). \quad (\text{B.2})$$

In phase p (for $p = 1, 2$, and E), from (3.16) and (3.17) we have

$$\mathbb{C}_p = \lambda_p \mathbf{I} \otimes \mathbf{I} + 2\mu \mathbb{I}.$$

Then

$$\begin{aligned}
\boldsymbol{\sigma} &= \mathbb{C}_p : \boldsymbol{\varepsilon} \\
&= (\lambda_p \mathbf{I} \otimes \mathbf{I} + 2\mu \mathbb{I}) : \boldsymbol{\varepsilon} \\
&= \lambda_p (\delta_{ij} \mathbf{e}_{ij} \otimes \delta_{kl} \mathbf{e}_{kl}) : \varepsilon_{mn} \mathbf{e}_{mn} + 2\mu \boldsymbol{\varepsilon} \\
&= \lambda_p \delta_{ij} \mathbf{e}_{ij} (\delta_{kl} \varepsilon_{mn} \mathbf{e}_{kl} : \mathbf{e}_{mn}) + 2\mu \boldsymbol{\varepsilon} \\
&= \lambda_p \delta_{ij} \mathbf{e}_{ij} (\delta_{kl} \varepsilon_{mn} \delta_{km} \delta_{ln}) + 2\mu \boldsymbol{\varepsilon} \quad (\text{by (B.1)}) \\
&= \lambda_p \mathbf{I} (\delta_{kl} \varepsilon_{kl}) + 2\mu \boldsymbol{\varepsilon} \\
&= \lambda_p \mathbf{I} (\varepsilon_{kk}) + 2\mu \boldsymbol{\varepsilon} \\
&= \lambda_p \text{Tr}(\boldsymbol{\varepsilon}) \mathbf{I} + 2\mu \boldsymbol{\varepsilon}, \tag{B.3}
\end{aligned}$$

which is (3.7).

From (B.2) we have

$$\text{Tr}(\boldsymbol{\varepsilon}) = \varepsilon_{kk} = \frac{1}{2} (\partial_k u_k + \partial_k u_k) = \frac{1}{2} (2 \nabla \cdot \mathbf{u}) = \nabla \cdot \mathbf{u}.$$

Thus from this and (B.3) we have

$$\boldsymbol{\sigma} = \lambda_p (\nabla \cdot \mathbf{u}) \mathbf{I} + 2\mu \frac{1}{2} (\nabla \mathbf{u} + \nabla \mathbf{u}^T) = \lambda_p (\nabla \cdot \mathbf{u}) \mathbf{I} + \mu (\nabla \mathbf{u} + \nabla \mathbf{u}^T),$$

which is (3.8). Using (B.2), the above equation can be equivalently written as

$$\boldsymbol{\sigma} = \lambda_p (\partial_m u_m) \delta_{ik} \mathbf{e}_{ik} + \mu (\partial_i u_k + \partial_k u_i) \mathbf{e}_{ik}. \tag{B.4}$$

In each phase we have

$$0 = \nabla \cdot \boldsymbol{\sigma} = \mathbf{e}_i \partial_i \cdot (\sigma_{jk} \mathbf{e}_j \otimes \mathbf{e}_k) = \partial_i \sigma_{jk} (\mathbf{e}_i \cdot \mathbf{e}_j) \mathbf{e}_k = \partial_i \sigma_{jk} \delta_{ij} \mathbf{e}_k = \partial_i \sigma_{ik} \mathbf{e}_k. \tag{B.5}$$

Thus, using our convention, the divergence of a matrix in $\mathbb{R}^d \otimes \mathbb{R}^d$ is a vector in \mathbb{R}^d whose k^{th} entry is the divergence of the k^{th} column of the matrix.

Inserting (B.4) into (B.5) gives (assuming \mathbf{u} is smooth enough in each phase — in other words, assuming ϕ is smooth enough in each phase)

$$\begin{aligned}
0 &= \partial_i (\lambda_p (\partial_m u_m) \delta_{ik} + \mu (\partial_i u_k + \partial_k u_i)) \mathbf{e}_k \\
&= \lambda_p \partial_i \partial_m u_m \delta_{ik} \mathbf{e}_k + \mu \partial_i \partial_i u_k \mathbf{e}_k + \mu \partial_i \partial_k u_i \mathbf{e}_k
\end{aligned}$$

$$\begin{aligned}
&= \lambda_p \mathbf{e}_k \partial_k \partial_m u_m + \mu \partial_i \partial_i u_k \mathbf{e}_k + \mu \mathbf{e}_k \partial_k \partial_i u_i \\
&= (\lambda_p + \mu) \mathbf{e}_k \partial_k \partial_i u_i + \mu \partial_i \partial_i u_k \mathbf{e}_k \\
&= (\lambda_p + \mu) \nabla(\nabla \cdot \mathbf{u}) + \mu \Delta \mathbf{u},
\end{aligned}$$

which, up to a minus sign, is $\mathcal{L}_p \mathbf{u}$ — see the explanation following (3.19). Therefore in phase p the displacement \mathbf{u} satisfies $\mathcal{L}_p \mathbf{u} = 0$ (for $p = 1, 2,$ and E), which is what we wanted to show.

B.1.2 Continuity Conditions

In this section we derive the continuity conditions on the displacement and normal stress (traction) across ∂D and $\partial \Omega$ that are imposed in (3.19).

First, the displacement \mathbf{u} is required to be continuous across ∂D and $\partial \Omega$ as long as there are no *dislocations*. In other words, we assume the materials in D , $\Omega \setminus \overline{D}$, and $\mathbb{R}^d \setminus \overline{\Omega}$ remain firmly bonded together — they are not allowed to separate at the boundary (so the normal component of \mathbf{u} remains continuous) and none of the materials can rotate along its boundary while the material bonded to it stays fixed or rotates by a different amount along the same boundary (this guarantees that the tangential component of \mathbf{u} remains continuous). These are reasonable assumptions in the applications we have in mind — if one is interested in determining the volume fraction of the inclusion it would be detrimental to damage the material so substantially in the process of taking the measurements.

Second, we now show that the normal stress must be continuous across the boundary of each component. (The argument presented here more or less follows that given by Griffiths [45, Section 7.3.6] for the continuity of the normal component of the magnetic field in electrodynamics, although we have adapted the terminology to our situation.) We focus on ∂D for definiteness. Suppose $\mathbf{x} \in \partial D$ and that the outward unit normal vector to ∂D at the point \mathbf{x} is \mathbf{n}_D — see Figure B.1. We draw an imaginary, wafer-thin cylinder C of height $h \ll 1$ and fixed infinitesimal radius L , centered at the point \mathbf{x} as shown in Figure B.1. Let C_0 , C_+ , and C_- denote the curved surface of the cylinder, the flat surface of the cylinder that is outside D , and the flat surface of the cylinder that is inside D , respectively. We assume $\boldsymbol{\sigma}$ is essentially constant on the ends of the cylinder, namely C_+ and C_- (we are implicitly

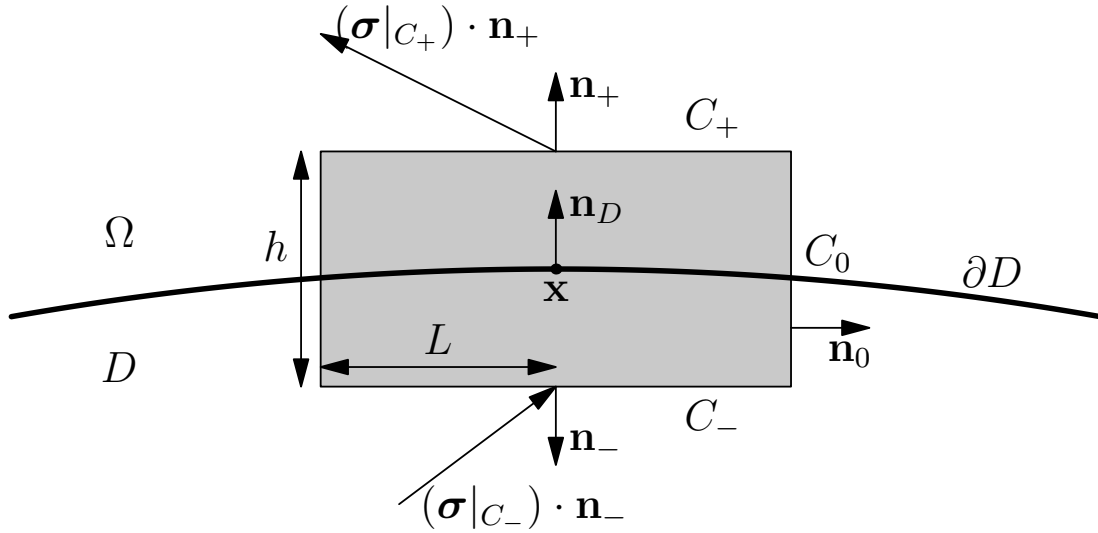


Figure B.1. The figure shows a plot of the cross-section of the cylinder discussed in the text. Note that the figure is not drawn to scale. The cylinder, of height $h \ll 1$ and infinitesimal radius L , is centered at the point $\mathbf{x} \in \partial D$. The outward unit normal to ∂D at \mathbf{x} is denoted \mathbf{n}_D . The boundary of D is indicated with a thick black line — the set D is below this line while the set $\Omega \setminus \bar{D}$ is above ∂D in the figure. The curved surface of the cylinder is labeled C_0 ; the flat surface of the cylinder that is outside of D is labeled C_+ and has outward unit normal vector \mathbf{n}_+ ; the flat surface of the cylinder that is inside D is labeled C_- and has outward unit normal vector \mathbf{n}_- . Finally, the vectors $(\boldsymbol{\sigma}|_{C_+}) \cdot \mathbf{n}_+$ and $(\boldsymbol{\sigma}|_{C_-}) \cdot \mathbf{n}_-$ denote the normal stress (traction) on the surfaces C_+ and C_- , respectively.

assuming $\boldsymbol{\sigma}$ is smooth). Also, let \mathbf{n}_0 , \mathbf{n}_+ and \mathbf{n}_- denote the outward unit normals to C_0 , C_+ , and C_- , respectively.

Since $\nabla \cdot \boldsymbol{\sigma} = 0$ by (3.6) on each side of ∂D , the divergence theorem implies

$$0 = \int_C \nabla \cdot \boldsymbol{\sigma} \, d\mathbf{x} = \int_{\partial C} \boldsymbol{\sigma} \cdot \mathbf{n} \, dS,$$

where \mathbf{n} is the outward unit normal vector to ∂C . This is equivalent to

$$0 = \int_{C_0} \boldsymbol{\sigma} \cdot \mathbf{n}_0 \, dS + \int_{C_+} \boldsymbol{\sigma} \cdot \mathbf{n}_+ \, dS + \int_{C_-} \boldsymbol{\sigma} \cdot \mathbf{n}_- \, dS. \quad (\text{B.6})$$

If $|\boldsymbol{\sigma} \cdot \mathbf{n}_0| \leq K$ for some constant $K > 0$ near ∂D , then the first integral vanishes in the limit $h \rightarrow 0^+$ since

$$\left| \int_{C_0} \boldsymbol{\sigma} \cdot \mathbf{n}_0 \, dS \right| \leq \int_{C_0} |\boldsymbol{\sigma} \cdot \mathbf{n}_0| \, dS \leq K \int_{C_0} dS = 2\pi K L h \rightarrow 0 \quad \text{as } h \rightarrow 0^+.$$

Since $\boldsymbol{\sigma}$ is assumed to be constant on the sets C_+ and C_- , (B.6) becomes

$$0 = ((\boldsymbol{\sigma}|_{C_+}) \cdot \mathbf{n}_+) \int_{C_+} dS + ((\boldsymbol{\sigma}|_{C_-}) \cdot \mathbf{n}_-) \int_{C_-} dS$$

$$= \pi L^2 \left((\boldsymbol{\sigma}|_{C_+}) \cdot \mathbf{n}_+ + (\boldsymbol{\sigma}|_{C_-}) \cdot \mathbf{n}_- \right). \quad (\text{B.7})$$

As long as ∂D is smooth enough, in the limit $h \rightarrow 0^+$ we have

$$(\boldsymbol{\sigma}|_{C_+}) \cdot \mathbf{n}_+ \rightarrow (\boldsymbol{\sigma}|_{\partial D^+}) \cdot \mathbf{n}_D \quad \text{and} \quad (\boldsymbol{\sigma}|_{C_-}) \cdot \mathbf{n}_- \rightarrow (\boldsymbol{\sigma}|_{\partial D^-}) \cdot (-\mathbf{n}_D).$$

Thus in the limit as $h \rightarrow 0^+$, (B.7) becomes (after dividing through by πL^2)

$$0 = (\boldsymbol{\sigma}|_{\partial D^+}) \cdot \mathbf{n}_D - (\boldsymbol{\sigma}|_{\partial D^-}) \cdot \mathbf{n}_D \quad \Leftrightarrow \quad (\boldsymbol{\sigma}|_{\partial D^+}) \cdot \mathbf{n}_D = (\boldsymbol{\sigma}|_{\partial D^-}) \cdot \mathbf{n}_D.$$

Therefore the normal stress must be continuous across ∂D . A similar argument shows that it must be continuous across $\partial \Omega$ as well.

B.2 Nonlocal Boundary Condition for a Disk

In this appendix we provide the details of the derivation of the boundary condition $\mathbf{P}(\mathbf{u}'_0, \mathbf{t}'_0, \mathbf{f}_0, \mathbf{F}_0)$ when Ω is a disk of radius R in \mathbb{R}^2 . The results are summarized in Section 3.6. Much of this work can be found in the books by Muskhelishvili [99] and England [30]. Recall that $\lambda_E = \lambda_2$.

B.2.1 Preliminaries

Let $\mathbf{e}_x = [1, 0]^T$ and $\mathbf{e}_y = [0, 1]^T$ denote the standard orthonormal Cartesian Basis for \mathbb{R}^2 , and let

$$\mathbf{e}_r = \cos \theta \mathbf{e}_x + \sin \theta \mathbf{e}_y \quad \text{and} \quad \mathbf{e}_\theta = -\sin \theta \mathbf{e}_x + \cos \theta \mathbf{e}_y \quad (\text{B.8})$$

denote the standard orthonormal polar basis for \mathbb{R}^2 , where θ denotes the angle measured counterclockwise from the x -axis. The inverse of (B.8) is

$$\mathbf{e}_x = \cos \theta \mathbf{e}_r - \sin \theta \mathbf{e}_\theta \quad \text{and} \quad \mathbf{e}_y = \sin \theta \mathbf{e}_r + \cos \theta \mathbf{e}_\theta. \quad (\text{B.9})$$

We denote the Cartesian Components of $\tilde{\mathbf{u}}_E$, the solution of (3.34), by \tilde{u}_E and \tilde{v}_E ; thus $\tilde{\mathbf{u}}_E = \tilde{u}_E \mathbf{e}_x + \tilde{v}_E \mathbf{e}_y$. Similarly, we denote the polar components of $\tilde{\mathbf{u}}_E$ by $\tilde{u}_{E,r}$ and $\tilde{u}_{E,\theta}$. By (B.9) we have

$$\tilde{\mathbf{u}}_E = \tilde{u}_E \mathbf{e}_x + \tilde{v}_E \mathbf{e}_y = \tilde{u}_E (\cos \theta \mathbf{e}_r - \sin \theta \mathbf{e}_\theta) + \tilde{v}_E (\sin \theta \mathbf{e}_r + \cos \theta \mathbf{e}_\theta) = \tilde{u}_{E,r} \mathbf{e}_r + \tilde{u}_{E,\theta} \mathbf{e}_\theta,$$

where

$$\tilde{u}_{E,r} = \tilde{u}_E \cos \theta + \tilde{v}_E \sin \theta \quad \text{and} \quad \tilde{u}_{E,\theta} = -\tilde{u}_E \sin \theta + \tilde{v}_E \cos \theta. \quad (\text{B.10})$$

We now introduce the change-of-basis matrix

$$\mathbf{R}_\theta = \begin{bmatrix} \cos \theta & \sin \theta \\ -\sin \theta & \cos \theta \end{bmatrix},$$

which will allow us to move back and forth between the Cartesian Basis $\{\mathbf{e}_x, \mathbf{e}_y\}$ and the polar basis $\{\mathbf{e}_r, \mathbf{e}_\theta\}$. For all $\theta \in \mathbb{R}$ we have $\mathbf{R}_\theta^T \mathbf{R}_\theta = \mathbf{R}_\theta \mathbf{R}_\theta^T = \mathbf{I}$, where $\mathbf{I} \in \text{Sym}(\mathbb{R}^2)$ is the identity matrix. Therefore $\mathbf{R}_\theta^{-1} = \mathbf{R}_\theta^T$, so \mathbf{R}_θ is an orthogonal matrix for each $\theta \in \mathbb{R}$. Using this matrix we see that the Cartesian Components and polar components of the displacement are related as follows:

$$\begin{bmatrix} \tilde{u}_{E,r} \\ \tilde{u}_{E,\theta} \end{bmatrix} = \mathbf{R}_\theta \begin{bmatrix} \tilde{u}_E \\ \tilde{v}_E \end{bmatrix} \quad \text{and} \quad \begin{bmatrix} \tilde{u}_E \\ \tilde{v}_E \end{bmatrix} = \mathbf{R}_\theta^T \begin{bmatrix} \tilde{u}_{E,r} \\ \tilde{u}_{E,\theta} \end{bmatrix}.$$

The stress tensor associated with the displacement $\tilde{\mathbf{u}}_E$ is denoted by $\tilde{\boldsymbol{\sigma}}_E$ and is in the space $\text{Sym}(\mathbb{R}^2)$; note that $\dim(\text{Sym}(\mathbb{R}^2)) = 3$, where $\dim(V)$ denotes the dimension of the subspace $V \subset \mathbb{R}^2$. On $\text{Sym}(\mathbb{R}^2)$ we use the orthogonal basis

$$\{\mathbf{e}_x \otimes \mathbf{e}_x, (\mathbf{e}_x \otimes \mathbf{e}_y + \mathbf{e}_y \otimes \mathbf{e}_x), \mathbf{e}_y \otimes \mathbf{e}_y\} = \left\{ \begin{bmatrix} 1 & 0 \\ 0 & 0 \end{bmatrix}, \begin{bmatrix} 0 & 1 \\ 1 & 0 \end{bmatrix}, \begin{bmatrix} 0 & 0 \\ 0 & 1 \end{bmatrix} \right\},$$

where the tensor product between two vectors \mathbf{b} and \mathbf{b}' in \mathbb{R}^2 is defined by $(\mathbf{b} \otimes \mathbf{b}')_{ij} = (\mathbf{b} \mathbf{b}'^T)_{ij} = b_i b'_j$ for $i, j = 1, 2$.

In the above basis, the stress tensor $\tilde{\boldsymbol{\sigma}}_E = \mathcal{S}_E \tilde{\mathbf{u}}_E$ (where \mathcal{S}_E is defined in (3.18)) can be written as

$$\tilde{\boldsymbol{\sigma}}_E = \tilde{\sigma}_{E,xx} \mathbf{e}_x \otimes \mathbf{e}_x + \tilde{\sigma}_{E,xy} (\mathbf{e}_x \otimes \mathbf{e}_y + \mathbf{e}_y \otimes \mathbf{e}_x) + \tilde{\sigma}_{E,yy} (\mathbf{e}_y \otimes \mathbf{e}_y). \quad (\text{B.11})$$

Using (B.9), we find

$$\begin{aligned} \mathbf{e}_x \otimes \mathbf{e}_x &= (\cos \theta \mathbf{e}_r - \sin \theta \mathbf{e}_\theta) \otimes (\cos \theta \mathbf{e}_r - \sin \theta \mathbf{e}_\theta) \\ &= \cos^2 \theta \mathbf{e}_r \otimes \mathbf{e}_r - \cos \theta \sin \theta (\mathbf{e}_r \otimes \mathbf{e}_\theta + \mathbf{e}_\theta \otimes \mathbf{e}_r) + \sin^2 \theta \mathbf{e}_\theta \otimes \mathbf{e}_\theta, \\ \mathbf{e}_x \otimes \mathbf{e}_y &= (\cos \theta \mathbf{e}_r - \sin \theta \mathbf{e}_\theta) \otimes (\sin \theta \mathbf{e}_r + \cos \theta \mathbf{e}_\theta) \\ &= \cos \theta \sin \theta \mathbf{e}_r \otimes \mathbf{e}_r + \cos^2 \theta \mathbf{e}_r \otimes \mathbf{e}_\theta - \sin^2 \theta \mathbf{e}_\theta \otimes \mathbf{e}_r - \cos \theta \sin \theta \mathbf{e}_\theta \otimes \mathbf{e}_\theta \\ \mathbf{e}_y \otimes \mathbf{e}_x &= (\sin \theta \mathbf{e}_r + \cos \theta \mathbf{e}_\theta) \otimes (\cos \theta \mathbf{e}_r - \sin \theta \mathbf{e}_\theta) \\ &= \cos \theta \sin \theta \mathbf{e}_r \otimes \mathbf{e}_r - \sin^2 \theta \mathbf{e}_r \otimes \mathbf{e}_\theta + \cos^2 \theta \mathbf{e}_\theta \otimes \mathbf{e}_r - \cos \theta \sin \theta \mathbf{e}_\theta \otimes \mathbf{e}_\theta \\ \mathbf{e}_y \otimes \mathbf{e}_y &= (\sin \theta \mathbf{e}_r + \cos \theta \mathbf{e}_\theta) \otimes (\sin \theta \mathbf{e}_r + \cos \theta \mathbf{e}_\theta) \\ &= \sin^2 \theta \mathbf{e}_r \otimes \mathbf{e}_r + \cos \theta \sin \theta (\mathbf{e}_r \otimes \mathbf{e}_\theta + \mathbf{e}_\theta \otimes \mathbf{e}_r) + \cos^2 \theta \mathbf{e}_\theta \otimes \mathbf{e}_\theta. \end{aligned} \quad (\text{B.12})$$

Inserting these expressions into (B.11) gives the following expression for the stress tensor in the polar basis:

$$\begin{aligned}
\tilde{\boldsymbol{\sigma}}_E &= \tilde{\sigma}_{E,xx}(\cos^2 \theta \mathbf{e}_r \otimes \mathbf{e}_r - \cos \theta \sin \theta (\mathbf{e}_r \otimes \mathbf{e}_\theta + \mathbf{e}_\theta \otimes \mathbf{e}_r) + \sin^2 \theta \mathbf{e}_\theta \otimes \mathbf{e}_\theta) \\
&\quad + \tilde{\sigma}_{E,xy}(\cos \theta \sin \theta \mathbf{e}_r \otimes \mathbf{e}_r + \cos^2 \theta \mathbf{e}_r \otimes \mathbf{e}_\theta - \sin^2 \theta \mathbf{e}_\theta \otimes \mathbf{e}_r - \cos \theta \sin \theta \mathbf{e}_\theta \otimes \mathbf{e}_\theta) \\
&\quad + \tilde{\sigma}_{E,xy}(\cos \theta \sin \theta \mathbf{e}_r \otimes \mathbf{e}_r - \sin^2 \theta \mathbf{e}_r \otimes \mathbf{e}_\theta + \cos^2 \theta \mathbf{e}_\theta \otimes \mathbf{e}_r - \cos \theta \sin \theta \mathbf{e}_\theta \otimes \mathbf{e}_\theta) \\
&\quad + \tilde{\sigma}_{E,yy}(\sin^2 \theta \mathbf{e}_r \otimes \mathbf{e}_r + \cos \theta \sin \theta (\mathbf{e}_r \otimes \mathbf{e}_\theta + \mathbf{e}_\theta \otimes \mathbf{e}_r) + \cos^2 \theta \mathbf{e}_\theta \otimes \mathbf{e}_\theta) \\
&= (\tilde{\sigma}_{E,xx} \cos^2 \theta + 2\tilde{\sigma}_{E,xy} \cos \theta \sin \theta + \tilde{\sigma}_{E,yy} \sin^2 \theta) \mathbf{e}_r \otimes \mathbf{e}_r \\
&\quad + (-\tilde{\sigma}_{E,xx} \cos \theta \sin \theta + \tilde{\sigma}_{E,xy}(\cos^2 \theta - \sin^2 \theta) + \tilde{\sigma}_{E,yy} \cos \theta \sin \theta) \mathbf{e}_r \otimes \mathbf{e}_\theta \\
&\quad + (-\tilde{\sigma}_{E,xx} \cos \theta \sin \theta + \tilde{\sigma}_{E,xy}(\cos^2 \theta - \sin^2 \theta) + \tilde{\sigma}_{E,yy} \cos \theta \sin \theta) \mathbf{e}_\theta \otimes \mathbf{e}_r \\
&\quad + (\tilde{\sigma}_{E,xx} \sin^2 \theta - 2\tilde{\sigma}_{E,xy} \cos \theta \sin \theta + \tilde{\sigma}_{E,yy} \cos^2 \theta) \mathbf{e}_\theta \otimes \mathbf{e}_\theta \\
&= \tilde{\sigma}_{E,rr} \mathbf{e}_r \otimes \mathbf{e}_r + \tilde{\sigma}_{E,r\theta} (\mathbf{e}_r \otimes \mathbf{e}_\theta + \mathbf{e}_\theta \otimes \mathbf{e}_r) + \tilde{\sigma}_{E,\theta\theta} \mathbf{e}_\theta \otimes \mathbf{e}_\theta, \tag{B.13}
\end{aligned}$$

where the polar components of $\tilde{\boldsymbol{\sigma}}_E$ are related to the Cartesian Components of $\tilde{\boldsymbol{\sigma}}_E$ by

$$\begin{aligned}
\tilde{\sigma}_{E,rr} &= \tilde{\sigma}_{E,xx} \cos^2 \theta + 2\tilde{\sigma}_{E,xy} \cos \theta \sin \theta + \tilde{\sigma}_{E,yy} \sin^2 \theta; \\
\tilde{\sigma}_{E,r\theta} &= -\tilde{\sigma}_{E,xx} \cos \theta \sin \theta + \tilde{\sigma}_{E,xy}(\cos^2 \theta - \sin^2 \theta) + \tilde{\sigma}_{E,yy} \cos \theta \sin \theta; \\
\tilde{\sigma}_{E,\theta\theta} &= \tilde{\sigma}_{E,xx} \sin^2 \theta - 2\tilde{\sigma}_{E,xy} \cos \theta \sin \theta + \tilde{\sigma}_{E,yy} \cos^2 \theta.
\end{aligned}$$

We note that one obtains the same relationships through the change-of-basis formula

$$\begin{bmatrix} \tilde{\sigma}_{E,rr} & \tilde{\sigma}_{E,r\theta} \\ \tilde{\sigma}_{E,r\theta} & \tilde{\sigma}_{E,\theta\theta} \end{bmatrix} = \mathbf{R}_\theta \begin{bmatrix} \tilde{\sigma}_{E,xx} & \tilde{\sigma}_{E,xy} \\ \tilde{\sigma}_{E,xy} & \tilde{\sigma}_{E,yy} \end{bmatrix} \mathbf{R}_\theta^T.$$

As in the book by England [30] (see also the book by Muskhelishvili [99]), it is convenient for us to use complex notation; in particular we write $\tilde{\mathbf{u}}_E = \tilde{u}_E + i\tilde{v}_E$, where $i = \sqrt{-1}$. The complex variable z can be written as $z = x + iy = re^{i\theta}$. The conjugate of z is $\bar{z} = x - iy = re^{-i\theta}$ and the modulus of z is $|z|^2 = z\bar{z} = x^2 + y^2 = r^2$. Thanks to (B.10) we can write

$$\tilde{u}_{E,r} + i\tilde{u}_{E,\theta} = e^{-i\theta}(\tilde{u}_E + i\tilde{v}_E). \tag{B.14}$$

This relationship is essentially due to the fact that R_\perp represents a clockwise rotation by angle θ in \mathbb{R}^2 — this same transformation is represented in the complex plane by multiplication by $e^{-i\theta}$. There are similar relationships between the polar and

Cartesian Components of the stress tensor, but we omit them since we do not explicitly use them.

As discussed by England [30, Chapter 4], there exist complex potentials $\Psi(z)$ and $\psi(z)$ such that

$$\begin{aligned}\tilde{u}_{E,r} + i\tilde{u}_{E,\theta} &= \frac{e^{-i\theta}}{2\mu} \left(\rho_E \Psi(z) - z \overline{\Psi'(z)} - \overline{\psi(z)} \right), \\ \tilde{\sigma}_{E,rr} + i\tilde{\sigma}_{E,r\theta} &= \Psi'(z) + \overline{\Psi'(z)} - \left(\bar{z} \overline{\Psi''(z)} + \frac{\bar{z}}{z} \overline{\psi'(z)} \right), \\ \tilde{\sigma}_{E,rr} + \tilde{\sigma}_{E,\theta\theta} &= 2 \left(\Psi'(z) + \overline{\Psi'(z)} \right),\end{aligned}\tag{B.15}$$

where $\Psi'(z) = \frac{d}{dz} \Psi(z)$, $\psi'(z) = \frac{d}{dz} \psi(z)$, and

$$\rho_E \equiv \frac{\lambda_E + 3\mu}{\lambda_E + \mu} > 0\tag{B.16}$$

($\rho_E > 0$ since $\lambda_E > -(2/d)\mu \geq -\mu$ by (3.9)).

As discussed by England [30, Section 4.1], the complex potentials are of the form

$$\Psi(z) = -\frac{X + iY}{2\pi(1 + \rho_E)} \log z + \Psi_0(z) \quad \text{and} \quad \psi(z) = \frac{\rho_E(X - iY)}{2\pi(1 + \rho_E)} \log z + \psi_0(z),$$

where Ψ_0 and ψ_0 are single-valued holomorphic functions in the region $|z| > R$. Since Ψ_0 and ψ_0 are holomorphic for $|z| > R$, they can be written as Laurent series:

$$\begin{aligned}\Psi(z) &= -\frac{X + iY}{2\pi(1 + \rho_E)} \log z + \sum_{n=1}^{\infty} C_n z^n + \sum_{n=0}^{\infty} \gamma_n z^{-n} \\ \psi(z) &= \frac{\rho_E(X - iY)}{2\pi(1 + \rho_E)} \log z + \sum_{n=1}^{\infty} D_n z^n + \sum_{n=0}^{\infty} \delta_n z^{-n},\end{aligned}\tag{B.17}$$

where the constants C_n, D_n, γ_n , and δ_n need to be determined.

B.2.2 The Solution $\tilde{\mathbf{u}}_E$

Next, we use (B.15) and (B.17) to determine the solution $\tilde{\mathbf{u}}_E$ to the problem (3.34).

Inserting (B.17) into (B.15), we find

$$\begin{aligned}\tilde{u}_{E,r} + i\tilde{u}_{E,\theta} &= \frac{e^{-i\theta}}{2\mu} \left(\rho_E \left(-\frac{X + iY}{2\pi(1 + \rho_E)} \log z + \sum_{n=1}^{\infty} C_n z^n + \sum_{n=0}^{\infty} \gamma_n z^{-n} \right) \right. \\ &\quad \left. - z \left(-\frac{X - iY}{2\pi(1 + \rho_E)} \frac{1}{\bar{z}} + \sum_{n=1}^{\infty} n \overline{C_n} \bar{z}^{n-1} + \sum_{n=0}^{\infty} -n \overline{\gamma_n} \bar{z}^{-n-1} \right) \right. \\ &\quad \left. - \left(\frac{\rho_E(X + iY)}{2\pi(1 + \rho_E)} \overline{\log z} + \sum_{n=1}^{\infty} \overline{D_n} \bar{z}^n + \sum_{n=0}^{\infty} \overline{\delta_n} \bar{z}^{-n} \right) \right).\end{aligned}\tag{B.18}$$

Evaluating this at $z = re^{i\theta}$ for $r \geq R$ gives

$$\begin{aligned}
& (\tilde{u}_{E,r} + i\tilde{u}_{E,\theta})|_{z=re^{i\theta}} = \tilde{u}_{E,r}(r, \theta) + i\tilde{u}_{E,\theta}(r, \theta) \\
&= \frac{e^{-i\theta}}{2\mu} \left(\rho_E \left(-\frac{X + iY}{2\pi(1 + \rho_E)} (\log r + i\theta) + \sum_{n=1}^{\infty} C_n r^n e^{in\theta} + \sum_{n=0}^{\infty} \gamma_n r^{-n} e^{-in\theta} \right) \right. \\
&\quad \left. - re^{i\theta} \left(-\frac{X - iY}{2\pi(1 + \rho_E)} r^{-1} e^{i\theta} + \sum_{n=1}^{\infty} n \overline{C}_n r^{n-1} e^{-i(n-1)\theta} + \sum_{n=0}^{\infty} -n \overline{\gamma}_n r^{-n-1} e^{i(n+1)\theta} \right) \right. \\
&\quad \left. - \left(\frac{\rho_E(X + iY)}{2\pi(1 + \rho_E)} (\log r - i\theta) + \sum_{n=1}^{\infty} \overline{D}_n r^n e^{-in\theta} + \sum_{n=0}^{\infty} \overline{\delta}_n r^{-n} e^{in\theta} \right) \right) \\
&= \frac{e^{-i\theta}}{2\mu} \left(-\frac{\rho_E(X + iY)}{2\pi(1 + \rho_E)} 2 \log r + \sum_{n=1}^{\infty} \rho_E C_n r^n e^{in\theta} + \sum_{n=0}^{\infty} \rho_E \gamma_n r^{-n} e^{-in\theta} \right. \\
&\quad \left. + \frac{X - iY}{2\pi(1 + \rho_E)} e^{2i\theta} - \sum_{n=1}^{\infty} n \overline{C}_n r^n e^{-i(n-2)\theta} + \sum_{n=0}^{\infty} n \overline{\gamma}_n r^{-n} e^{i(n+2)\theta} \right. \\
&\quad \left. - \sum_{n=1}^{\infty} \overline{D}_n r^n e^{-in\theta} - \sum_{n=0}^{\infty} \overline{\delta}_n r^{-n} e^{in\theta} \right).
\end{aligned}$$

Distributing $e^{-i\theta}$ gives

$$\begin{aligned}
& \frac{1}{2\mu} \left(-\frac{\rho_E(X + iY)}{2\pi(1 + \rho_E)} (2 \log r) e^{-i\theta} + \sum_{n=1}^{\infty} \rho_E C_n r^n e^{i(n-1)\theta} + \sum_{n=0}^{\infty} \rho_E \gamma_n r^{-n} e^{-i(n+1)\theta} \right. \\
&\quad \left. + \frac{X - iY}{2\pi(1 + \rho_E)} e^{i\theta} - \sum_{n=1}^{\infty} n \overline{C}_n r^n e^{-i(n-1)\theta} + \sum_{n=0}^{\infty} n \overline{\gamma}_n r^{-n} e^{i(n+1)\theta} \right. \\
&\quad \left. - \sum_{n=1}^{\infty} \overline{D}_n r^n e^{-i(n+1)\theta} - \sum_{n=0}^{\infty} \overline{\delta}_n r^{-n} e^{i(n-1)\theta} \right).
\end{aligned}$$

Next, we change the sum indices to obtain

$$\begin{aligned}
& \frac{1}{2\mu} \left(-\frac{\rho_E(X + iY)}{2\pi(1 + \rho_E)} (2 \log r) e^{-i\theta} + \sum_{n=0}^{\infty} \rho_E C_{n+1} r^{n+1} e^{in\theta} + \sum_{n=1}^{\infty} \rho_E \gamma_{n-1} r^{-(n-1)} e^{-in\theta} \right. \\
&\quad \left. + \frac{X - iY}{2\pi(1 + \rho_E)} e^{i\theta} - \sum_{n=0}^{\infty} (n+1) \overline{C}_{n+1} r^{n+1} e^{-in\theta} + \sum_{n=1}^{\infty} (n-1) \overline{\gamma}_{n-1} r^{-(n-1)} e^{in\theta} \right. \\
&\quad \left. - \sum_{n=2}^{\infty} \overline{D}_{n-1} r^{n-1} e^{-in\theta} - \sum_{n=-1}^{\infty} \overline{\delta}_{n+1} r^{-(n+1)} e^{in\theta} \right).
\end{aligned}$$

It will be convenient for us to separate the logarithmic terms, terms of order $n = 0$ and $n = 1$, and terms of order $n \geq 2$. In particular, this will make it easier for us

to compare terms in corresponding Fourier Expansions. Applying this to the above expression gives

$$\begin{aligned}
& \frac{1}{2\mu} \left(-\frac{\rho_E(X + iY)}{2\pi(1 + \rho_E)}(2 \log r)e^{-i\theta} + \rho_EC_1r + \rho_EC_2r^2e^{i\theta} + \sum_{n=2}^{\infty} \rho_EC_{n+1}r^{n+1}e^{in\theta} \right. \\
& \quad + \rho_E\gamma_0e^{-i\theta} + \sum_{n=2}^{\infty} \rho_E\gamma_{n-1}r^{-(n-1)}e^{-in\theta} + \frac{X - iY}{2\pi(1 + \rho_E)}e^{i\theta} \\
& \quad - \overline{C_1}r - 2\overline{C_2}r^2e^{-i\theta} - \sum_{n=2}^{\infty} (n+1)\overline{C_{n+1}}r^{n+1}e^{-in\theta} \\
& \quad + \sum_{n=2}^{\infty} (n-1)\overline{\gamma_{n-1}}r^{-(n-1)}e^{in\theta} - \sum_{n=2}^{\infty} \overline{D_{n-1}}r^{n-1}e^{-in\theta} \\
& \quad \left. - \overline{\delta_0}e^{-i\theta} - \overline{\delta_1}r^{-1} - \overline{\delta_2}r^{-2}e^{i\theta} - \sum_{n=2}^{\infty} \overline{\delta_{n+1}}r^{-(n+1)}e^{in\theta} \right).
\end{aligned}$$

Finally, we collect terms of the same order in $e^{in\theta}$ and find

$$\begin{aligned}
& \tilde{u}_{E,r}(r, \theta) + i\tilde{u}_{E,\theta}(r, \theta) \\
& = \frac{1}{2\mu} \left((\rho_EC_1r - \overline{C_1}r - \overline{\delta_1}r^{-1}) \right. \\
& \quad + \left(\rho_EC_2r^2 + \frac{X - iY}{2\pi(1 + \rho_E)} - \overline{\delta_2}r^{-2} \right) e^{i\theta} \\
& \quad + \left(-\frac{\rho_E(X + iY)}{2\pi(1 + \rho_E)}(2 \log r) + \rho_E\gamma_0 - 2\overline{C_2}r^2 - \overline{\delta_0} \right) e^{-i\theta} \tag{B.19} \\
& \quad + \sum_{n=2}^{\infty} (\rho_EC_{n+1}r^{n+1} + (n-1)\overline{\gamma_{n-1}}r^{-(n-1)} - \overline{\delta_{n+1}}r^{-(n+1)}) e^{in\theta} \\
& \quad \left. + \sum_{n=2}^{\infty} (\rho_E\gamma_{n-1}r^{-(n-1)} - (n+1)\overline{C_{n+1}}r^{n+1} - \overline{D_{n-1}}r^{n-1}) e^{-in\theta} \right).
\end{aligned}$$

For $r \gg 1$ (B.19) implies

$$\begin{aligned}
& \tilde{u}_{E,r}(r, \theta) + i\tilde{u}_{E,\theta}(r, \theta) \\
& \approx \frac{1}{2\mu} \left((\rho_EC_1 - \overline{C_1})r + \left(\rho_EC_2r^2 + \frac{X - iY}{2\pi(1 + \rho_E)} \right) e^{i\theta} \right. \\
& \quad \left(-\frac{\rho_E(X + iY)}{2\pi(1 + \rho_E)}(2 \log r) + (\rho_E\gamma_0 - \overline{\delta_0}) - 2\overline{C_2}r^2 \right) e^{-i\theta} \\
& \quad \left. + \sum_{n=2}^{\infty} \rho_EC_{n+1}r^{n+1}e^{in\theta} + \sum_{n=2}^{\infty} (-(n+1)\overline{C_{n+1}}r^{n+1} - \overline{D_{n-1}}r^{n-1}) e^{-in\theta} \right). \tag{B.20}
\end{aligned}$$

Since we are requiring $(\tilde{u}_{E,r} + i\tilde{u}_{E,\theta}) \rightarrow 0$ as $r = |\mathbf{x}| \rightarrow \infty$, the coefficients of $e^{in\theta}$ in (B.20) must be zero for each $n \in \mathbb{Z}$ (due to the uniqueness of Fourier Expansions). In order to guarantee that this limit condition holds, for all large r we must have

$$(\rho_E C_1 - \overline{C_1})r + \rho_E C_2 r^2 + \frac{X - iY}{2\pi(1 + \rho_E)} = 0 \quad (\text{B.21a})$$

$$-\frac{\rho_E(X + iY)}{2\pi(1 + \rho_E)}(2 \log r) + (\rho_E \gamma_0 - \overline{\delta_0}) - 2\overline{C_2}r^2 = 0 \quad (\text{B.21b})$$

$$\rho_E C_{n+1} r^{n+1} = 0 \quad (n \geq 2) \quad (\text{B.21c})$$

$$-(n+1)\overline{C_{n+1}}r^{n+1} - \overline{D_{n-1}}r^{n-1} = 0 \quad (n \geq 2). \quad (\text{B.21d})$$

From (B.21c) we immediately have $C_n = 0$ for $n \geq 3$. Then (B.21d) implies $\overline{D_{n-1}} = 0$ for $n \geq 2$, so $D_n = 0$ for $n \geq 1$. Since (B.21b) must hold for all $r \gg 1$, we require $X = Y = 0$, $\rho_E \gamma_0 - \overline{\delta_0} = 0$, and $\overline{C_2} = 0$, so $C_2 = 0$. Since $C_2 = 0$ and $X = Y = 0$, (B.21a) implies $\rho_E C_1 - \overline{C_1} = 0$. If we add this equation to the negative its conjugate we obtain

$$(\rho_E + 1)(C_1 - \overline{C_1}) = 0. \quad (\text{B.22})$$

By (B.16) and (3.9),

$$\rho_E + 1 = \frac{\lambda_E + 3\mu}{\lambda_E + \mu} + 1 = \frac{2(\lambda_E + 2\mu)}{\lambda_E + \mu} > 0.$$

This and (B.22) imply C_1 is real. However, if C_1 is real then (B.21a) implies $(\rho_E - 1)C_1 = 0$, which implies $C_1 = 0$ since

$$\rho_E - 1 = \frac{\lambda_E + 3\mu}{\lambda_E + \mu} - 1 = \frac{2\mu}{\lambda_E + \mu} > 0$$

by (3.9). To summarize, then, we have

$$\rho_E \gamma_0 - \overline{\delta_0} = 0; \quad X = Y = 0; \quad C_n = D_n = 0 \quad \text{for } n \geq 1. \quad (\text{B.23})$$

Remark B.1 *If we require the solution to remain bounded instead of going to zero, (B.21) still implies $X = Y = 0$ and $C_n = D_n = 0$ for $n \geq 1$. However, the coefficient $\rho_E \gamma_0 - \overline{\delta_0}$ remains undetermined. As we will see in Section B.2.3, the constant $\rho_E \gamma_0 - \overline{\delta_0}$ has no effect on the stress $\tilde{\boldsymbol{\sigma}}_E$.*

Finally, (B.17) and (B.23) imply

$$\Psi(x) = \sum_{n=0}^{\infty} \gamma_n z^{-n} \quad \text{and} \quad \psi(x) = \sum_{n=0}^{\infty} \delta_n z^{-n}; \quad (\text{B.24})$$

by (B.18) and (B.23), the displacement $\tilde{\mathbf{u}}_E$ becomes

$$\tilde{u}_{E,r} + i\tilde{u}_{E,\theta} = \frac{e^{-i\theta}}{2\mu} \left(\sum_{n=0}^{\infty} \rho_E \gamma_n z^{-n} + \sum_{n=0}^{\infty} n \overline{\gamma_n} z \bar{z}^{-n-1} - \sum_{n=0}^{\infty} \overline{\delta_n} \bar{z}^{-n} \right).$$

Using (B.19) we can evaluate this at $z = Re^{i\theta}$ (assuming $\tilde{u}_{E,r} + i\tilde{u}_{E,\theta}$ is continuous up to ∂B_R from outside B_R); in particular we have

$$\begin{aligned} (\tilde{u}_{E,r} + i\tilde{u}_{E,\theta})|_{\partial B_R^+} &= \tilde{u}_{E,r}(R^+, \theta) + i\tilde{u}_{E,\theta}(R^+, \theta) \\ &= \frac{1}{2\mu} \left(-\overline{\delta_1} R^{-1} - \overline{\delta_2} R^{-2} e^{i\theta} + (\rho_E \gamma_0 - \overline{\delta_0}) e^{-i\theta} \right. \\ &\quad \left. + \sum_{n=2}^{\infty} \left((n-1) \overline{\gamma_{n-1}} R^{-(n-1)} - \overline{\delta_{n+1}} R^{-(n+1)} \right) e^{in\theta} \right. \\ &\quad \left. + \sum_{n=2}^{\infty} \rho_E \gamma_{n-1} R^{-(n-1)} e^{-in\theta} \right). \end{aligned} \quad (\text{B.25})$$

From (3.34), we must have $\tilde{u}_{E,r}(R^+, \theta) + i\tilde{u}_{E,\theta}(R^+, \theta) = \tilde{u}_r(\theta) + i\tilde{u}_\theta(\theta)$. We now expand $\tilde{u}_r + i\tilde{u}_\theta$ in a Fourier Series, namely

$$\tilde{u}_r(\theta) + i\tilde{u}_\theta(\theta) = \sum_{n=-\infty}^{\infty} \tilde{u}_n e^{in\theta} = \tilde{u}_0 + \tilde{u}_1 e^{i\theta} + \tilde{u}_{-1} e^{-i\theta} + \sum_{n=2}^{\infty} \tilde{u}_n e^{in\theta} + \sum_{n=2}^{\infty} \tilde{u}_{-n} e^{-in\theta}, \quad (\text{B.26})$$

where for each $n \in \mathbb{Z}$ we have

$$\tilde{u}_n = \frac{1}{2\pi} \int_0^{2\pi} (\tilde{u}_r(\theta) + i\tilde{u}_\theta(\theta)) e^{-in\theta} d\theta.$$

Terms of the same order in $e^{in\theta}$ in (B.25) and (B.26) must be equal. In other words, we must have

$$\begin{aligned} \frac{1}{2\mu} (-\overline{\delta_1} R^{-1}) &= \tilde{u}_0, \\ \frac{1}{2\mu} (-\overline{\delta_2} R^{-2}) &= \tilde{u}_1, \\ \frac{1}{2\mu} (\rho_E \gamma_0 - \overline{\delta_0}) &= \tilde{u}_{-1}, \\ \frac{1}{2\mu} \left((n-1) \overline{\gamma_{n-1}} R^{-(n-1)} - \overline{\delta_{n+1}} R^{-(n+1)} \right) &= \tilde{u}_n \quad (n \geq 2), \\ \text{and } \frac{1}{2\mu} (\rho_E \gamma_{n-1} R^{-(n-1)}) &= \tilde{u}_{-n} \quad (n \geq 2). \end{aligned}$$

From this we find that the coefficients γ_n and δ_n are

$$\begin{aligned}
\delta_1 &= -2\mu R \overline{\tilde{u}_0}, \\
\delta_2 &= -2\mu R^2 \overline{\tilde{u}_1}, \\
\rho_E \gamma_0 - \delta_0 &= 2\mu \tilde{u}_{-1}, \\
\delta_{n+1} &= 2\mu R^{n+1} \left(\frac{n-1}{\rho_E} \overline{\tilde{u}_{-n}} - \overline{\tilde{u}_n} \right) \quad (n \geq 2), \\
\text{and } \gamma_{n-1} &= \frac{2\mu R^{n-1}}{\rho_E} \tilde{u}_{-n} \quad (n \geq 2).
\end{aligned} \tag{B.27}$$

Then by (B.25) and (B.27) we have

$$\begin{aligned}
&\tilde{u}_{E,r}(r, \theta) + i\tilde{u}_{E,\theta}(r, \theta) \\
&= \frac{1}{2\mu} \left(-\overline{\delta_1} r^{-1} - \overline{\delta_2} r^{-2} e^{i\theta} + (\rho_E \gamma_0 - \overline{\delta_0}) e^{-i\theta} \right. \\
&\quad \left. + \sum_{n=2}^{\infty} \left((n-1) \overline{\gamma_{n-1}} r^{-(n-1)} - \overline{\delta_{n+1}} r^{-(n+1)} \right) e^{in\theta} + \sum_{n=2}^{\infty} \rho_E \gamma_{n-1} r^{-(n-1)} e^{-in\theta} \right) \\
&= \tilde{u}_0 R r^{-1} + \tilde{u}_1 R^2 r^{-2} e^{i\theta} + \tilde{u}_{-1} e^{-i\theta} \\
&\quad + \sum_{n=2}^{\infty} \left((n-1) \frac{R^{n-1}}{\rho_E} \overline{\tilde{u}_{-n}} r^{-(n-1)} - R^{n+1} \left(\frac{n-1}{\rho_E} \overline{\tilde{u}_{-n}} - \tilde{u}_n \right) r^{-(n+1)} \right) e^{in\theta} \\
&\quad + \sum_{n=2}^{\infty} \rho_E \frac{R^{n-1}}{\rho_E} \tilde{u}_{-n} r^{-(n-1)} e^{-in\theta} \\
&= \tilde{u}_0 R r^{-1} + \tilde{u}_1 R^2 r^{-2} e^{i\theta} + \tilde{u}_{-1} e^{-i\theta} \\
&\quad + \sum_{n=2}^{\infty} \left(\tilde{u}_n R^{n+1} r^{-(n+1)} + \left(\frac{n-1}{\rho_E} \right) \overline{\tilde{u}_{-n}} R^{n-1} r^{-(n+1)} (r^2 - R^2) \right) e^{in\theta} \\
&\quad + \sum_{n=2}^{\infty} \tilde{u}_{-n} R^{n-1} r^{-(n-1)} e^{-in\theta}.
\end{aligned}$$

This simplifies to

$$\begin{aligned}
&\tilde{u}_{E,r}(r, \theta) + i\tilde{u}_{E,\theta}(r, \theta) \\
&= \tilde{u}_0 R r^{-1} + \sum_{n=1}^{\infty} \tilde{u}_{-n} R^{n-1} r^{-(n-1)} e^{-in\theta} \\
&\quad + \sum_{n=1}^{\infty} \left(\tilde{u}_n R^{n+1} r^{-(n+1)} + \left(\frac{n-1}{\rho_E} \right) \overline{\tilde{u}_{-n}} R^{n-1} r^{-(n+1)} (r^2 - R^2) \right) e^{in\theta},
\end{aligned} \tag{B.28}$$

which is (3.46). Note that as $r \rightarrow R^+$ we have (from (B.26) and (B.28))

$$\tilde{u}_{E,r}(R^+, \theta) + i\tilde{u}_{E,\theta}(R^+, \theta) = \tilde{u}_0 + \sum_{n=1}^{\infty} \tilde{u}_{-n} e^{-in\theta} + \sum_{n=1}^{\infty} \tilde{u}_n e^{in\theta} = \tilde{u}_r(\theta) + i\tilde{u}_\theta(\theta),$$

as required.

B.2.3 Derivation of Λ_E

We now derive the Exterior Dirichlet-to-Neumann Map Λ_E . Recall from (3.35) that

$$\Lambda_E(\tilde{\mathbf{u}}) = (\tilde{\boldsymbol{\sigma}}_E|_{\partial B_R^+}) \cdot \mathbf{n}_{B_R}.$$

Thus, we need to compute the traction around ∂B_R due to the displacement $\tilde{u}_{E,r} + i\tilde{u}_{E,\theta}$.

Using (B.13), the fact that $\mathbf{n}_{B_R} = \mathbf{e}_r$, and the identities $\mathbf{e}_r \cdot \mathbf{e}_r = 1$ and $\mathbf{e}_r \cdot \mathbf{e}_\theta = \mathbf{e}_\theta \cdot \mathbf{e}_r = 0$ we have

$$\begin{aligned} & (\tilde{\boldsymbol{\sigma}}_E|_{\partial B_R^+}) \cdot \mathbf{e}_r \\ &= \left((\tilde{\sigma}_{E,rr}|_{\partial B_R^+}) \mathbf{e}_r \otimes \mathbf{e}_r + (\tilde{\sigma}_{E,r\theta}|_{\partial B_R^+}) (\mathbf{e}_r \otimes \mathbf{e}_\theta + \mathbf{e}_\theta \otimes \mathbf{e}_r) + (\tilde{\sigma}_{E,\theta\theta}|_{\partial B_R^+}) \mathbf{e}_\theta \otimes \mathbf{e}_\theta \right) \cdot \mathbf{e}_r \\ &= (\tilde{\sigma}_{E,rr}|_{\partial B_R^+}) \mathbf{e}_r (\mathbf{e}_r \cdot \mathbf{e}_r) + (\tilde{\sigma}_{E,r\theta}|_{\partial B_R^+}) \mathbf{e}_r (\mathbf{e}_\theta \cdot \mathbf{e}_r) \\ &\quad + (\tilde{\sigma}_{E,r\theta}|_{\partial B_R^+}) \mathbf{e}_\theta (\mathbf{e}_r \cdot \mathbf{e}_r) + (\tilde{\sigma}_{E,\theta\theta}|_{\partial B_R^+}) \mathbf{e}_\theta (\mathbf{e}_\theta \cdot \mathbf{e}_r) \\ &= (\tilde{\sigma}_{E,rr}|_{\partial B_R^+}) \mathbf{e}_r + (\tilde{\sigma}_{E,r\theta}|_{\partial B_R^+}) \mathbf{e}_\theta. \end{aligned}$$

Then (B.15) and (B.24) imply

$$\begin{aligned} \tilde{\sigma}_{E,rr} + i\tilde{\sigma}_{E,r\theta} &= \Psi'(z) + \overline{\Psi'(z)} - \left(\overline{z\Psi''(x)} + \frac{\bar{z}}{z} \overline{\psi'(z)} \right) \\ &= \sum_{n=0}^{\infty} -n\gamma_n z^{-n-1} + \sum_{n=0}^{\infty} -n\overline{\gamma_n} z^{-n-1} \\ &\quad - \sum_{n=0}^{\infty} n(n+1)\overline{\gamma_n} z^{-n-1} - \sum_{n=0}^{\infty} -n\overline{\delta_n} \frac{\bar{z}^{-n}}{z}. \end{aligned}$$

If we evaluate this at $z = re^{i\theta}$ we find

$$\begin{aligned} & (\tilde{\sigma}_{E,rr} + i\tilde{\sigma}_{E,r\theta})|_{z=re^{i\theta}} = \tilde{\sigma}_{E,rr}(r, \theta) + i\tilde{\sigma}_{E,r\theta}(r, \theta) \\ &= - \sum_{n=0}^{\infty} n\gamma_n r^{-(n+1)} e^{-i(n+1)\theta} - \sum_{n=0}^{\infty} n\overline{\gamma_n} r^{-(n+1)} e^{i(n+1)\theta} \\ &\quad - \sum_{n=0}^{\infty} n(n+1)\overline{\gamma_n} r^{-(n+1)} e^{i(n+1)\theta} + \sum_{n=0}^{\infty} n\overline{\delta_n} r^{-(n+1)} e^{i(n-1)\theta} \\ &= - \sum_{n=1}^{\infty} (n-1)\gamma_{n-1} r^{-n} e^{-in\theta} - \sum_{n=1}^{\infty} (n-1)\overline{\gamma_{n-1}} r^{-n} e^{in\theta} \\ &\quad - \sum_{n=1}^{\infty} (n-1)n\overline{\gamma_{n-1}} r^{-n} e^{in\theta} + \sum_{n=-1}^{\infty} (n+1)\overline{\delta_{n+1}} r^{-(n+2)} e^{in\theta}. \end{aligned}$$

Next we simplify and collect like terms in $e^{in\theta}$ to find

$$\begin{aligned}
& \tilde{\sigma}_{E,rr}(r, \theta) + i\tilde{\sigma}_{E,r\theta}(r, \theta) \\
&= -\sum_{n=2}^{\infty} (n-1)\gamma_{n-1}r^{-n}e^{-in\theta} - \sum_{n=2}^{\infty} (n-1)(n+1)\overline{\gamma_{n-1}}r^{-n}e^{in\theta} \\
&\quad + \overline{\delta_1}r^{-2} + 2\overline{\delta_2}r^{-3}e^{i\theta} + \sum_{n=2}^{\infty} (n+1)\overline{\delta_{n+1}}r^{-(n+2)}e^{in\theta} \\
&= \overline{\delta_1}r^{-2} + 2\overline{\delta_2}r^{-3}e^{i\theta} - \sum_{n=2}^{\infty} (n-1)\gamma_{n-1}r^{-n}e^{-in\theta} \\
&\quad + \sum_{n=2}^{\infty} (\overline{\delta_{n+1}}r^{-2} - (n-1)\overline{\gamma_{n-1}})(n+1)r^{-n}e^{in\theta}.
\end{aligned}$$

Note that this goes to zero as $r = |\mathbf{x}| \rightarrow \infty$.

We now evaluate this on ∂B_R . Using (B.27) (and assuming $\tilde{\sigma}_{E,rr} + i\tilde{\sigma}_{E,r\theta}$ is continuous up to ∂B_R from outside B_R) we have

$$\begin{aligned}
& \tilde{\sigma}_{E,rr}(R^+, \theta) + i\tilde{\sigma}_{E,r\theta}(R^+, \theta) \\
&= -2\mu\tilde{u}_0R^{-1} - 4\mu\tilde{u}_1R^{-1}e^{i\theta} - \sum_{n=2}^{\infty} (n-1)\frac{2\mu R^{n-1}}{\rho_E}\tilde{u}_{-n}R^{-n}e^{-in\theta} \\
&\quad + \sum_{n=2}^{\infty} \left(2\mu R^{n+1} \left(\frac{n-1}{\rho_E}\tilde{u}_{-n} - \tilde{u}_n \right) R^{-2} \right. \\
&\quad \quad \left. - (n-1)\frac{2\mu R^{n-1}}{\rho_E}\tilde{u}_{-n} \right) (n+1)R^{-n}e^{in\theta} \\
&= -\frac{2\mu}{R}\tilde{u}_0 - \frac{4\mu}{R}\tilde{u}_1e^{i\theta} - \sum_{n=2}^{\infty} \frac{2\mu(n-1)}{R\rho_E}\tilde{u}_{-n}e^{-in\theta} - \sum_{n=2}^{\infty} \frac{2\mu(n+1)}{R}\tilde{u}_ne^{in\theta} \\
&= \sum_{n=0}^{\infty} \left(-\frac{2\mu}{R} \right) (n+1)\tilde{u}_ne^{in\theta} + \sum_{n=2}^{\infty} \left(-\frac{2\mu}{R\rho_E} \right) (n-1)\tilde{u}_{-n}e^{-in\theta}. \tag{B.29}
\end{aligned}$$

Finally, we expand $\tilde{\sigma}_{E,rr}(R^+, \theta) + i\tilde{\sigma}_{E,r\theta}(R^+, \theta)$ in a Fourier Series; we have

$$\begin{aligned}
\Lambda_E(\tilde{u}_r + i\tilde{u}_\theta) &= \tilde{\sigma}_{E,rr}(R^+, \theta) + i\tilde{\sigma}_{E,r\theta}(R^+, \theta) \\
&= \sum_{n=0}^{\infty} \tilde{\sigma}_ne^{in\theta} + \tilde{\sigma}_{-1}e^{-i\theta} + \sum_{n=2}^{\infty} \tilde{\sigma}_{-n}e^{-in\theta}, \tag{B.30}
\end{aligned}$$

where

$$\tilde{\sigma}_n = \frac{1}{2\pi} \int_0^{2\pi} (\tilde{\sigma}_{E,rr}(R^+, \theta) + i\tilde{\sigma}_{E,r\theta}(R^+, \theta)) e^{-in\theta} d\theta.$$

Terms of the same order in $e^{in\theta}$ in (B.29) and (B.30) must be equal. This implies

$$\begin{cases} \tilde{\sigma}_n = -\frac{2\mu}{R}(n+1)\tilde{u}_n & (n \geq 0), \\ \tilde{\sigma}_{-n} = -\frac{2\mu}{R\rho_E}(n-1)\tilde{u}_{-n} & (n \geq 2), \\ \tilde{\sigma}_{-1} = 0, \end{cases}$$

which is (3.48).

B.2.4 The Boundary Condition $\mathbf{P}(\mathbf{u}'_0, \mathbf{t}'_0, \mathbf{f}_0, \mathbf{F}_0) = 0$

The main goal of this section is to write an explicit formula for the boundary condition $\mathbf{P}(\mathbf{u}'_0, \mathbf{t}'_0, \mathbf{f}_0, \mathbf{F}_0) = 0$, where \mathbf{u}' solves (3.32),

$$\mathbf{P}(\mathbf{u}'_0, \mathbf{t}'_0, \mathbf{f}_0, \mathbf{F}_0) \equiv \mathbf{t}'_0 - \Lambda_E(\mathbf{u}'_0 - \mathbf{f}_0) - \mathbf{F}_0,$$

and \mathbf{u}'_0 , \mathbf{t}'_0 , \mathbf{f}_0 , and \mathbf{F}_0 are defined in (3.33).

First we define the stress tensor due to the displacement \mathbf{f} by

$$\mathbf{F} \equiv \mathcal{S}_E \mathbf{f} = \mathcal{S}_E \nabla g = \lambda_E \Delta g \mathbf{I} + 2\mu \nabla \nabla g, \quad (\text{B.31})$$

where the last equality holds by (3.22) since $\mathbf{f} = \nabla g$. Since our goal is to write everything in Fourier Space, we begin by rewriting the stress tensor \mathbf{F} in the polar basis $\{\mathbf{e}_r, \mathbf{e}_\theta\}$.

The second-order identity tensor \mathbf{I} is invariant under the change from Cartesian Coordinates to polar coordinates due to (B.12); in particular we have

$$\begin{aligned} \mathbf{I} &= \mathbf{e}_x \otimes \mathbf{e}_x + \mathbf{e}_y \otimes \mathbf{e}_y \\ &= \cos^2 \theta \mathbf{e}_r \otimes \mathbf{e}_r - \cos \theta \sin \theta (\mathbf{e}_r \otimes \mathbf{e}_\theta + \mathbf{e}_\theta \otimes \mathbf{e}_r) + \sin^2 \theta \mathbf{e}_\theta \otimes \mathbf{e}_\theta \\ &\quad + \sin^2 \theta \mathbf{e}_r \otimes \mathbf{e}_r + \cos \theta \sin \theta (\mathbf{e}_r \otimes \mathbf{e}_\theta + \mathbf{e}_\theta \otimes \mathbf{e}_r) + \cos^2 \theta \mathbf{e}_\theta \otimes \mathbf{e}_\theta \\ &= (\cos^2 \theta + \sin^2 \theta) \mathbf{e}_r \otimes \mathbf{e}_r + (\sin^2 \theta + \cos^2 \theta) \mathbf{e}_\theta \otimes \mathbf{e}_\theta \\ &= \mathbf{e}_r \otimes \mathbf{e}_r + \mathbf{e}_\theta \otimes \mathbf{e}_\theta. \end{aligned} \quad (\text{B.32})$$

Note that (B.8) implies

$$\frac{\partial}{\partial \theta} \mathbf{e}_r = \mathbf{e}_\theta, \quad \frac{\partial}{\partial \theta} \mathbf{e}_\theta = -\mathbf{e}_r, \quad \text{and} \quad \frac{\partial}{\partial r} \mathbf{e}_r = \frac{\partial}{\partial r} \mathbf{e}_\theta = 0.$$

In the Cartesian Basis the gradient operator is

$$\nabla = \mathbf{e}_x \frac{\partial}{\partial x} + \mathbf{e}_y \frac{\partial}{\partial y}.$$

Using (B.8) this becomes

$$\nabla = (\cos \theta \mathbf{e}_r - \sin \theta \mathbf{e}_\theta) \frac{\partial}{\partial x} + (\sin \theta \mathbf{e}_r + \cos \theta \mathbf{e}_\theta) \frac{\partial}{\partial y}. \quad (\text{B.33})$$

Since $x = r \cos \theta$, $y = r \sin \theta$, $r = \sqrt{x^2 + y^2}$, and $\theta = \arctan(y/x) + C$ (where $C = 0$ or $C = \pi$ depending on which quadrant the point (x, y) is in), we can compute the derivatives of the polar coordinates with respect to the Cartesian Coordinates:

$$\begin{aligned} \frac{\partial r}{\partial x} &= \frac{x}{r} = \cos \theta & \frac{\partial r}{\partial y} &= \frac{y}{r} = \sin \theta \\ \frac{\partial \theta}{\partial x} &= -\frac{y}{r^2} = -\frac{\sin \theta}{r} & \frac{\partial \theta}{\partial y} &= \frac{x}{r^2} = \frac{\cos \theta}{r}. \end{aligned} \tag{B.34}$$

This in combination with the Chain Rule implies

$$\begin{aligned} \frac{\partial}{\partial x} &= \frac{\partial r}{\partial x} \frac{\partial}{\partial r} + \frac{\partial \theta}{\partial x} \frac{\partial}{\partial \theta} = \cos \theta \frac{\partial}{\partial r} - \frac{\sin \theta}{r} \frac{\partial}{\partial \theta}; \\ \frac{\partial}{\partial y} &= \frac{\partial r}{\partial y} \frac{\partial}{\partial r} + \frac{\partial \theta}{\partial y} \frac{\partial}{\partial \theta} = \sin \theta \frac{\partial}{\partial r} + \frac{\cos \theta}{r} \frac{\partial}{\partial \theta}. \end{aligned} \tag{B.35}$$

Inserting (B.34) and (B.35) into (B.33) gives

$$\begin{aligned} \nabla &= (\cos \theta \mathbf{e}_r - \sin \theta \mathbf{e}_\theta) \left(\cos \theta \frac{\partial}{\partial r} - \frac{\sin \theta}{r} \frac{\partial}{\partial \theta} \right) \\ &\quad + (\sin \theta \mathbf{e}_r + \cos \theta \mathbf{e}_\theta) \left(\sin \theta \frac{\partial}{\partial r} + \frac{\cos \theta}{r} \frac{\partial}{\partial \theta} \right) \\ &= \mathbf{e}_r \left(\cos^2 \theta \frac{\partial}{\partial r} - \frac{\cos \theta \sin \theta}{r} \frac{\partial}{\partial \theta} + \sin^2 \theta \frac{\partial}{\partial r} + \frac{\cos \theta \sin \theta}{r} \frac{\partial}{\partial \theta} \right) \\ &\quad + \mathbf{e}_\theta \left(-\cos \theta \sin \theta \frac{\partial}{\partial r} + \frac{\sin^2 \theta}{r} \frac{\partial}{\partial \theta} + \cos \theta \sin \theta \frac{\partial}{\partial r} + \frac{\cos^2 \theta}{r} \frac{\partial}{\partial \theta} \right) \\ &= \mathbf{e}_r \frac{\partial}{\partial r} + \mathbf{e}_\theta \frac{1}{r} \frac{\partial}{\partial \theta}, \end{aligned}$$

which is the gradient operator in polar coordinates. Using this we see that the operator $\nabla \nabla = \nabla \otimes \nabla$ is given by

$$\begin{aligned} \nabla \otimes \nabla &= \left(\mathbf{e}_r \frac{\partial}{\partial r} + \mathbf{e}_\theta \frac{1}{r} \frac{\partial}{\partial \theta} \right) \otimes \left(\mathbf{e}_r \frac{\partial}{\partial r} + \mathbf{e}_\theta \frac{1}{r} \frac{\partial}{\partial \theta} \right) \\ &= \mathbf{e}_r \otimes \mathbf{e}_r \frac{\partial^2}{\partial r^2} + \mathbf{e}_r \otimes \mathbf{e}_\theta \frac{\partial}{\partial r} \left(\frac{1}{r} \frac{\partial}{\partial \theta} \right) \\ &\quad + \mathbf{e}_\theta \otimes \frac{1}{r} \frac{\partial}{\partial \theta} \left(\mathbf{e}_r \frac{\partial}{\partial r} \right) + \frac{1}{r^2} \mathbf{e}_\theta \otimes \frac{\partial}{\partial \theta} \left(\mathbf{e}_\theta \frac{\partial}{\partial \theta} \right) \\ &= \mathbf{e}_r \otimes \mathbf{e}_r \frac{\partial^2}{\partial r^2} + \mathbf{e}_r \otimes \mathbf{e}_\theta \left(\frac{1}{r} \frac{\partial^2}{\partial r \partial \theta} - \frac{1}{r^2} \frac{\partial}{\partial \theta} \right) \\ &\quad + \mathbf{e}_\theta \otimes \frac{1}{r} \left(\mathbf{e}_r \frac{\partial^2}{\partial \theta \partial r} + \mathbf{e}_\theta \frac{\partial}{\partial r} \right) + \frac{1}{r^2} \mathbf{e}_\theta \otimes \left(\mathbf{e}_\theta \frac{\partial^2}{\partial \theta^2} - \mathbf{e}_r \frac{\partial}{\partial \theta} \right) \end{aligned}$$

$$\begin{aligned}
&= \mathbf{e}_r \otimes \mathbf{e}_r \left(\frac{\partial^2}{\partial r^2} \right) + \mathbf{e}_r \otimes \mathbf{e}_\theta \left(\frac{1}{r} \frac{\partial^2}{\partial r \partial \theta} - \frac{1}{r^2} \frac{\partial}{\partial \theta} \right) \\
&\quad + \mathbf{e}_\theta \otimes \mathbf{e}_r \left(\frac{1}{r} \frac{\partial^2}{\partial \theta \partial r} - \frac{1}{r^2} \frac{\partial}{\partial \theta} \right) + \mathbf{e}_\theta \otimes \mathbf{e}_\theta \left(\frac{1}{r} \frac{\partial}{\partial r} + \frac{1}{r^2} \frac{\partial^2}{\partial \theta^2} \right).
\end{aligned}$$

Since we are taking $\Omega = B_R$, we have $\mathbf{n}_{B_R} = \mathbf{e}_r$; then the above equation implies that the radial component of the double gradient of g is

$$\begin{aligned}
\nabla \nabla g \cdot \mathbf{e}_r &= \left(\mathbf{e}_r \otimes \mathbf{e}_r \left(\frac{\partial^2 g}{\partial r^2} \right) + \mathbf{e}_r \otimes \mathbf{e}_\theta \left(\frac{1}{r} \frac{\partial^2 g}{\partial r \partial \theta} - \frac{1}{r^2} \frac{\partial g}{\partial \theta} \right) \right. \\
&\quad \left. + \mathbf{e}_\theta \otimes \mathbf{e}_r \left(\frac{1}{r} \frac{\partial^2 g}{\partial \theta \partial r} - \frac{1}{r^2} \frac{\partial g}{\partial \theta} \right) + \mathbf{e}_\theta \otimes \mathbf{e}_\theta \left(\frac{1}{r} \frac{\partial g}{\partial r} + \frac{1}{r^2} \frac{\partial^2 g}{\partial \theta^2} \right) \right) \cdot \mathbf{e}_r \\
&= \frac{\partial^2 g}{\partial r^2} \mathbf{e}_r (\mathbf{e}_r \cdot \mathbf{e}_r) + \left(\frac{1}{r} \frac{\partial^2 g}{\partial r \partial \theta} - \frac{1}{r^2} \frac{\partial g}{\partial \theta} \right) \mathbf{e}_r (\mathbf{e}_\theta \cdot \mathbf{e}_r) \\
&\quad + \left(\frac{1}{r} \frac{\partial^2 g}{\partial \theta \partial r} - \frac{1}{r^2} \frac{\partial g}{\partial \theta} \right) \mathbf{e}_\theta (\mathbf{e}_r \cdot \mathbf{e}_r) + \left(\frac{1}{r} \frac{\partial g}{\partial r} + \frac{1}{r^2} \frac{\partial^2 g}{\partial \theta^2} \right) \mathbf{e}_\theta (\mathbf{e}_\theta \cdot \mathbf{e}_r) \\
&= \frac{\partial^2 g}{\partial r^2} \mathbf{e}_r + \left(\frac{1}{r} \frac{\partial^2 g}{\partial \theta \partial r} - \frac{1}{r^2} \frac{\partial g}{\partial \theta} \right) \mathbf{e}_\theta. \tag{B.36}
\end{aligned}$$

Finally, the Laplacian in polar coordinates is

$$\begin{aligned}
\Delta &= \left(\mathbf{e}_r \frac{\partial}{\partial r} + \mathbf{e}_\theta \frac{1}{r} \frac{\partial}{\partial \theta} \right) \cdot \left(\mathbf{e}_r \frac{\partial}{\partial r} + \mathbf{e}_\theta \frac{1}{r} \frac{\partial}{\partial \theta} \right) \\
&= (\mathbf{e}_r \cdot \mathbf{e}_r) \frac{\partial^2}{\partial r^2} + (\mathbf{e}_r \cdot \mathbf{e}_\theta) \frac{\partial}{\partial r} \left(\frac{1}{r} \frac{\partial}{\partial \theta} \right) + \mathbf{e}_\theta \cdot \frac{1}{r} \frac{\partial}{\partial \theta} \left(\mathbf{e}_r \frac{\partial}{\partial r} \right) + \frac{1}{r^2} \mathbf{e}_\theta \cdot \frac{\partial}{\partial \theta} \left(\mathbf{e}_\theta \frac{\partial}{\partial \theta} \right) \\
&= \frac{\partial^2}{\partial r^2} + \mathbf{e}_\theta \cdot \frac{1}{r} \left(\mathbf{e}_r \frac{\partial^2}{\partial \theta \partial r} + \mathbf{e}_\theta \frac{\partial}{\partial r} \right) + \frac{1}{r^2} \mathbf{e}_\theta \cdot \left(\mathbf{e}_\theta \frac{\partial^2}{\partial \theta^2} - \mathbf{e}_r \frac{\partial}{\partial \theta} \right) \\
&= \frac{\partial^2}{\partial r^2} + (\mathbf{e}_\theta \cdot \mathbf{e}_r) \frac{1}{r} \frac{\partial^2}{\partial \theta \partial r} + (\mathbf{e}_\theta \cdot \mathbf{e}_\theta) \frac{1}{r} \frac{\partial}{\partial r} + (\mathbf{e}_\theta \cdot \mathbf{e}_\theta) \frac{1}{r^2} \frac{\partial^2}{\partial \theta^2} - (\mathbf{e}_\theta \cdot \mathbf{e}_r) \frac{1}{r^2} \frac{\partial}{\partial \theta} \\
&= \frac{\partial^2}{\partial r^2} + \frac{1}{r} \frac{\partial}{\partial r} + \frac{1}{r^2} \frac{\partial^2}{\partial \theta^2}. \tag{B.37}
\end{aligned}$$

Therefore by (B.31), (B.32), (B.36), and (B.37) we have

$$\begin{aligned}
\mathbf{F} \cdot \mathbf{e}_r &= (\lambda_E \Delta g \mathbf{I} + 2\mu \nabla \nabla g) \cdot \mathbf{e}_r \\
&= \lambda_E \Delta g ((\mathbf{e}_r \otimes \mathbf{e}_r) + (\mathbf{e}_\theta \otimes \mathbf{e}_\theta)) \cdot \mathbf{e}_r + 2\mu \nabla \nabla g \cdot \mathbf{e}_r \\
&= \lambda_E \Delta g (\mathbf{e}_r (\mathbf{e}_r \cdot \mathbf{e}_r) + \mathbf{e}_\theta (\mathbf{e}_\theta \cdot \mathbf{e}_r)) + 2\mu \nabla \nabla g \cdot \mathbf{e}_r \\
&= \lambda_E \Delta g \mathbf{e}_r + 2\mu \nabla \nabla g \cdot \mathbf{e}_r \\
&= \lambda_E \left(\frac{\partial^2 g}{\partial r^2} + \frac{1}{r} \frac{\partial g}{\partial r} + \frac{1}{r^2} \frac{\partial^2 g}{\partial \theta^2} \right) \mathbf{e}_r + 2\mu \left(\frac{\partial^2 g}{\partial r^2} \mathbf{e}_r + \left(\frac{1}{r} \frac{\partial^2 g}{\partial \theta \partial r} - \frac{1}{r^2} \frac{\partial g}{\partial \theta} \right) \mathbf{e}_\theta \right).
\end{aligned}$$

In complex notation, we write $\mathbf{F} \cdot \mathbf{e}_r = F_{rr} + iF_{r\theta}$ where

$$\begin{aligned} F_{rr} &= (\mathbf{F} \cdot \mathbf{e}_r) \cdot \mathbf{e}_r = (\lambda_E + 2\mu) \frac{\partial^2 g}{\partial r^2} + \lambda_E \left(\frac{1}{r} \frac{\partial g}{\partial r} + \frac{1}{r^2} \frac{\partial^2 g}{\partial \theta^2} \right) \\ F_{r\theta} &= (\mathbf{F} \cdot \mathbf{e}_r) \cdot \mathbf{e}_\theta = 2\mu \left(\frac{1}{r} \frac{\partial^2 g}{\partial \theta \partial r} - \frac{1}{r^2} \frac{\partial g}{\partial \theta} \right). \end{aligned} \quad (\text{B.38})$$

We now expand $F_{rr} + iF_{r\theta}$ in a Fourier Series around ∂B_r for $r \geq R$. Then

$$(\mathbf{F}|_{\partial B_r}) \cdot \mathbf{e}_r = (F_{rr} + iF_{r\theta})|_{z=re^{i\theta}} = F_{rr}(r, \theta) + iF_{r\theta}(r, \theta) = \sum_{n=-\infty}^{\infty} F_n(r) e^{in\theta}, \quad (\text{B.39})$$

where

$$F_n(r) = \frac{1}{2\pi} \int_0^{2\pi} (F_{rr}(r, \theta) + iF_{r\theta}(r, \theta)) e^{-in\theta} d\theta.$$

The coefficients $F_n(r)$ can also be determined in terms of the function g . In particular, we expand g in a Fourier Series around the circle ∂B_r ; we have

$$g(r, \theta) = \sum_{n=-\infty}^{\infty} g_n(r) e^{in\theta}, \quad \text{where} \quad g_n(r) = \frac{1}{2\pi} \int_0^{2\pi} g(r, \theta) e^{-in\theta} d\theta. \quad (\text{B.40})$$

Then, due to (B.40) and the fact that g is infinitely differentiable (as discussed in Section 3.4), the following formula holds for any nonnegative integers p and q with $p + q = m$:

$$\frac{\partial^m g}{\partial r^p \partial \theta^q}(r, \theta) = \sum_{n=-\infty}^{\infty} (in)^q \frac{\partial^p g_n(r)}{\partial r^p} e^{in\theta}. \quad (\text{B.41})$$

Then (B.38), (B.39), and (B.41) imply

$$\begin{aligned} F_{rr}(r, \theta) + iF_{r\theta}(r, \theta) &= \sum_{n=-\infty}^{\infty} F_n(r) e^{in\theta} \\ &= (\lambda_E + 2\mu) \frac{\partial^2 g}{\partial r^2} + \lambda_E \left(\frac{1}{r} \frac{\partial g}{\partial r} + \frac{1}{r^2} \frac{\partial^2 g}{\partial \theta^2} \right) + i2\mu \left(\frac{1}{r} \frac{\partial^2 g}{\partial \theta \partial r} - \frac{1}{r^2} \frac{\partial g}{\partial \theta} \right) \\ &= (\lambda_E + 2\mu) \sum_{n=-\infty}^{\infty} \frac{\partial^2 g_n(r)}{\partial r^2} e^{in\theta} + \lambda_E \sum_{n=-\infty}^{\infty} \frac{1}{r} \frac{\partial g_n(r)}{\partial r} e^{in\theta} \\ &\quad + \lambda_E \sum_{n=-\infty}^{\infty} \frac{(in)^2}{r^2} g_n(r) e^{in\theta} + i2\mu \left(\sum_{n=-\infty}^{\infty} \frac{in}{r} \frac{\partial g_n(r)}{\partial r} - \sum_{n=-\infty}^{\infty} \frac{in}{r^2} g_n(r) \right) \\ &= \sum_{n=-\infty}^{\infty} \left((\lambda_E + 2\mu) \frac{\partial^2 g_n(r)}{\partial r^2} + \lambda_E \left(\frac{1}{r} \frac{\partial g_n(r)}{\partial r} - \frac{n^2}{r^2} g_n(r) \right) \right. \\ &\quad \left. + 2\mu \left(-\frac{n}{r} \frac{\partial g_n(r)}{\partial r} + \frac{n}{r^2} g_n(r) \right) \right) e^{in\theta}. \end{aligned}$$

Terms of the same order in $e^{in\theta}$ must be equal; this gives

$$F_n(r) = (\lambda_E + 2\mu) \frac{\partial^2 g_n(r)}{\partial r^2} + \lambda_E \left(\frac{1}{r} \frac{\partial g_n(r)}{\partial r} - \frac{n^2}{r^2} g_n(r) \right) + 2\mu \left(-\frac{n}{r} \frac{\partial g_n(r)}{\partial r} + \frac{n}{r^2} g_n(r) \right).$$

In particular, taking $r \rightarrow R^+$ and assuming all quantities in the above expression are continuous up to ∂B_R from outside B_R gives

$$\begin{aligned} F_n(R^+) &= (\lambda_E + 2\mu) \left. \frac{\partial^2 g_n(r)}{\partial r^2} \right|_{r \rightarrow R^+} + \lambda_E \left(\left. \frac{1}{R} \frac{\partial g_n(r)}{\partial r} \right|_{r \rightarrow R^+} - \frac{n^2}{R^2} g_n(R^+) \right) \\ &\quad + 2\mu \left(-\left. \frac{n}{R} \frac{\partial g_n(r)}{\partial r} \right|_{r \rightarrow R^+} + \frac{n}{R^2} g_n(R^+) \right), \end{aligned} \quad (\text{B.42})$$

where for a function h defined for $r > R$ we define

$$h(r)|_{r \rightarrow R^+} \equiv \lim_{r \rightarrow R^+} h(r).$$

Recall from (3.33) that $\mathbf{F}_0 \equiv (\mathbf{F}|_{\partial B_R^+}) \cdot \mathbf{e}_r$. Since

$$(\mathbf{F}|_{\partial B_R^+}) \cdot \mathbf{e}_r = \sum_{n=-\infty}^{\infty} F_n(R^+) e^{in\theta} \quad (\text{B.43})$$

by (B.39), we define $F_{0,n} \equiv F_n(R^+)$ so that

$$F_{0,r}(\theta) + iF_{0,\theta}(\theta) = \sum_{n=-\infty}^{\infty} F_{0,n} e^{in\theta}. \quad (\text{B.44})$$

Inserting the last two equations into (B.42) gives (3.51). The remainder of the derivation for \mathbf{P} is given in Section 3.6.2.

B.3 Verification of Our Results

In this section we verify that our formula for the Exterior DtN Map in (3.47)–(3.48) is equivalent to that in (3.54), which was obtained by Han and Wu [52, 53].

According to (3.47) and (3.48) we have

$$\begin{aligned} \tilde{\sigma}_{E,rr}(R^+, \theta) + i\tilde{\sigma}_{E,r\theta}(R^+, \theta) &= \Lambda_E(\tilde{u}_r + i\tilde{u}_\theta) \\ &= \sum_{n=0}^{\infty} -\frac{2\mu}{R}(n+1)\tilde{u}_n e^{in\theta} + \sum_{n=-\infty}^{-1} -\frac{2\mu}{R\rho_E}(-n-1)\tilde{u}_n e^{in\theta}, \end{aligned} \quad (\text{B.45})$$

where, by (3.45) and (B.14),

$$\tilde{u}_n = \frac{1}{2\pi} \int_0^{2\pi} (\tilde{u}_{E,r}(R^+, \theta') + i\tilde{u}_{E,\theta}(R^+, \theta')) e^{-in\theta'} d\theta'$$

$$\begin{aligned}
&= \frac{1}{2\pi} \int_0^{2\pi} (\tilde{u}_r(\theta') + i\tilde{u}_\theta(\theta')) e^{-in\theta'} d\theta' \\
&= \frac{1}{2\pi} \int_0^{2\pi} (\tilde{u}(\theta') + i\tilde{v}(\theta')) e^{-i(n+1)\theta'} d\theta'.
\end{aligned}$$

Inserting this into (B.45) we find

$$\begin{aligned}
&\tilde{\sigma}_{E,rr}(R^+, \theta) + i\tilde{\sigma}_{E,r\theta}(R^+, \theta) \\
&= \sum_{n=0}^{\infty} -\frac{2\mu(n+1)}{2\pi R} \left(\int_0^{2\pi} (\tilde{u}(\theta') + i\tilde{v}(\theta')) e^{-i(n+1)\theta'} d\theta' \right) e^{in\theta} \\
&\quad + \sum_{n=-\infty}^{-1} \frac{2\mu(n+1)}{2\pi R\rho_E} \left(\int_0^{2\pi} (\tilde{u}(\theta') + i\tilde{v}(\theta')) e^{-i(n+1)\theta'} d\theta' \right) e^{in\theta} \\
&= \sum_{n=1}^{\infty} -\frac{2\mu n}{2\pi R} \left(\int_0^{2\pi} (\tilde{u}(\theta') + i\tilde{v}(\theta')) e^{-in\theta'} d\theta' \right) e^{i(n-1)\theta} \\
&\quad + \sum_{n=-\infty}^0 \frac{2\mu n}{2\pi R\rho_E} \left(\int_0^{2\pi} (\tilde{u}(\theta') + i\tilde{v}(\theta')) e^{-in\theta'} d\theta' \right) e^{i(n-1)\theta}.
\end{aligned}$$

We now multiply both sides of the above equation by $e^{i\theta}$; this gives

$$(\tilde{\sigma}_{E,rr}(R^+, \theta) + i\tilde{\sigma}_{E,r\theta}(R^+, \theta)) e^{i\theta} = \quad (\text{B.46})$$

$$\begin{aligned}
&\sum_{n=1}^{\infty} -\frac{2\mu n}{2\pi R} \int_0^{2\pi} (\tilde{u}(\theta') + i\tilde{v}(\theta')) e^{in(\theta-\theta')} d\theta' \\
&\quad + \sum_{n=-\infty}^{-1} \frac{2\mu n}{2\pi R\rho_E} \int_0^{2\pi} (\tilde{u}(\theta') + i\tilde{v}(\theta')) e^{in(\theta-\theta')} d\theta', \quad (\text{B.47})
\end{aligned}$$

where we have omitted the $n = 0$ term from the second sum in the last expression. By (B.14), the left-hand side of this expression gives the Cartesian Components of the traction around ∂B_R . Denoting these components by \tilde{X} and \tilde{Y} , respectively, we find

$$(\tilde{\sigma}_{E,rr}(R^+, \theta) + i\tilde{\sigma}_{E,r\theta}(R^+, \theta)) e^{i\theta} = \tilde{X}(R^+, \theta) + i\tilde{Y}(R^+, \theta). \quad (\text{B.48})$$

Using integration by parts and recalling that $\tilde{u} + i\tilde{v}$ and $e^{in\theta}$ are periodic on $[0, 2\pi]$ for any integer n , we find

$$\begin{aligned}
&\int_0^{2\pi} (\tilde{u}(\theta') + i\tilde{v}(\theta')) e^{-in(\theta-\theta')} d\theta' \\
&= -(\tilde{u}(\theta') + i\tilde{v}(\theta')) \frac{e^{in(\theta-\theta')}}{in} \Big|_{\theta'=0}^{2\pi} + \int_0^{2\pi} \left(\frac{d}{d\theta'} (\tilde{u}(\theta') + i\tilde{v}(\theta')) \right) \frac{e^{in(\theta-\theta')}}{in} d\theta' \\
&= \int_0^{2\pi} \left(\frac{d}{d\theta'} (\tilde{u}(\theta') + i\tilde{v}(\theta')) \right) \frac{e^{in(\theta-\theta')}}{in} d\theta'. \quad (\text{B.49})
\end{aligned}$$

We integrate by parts again to find

$$\int_0^{2\pi} \left(\frac{d}{d\theta'} (\tilde{u}(\theta') + i\tilde{v}(\theta')) \right) \frac{e^{in(\theta-\theta')}}{in} d\theta' \quad (\text{B.50})$$

$$\begin{aligned} &= \left(\frac{d}{d\theta'} (\tilde{u}(\theta') + i\tilde{v}(\theta')) \right) \frac{e^{in(\theta-\theta')}}{n^2} \Big|_{\theta'=0}^{2\pi} \\ &\quad - \int_0^{2\pi} \left(\frac{d^2}{d\theta'^2} (\tilde{u}(\theta') + i\tilde{v}(\theta')) \right) \frac{e^{in(\theta-\theta')}}{n^2} d\theta' \\ &= - \int_0^{2\pi} \left(\frac{d^2}{d\theta'^2} (\tilde{u}(\theta') + i\tilde{v}(\theta')) \right) \frac{e^{in(\theta-\theta')}}{n^2} d\theta'. \end{aligned} \quad (\text{B.51})$$

Thus (B.49) and (B.51) imply

$$\int_0^{2\pi} (\tilde{u}(\theta') + i\tilde{v}(\theta')) e^{-in(\theta-\theta')} d\theta' = - \int_0^{2\pi} \left(\frac{d^2}{d\theta'^2} (\tilde{u}(\theta') + i\tilde{v}(\theta')) \right) \frac{e^{in(\theta-\theta')}}{n^2} d\theta'. \quad (\text{B.52})$$

Inserting (B.52) into (B.47) and (B.48) gives

$$\begin{aligned} \tilde{X}(R^+, \theta) + i\tilde{Y}(R^+, \theta) &= \sum_{n=1}^{\infty} \frac{\mu}{\pi R} \int_0^{2\pi} \left(\frac{d^2}{d\theta'^2} (\tilde{u}(\theta') + i\tilde{v}(\theta')) \right) \frac{e^{in(\theta-\theta')}}{n} d\theta' \\ &\quad - \sum_{n=-\infty}^{-1} \frac{\mu}{\pi R \rho_E} \int_0^{2\pi} \left(\frac{d^2}{d\theta'^2} (\tilde{u}(\theta') + i\tilde{v}(\theta')) \right) \frac{e^{in(\theta-\theta')}}{n} d\theta'. \end{aligned} \quad (\text{B.53})$$

We begin with the real part of (B.53); we have

$$\begin{aligned} \tilde{X}(R^+, \theta) &= \sum_{n=1}^{\infty} \frac{\mu}{\pi R} \int_0^{2\pi} \left(\left(\frac{d^2 \tilde{u}(\theta')}{d\theta'^2} \right) \frac{\cos n(\theta - \theta')}{n} - \left(\frac{d^2 \tilde{v}(\theta')}{d\theta'^2} \right) \frac{\sin n(\theta - \theta')}{n} \right) d\theta' \\ &\quad - \sum_{n=-\infty}^{-1} \frac{\mu}{\pi R \rho_E} \int_0^{2\pi} \left(\left(\frac{d^2 \tilde{u}(\theta')}{d\theta'^2} \right) \frac{\cos n(\theta - \theta')}{n} \right. \\ &\quad \left. - \left(\frac{d^2 \tilde{v}(\theta')}{d\theta'^2} \right) \frac{\sin n(\theta - \theta')}{n} \right) d\theta' \\ &= \sum_{n=1}^{\infty} \frac{\mu}{\pi R} \int_0^{2\pi} \left(\left(\frac{d^2 \tilde{u}(\theta')}{d\theta'^2} \right) \frac{\cos n(\theta - \theta')}{n} - \left(\frac{d^2 \tilde{v}(\theta')}{d\theta'^2} \right) \frac{\sin n(\theta - \theta')}{n} \right) d\theta' \\ &\quad + \sum_{n=1}^{\infty} \frac{\mu}{\pi R \rho_E} \int_0^{2\pi} \left(\left(\frac{d^2 \tilde{u}(\theta')}{d\theta'^2} \right) \frac{\cos n(\theta - \theta')}{n} \right. \\ &\quad \left. + \left(\frac{d^2 \tilde{v}(\theta')}{d\theta'^2} \right) \frac{\sin n(\theta - \theta')}{n} \right) d\theta' \end{aligned}$$

$$\begin{aligned}
&= \sum_{n=1}^{\infty} \frac{\mu}{\pi R} \left(1 + \frac{1}{\rho_E}\right) \int_0^{2\pi} \left(\frac{d^2 \tilde{u}(\theta')}{d\theta'^2}\right) \frac{\cos n(\theta - \theta')}{n} d\theta' \\
&\quad + \sum_{n=1}^{\infty} \frac{\mu}{\pi R} \left(-1 + \frac{1}{\rho_E}\right) \int_0^{2\pi} \left(\frac{d^2 \tilde{v}(\theta')}{d\theta'^2}\right) \frac{\sin n(\theta - \theta')}{n} d\theta'.
\end{aligned}$$

We handle the imaginary part of (B.53) similarly. In particular, we have

$$\begin{aligned}
\tilde{Y}(R^+, \theta) &= \sum_{n=1}^{\infty} \frac{\mu}{\pi R} \int_0^{2\pi} \left(\left(\frac{d^2 \tilde{u}(\theta')}{d\theta'^2}\right) \frac{\sin n(\theta - \theta')}{n} + \left(\frac{d^2 \tilde{v}(\theta')}{d\theta'^2}\right) \frac{\cos n(\theta - \theta')}{n} \right) d\theta' \\
&\quad + \sum_{n=1}^{\infty} \frac{\mu}{\pi R \rho_E} \int_0^{2\pi} \left(- \left(\frac{d^2 \tilde{u}(\theta')}{d\theta'^2}\right) \frac{\sin n(\theta - \theta')}{n} \right. \\
&\quad \quad \left. + \left(\frac{d^2 \tilde{v}(\theta')}{d\theta'^2}\right) \frac{\cos n(\theta - \theta')}{n} \right) d\theta' \\
&= \sum_{n=1}^{\infty} \frac{\mu}{\pi R} \left(1 - \frac{1}{\rho_E}\right) \int_0^{2\pi} \left(\frac{d^2 \tilde{u}(\theta')}{d\theta'^2}\right) \frac{\sin n(\theta - \theta')}{n} d\theta' \\
&\quad + \sum_{n=1}^{\infty} \frac{\mu}{\pi R} \left(1 + \frac{1}{\rho_E}\right) \int_0^{2\pi} \left(\frac{d^2 \tilde{v}(\theta')}{d\theta'^2}\right) \frac{\cos n(\theta - \theta')}{n} d\theta'.
\end{aligned}$$

Finally, from the statement following (3.54) we have

$$\eta = \frac{\mu}{\lambda_E + \mu} \Leftrightarrow \lambda_E = \frac{\mu(1 - \eta)}{\eta}.$$

Using this and (B.16), we find

$$1 + \frac{1}{\rho_E} = 1 + \frac{\lambda_E + \mu}{\lambda_E + 3\mu} = \frac{2(\lambda_E + 2\mu)}{\lambda_E + 3\mu} = \frac{2\left(\frac{\mu(1-\eta)}{\eta} + 2\mu\right)}{\frac{\mu(1-\eta)}{\eta} + 3\mu} = \frac{2\mu(1 + \eta)}{\mu(1 + 2\eta)} = \frac{2 + 2\eta}{1 + 2\eta}$$

and

$$-1 + \frac{1}{\rho_E} = -1 + \frac{\lambda_E + \mu}{\lambda_E + 3\mu} = \frac{-2\mu}{\lambda_E + 3\mu} = \frac{-2\mu}{\frac{\mu(1-\eta)}{\eta} + 3\mu} = \frac{-2\mu\eta}{\mu(1 + 2\eta)} = \frac{-2\eta}{1 + 2\eta}.$$

Inserting these expressions into (2.51) and (2.52) gives (3.54), so our formula for Λ_E agrees with that of Han and Wu [52, 53].

APPENDIX C

APPENDIX TO CHAPTER 4

In Section C.1, we provide a brief derivation of the relationship between the complex conductivity and complex permittivity used in Chapters 2 and 4, respectively. Next, we provide justification of the Leibniz Integration Rule in Section C.2. Sections C.3–C.5 are devoted to proving that V satisfies the constraints imposed in (4.12). In Section C.6, we prove that $V \in L^2_{\text{loc}}(\mathbb{R}^2)$. Finally, in Section C.7, we use distribution theory to provide an heuristic justification of (4.17).

C.1 Complex Conductivity and Permittivity

In this section we discuss the relationship between the complex conductivity utilized in Chapter 2 and the complex permittivity (also called the complex dielectric constant if we choose units so that vacuum has permittivity equal to 1). In particular, we wish to derive (4.2) from the Maxwell Equations in the same manner that we derived (2.7). Beginning from (2.5), we arrive at (2.6a) and (2.6b) just as in Section 2.1. However, we rewrite (2.6b) in a slightly different (equivalent) form. We have

$$\nabla \times \widehat{\mathbf{E}}(\mathbf{x}, \omega) = i\omega\mu'(\mathbf{x}, \omega)\widehat{\mathbf{H}}(\mathbf{x}, \omega), \quad (\text{C.1a})$$

$$\nabla \times \widehat{\mathbf{H}}(\mathbf{x}, \omega) = \sigma'(\mathbf{x}, \omega)\widehat{\mathbf{E}}(\mathbf{x}, \omega) - i\omega\varepsilon'(\mathbf{x}, \omega)\widehat{\mathbf{E}}(\mathbf{x}, \omega) = -i\omega\varepsilon(\mathbf{x}, \omega)\widehat{\mathbf{E}}(\mathbf{x}, \omega), \quad (\text{C.1b})$$

where $\varepsilon(\mathbf{x}, \omega) = \varepsilon'(\mathbf{x}, \omega) + i\sigma'(\mathbf{x}, \omega)/\omega$. The displacement field is defined by $\widehat{\mathbf{D}}(\mathbf{x}, \omega) \equiv \varepsilon(\mathbf{x}, \omega)\widehat{\mathbf{E}}(\mathbf{x}, \omega)$. In the medium under consideration, if the wavelengths and attenuation lengths of the displacement and magnetic fields are large compared with the dimensions of the body then we may neglect the right-hand side of (C.1a) (just as in Section 2.1). This gives $\nabla \times \widehat{\mathbf{E}}(\mathbf{x}, \omega) = 0$ so that $\widehat{\mathbf{E}}(\mathbf{x}, \omega) = -\nabla\widehat{V}(\mathbf{x}, \omega)$ for some potential $\widehat{V}(\mathbf{x}, \omega)$ as long as the set under consideration is simply connected. In the case of the slab or cylindrical superlens the set under consideration is typically all of \mathbb{R}^2 or \mathbb{R}^3 , or a large ball in the case of the cylindrical lens, all of which are

simply connected. Since the divergence of a curl is always zero, taking the divergence of (C.1b) gives $\nabla \cdot [\varepsilon(\mathbf{x}, \omega) \nabla \widehat{V}(\mathbf{x}, \omega)] = 0$. As in Chapter 2, we remove the hats for notational convenience. Finally, comparing (C.1b) and (2.6b) we see that the relationship between the complex conductivity and complex dielectric constant is

$$\sigma(\mathbf{x}, \omega) = -i\omega\varepsilon(\mathbf{x}, \omega).$$

C.2 The Leibniz Integration Rule

In this section we present a proof of the following theorem, also known as the Leibniz Integration Rule. In all of our applications of this theorem in the text, one of the functions p, q is a constant while the other is linear.

Theorem C.1 *Let $X \subset \mathbb{R}$ be a nontrivial open interval and let $p, q : X \rightarrow \mathbb{R}$ be differentiable on X such that $p(x) \leq q(x)$ for all $x \in X$. Define $\tilde{p} \equiv \inf_{x \in X} p(x)$ and $\tilde{q} \equiv \sup_{x \in X} q(x)$. Suppose that $f : (\tilde{p}, \tilde{q}) \times X \rightarrow \mathbb{C}$ is a map with the following properties.*

- (i) *For any $x \in X$, the map $s \mapsto f(s, x)$ is in $L^1((\tilde{p}, \tilde{q}))$.*
- (ii) *For almost every $s \in (\tilde{p}, \tilde{q})$, the map $X \rightarrow \mathbb{C}$, $x \mapsto f(s, x)$ is differentiable with derivative $\frac{\partial f}{\partial x}$.*
- (iii) *$h \equiv \sup_{x \in X} |\frac{\partial f}{\partial x}(\cdot, x)| \in L^1((\tilde{p}, \tilde{q}))$.*

Then, for almost every $x \in X$,

$$\frac{\partial}{\partial x} \int_{p(x)}^{q(x)} f(s, x) ds = f(q(x), x)q'(x) - f(p(x), x)p'(x) + \int_{p(x)}^{q(x)} \frac{\partial f}{\partial x}(s, x) ds.$$

Proof of Theorem C.1: This proof is essentially the same as that given by Flanders [34] and Kaplan [69, Section 4.9]. We define

$$\Phi(u, v, x) \equiv \int_u^v f(s, x) ds,$$

where $u = p(x)$ and $v = q(x)$. Then the Chain Rule implies that

$$\frac{d}{dx} \Phi(p(x), q(x), x) = \frac{\partial \Phi}{\partial u} p'(x) + \frac{\partial \Phi}{\partial v} q'(x) + \frac{\partial \Phi}{\partial x}.$$

Since $(u, v) \subseteq (\tilde{p}, \tilde{q})$, assumption (i) implies that $f(\cdot, x) \in L^1((u, v))$ for each $x \in X$. Then the fundamental theorem of calculus [113, Theorem 7.11] implies that

$$\frac{\partial \Phi}{\partial u} = -f(u, x) \quad \text{and} \quad \frac{\partial \Phi}{\partial v} = f(v, x)$$

for almost every $u \in (\tilde{p}, \sup_{x \in X} p(x))$ and almost every $v \in (\inf_{x \in X} q(x), \tilde{q})$.

Additionally, assumptions (i)–(iii) imply that f satisfies the hypotheses of Theorem 4.2; thus

$$\frac{\partial \Phi}{\partial x} = \int_u^v \frac{\partial f}{\partial x}(s, x) ds.$$

This completes the proof.

C.3 Some Properties of \widehat{V}

In this section we prove some useful lemmas regarding the Fourier Transform of the potential, namely $\widehat{V}(x, k)$. The main result of this section is stated in Theorem C.3.

C.3.1 The Potential $\widehat{V}_c(x, k)$

In this section we prove the following lemma.

Lemma C.1 *Let $\rho \in \mathcal{P}$, $\beta > 0$, and λ be feasible. Then for every $0 < \delta \leq \delta_\mu$ we have $(1 + |\cdot|^r)\widehat{V}_c(x, \cdot) \in L^2(\mathbb{R})$ for every $r \geq 0$ and every $x < 0$.*

Proof of Lemma C.1: Recall from (4.20) that $\widehat{V}_c(x, k) = A_k e^{|k|x}$, where A_k is given in (4.34). Since $\mu = \delta + \lambda\delta^\beta \geq 0$ for $0 < \delta \leq \delta_\mu$, we have $\lambda\delta^\beta \geq -\delta$ for $0 < \delta \leq \delta_\mu$. Then $4 + \delta(\mu - \delta) = 4 + \lambda\delta^{\beta+1} \geq 4 - \delta^2 \geq 4 - \delta_\mu^2 \geq 3$ since $\delta_\mu < 1$. Then Lemma 4.2 implies

$$\|k|\psi_k^+ + \psi_k^-\|^2 \geq \frac{\delta^2(\delta + \mu)^2}{4(1 + \delta^2)} |k|^2 e^{2|k|a} \quad (\text{C.2})$$

for all $k \in \mathbb{R}$ and for $0 < \delta \leq \delta_\mu$.

Then, for every $k \in \mathbb{R}$ and each $0 < \delta \leq \delta_\mu$, (C.2) implies that

$$|A_k|^2 = \frac{|I_k|^2}{e^{-2|k|a} \|k|\psi_k^+ + \psi_k^-\|^2} \leq \frac{4(1 + \delta^2)}{\delta^2(\delta + \mu)^2} \cdot \frac{|I_k|^2}{|k|^2 e^{-2|k|a} e^{2|k|a}} = \widetilde{C}_c(\delta) \frac{|I_k|^2}{|k|^2}, \quad (\text{C.3})$$

where

$$\widetilde{C}_c(\delta) \equiv \frac{4(1 + \delta^2)}{\delta^2(\delta + \mu)^2} = \frac{4(1 + \delta^2)}{\delta^2(2\delta + \lambda\delta^\beta)^2} > 0$$

($\tilde{C}_c(\delta)$ is not infinite for fixed $\delta > 0$ since $\mu \geq 0$ for $0 < \delta \leq \delta_\mu$). Then, thanks to Lemma 4.1, the above bound on $|A_k|^2$ becomes

$$|A_k|^2 \leq C_c(\delta) \frac{e^{-2|k|d_0}}{|k|^2}, \quad (\text{C.4})$$

where $C_c(\delta)$ is defined as

$$0 < C_c(\delta) \equiv (d_1 - d_0) \|\rho\|_{L^2(\mathcal{M})}^2 \tilde{C}_c(\delta) < \infty.$$

Note that $|A_k|^2$ is an even function of k if ρ is real due to (4.30), (4.31), (4.34), and Lemma 4.1. Thus, $|\widehat{V}_c(x, k)|^2$ is an even function of k as well (by (4.20)). Then for every $x < 0$ and for every $r \geq 0$ we have

$$\int_{-\infty}^{\infty} (1 + |k|^r)^2 |\widehat{V}_c(x, k)|^2 dk = 2 \int_0^{\infty} (1 + k^r)^2 |\widehat{V}_c(x, k)|^2 dk. \quad (\text{C.5})$$

Then, for $0 \leq k \leq 1$, $x < 0$, $r \geq 0$, and $0 < \delta \leq \delta_\mu$, we have, by (C.3) and Lemma 4.1, that

$$|\widehat{V}_c(x, k)|^2 = |A_k|^2 e^{2|k|x} \leq \tilde{C}_c(\delta) \frac{|I_k|^2}{k^2} e^{2kx} \leq \tilde{C}_c(\delta) C_I^2. \quad (\text{C.6})$$

Analogously, for $k \geq 1$, $x < 0$, $r \geq 0$, and $0 < \delta \leq \delta_\mu$, (C.4) and Lemma 4.1 imply that we have

$$|\widehat{V}_c(x, k)|^2 = |A_k|^2 e^{2|k|x} \leq C_c(\delta) \frac{e^{-2kd_0} e^{2kx}}{k^2} \leq C_c(\delta) \frac{e^{-2kd_0}}{k^2}. \quad (\text{C.7})$$

Inserting the bounds from (C.6) and (C.7) into (C.5) we find, for all $x < 0$ and $r \geq 0$, that

$$\begin{aligned} & \int_{-\infty}^{\infty} (1 + |k|^r)^2 |\widehat{V}_c(x, k)|^2 dk \\ & \leq 2\tilde{C}_c(\delta) C_I^2 \int_0^1 (1 + k^r)^2 dk + 2C_c(\delta) \int_1^{\infty} (1 + k^r)^2 \frac{e^{-2kd_0}}{k^2} dk \\ & \leq 8\tilde{C}_c(\delta) C_I^2 + 2C_c(\delta) \int_1^{\infty} (1 + k^r)^2 \frac{e^{-2kd_0}}{k^2} dk. \end{aligned} \quad (\text{C.8})$$

The integral in (C.8) converges since $d_0 > 0$. This completes the proof.

C.3.2 The Potential $\widehat{V}_s(x, k)$

The next lemma is the analogue of Lemma C.1 for $\widehat{V}_s(x, k)$.

Lemma C.2 *Let $\rho \in \mathcal{P}$, $\beta > 0$, and λ be feasible. Then for every $0 < \delta \leq \delta_\mu$ we have $(1 + |\cdot|^r)\widehat{V}_s(x, \cdot) \in L^2(\mathbb{R})$ for every $r \geq 0$ and every $0 \leq x \leq a$.*

Proof of Lemma C.2: Recall from (4.27) that

$$\widehat{V}_s(x, k) = \frac{A_k}{2\chi_c} [(\chi_c + 1)e^{|k|x} + (\chi_c - 1)e^{-|k|x}]. \quad (\text{C.9})$$

Performing computations similar to those leading up to (4.45) and (4.46), we find that

$$\left| \frac{\chi_c + 1}{\chi_c} \right|^2 = \frac{(\delta + \mu)^2}{1 + \delta^2} \quad \text{and} \quad \left| \frac{\chi_c - 1}{\chi_c} \right|^2 = \frac{4 + (\mu - \delta)^2}{1 + \delta^2}.$$

Then, for all $0 \leq x \leq a$ and $k \in \mathbb{R}$, and since $(p + q)^2 \leq 2p^2 + 2q^2$ for any $p, q \in \mathbb{R}$,

$$\begin{aligned} |\widehat{V}_s(x, k)|^2 &= \frac{|A_k|^2}{4} \left| \left(\frac{\chi_c + 1}{\chi_c} \right) e^{|k|x} + \left(\frac{\chi_c - 1}{\chi_c} \right) e^{-|k|x} \right|^2 & (\text{C.10}) \\ &\leq \frac{|A_k|^2}{4} \left(\left| \frac{\chi_c + 1}{\chi_c} \right| e^{|k|x} + \left| \frac{\chi_c - 1}{\chi_c} \right| e^{-|k|x} \right)^2 \\ &\leq \frac{|A_k|^2}{2} \left(\left| \frac{\chi_c + 1}{\chi_c} \right|^2 e^{2|k|x} + \left| \frac{\chi_c - 1}{\chi_c} \right|^2 e^{-2|k|x} \right) \\ &\leq \frac{\widetilde{C}_s(\delta)|A_k|^2}{2} (e^{2|k|x} + e^{-2|k|x}) \\ &\leq \widetilde{C}_s(\delta)|A_k|^2 e^{2|k|a}; & (\text{C.11}) \end{aligned}$$

we have defined

$$\widetilde{C}_s(\delta) \equiv \max \left\{ \left| \frac{\chi_c + 1}{\chi_c} \right|^2, \left| \frac{\chi_c - 1}{\chi_c} \right|^2 \right\} = \begin{cases} \frac{4 + (\mu - \delta)^2}{1 + \delta^2} & \text{if } \mu\delta \leq 1, \\ \frac{(\delta + \mu)^2}{1 + \delta^2} & \text{otherwise.} \end{cases}$$

Note that $\widetilde{C}_s \rightarrow 4$ as $\delta \rightarrow 0^+$.

For $0 \leq k \leq 1$, $0 \leq x \leq a$, $r \geq 0$, and $0 < \delta \leq \delta_\mu$, (C.3), (C.11), and Lemma 4.1 imply that

$$|\widehat{V}_s(x, k)|^2 \leq \widetilde{C}_s(\delta)|A_k|^2 e^{2|k|x} \leq \widetilde{C}_s(\delta)\widetilde{C}_c(\delta) \frac{|I_k|^2}{k^2} e^{2kx} \leq \widetilde{C}_s(\delta)\widetilde{C}_c(\delta)C_I^2 e^{2a}. \quad (\text{C.12})$$

Similarly, for $k \geq 1$, $0 \leq x \leq a$, $r \geq 0$, and $0 < \delta \leq \delta_\mu$, (C.4), (C.11), and Lemma 4.1 imply that

$$|\widehat{V}_s(x, k)|^2 \leq \widetilde{C}_s(\delta) |A_k|^2 e^{2|k|x} \leq \widetilde{C}_s(\delta) C_c(\delta) \frac{e^{-2kd_0} e^{2kx}}{k^2} \leq \widetilde{C}_s(\delta) C_c(\delta) \frac{e^{-2k(d_0-a)}}{k^2}. \quad (\text{C.13})$$

Since $|\widehat{V}_s(x, k)|^2$ is an even function of k (see (C.10)), (C.12) and (C.13) imply, for $0 \leq x \leq a$, $r \geq 0$, and $0 < \delta \leq \delta_\mu$, that

$$\begin{aligned} & \int_{-\infty}^{\infty} (1 + |k|^r)^2 |\widehat{V}_s(x, k)|^2 dk \\ &= 2 \int_0^{\infty} (1 + k^r)^2 |\widehat{V}_s(x, k)|^2 dk \\ &= 2 \int_0^1 (1 + k^r)^2 |\widehat{V}_s(x, k)|^2 dk + 2 \int_1^{\infty} (1 + k^r)^2 |\widehat{V}_s(x, k)|^2 dk \\ &\leq 2\widetilde{C}_s(\delta)\widetilde{C}_c(\delta)C_I^2 e^{2a} \int_0^1 (1 + k^r)^2 dk + 2\widetilde{C}_s(\delta)C_c(\delta) \int_1^{\infty} (1 + k^r)^2 \frac{e^{-2k(d_0-a)}}{k^2} dk \\ &\leq 8\widetilde{C}_s(\delta)\widetilde{C}_c(\delta)C_I^2 e^{2a} + 2\widetilde{C}_s(\delta)C_c(\delta) \int_1^{\infty} (1 + k^r)^2 \frac{e^{-2k(d_0-a)}}{k^2} dk. \end{aligned} \quad (\text{C.14})$$

The integral in (C.14) converges since $d_0 > a$. This completes the proof.

C.3.3 The Potential $\widehat{V}_m(x, k)$

The first lemma of this section is analogous to Lemmas 4.1 and 4.12. For $x \in [d_0, d_1]$ we define

$$H_k(x) \equiv e^{|k|x} \int_x^{d_1} \widehat{\rho}(s, k) e^{-|k|s} ds + e^{-|k|x} \int_{d_0}^x \widehat{\rho}(s, k) e^{|k|s} ds. \quad (\text{C.15})$$

Lemma C.3 *Suppose $\rho \in \mathcal{P}$ (where \mathcal{P} is defined in (4.3)) and that, for $d_0 \leq x \leq d_1$, $H_k(x)$ is defined as in (C.15). Then, for every $x \in [d_0, d_1]$, $H_k(x)$ satisfies the following properties:*

1. for all $k \in \mathbb{R}$, $|H_k(x)|^2 \leq 2(d_1 - d_0) \int_{d_0}^{d_1} |\widehat{\rho}(s, k)|^2 ds \leq 2(d_1 - d_0) \|\rho\|_{L^2(\mathcal{M})}^2$;
2. if ρ is real-valued, then $|H_k(x)|^2$ is an even function of k for $k \in \mathbb{R}$;
3. $H_k(x)$ is continuous at k for each $k \in \mathbb{R}$;
4. $\lim_{k \rightarrow 0} H_k(x) = H_0(x) = 0$;

5. for each $x \in [d_0, d_1]$, $\lim_{k \rightarrow 0} \frac{|H_k(x)|}{|k|} = |C_{12}(x)| < \infty$, where C_{12} is defined in (C.16) and (C.17); moreover, there is a positive constant C_H (defined in (C.19)), independent of x , such that $|H_k(x)|/|k| \leq C_H$ for all $d_0 \leq x \leq d_1$ and all $k \in [0, 1]$.

Proof of Lemma C.3: Although the proof of this lemma is essentially the same as the proof of Lemma 4.12, we compute the bound in item (1) and the constants C_{12} and C_H to highlight the differences between this lemma and Lemma 4.12. By definition we have

$$\begin{aligned}
|H_k(x)|^2 &= \left| \int_x^{d_1} \widehat{\rho}(s, k) e^{-|k|(s-x)} ds + \int_{d_0}^x \widehat{\rho}(s, k) e^{|k|(s-x)} ds \right|^2 \\
&\leq 2 \left| \int_x^{d_1} \widehat{\rho}(s, k) e^{-|k|(s-x)} ds \right|^2 + 2 \left| \int_{d_0}^x \widehat{\rho}(s, k) e^{|k|(s-x)} ds \right|^2 \\
&\leq 2 \int_x^{d_1} |\widehat{\rho}(s, k)|^2 ds \int_x^{d_1} e^{-2|k|(s-x)} ds + 2 \int_{d_0}^x |\widehat{\rho}(s, k)|^2 ds \int_{d_0}^x e^{2|k|(s-x)} ds \\
&\leq 2(d_1 - x) \int_x^{d_1} |\widehat{\rho}(s, k)|^2 ds + 2(x - d_0) \int_{d_0}^x |\widehat{\rho}(s, k)|^2 ds \\
&\leq 2(d_1 - x) \int_{d_0}^{d_1} |\widehat{\rho}(s, k)|^2 ds + 2(x - d_0) \int_{d_0}^{d_1} |\widehat{\rho}(s, k)|^2 ds \\
&= 2(d_1 - d_0) \int_{d_0}^{d_1} |\widehat{\rho}(s, k)|^2 ds \\
&= 2(d_1 - d_0) \int_{d_0}^{d_1} \int_{h_0}^{h_1} |\rho(s, y)|^2 dy ds \\
&= 2(d_1 - d_0) \|\rho\|_{L^2(\mathcal{M})}^2,
\end{aligned}$$

where the second-to-last step holds by the Plancherel Theorem. This bound holds for all $x \in [d_0, d_1]$ and all $k \in \mathbb{R}$.

Next, just as in the proof of Lemma 4.12, one can show that $H_k(x)$ is differentiable as a function of k on $(0, k_*)$, where $k_* > 0$ is arbitrary. (In particular, one can prove that the integrals $\int_x^{d_1} \widehat{\rho}(s, k) e^{-ks} ds$ and $\int_{d_0}^x \widehat{\rho}(s, k) e^{ks} ds$ are differentiable with respect to k on $(0, k_*)$ for any fixed $x \in [d_0, d_1]$; since $e^{|k|x}$ and $e^{-|k|x}$ are differentiable for all

x and all $k > 0$, $H_k(x)$ is differentiable with respect to k for $k \in (0, k_*)$.) Then, by item (4) of this lemma,

$$\begin{aligned} \lim_{k \rightarrow 0^+} \frac{H_k(x)}{k} &= \lim_{k \rightarrow 0^+} \frac{\partial H_k(x)}{\partial k} \\ &= \lim_{k \rightarrow 0^+} \left[e^{kx} \int_x^{d_1} -s\widehat{\rho}(s, k)e^{-ks} + \frac{\partial \widehat{\rho}}{\partial k}(s, k)e^{-ks} ds + xe^{kx} \int_x^{d_1} \widehat{\rho}(s, k)e^{-ks} ds \right. \\ &\quad \left. + e^{-kx} \int_{d_0}^x s\widehat{\rho}(s, k)e^{ks} + \frac{\partial \widehat{\rho}}{\partial k}(s, k)e^{ks} ds - xe^{-kx} \int_{d_0}^x \widehat{\rho}(s, k)e^{ks} ds \right] \\ &= \int_x^{d_1} -s\widehat{\rho}(s, 0) + \frac{\partial \widehat{\rho}}{\partial k}(s, 0) ds + x \int_x^{d_1} \widehat{\rho}(s, 0) ds \\ &\quad + \int_{d_0}^x s\widehat{\rho}(s, 0) + \frac{\partial \widehat{\rho}}{\partial k}(s, 0) ds - x \int_{d_0}^x \widehat{\rho}(s, 0) ds \end{aligned} \quad (\text{C.16})$$

$$\begin{aligned} &= \int_x^{d_1} \int_{h_0}^{h_1} -s\rho(s, y) - iy\rho(s, y) dy ds + x \int_x^{d_1} \int_{h_0}^{h_1} \rho(s, y) dy ds \\ &\quad + \int_{d_0}^x \int_{h_0}^{h_1} s\rho(s, y) - iy\rho(s, y) dy ds - x \int_{d_0}^x \int_{h_0}^{h_1} \rho(s, y) dy ds \end{aligned} \quad (\text{C.17})$$

$$\equiv C_{12}(x).$$

Since C_{12} depends on x , we have to be a bit careful when we derive the final bound in item (5). Note that $C_{12}(x)$ is well defined and finite for each $x \in [d_0, d_1]$ since $\rho \in L^1(\mathcal{M})$. In fact, for $x \in [d_0, d_1]$,

$$\begin{aligned} |C_{12}(x)| &\leq \int_{d_0}^{d_1} \int_{h_0}^{h_1} |s||\rho(s, y)| + |y||\rho(s, y)| dy ds + |x| \int_{d_0}^{d_1} \int_{h_0}^{h_1} |\rho(s, y)| dy ds \\ &\quad + \int_{d_0}^{d_1} \int_{h_0}^{h_1} |s||\rho(s, y)| + |y||\rho(s, y)| dy ds + |x| \int_{d_0}^{d_1} \int_{h_0}^{h_1} |\rho(s, y)| dy ds \\ &\leq (4d_1 + 2C_h)\|\rho\|_{L^1(\mathcal{M})}; \end{aligned} \quad (\text{C.18})$$

For $x \in [d_0, d_1]$ and for $k \in (0, k_*)$ we have

$$\begin{aligned} \left| \frac{\partial H_k(x)}{\partial k} \right| &\leq e^{k_*d_1} \int_{d_0}^{d_1} |s\widehat{\rho}(s, k)| ds + \int_{d_0}^{d_1} \left| \frac{\partial \widehat{\rho}}{\partial k}(s, k) \right| ds + d_1 e^{k_*d_1} \int_{d_0}^{d_1} |\widehat{\rho}(s, k)| ds \\ &\quad + \int_{d_0}^{d_1} |s\widehat{\rho}(s, k)e^{k_*d_1}| ds + \int_{d_0}^{d_1} \left| \frac{\partial \widehat{\rho}}{\partial k}(s, k) \right| e^{k_*d_1} ds \\ &\quad + d_1 \int_{d_0}^{d_1} |\widehat{\rho}(s, k)| e^{k_*d_1} ds \end{aligned}$$

$$\begin{aligned}
&\leq 4d_1 e^{k_* d_1} \int_{d_0}^{d_1} \int_{h_0}^{h_1} |\rho(s, y)| dy ds + (1 + e^{k_* d_1}) \int_{d_0}^{d_1} \int_{h_0}^{h_1} |y \rho(s, y)| dy ds \\
&\leq [4d_1 e^{k_* d_1} + C_h(1 + e^{k_* d_1})] \|\rho\|_{L^1(\mathcal{M})} \\
&\equiv \frac{C_H}{2}; \tag{C.19}
\end{aligned}$$

Note that (C.18) implies that $|C_{12}(x)| \leq C_H/2$ for all $x \in [d_0, d_1]$.

For each $x \in [d_0, d_1]$, $H_k(x)$ is continuous as a function of k on $[0, k_*]$ (as long as we define $H_k(x)/k = C_{12}(x)$ at $k = 0$) and differentiable as a function of k on $(0, k_*)$. Thus the real and imaginary parts of $H_k(x)$, namely $\Re H_k(x)$ and $\Im H_k(x)$, respectively, satisfy the same properties. In particular, $\Re H_0(x) = \Im H_0(x) = 0$ and, since $|\Re z| \leq |z|$ and $|\Im z| \leq |z|$ for any complex number z ,

$$\left| \frac{\partial[\Re H_k(x)]}{\partial k} \right| \leq \frac{C_H}{2} \quad \text{and} \quad \left| \frac{\partial[\Im H_k(x)]}{\partial k} \right| \leq \frac{C_H}{2}$$

for all $k \in (0, k_*)$ due to (C.19). Then the mean value theorem for derivatives implies that for each $k \in (0, k_*)$ there is a $0 < k_{**} < k_*$ such that

$$\left| \frac{\Re H_k(x) - \Re H_0(x)}{k - 0} \right| = \left| \frac{\Re H_k(x)}{k} \right| = \left| \frac{\partial[\Re H_k(x)]}{\partial k} \right|_{k=k_{**}} \leq \frac{C_H}{2}$$

for all $k \in (0, k_*)$. Similarly, $|\Im H_k(x)|/k \leq C_H/2$ for all $k \in (0, k_*)$. This implies that

$$\frac{|H_k(x)|}{k} \leq \frac{|\Re H_k(x)| + |\Im H_k(x)|}{k} \leq C_H$$

for all $x \in [d_0, d_1]$ and for all $k \in (0, k_*)$. Finally, (C.18) implies that $k^{-1}|H_k(x)| \leq |C_{12}(x)| \leq C_H/2$ at $k = 0$. Since $k_* > 0$ is arbitrary,

$$\frac{|H_k(x)|}{k} \leq C_H$$

for all $x \in [d_0, d_1]$ and all $k \in [0, 1]$. This completes the proof.

Finally, the next lemma is the analogue of Lemmas C.1 and C.2 for $\widehat{V}_m(x, k)$.

Lemma C.4 *Let $\rho \in \mathcal{P}$, $\beta > 0$, and λ be feasible. Then there exists $0 < \delta_m(\beta, \lambda) \leq \delta_\mu$ such that, for every $0 < \delta \leq \delta_m$, $(1 + |\cdot|^r)\widehat{V}_m(x, \cdot) \in L^2(\mathbb{R})$ for every $r \geq 0$ and every $x \in (a, d_0) \cup (d_1, \infty)$; when $x \in [d_0, d_1]$, $(1 + |\cdot|^r)\widehat{V}_m(x, \cdot) \in L^2(\mathbb{R})$ for $0 \leq r \leq 1$.*

Proof of Lemma C.4: First we choose $0 < \delta_m(\beta, \lambda) \leq \delta_\mu$ small enough so that $\delta(\mu - \delta) - 4 \leq 0$ for $0 < \delta \leq \delta_m$. Then Lemma 4.3 implies, for $0 < \delta \leq \delta_m$, that

$$\left| \psi_k^+ - \frac{1}{|k|} \psi_k^- \right|^2 \leq \tilde{C}_m(\delta)(e^{2|k|a} + e^{-2|k|a}) \leq 2\tilde{C}_m(\delta)e^{2|k|a}, \quad (\text{C.20})$$

where

$$\tilde{C}_m(\delta) = \frac{1}{4(1 + \delta^2)} \max \{ (\delta + \mu)^2(4 + \delta^2), \delta^2(4 + (\mu - \delta)^2) \}.$$

Note that $\tilde{C}_m(\delta) \rightarrow 0$ as $\delta \rightarrow 0^+$.

If necessary, we redefine δ_m so that the following inequalities hold for $0 < \delta \leq \delta_m$:

$$\begin{aligned} \left| \psi_k^+ + \frac{1}{|k|} \psi_k^- \right|^2 &= \frac{1}{4(1 + \delta^2)} \left[\delta^2(\delta + \mu)^2 e^{2|k|a} + 2\delta(\delta + \mu)(4 + \delta(\mu - \delta)) \right. \\ &\quad \left. + (4 + (\mu - \delta)^2)(4 + \delta^2)e^{-2|k|a} \right] \\ &\leq \frac{1}{4}(10e^{2|k|a} + 10 + 20e^{-2|k|a}) \\ &\leq \frac{1}{4}(20e^{2|k|a} + 20e^{-2|k|a}) \\ &= 5(e^{2|k|a} + e^{-2|k|a}) \\ &\leq 10e^{2|k|a}. \end{aligned} \quad (\text{C.21})$$

From (4.33) we have

$$\begin{aligned} \widehat{V}_m(x, k) &= e^{|k|x} \left[\frac{A_k \psi_k^+ e^{-|k|a}}{2} + \frac{A_k \psi_k^- e^{-|k|a}}{2|k|} - \frac{1}{2|k|} \int_a^x \widehat{\rho}(s, k) e^{-|k|s} ds \right] \\ &\quad + e^{-|k|x} \left[\frac{A_k \psi_k^+ e^{|k|a}}{2} - \frac{A_k \psi_k^- e^{|k|a}}{2|k|} + \frac{1}{2|k|} \int_a^x \widehat{\rho}(s, k) e^{|k|s} ds \right] \\ &= \frac{e^{|k|x}}{2} \left[A_k e^{-|k|a} \left(\psi_k^+ + \frac{\psi_k^-}{|k|} \right) - \frac{1}{|k|} \int_a^x \widehat{\rho}(s, k) e^{-|k|s} ds \right] \\ &\quad + \frac{e^{-|k|x}}{2} \left[A_k e^{|k|a} \left(\psi_k^+ - \frac{\psi_k^-}{|k|} \right) + \frac{1}{|k|} \int_a^x \widehat{\rho}(s, k) e^{|k|s} ds \right]. \end{aligned} \quad (\text{C.22})$$

We break the proof into three cases, namely $a < x < d_0$, $x > d_1$, and $d_0 \leq x \leq d_1$.

C.3.3.1 Case I: $a < x < d_0$

Since $\text{supp } \rho \subseteq [d_0, d_1] \times [h_0, h_1]$, if $a < x < d_0$, then $\int_a^x \widehat{\rho}(s, k) e^{\pm|k|s} ds = 0$. Thus for $a < x < d_0$ we have, from (C.20), (C.21), and (C.22), that

$$\begin{aligned}
|\widehat{V}_m(x, k)|^2 &= \left| \frac{e^{|k|x}}{2} \left[A_k e^{-|k|a} \left(\psi_k^+ + \frac{\psi_k^-}{|k|} \right) \right] + \frac{e^{-|k|x}}{2} \left[A_k e^{|k|a} \left(\psi_k^+ - \frac{\psi_k^-}{|k|} \right) \right] \right|^2 \\
&= \frac{|A_k|^2}{4} \left| e^{|k|(x-a)} \left(\psi_k^+ + \frac{\psi_k^-}{|k|} \right) + e^{-|k|(x-a)} \left(\psi_k^+ - \frac{\psi_k^-}{|k|} \right) \right|^2 \\
&\leq \frac{|A_k|^2}{4} \left[e^{|k|(x-a)} \left| \psi_k^+ + \frac{\psi_k^-}{|k|} \right| + e^{-|k|(x-a)} \left| \psi_k^+ - \frac{\psi_k^-}{|k|} \right| \right]^2 \\
&\leq \frac{|A_k|^2}{2} \left[e^{2|k|(x-a)} \left| \psi_k^+ + \frac{\psi_k^-}{|k|} \right|^2 + e^{-2|k|(x-a)} \left| \psi_k^+ - \frac{\psi_k^-}{|k|} \right|^2 \right] \\
&\leq \frac{|A_k|^2}{2} (10e^{2|k|(x-a)} e^{2|k|a} + 2\widetilde{C}_m(\delta) e^{-2|k|(x-a)} e^{2|k|a}) \\
&\leq |A_k|^2 e^{2|k|a} [5e^{2|k|(x-a)} + \widetilde{C}_m(\delta) e^{-2|k|(x-a)}] \\
&\leq C_m(\delta) |A_k|^2 e^{2|k|x}, \tag{C.23}
\end{aligned}$$

where $C_m(\delta) = \max\{5, \widetilde{C}_m(\delta)\}$. Since $|\widehat{V}_m(x, k)|^2$ is an even function of k (by (C.22)), we have

$$\begin{aligned}
&\int_{-\infty}^{\infty} (1 + |k|^r)^2 |\widehat{V}_m(x, k)|^2 dk \\
&\leq 2C_m(\delta) \int_0^{\infty} (1 + k^r)^2 |A_k|^2 e^{2kx} dk \\
&= 2C_m(\delta) \left[\int_0^1 (1 + k^r)^2 |A_k|^2 e^{2kx} dk + \int_1^{\infty} (1 + k^r)^2 |A_k|^2 e^{2kx} dk \right]. \tag{C.24}
\end{aligned}$$

Note that, up to multiplication by $C_m(\delta)$, (C.24) is the same as (C.5). Thus, we can apply the computations following (C.5) to find, for $a < x < d_0$, that

$$\begin{aligned}
\int_{-\infty}^{\infty} (1 + |k|^r)^2 |\widehat{V}_m(x, k)|^2 dk &\leq 8C_m(\delta) \widetilde{C}_c(\delta) C_I^2 \\
&\quad + 2C_m(\delta) C_c(\delta) \int_1^{\infty} (1 + k^r)^2 \frac{e^{2k(x-d_0)}}{k^2} dk
\end{aligned}$$

For $r \geq 0$, the above integral on the right-hand side converges if $a < x < d_0$, which gives us the desired result.

C.3.3.2 Case II: $x > d_1$

By our choice of A_k in (4.34) and (4.35) and the fact that $\text{supp } \rho \subseteq [d_0, d_1] \times [h_0, h_1]$, for $x > d_1$ (C.22) becomes

$$\begin{aligned} \widehat{V}_m(x, k) &= \frac{e^{|k|x}}{2} \left[A_k e^{-|k|a} \left(\psi_k^+ + \frac{\psi_k^-}{|k|} \right) - \frac{1}{|k|} \int_{d_0}^{d_1} \widehat{\rho}(s, k) e^{-|k|s} ds \right] \\ &\quad + \frac{e^{-|k|x}}{2} \left[A_k e^{|k|a} \left(\psi_k^+ - \frac{\psi_k^-}{|k|} \right) + \frac{1}{|k|} \int_{d_0}^{d_1} \widehat{\rho}(s, k) e^{|k|s} ds \right] \\ &= \frac{e^{-|k|x}}{2} \left[A_k e^{|k|a} \left(\psi_k^+ - \frac{\psi_k^-}{|k|} \right) \right] + \frac{J_k(x)}{2|k|}, \end{aligned} \quad (\text{C.25})$$

where $J_k(x)$ is defined in (4.96). Then, for $x > d_1$ and $0 < \delta \leq \delta_m$, (C.20) implies

$$\begin{aligned} |\widehat{V}_m(x, k)|^2 &= \left| \frac{e^{-|k|x}}{2} \left[A_k e^{|k|a} \left(\psi_k^+ - \frac{\psi_k^-}{|k|} \right) \right] + \frac{J_k(x)}{2|k|} \right|^2 \\ &\leq \left[\frac{e^{-|k|(x-a)}}{2} |A_k| \left| \psi_k^+ - \frac{\psi_k^-}{|k|} \right| + \frac{|J_k(x)|}{2|k|} \right]^2 \\ &\leq \frac{|A_k|^2 e^{-2|k|(x-a)}}{2} \left| \psi_k^+ - \frac{\psi_k^-}{|k|} \right|^2 + \frac{|J_k(x)|^2}{2|k|^2} \\ &\leq \widetilde{C}_m(\delta) \frac{|A_k|^2 e^{-2|k|(x-a)}}{2} (e^{2|k|a} + e^{-2|k|a}) + \frac{|J_k(x)|^2}{2|k|^2} \\ &\leq \widetilde{C}_m(\delta) |A_k|^2 e^{-2|k|(x-2a)} + \frac{|J_k(x)|^2}{2|k|^2}. \end{aligned} \quad (\text{C.26})$$

Then

$$\begin{aligned} &\int_{-\infty}^{\infty} (1 + |k|^r)^2 |\widehat{V}_m(x, k)|^2 dk \\ &\leq \int_{-\infty}^{\infty} (1 + |k|^r)^2 \left[\widetilde{C}_m(\delta) |A_k|^2 e^{-2|k|(x-2a)} + \frac{|J_k(x)|^2}{2|k|^2} \right] dk \\ &= 2\widetilde{C}_m(\delta) \int_0^{\infty} (1 + k^r)^2 |A_k|^2 e^{-2k(x-2a)} dk + \int_0^{\infty} (1 + k^r)^2 \frac{|J_k(x)|^2}{k^2} dk \end{aligned}$$

since for all $x > d_1$, $|J_k(x)|^2$ is an even function of k by Lemma 4.12. Next, we combine the bounds from (C.3), (C.4), Lemma 4.1, and Lemma 4.12 to find a bound on the above expression. We have

$$\begin{aligned}
& \int_{-\infty}^{\infty} (1 + |k|^r)^2 |\widehat{V}_m(x, k)|^2 dk \\
& \leq 2\widetilde{C}_m(\delta) \left[\widetilde{C}_c(\delta) \int_0^1 (1 + k^r)^2 \frac{|I_k|^2}{k^2} e^{-2k(x-2a)} dk \right. \\
& \quad \left. + C_c(\delta) \int_1^{\infty} (1 + k^r)^2 \frac{e^{-2k(x-2a+d_0)}}{k^2} dk \right] \\
& \quad + \int_0^1 (1 + k^r)^2 \frac{|J_k(x)|^2}{k^2} dk + \int_1^{\infty} (1 + k^r)^2 \frac{|J_k(x)|^2}{k^2} dk \\
& \leq 2\widetilde{C}_m(\delta) \left[4\widetilde{C}_c(\delta) C_I^2 \int_0^1 e^{-2k(x-2a)} dk + C_c(\delta) \int_1^{\infty} (1 + k^r)^2 \frac{e^{-2k(x-2a+d_0)}}{k^2} dk \right] \\
& \quad + 4C_J^2 + (d_1 - d_0) \|\rho\|_{L^2(\mathcal{M})}^2 \int_1^{\infty} (1 + k^r)^2 \frac{e^{-2k(x-d_1)}}{k^2} dk. \tag{C.27}
\end{aligned}$$

The first integral in (C.27) converges for all x . The second integral converges for $x > 2a - d_0$; however, since $d_0 > a \Leftrightarrow 2a - d_0 < a$ and $x > d_1 > d_0 > a$, we have $x > 2a - d_0$ and therefore the second integral converges. The last integral also converges for $x > d_1$. Thus

$$\int_{-\infty}^{\infty} (1 + |k|^r)^2 |\widehat{V}_m(x, k)|^2 dk < \infty$$

for all $x > d_1$ and all $r \geq 0$, which is what we wanted to show.

C.3.3.3 Case III: $d_0 \leq x \leq d_1$

From (C.22), (4.34), and (4.35) we have, for $d_0 \leq x \leq d_1$, that

$$\begin{aligned}
\widehat{V}_m(x, k) &= \frac{e^{|k|x}}{2} \left[A_k e^{-|k|a} \left(\psi_k^+ + \frac{\psi_k^-}{|k|} \right) - \frac{1}{|k|} \int_a^x \widehat{\rho}(s, k) e^{-|k|s} ds \right] \\
& \quad + \frac{e^{-|k|x}}{2} \left[A_k e^{|k|a} \left(\psi_k^+ - \frac{\psi_k^-}{|k|} \right) + \frac{1}{|k|} \int_a^x \widehat{\rho}(s, k) e^{|k|s} ds \right] \\
&= \frac{e^{|k|x}}{2} \left[\frac{1}{|k|} \int_{d_0}^{d_1} \widehat{\rho}(s, k) e^{-|k|s} ds - \frac{1}{|k|} \int_{d_0}^x \widehat{\rho}(s, k) e^{-|k|s} ds \right] \\
& \quad + \frac{e^{-|k|x}}{2} \left[A_k e^{|k|a} \left(\psi_k^+ - \frac{\psi_k^-}{|k|} \right) + \frac{1}{|k|} \int_a^x \widehat{\rho}(s, k) e^{|k|s} ds \right]
\end{aligned}$$

$$= \frac{e^{-|k|x}}{2} A_k e^{|k|a} \left(\psi_k^+ - \frac{\psi_k^-}{|k|} \right) + \frac{H_k(x)}{2|k|}, \quad (\text{C.28})$$

where $H_k(x)$ is defined in (C.15). Then for $x \in [d_0, d_1]$ and each $k \in \mathbb{R}$ we have

$$\begin{aligned} |\widehat{V}_m(x, k)|^2 &= \left| \frac{e^{-|k|x}}{2} A_k e^{|k|a} \left(\psi_k^+ - \frac{\psi_k^-}{|k|} \right) + \frac{H_k(x)}{2|k|} \right|^2 \\ &\leq \left[\frac{e^{-|k|x}}{2} |A_k| e^{|k|a} \left| \psi_k^+ - \frac{\psi_k^-}{|k|} \right| + \frac{|H_k(x)|}{2|k|} \right]^2 \\ &\leq \frac{e^{-2|k|(x-a)}}{2} |A_k|^2 \left| \psi_k^+ - \frac{\psi_k^-}{|k|} \right|^2 + \frac{|H_k(x)|^2}{2|k|^2}. \end{aligned} \quad (\text{C.29})$$

Note that this is an even function of k . Thus (C.20) and (C.29) imply, for $x \in [d_0, d_1]$ and $0 < \delta \leq \delta_\mu$, that

$$\begin{aligned} &\int_{-\infty}^{\infty} (1 + |k|^r)^2 |\widehat{V}_m(x, k)|^2 dk \\ &\leq \int_{-\infty}^{\infty} (1 + |k|^r)^2 \left[\frac{e^{-2|k|(x-a)}}{2} |A_k|^2 \left| \psi_k^+ - \frac{\psi_k^-}{|k|} \right|^2 + \frac{|H_k(x)|^2}{2|k|^2} \right] dk \\ &= \int_0^{\infty} (1 + k^r)^2 \left[e^{-2k(x-a)} |A_k|^2 \left| \psi_k^+ - \frac{\psi_k^-}{k} \right|^2 + \frac{|H_k(x)|^2}{k^2} \right] dk \\ &\leq 2\widetilde{C}_m(\delta) \left[\int_0^1 (1 + k^r)^2 e^{-2k(x-2a)} |A_k|^2 dk + \int_1^{\infty} (1 + k^r)^2 e^{-2k(x-2a)} |A_k|^2 dk \right] \\ &\quad + \int_0^1 (1 + k^r)^2 \frac{|H_k(x)|^2}{k^2} dk + \int_1^{\infty} (1 + k^r)^2 \frac{|H_k(x)|^2}{k^2} dk. \end{aligned}$$

Then (C.3), (C.4), and Lemmas 4.1 and C.3 imply that this is less than or equal to

$$\begin{aligned} &2\widetilde{C}_m(\delta) \left\{ 4\widetilde{C}_c(\delta) \int_0^1 e^{-2k(x-2a)} \frac{|I_k|^2}{k^2} dk + C_c(\delta) \int_1^{\infty} (1 + k^r)^2 \left[\frac{e^{-2k(x-2a+d_0)}}{k^2} \right] dk \right\} \\ &\quad + 4 \int_0^1 C_H^2 dk + \int_1^{\infty} (1 + k^r)^2 \frac{|H_k(x)|^2}{k^2} dk \\ &\leq 2\widetilde{C}_m(\delta) \left\{ 4\widetilde{C}_c(\delta) C_I^2 \int_0^1 e^{-2k(x-2a)} dk + C_c(\delta) \int_1^{\infty} (1 + k^r)^2 \left[\frac{e^{-2k(x-2a+d_0)}}{k^2} \right] dk \right\} \\ &\quad + 4C_H^2 + \int_1^{\infty} (1 + k^r)^2 \frac{|H_k(x)|^2}{k^2} dk. \end{aligned} \quad (\text{C.30})$$

The first integral in (C.30) converges for all $x \in [d_0, d_1]$. The second integral converges as long as $x > 2a - d_0$; however, since $d_0 > a \Leftrightarrow 2a - d_0 < a$, $x > 2a - d_0$ for all $x \in [d_0, d_1]$. We now consider the last integral in the cases $r = 0$ and $0 < r \leq 1$ separately.

First take $r = 0$. Then Lemma C.3 implies

$$\int_1^\infty (1 + k^0)^2 \frac{|H_k(x)|^2}{k^2} dk \leq (d_1 - d_0) \|\rho\|_{L^2(\mathcal{M})}^2 \int_1^\infty \frac{1}{k^2} dk = (d_1 - d_0) \|\rho\|_{L^2(\mathcal{M})}^2 < \infty. \quad (\text{C.31})$$

Next, we take $0 < r \leq 1$; then (C.31), Lemma C.3, the Plancherel Theorem, and the fact that $(1 + k^r)^2 \leq 2 + 2k^{2r}$ imply

$$\begin{aligned} \int_1^\infty (1 + k^r)^2 \frac{|H_k(x)|^2}{k^2} dk &\leq 2 \int_1^\infty \frac{|H_k(x)|^2}{k^2} dk + 2 \int_1^\infty k^{2r-2} |H_k(x)|^2 dk \\ &\leq 2 \int_1^\infty \frac{|H_k(x)|^2}{k^2} dk + 2 \int_1^\infty |H_k(x)|^2 dk \\ &\leq 2(d_1 - d_0) \|\rho\|_{L^2(\mathcal{M})}^2 + 2 \int_0^\infty |H_k(x)|^2 dk \\ &= 2(d_1 - d_0) \|\rho\|_{L^2(\mathcal{M})}^2 + \int_{-\infty}^\infty |H_k(x)|^2 dk \\ &\leq 2(d_1 - d_0) \|\rho\|_{L^2(\mathcal{M})}^2 + 2(d_1 - d_0) \int_{-\infty}^\infty \int_{d_0}^{d_1} |\widehat{\rho}(s, k)|^2 ds dk \\ &= 2(d_1 - d_0) \|\rho\|_{L^2(\mathcal{M})}^2 + 2(d_1 - d_0) \int_{d_0}^{d_1} \int_{-\infty}^\infty |\widehat{\rho}(s, k)|^2 dk ds \\ &= 2(d_1 - d_0) \|\rho\|_{L^2(\mathcal{M})}^2 + 2(d_1 - d_0) \int_{d_0}^{d_1} \int_{-\infty}^\infty |\rho(s, y)|^2 dy ds \\ &= 4(d_1 - d_0) \|\rho\|_{L^2(\mathcal{M})}^2. \end{aligned}$$

This completes the proof.

C.3.4 Summary

We begin by introducing some notation; the following definition can be found in the book by Evans [32, Appendix A].

Definition C.1 (a) A vector of the form $\alpha = (\alpha_1, \dots, \alpha_n)$, where each component α_i is a nonnegative integer, is called a multiindex of order $|\alpha| = \alpha_1 + \dots + \alpha_n$.

(b) Given a multiindex α , define

$$D^\alpha u(\mathbf{x}) \equiv \frac{\partial^{|\alpha|} u(\mathbf{x})}{\partial x_1^{\alpha_1} \cdots \partial x_n^{\alpha_n}} = \partial_{x_1}^{\alpha_1} \cdots \partial_{x_n}^{\alpha_n} u.$$

The following two definitions can also be found in the book by Evans [32, Chapter 5].

Definition C.2 Let $U \subset \mathbb{R}^n$ be open (where $n \geq 1$ is an integer); suppose $u, v \in L^1_{\text{loc}}(U)$ and α is a multiindex. We say that v is the α^{th} -weak derivative of u , written $D^\alpha u = v$, provided

$$\int_U u D^\alpha \phi \, d\mathbf{x} = (-1)^{|\alpha|} \int_U v \phi \, d\mathbf{x}$$

for all test functions $\phi \in C_c^\infty(U)$ (which is the set of all infinitely differentiable functions with compact support in U).

Definition C.3 Let r be a nonnegative integer. The Sobolev Space $H^r(U)$ consists of functions $u : U \rightarrow \mathbb{C}$ with $u \in L^1_{\text{loc}}(U)$ such that for each multiindex α with $|\alpha| \leq r$, $D^\alpha u$ exists in the weak sense and belongs to $L^2(U)$.

The statement and proof of the following theorem can be found in the book by Evans [32, Chapter 5].

Theorem C.2 Let r be a nonnegative integer. A function $u \in L^2(\mathbb{R})$ belongs to $H^r(\mathbb{R})$ if and only if

$$(1 + |k|^r) \widehat{u} \in L^2(\mathbb{R}).$$

Theorem C.3 Let $\rho \in \mathcal{P}$, $\beta > 0$, and λ be feasible. Then there exists $0 < \delta_m(\beta, \lambda) \leq \delta_\mu$ such that, for every $0 < \delta \leq \delta_m$ and almost every $x \in \mathbb{R}$, $V(x, \cdot) \in H^1(\mathbb{R})$.

Proof of Theorem C.3: First, note that Lemmas C.1, C.2, and C.4 and the Plancherel Theorem imply, for almost every $x \in \mathbb{R}$, that

$$\int_{-\infty}^{\infty} |V(x, y)|^2 \, dy = \int_{-\infty}^{\infty} |\widehat{V}(x, k)|^2 \, dk < \infty, \quad (\text{C.32})$$

so $V(x, \cdot) \in L^2(\mathbb{R})$ for almost every $x \in \mathbb{R}$. Furthermore, according to Theorem C.2, Lemmas C.1, C.2, and C.4 imply that $V(x, \cdot) \in H^1(\mathbb{R})$ for almost every $x \in \mathbb{R}$. This completes the proof.

Remark C.1 Lemmas C.1, C.2, and C.4 imply that $\widehat{V}(x, \cdot) \in H^r(\mathbb{R})$ for every nonnegative integer r and for all $x \in (-\infty, d_0) \cup (d_1, \infty)$. In particular, (C.32) holds for all $x \in (-\infty, d_0) \cup (d_1, \infty)$ since V is harmonic and therefore smooth there.

C.4 Some Properties of $\frac{\partial V}{\partial x}$

In this section we prove that $\partial V(x, \cdot)/\partial x \in L^2(\mathbb{R})$ for almost every $x \in \mathbb{R}$.

C.4.1 The Field $\frac{\partial V_c}{\partial x}$

We begin in the region $x < 0$.

Lemma C.5 Let $\rho \in \mathcal{P}$, $\beta > 0$, and λ be feasible. Then for every $0 < \delta \leq \delta_\mu$ and every $x < 0$ we have

$$\frac{\partial V_c}{\partial x}(x, \cdot) \in L^2(\mathbb{R}).$$

Proof of Lemma C.5: Fix $x < 0$. By (4.20) we have

$$\frac{\partial \widehat{V}}{\partial x}(x, k) = \frac{\partial \widehat{V}_c}{\partial x}(x, k) = |k|A_k e^{k|x} = |k|\widehat{V}_c(x, k).$$

Then, for every $x < 0$,

$$\int_{-\infty}^{\infty} \left| \frac{\partial \widehat{V}}{\partial x}(x, k) \right|^2 dk = \int_{-\infty}^{\infty} |k|^2 |\widehat{V}_c(x, k)|^2 dk \leq \int_{-\infty}^{\infty} (1 + |k|)^2 |\widehat{V}_c(x, k)|^2 dk < \infty$$

by Lemma C.1. Then the Plancherel Theorem implies, for every $x < 0$, that

$$\int_{-\infty}^{\infty} \left| \frac{\partial V}{\partial x}(x, y) \right|^2 dy = \int_{-\infty}^{\infty} \left| \frac{\partial \widehat{V}}{\partial x}(x, k) \right|^2 dk < \infty.$$

This completes the proof.

C.4.2 The Field $\frac{\partial V_s}{\partial x}$

We now consider the region $0 \leq x \leq a$.

Lemma C.6 Let $\rho \in \mathcal{P}$, $\beta > 0$, and λ be feasible. Then for every $0 < \delta \leq \delta_\mu$ and every $0 < x < a$ we have

$$\frac{\partial V}{\partial x}(x, \cdot) \in L^2(\mathbb{R}).$$

Proof of Lemma C.6: Thanks to (4.27), for every $0 < x < a$ we have

$$\frac{\partial \widehat{V}}{\partial x}(x, k) = \frac{\partial \widehat{V}_s}{\partial x}(x, k) = \frac{|k|A_k}{2\chi_c} [(\chi_c + 1)e^{|k|x} - (\chi_c - 1)e^{-|k|x}].$$

Then for every $0 \leq x \leq a$

$$\begin{aligned} \left| \frac{\partial \widehat{V}}{\partial x}(x, k) \right|^2 &= \frac{|k|^2 |A_k|^2}{4} \left| \left(\frac{\chi_c + 1}{\chi_c} \right) e^{|k|x} - \left(\frac{\chi_c - 1}{\chi_c} \right) e^{-|k|x} \right|^2 \\ &\leq \frac{(1 + |k|)^2 |A_k|^2}{4} \left(\left| \frac{\chi_c + 1}{\chi_c} \right| e^{|k|x} + \left| \frac{\chi_c - 1}{\chi_c} \right| e^{-|k|x} \right)^2 \\ &\leq \frac{(1 + |k|)^2 |A_k|^2}{2} \left(\left| \frac{\chi_c + 1}{\chi_c} \right|^2 e^{2|k|x} + \left| \frac{\chi_c - 1}{\chi_c} \right|^2 e^{-2|k|x} \right) \\ &\leq \frac{\widetilde{C}_s(\delta)(1 + |k|)^2 |A_k|^2}{2} (e^{2|k|x} + e^{-2|k|x}) \\ &\leq \widetilde{C}_s(\delta)(1 + |k|)^2 |A_k|^2 e^{2|k|a}. \end{aligned}$$

In Lemma C.2 we proved that this expression is integrable as a function of k for every $0 < x < a$ (see (C.11)). Then, for every $0 < x < a$, the Plancherel Theorem implies

$$\int_{-\infty}^{\infty} \left| \frac{\partial V}{\partial x}(x, y) \right|^2 dy = \int_{-\infty}^{\infty} \left| \frac{\partial \widehat{V}_s}{\partial x}(x, k) \right|^2 dk < \infty.$$

This completes the proof.

C.4.3 The Field $\frac{\partial V_m}{\partial x}$

Lemma C.7 *Let $\rho \in \mathcal{P}$, $\beta > 0$, and λ be feasible. Then there exists $0 < \delta_m(\beta, \lambda) \leq \delta_\mu$ such that, for every $0 < \delta \leq \delta_m$,*

$$\frac{\partial V}{\partial x}(x, \cdot) \in L^2(\mathbb{R})$$

for almost every $x > a$.

Proof of Lemma C.7: We break the proof up into three cases. In all three cases we assume that $0 < \delta \leq \delta_m$.

C.4.3.1 Case I: $a < x < d_0$

If $a < x < d_0$, then (C.22) implies

$$\widehat{V}(x, k) = \widehat{V}_m(x, k) = \frac{e^{|k|x}}{2} \left[A_k e^{-|k|a} \left(\psi_k^+ + \frac{\psi_k^-}{|k|} \right) \right] + \frac{e^{-|k|x}}{2} \left[A_k e^{|k|a} \left(\psi_k^+ - \frac{\psi_k^-}{|k|} \right) \right].$$

Then, for each $x \in (a, d_0)$,

$$\frac{\partial \widehat{V}_m}{\partial x}(x, k) = \frac{|k|A_k}{2} \left[e^{|k|x} e^{-|k|a} \left(\psi_k^+ + \frac{\psi_k^-}{|k|} \right) - e^{-|k|x} e^{|k|a} \left(\psi_k^+ - \frac{\psi_k^-}{|k|} \right) \right].$$

Using the fact that $|k|^2 \leq (1 + |k|)^2$ for all $k \in \mathbb{R}$ and following the arguments leading to (C.23) we see that

$$\begin{aligned} \left| \frac{\partial \widehat{V}_m}{\partial x}(x, k) \right|^2 &= \frac{|k|^2 |A_k|^2}{4} \left| e^{|k|x} e^{-|k|a} \left(\psi_k^+ + \frac{\psi_k^-}{|k|} \right) - e^{-|k|x} e^{|k|a} \left(\psi_k^+ - \frac{\psi_k^-}{|k|} \right) \right|^2 \\ &\leq \frac{(1 + |k|)^2 |A_k|^2}{4} \left[e^{|k|(x-a)} \left| \psi_k^+ + \frac{\psi_k^-}{|k|} \right| + e^{-|k|(x-a)} \left| \psi_k^+ - \frac{\psi_k^-}{|k|} \right| \right]^2 \\ &\leq (1 + |k|)^2 C_m(\delta) |A_k|^2 e^{2|k|x}; \end{aligned}$$

this last expression was shown to be integrable (as a function of k) for all $a < x < d_0$ in Case I of Lemma C.4. Then the Plancherel Theorem implies that

$$\int_{-\infty}^{\infty} \left| \frac{\partial V}{\partial x}(x, y) \right|^2 dy = \int_{-\infty}^{\infty} \left| \frac{\partial \widehat{V}_m}{\partial x}(x, k) \right|^2 dk < \infty$$

for $a < x < d_0$.

C.4.3.2 Case II: $x > d_1$

For $x > d_1$, (4.96) and (C.25) imply that

$$\widehat{V}(x, k) = \widehat{V}_m(x, k) = \frac{e^{-|k|x}}{2} \left[A_k e^{|k|a} \left(\psi_k^+ - \frac{\psi_k^-}{|k|} \right) + \frac{1}{|k|} \int_{d_0}^{d_1} \widehat{\rho}(s, k) e^{|k|s} ds \right].$$

Thus

$$\frac{\partial \widehat{V}_m}{\partial x}(x, k) = -|k| \frac{e^{-|k|x}}{2} \left[A_k e^{|k|a} \left(\psi_k^+ - \frac{\psi_k^-}{|k|} \right) + \frac{1}{|k|} \int_{d_0}^{d_1} \widehat{\rho}(s, k) e^{|k|s} ds \right] = -|k| \widehat{V}_m(x, k), \quad (\text{C.33})$$

so

$$\left| \frac{\partial \widehat{V}_m}{\partial x}(x, k) \right|^2 = |k|^2 |\widehat{V}_m(x, k)|^2 \leq (1 + |k|)^2 |\widehat{V}_m(x, k)|^2.$$

This last expression was shown to be integrable (as a function of k) for all $x > d_1$ in Case II of Lemma C.4. Thus the Plancherel Theorem implies, for every $x > d_1$, that

$$\int_{-\infty}^{\infty} \left| \frac{\partial V}{\partial x}(x, y) \right|^2 dy = \int_{-\infty}^{\infty} \left| \frac{\partial \widehat{V}_m}{\partial x}(x, k) \right|^2 dk < \infty.$$

C.4.3.3 Case III: $d_0 \leq x \leq d_1$

For $x \in [d_0, d_1]$, (C.15) and (C.28) imply that

$$\begin{aligned} \widehat{V}(x, k) &= \widehat{V}_m(x, k) \\ &= \frac{e^{-|k|x}}{2} A_k e^{|k|a} \left(\psi_k^+ - \frac{\psi_k^-}{|k|} \right) + \frac{H_k(x)}{2|k|} \\ &= \frac{e^{-|k|x}}{2} A_k e^{|k|a} \left(\psi_k^+ - \frac{\psi_k^-}{|k|} \right) \\ &\quad + \frac{1}{2|k|} \left[e^{|k|x} \int_x^{d_1} \widehat{\rho}(s, k) e^{-|k|s} ds + e^{-|k|x} \int_{d_0}^x \widehat{\rho}(s, k) e^{|k|s} ds \right]. \end{aligned}$$

Then the Leibniz Rule (discussed in Section C.2) implies, for almost every $x \in (d_0, d_1)$, that

$$\begin{aligned} \frac{\partial \widehat{V}_m}{\partial x}(x, k) &= -|k| \frac{e^{-|k|x}}{2} A_k e^{|k|a} \left(\psi_k^+ - \frac{\psi_k^-}{|k|} \right) \\ &\quad + \frac{1}{2|k|} \left[|k| e^{|k|x} \int_x^{d_1} \widehat{\rho}(s, k) e^{-|k|s} ds - e^{|k|x} \widehat{\rho}(x, k) e^{-|k|x} \right. \\ &\quad \left. - |k| e^{-|k|x} \int_{d_0}^x \widehat{\rho}(s, k) e^{|k|s} ds + e^{-|k|x} \widehat{\rho}(x, k) e^{|k|x} \right] \\ &= -|k| \frac{e^{-|k|x}}{2} A_k e^{|k|a} \left(\psi_k^+ - \frac{\psi_k^-}{|k|} \right) \\ &\quad + \frac{e^{|k|x}}{2} \int_x^{d_1} \widehat{\rho}(s, k) e^{-|k|s} ds - \frac{e^{-|k|x}}{2} \int_{d_0}^x \widehat{\rho}(s, k) e^{|k|s} ds. \end{aligned}$$

Then, for almost every $x \in (d_0, d_1)$,

$$\begin{aligned} \left| \frac{\partial \widehat{V}_m}{\partial x}(x, k) \right|^2 &= \left| -|k| \frac{e^{-|k|x}}{2} A_k e^{|k|a} \left(\psi_k^+ - \frac{\psi_k^-}{|k|} \right) \right. \\ &\quad \left. + \frac{e^{|k|x}}{2} \int_x^{d_1} \widehat{\rho}(s, k) e^{-|k|s} ds - \frac{e^{-|k|x}}{2} \int_{d_0}^x \widehat{\rho}(s, k) e^{|k|s} ds \right|^2 \end{aligned}$$

$$\begin{aligned} &\leq \frac{(1 + |k|)^2 e^{-2|k|(x-a)}}{2} |A_k|^2 \left| \psi_k^+ - \frac{\psi_k^-}{|k|} \right|^2 \\ &\quad + \frac{1}{2} \left| e^{|k|x} \int_x^{d_1} \widehat{\rho}(s, k) e^{-|k|s} ds - e^{-|k|x} \int_{d_0}^x \widehat{\rho}(s, k) e^{|k|s} ds \right|^2. \end{aligned} \quad (\text{C.34})$$

The first term in (C.34) was shown to be integrable (as a function of k) for every $x \in [d_0, d_1]$ in Case III of Lemma C.4. We now show that the second term is integrable.

For all $k \in \mathbb{R}$ we have

$$\begin{aligned} &\frac{1}{2} \left| e^{|k|x} \int_x^{d_1} \widehat{\rho}(s, k) e^{-|k|s} ds - e^{-|k|x} \int_{d_0}^x \widehat{\rho}(s, k) e^{|k|s} ds \right|^2 \\ &\leq \frac{1}{2} \left[\left| \int_x^{d_1} \widehat{\rho}(s, k) e^{-|k|(s-x)} ds \right|^2 + \left| \int_{d_0}^x \widehat{\rho}(s, k) e^{|k|(s-x)} ds \right|^2 \right] \\ &\leq \left| \int_x^{d_1} \widehat{\rho}(s, k) e^{-|k|(s-x)} ds \right|^2 + \left| \int_{d_0}^x \widehat{\rho}(s, k) e^{|k|(s-x)} ds \right|^2 \\ &\leq \int_x^{d_1} |\widehat{\rho}(s, k)|^2 ds + \int_{d_0}^x |\widehat{\rho}(s, k)|^2 ds \\ &= \int_{d_0}^{d_1} |\widehat{\rho}(x, k)|^2 ds. \end{aligned}$$

Then the Plancherel Theorem implies that

$$\int_{-\infty}^{\infty} \int_{d_0}^{d_1} |\widehat{\rho}(x, k)|^2 ds dk = \int_{d_0}^{d_1} \int_{-\infty}^{\infty} |\widehat{\rho}(x, k)|^2 dk ds = \int_{d_0}^{d_1} \int_{-\infty}^{\infty} |\rho(x, y)|^2 dy ds < \infty.$$

Therefore the second term in (C.34) is integrable for almost every $x \in (d_0, d_1)$.

Finally, the Plancherel Theorem and (C.34) imply, for almost every $x \in (d_0, d_1)$, that

$$\int_{-\infty}^{\infty} \left| \frac{\partial V}{\partial x}(x, y) \right|^2 dy = \int_{-\infty}^{\infty} \left| \frac{\partial \widehat{V}_m}{\partial x}(x, k) \right|^2 dk < \infty.$$

This completes the proof.

C.4.4 Summary

The results from Lemmas C.5–C.7 lead immediately to the following theorem.

Theorem C.4 *Let $\rho \in \mathcal{P}$, $\beta > 0$, and λ be feasible. Then for every $0 < \delta \leq \delta_m$ (where δ_m is defined in Lemma C.4) and for almost every $x \in \mathbb{R}$,*

$$\frac{\partial V}{\partial x}(x, \cdot) \in L^2(\mathbb{R}).$$

Remark C.2 *Since the operator $\partial/\partial x$ essentially turns into multiplication by $|k|$ in Fourier Space, Lemmas C.5–C.6 and Lemma C.7 (Cases I and II) can be extended to show that*

$$\frac{\partial^n V}{\partial x^n}(x, \cdot) \in L^2(\mathbb{R})$$

for every positive integer n and for every $x \in (-\infty, 0) \cup (0, a) \cup (a, d_0) \cup (d_1, \infty)$.

C.5 Continuity Conditions

In this section we prove that the potential V satisfies the continuity conditions at $x = 0$ and $x = a$ and the limit condition as $|x| \rightarrow \infty$ from (4.12). The next theorem can be found in the book by Rudin [113, Theorem 9.14].

Theorem C.5 *If $f \in L^2(\mathbb{R})$ and $\hat{f} \in L^1(\mathbb{R})$, then*

$$f(y) = \frac{1}{2\pi} \int_{-\infty}^{\infty} \hat{f}(k) e^{iky} dk$$

for almost every $y \in \mathbb{R}$.

In the following theorem we prove that V satisfies the continuity conditions across the boundaries of the slab. It is a consequence of the fact that $\widehat{V}(x, \cdot) \in L^2(\mathbb{R}) \cap L^1(\mathbb{R})$ for x near the slab boundaries, Theorem C.5, the dominated convergence theorem, the fact that $\widehat{V}(x, k)$ is continuous as a function of x near the edges of the slab, and the fact that \widehat{V} satisfies similar continuity conditions for all $k \in \mathbb{R}$.

Theorem C.6 *Let $\rho \in \mathcal{P}$, $\beta > 0$, and λ be feasible. Then for every $0 < \delta \leq \delta_m$ (where δ_m is defined in Lemma C.4) and almost every $y \in \mathbb{R}$ the following hold:*

1. $\lim_{x \rightarrow 0^-} V(x, y) = \lim_{x \rightarrow 0^+} V(x, y);$
2. $\lim_{x \rightarrow 0^-} \varepsilon_c[\partial V(x, y)/\partial x] = \lim_{x \rightarrow 0^+} \varepsilon_s[\partial V(x, y)/\partial x];$
3. $\lim_{x \rightarrow a^-} V(x, y) = \lim_{x \rightarrow a^+} V(x, y);$
4. $\lim_{x \rightarrow a^-} \varepsilon_s[\partial V(x, y)/\partial x] = \lim_{x \rightarrow a^+} \varepsilon_m[\partial V(x, y)/\partial x];$
5. $\lim_{x \rightarrow -\infty} [\partial V(x, y)/\partial x] = 0;$
6. $\lim_{x \rightarrow \infty} [\partial V(x, y)/\partial x] = 0.$

Proof of Theorem C.6: We prove items (1) and (6) of this lemma; the proofs of the remaining items are similar.

- (1) First, for every $x < 0$, $V(x, \cdot) \in L^2(\mathbb{R})$ by Lemma C.1 (since $\widehat{V}(x, \cdot) \in L^2(\mathbb{R})$ for all $x < 0$ and by the Plancherel Theorem). Next, note that $\widehat{V}_c(x, k)$ is continuous as a function of x for $x < 0$ and for each $k \in \mathbb{R}$ by (4.20).

From (C.6) and (C.7) we have, for all $x < 0$ and $0 < \delta \leq \delta_\mu$, that

$$|\widehat{V}_c(x, k)| \leq \begin{cases} [\widetilde{C}_c(\delta)]^{1/2} C_I & \text{for } 0 \leq k \leq 1, \\ [C_c(\delta)]^{1/2} \left(\frac{e^{-kd_0}}{k} \right) & \text{for } k \geq 1. \end{cases}$$

Since $|\widehat{V}_c(x, k)|$ is even as a function of k for each $x < 0$, similar bounds hold for $k \leq 0$; in particular we have

$$|\widehat{V}_c(x, k)| \leq \widetilde{V}_c(k) \equiv \begin{cases} [\widetilde{C}_c(\delta)]^{1/2} C_I & \text{for } |k| \leq 1, \\ [C_c(\delta)]^{1/2} \left(\frac{e^{-|k|d_0}}{|k|} \right) & \text{for } |k| \geq 1. \end{cases}$$

Because $\widetilde{V}_c(k) \in L^1(\mathbb{R})$, $\widehat{V}(x, \cdot) \in L^1(\mathbb{R})$ for all $x < 0$. Then Theorem C.5 implies, for every $x < 0$ and almost every $y \in \mathbb{R}$, that

$$V(x, y) = V_c(x, y) = \frac{1}{2\pi} \int_{-\infty}^{\infty} \widehat{V}_c(x, k) e^{iky} dk.$$

Furthermore, because $\widetilde{V}_c(k)$ is in $L^1(\mathbb{R})$, the dominated convergence theorem (see Theorem 1.34 and Remark 9.3(a) in the book by Rudin [113]) implies, for almost every $y \in \mathbb{R}$, that

$$\begin{aligned} \lim_{x \rightarrow 0^-} V(x, y) &= \frac{1}{2\pi} \lim_{x \rightarrow 0^-} \int_{-\infty}^{\infty} \widehat{V}_c(x, k) e^{iky} dk \\ &= \frac{1}{2\pi} \int_{-\infty}^{\infty} \lim_{x \rightarrow 0^-} \widehat{V}_c(x, k) e^{iky} dk \\ &= \frac{1}{2\pi} \int_{-\infty}^{\infty} \widehat{V}_c(0, k) e^{iky} dk \\ &= \frac{1}{2\pi} \int_{-\infty}^{\infty} \widehat{V}_s(0, k) e^{iky} dk \end{aligned} \tag{C.35}$$

by (4.22).

Similarly (see (C.12) and (C.13)), for every $0 \leq x \leq a$ and $0 < \delta \leq \delta_\mu$,

$$|\widehat{V}_s(x, k)| \leq \widetilde{V}_s(k) \equiv \begin{cases} [\widetilde{C}_s(\delta)\widetilde{C}_c(\delta)]^{1/2}C_I e^a & \text{for } |k| \leq 1, \\ [\widetilde{C}_s(\delta)C_c(\delta)]^{1/2} \left(\frac{e^{-|k|(d_0-a)}}{|k|} \right) & \text{for } |k| \geq 1. \end{cases}$$

Then, since $\widetilde{V}_s(k) \in L^1(\mathbb{R})$, for almost every $y \in \mathbb{R}$

$$\begin{aligned} \lim_{x \rightarrow 0^+} V(x, y) &= \frac{1}{2\pi} \lim_{x \rightarrow 0^+} \int_{-\infty}^{\infty} \widehat{V}_s(x, k) e^{iky} dk \\ &= \frac{1}{2\pi} \int_{-\infty}^{\infty} \lim_{x \rightarrow 0^+} \widehat{V}_s(x, k) e^{iky} dk \\ &= \frac{1}{2\pi} \int_{-\infty}^{\infty} \widehat{V}_s(0, k) e^{iky} dk. \end{aligned} \tag{C.36}$$

Then (C.35) and (C.36) imply

$$\lim_{x \rightarrow 0^-} V(x, y) = \lim_{x \rightarrow 0^+} V(x, y)$$

for almost every $y \in \mathbb{R}$.

- (6) Let $x_* > \max\{2a, d_1\}$. Following the proof of Lemma C.4, Case II, we find, for all $x \geq x_*$ and $0 < \delta \leq \delta_\mu$ (see (C.26), (C.27), and (C.33)), that

$$\left| \frac{\partial V_m}{\partial x}(x, k) \right| \leq \widetilde{V}_m(k) \equiv \begin{cases} [\widetilde{C}_m(\delta)\widetilde{C}_c(\delta)]^{1/2}C_I + \frac{C_J}{2} & \text{if } |k| \leq 1, \\ [\widetilde{C}_m(\delta)C_c(\delta)]^{1/2} e^{-|k|(x_*-2a+d_0)} \\ \quad + (d_1 - d_0)^{1/2} \|\rho\|_{L^2(\mathcal{M})} e^{-|k|(x_*-d_1)} & \text{if } |k| \geq 1. \end{cases}$$

Since $x_* > d_0 - 2a$ and $x_* > d_1$, $V_m(k) \in L^1(\mathbb{R})$. Then Theorem C.5, the dominated convergence theorem, and (4.28) imply, for almost every $y \in \mathbb{R}$, that

$$\lim_{x \rightarrow \infty} V(x, y) = \frac{1}{2\pi} \lim_{x \rightarrow \infty} \int_{-\infty}^{\infty} \widehat{V}_m(x, k) e^{iky} dk = \frac{1}{2\pi} \int_{-\infty}^{\infty} \lim_{x \rightarrow \infty} \widehat{V}_m(x, k) e^{iky} dk = 0.$$

This completes the proof.

C.6 Some Properties of V

In this section we prove several lemmas that establish useful properties of the complex potential V . In particular, we prove that $V \in L^2_{\text{loc}}(\mathbb{R}^2) \cap H^1(\mathring{\mathcal{S}})$. The main results are summarized in Theorem C.7.

C.6.1 The Potential V_c

In this section we prove the following lemma.

Lemma C.8 *Let $\rho \in \mathcal{P}$, $\beta > 0$, and λ be feasible. Then for every $0 < \delta \leq \delta_\mu$ we have $V \in L^2_{\text{loc}}(\mathcal{C})$.*

Proof of Lemma C.8: Let $(x, y) \in \mathcal{C} = \{(x, y) \in \mathbb{R}^2 : x < 0\}$, $\eta > 0$ be arbitrary, and define

$$\mathcal{C}_\eta \equiv \{(x, y) \in \mathbb{R}^2 : -\eta < x < 0\}.$$

Then, by (4.48),

$$\int_{\mathcal{C}_\eta} |V|^2 d\mathbf{x} = \int_{-\eta}^0 \int_{-\infty}^{\infty} |V_c(x, y)|^2 dy dx = \int_{-\eta}^0 \int_{-\infty}^{\infty} |\widehat{V}_c(x, k)|^2 dk dx. \quad (\text{C.37})$$

(The Plancherel Theorem holds in this case since $V_c(x, \cdot) \in L^2(\mathbb{R})$ for each $x < 0$ by Lemma C.1.)

Lemma C.1 implies, for $x < 0$ and $0 < \delta \leq \delta_\mu$, that

$$\int_{-\infty}^{\infty} |\widehat{V}_c(x, k)|^2 dk \leq C,$$

where C is a positive constant independent of x — see (C.8). Inserting this into (C.37) gives

$$\int_{\mathcal{C}_\eta} |V|^2 d\mathbf{x} \leq C \int_{-\eta}^0 dx = C\eta < \infty.$$

This completes the proof.

Remark C.3 *Even if we used a tighter bound on $|\widehat{V}_c(x, k)|^2$ in the proof of Lemma C.8 (e.g., the second to last expressions in (C.6) and (C.7)), switched the order of integration in (C.37), and computed the integral with respect to x exactly, we would still only obtain $V_c \in L^2_{\text{loc}}(\mathcal{C})$.*

C.6.2 The Potential V_s

In this section we prove the following lemma.

Lemma C.9 *Let $\rho \in \mathcal{P}$, $\beta > 0$, and λ be feasible. Then for every $0 < \delta \leq \delta_\mu$ we have $V \in H^1(\mathring{\mathcal{S}})$.*

Proof of Lemma C.9: Let $(x, y) \in \mathring{\mathcal{S}} = \{(x, y) \in \mathbb{R}^2 : 0 \leq x \leq a\}$. Then by (4.48) (which holds since $V_s(x, \cdot) \in L^2(\mathbb{R})$ for all $x \in [0, a]$ by Lemma C.2) we have

$$\int_{\mathcal{S}} |V|^2 d\mathbf{x} = \int_0^a \int_{-\infty}^{\infty} |V_s(x, y)|^2 dy dx = \int_0^a \int_{-\infty}^{\infty} |\widehat{V}_s(x, k)|^2 dk dx. \quad (\text{C.38})$$

In Lemma C.2, we showed that there is a constant $C > 0$, independent of x , such that

$$\int_{-\infty}^{\infty} |\widehat{V}_s(x, k)|^2 dk \leq C$$

for all $0 \leq x \leq a$ and $0 < \delta \leq \delta_\mu$ (see (C.14)). Then (C.38) implies that $V \in L^2(\mathcal{S})$ since

$$\int_{\mathcal{S}} |V|^2 d\mathbf{x} \leq C \int_0^a dx = Ca < \infty.$$

Similarly, by the Plancherel Theorem, we have

$$\begin{aligned} \int_{\mathring{\mathcal{S}}} |\nabla V|^2 d\mathbf{x} &= \int_0^a \int_{-\infty}^{\infty} \left| \frac{\partial V_s}{\partial x}(x, y) \right|^2 + \left| \frac{\partial V_s}{\partial y}(x, y) \right|^2 dy dx \\ &= \int_0^a \int_{-\infty}^{\infty} \left| \frac{\partial \widehat{V}_s}{\partial x}(x, k) \right|^2 + \left| \frac{\partial \widehat{V}_s}{\partial y}(x, k) \right|^2 dk dx \\ &= \int_0^a \int_{-\infty}^{\infty} \left| \frac{\partial \widehat{V}_s}{\partial x}(x, k) \right|^2 + |k|^2 |\widehat{V}_s(x, k)|^2 dk dx. \end{aligned} \quad (\text{C.39})$$

In Lemmas C.6 and C.2 we showed that there exist positive constants C and C' , independent of x such that

$$\int_{-\infty}^{\infty} \left| \frac{\partial \widehat{V}_s}{\partial x}(x, k) \right|^2 dk \leq C \quad \text{and} \quad \int_{-\infty}^{\infty} |k|^2 |\widehat{V}_s(x, k)|^2 dk \leq C',$$

respectively, for $0 < x < a$ and $0 < \delta \leq \delta_\mu$. Inserting these bounds into (C.39) gives

$$\int_{\mathring{\mathcal{S}}} |\nabla V|^2 d\mathbf{x} \leq (C + C') \int_0^a dx = (C + C')a < \infty.$$

Thus $\nabla V \in L^2(\mathring{\mathcal{S}})$; since $V \in L^2(\mathring{\mathcal{S}})$ as well, $V \in H^1(\mathring{\mathcal{S}})$. This completes the proof.

C.6.3 The Potential V_m

Finally, in this section we prove the following lemma.

Lemma C.10 *Let $\rho \in \mathcal{P}$, $\beta > 0$, and λ be feasible. Then for every $0 < \delta \leq \delta_m$ (where δ_m is defined in Lemma C.4) we have $V \in L^2_{\text{loc}}(\mathcal{M})$.*

Proof of Lemma C.10: Let $(x, y) \in \mathcal{M} = \{(x, y) \in \mathbb{R}^2 : x > a\}$, $\eta > 0$ be arbitrary, and define

$$\mathcal{M}_\eta \equiv \{(x, y) \in \mathbb{R}^2 : a < x < \eta\}.$$

Then for every $a < x < \eta$, $V(x, \cdot) \in L^2(\mathbb{R})$ by Lemma C.4. Thus the Plancherel Theorem implies

$$\int_{\mathcal{M}_\eta} |V|^2 d\mathbf{x} = \int_a^\eta \int_{-\infty}^\infty |V_m(x, y)|^2 dy dx = \int_a^\eta \int_{-\infty}^\infty |\widehat{V}_m(x, k)|^2 dk dx.$$

If $\eta > d_1$ this becomes

$$\begin{aligned} \int_{\mathcal{M}_\eta} |V|^2 d\mathbf{x} &= \int_{-\infty}^\infty \int_a^{d_0} |\widehat{V}_m(x, k)|^2 dx dk \\ &\quad + \int_{-\infty}^\infty \int_{d_0}^{d_1} |\widehat{V}_m(x, k)|^2 dx dk + \int_{-\infty}^\infty \int_{d_1}^\eta |\widehat{V}_m(x, k)|^2 dx dk. \end{aligned} \quad (\text{C.40})$$

We begin by considering the first integral in (C.40). From (C.3), (C.4), (C.23), and Lemma 4.1 we have, for $0 < \delta \leq \delta_m$, that

$$\begin{aligned} &\int_{-\infty}^\infty \int_a^{d_0} |\widehat{V}_m(x, k)|^2 dx dk \\ &\leq C_m(\delta) \int_{-\infty}^\infty \int_a^{d_0} |A_k|^2 e^{2|k|x} dx dk \\ &\leq C_m(\delta)(d_0 - a) \int_{-\infty}^\infty |A_k|^2 e^{2|k|d_0} dk \\ &= 2C_m(\delta)(d_0 - a) \int_0^\infty |A_k|^2 e^{2kd_0} dk \\ &= 2C_m(\delta)(d_0 - a) \left(\int_0^1 |A_k|^2 e^{2kd_0} dk + \int_1^\infty |A_k|^2 e^{2kd_0} dk \right) \\ &\leq 2C_m(\delta)(d_0 - a) \left[\widetilde{C}_c(\delta) \int_0^1 \frac{|I_k|^2}{k^2} e^{2kd_0} dk + C_c(\delta) \int_1^\infty \frac{e^{-2kd_0}}{k^2} e^{2kd_0} dk \right] \\ &\leq 2C_m(\delta)(d_0 - a) [\widetilde{C}_c(\delta) C_I^2 e^{2d_0} + C_c(\delta)]. \end{aligned}$$

We now focus our efforts on the third integral in (C.40). From (C.3), (C.4), (C.26), Lemma 4.1, and Lemma 4.12 we find that the following bounds hold for $0 < \delta \leq \delta_m$:

$$\int_{-\infty}^\infty \int_{d_1}^\eta |\widehat{V}_m(x, k)|^2 dx dk \leq \widetilde{C}_m(\delta) \int_{-\infty}^\infty \int_{d_1}^\eta |A_k|^2 e^{-2|k|(x-2a)} + \frac{|J_k(x)|^2}{2|k|^2} dx dk$$

$$\begin{aligned}
&= 2\tilde{C}_m(\delta) \left[\int_0^1 \int_{d_1}^\eta \tilde{C}_c(\delta) \frac{|I_k|^2}{k^2} e^{-2k(x-2a)} + \frac{|J_k(x)|^2}{2k^2} dx dk \right. \\
&\quad \left. + \int_1^\infty \int_{d_1}^\eta C_c(\delta) \frac{e^{-2kd_0}}{k^2} e^{-2k(x-2a)} + \frac{|J_k(x)|^2}{2k^2} dx dk \right] \\
&\leq 2\tilde{C}_m(\delta) \left[\int_0^1 \int_{d_1}^\eta \tilde{C}_c(\delta) C_I^2 e^{-2k(x-2a)} + \frac{C_J^2}{2} dx dk \right. \\
&\quad \left. + \int_1^\infty \int_{d_1}^\eta C_c(\delta) \frac{e^{-2kd_0}}{k^2} e^{-2k(x-2a)} + (d_1 - d_0) \|\rho\|_{L^2(\mathcal{M})}^2 \frac{e^{-2k(x-d_1)}}{2k^2} dx dk \right] \\
&= 2\tilde{C}_m(\delta) \left\{ \int_0^1 \tilde{C}_c(\delta) C_I^2 \left[\frac{e^{-2k(d_1-2a)} - e^{-2k(\eta-2a)}}{2k} \right] + \frac{C_J^2}{2} (\eta - d_1) dk \right. \\
&\quad \left. + \int_1^\infty C_c(\delta) \left[\frac{e^{-2k(d_1+d_0-2a)} - e^{-2k(\eta+d_0-2a)}}{2k^3} \right] \right. \\
&\quad \left. + (d_1 - d_0) \|\rho\|_{L^2(\mathcal{M})}^2 \left[\frac{1 - e^{-2k(\eta-d_1)}}{2k^3} \right] dk \right\}.
\end{aligned}$$

The first integral converges since $(2k)^{-1}[e^{-2k(d_1-2a)} - e^{-2k(\eta-2a)}] \rightarrow \eta - d_1$ as $k \rightarrow 0^+$.

The second integral converges since $d_1 + d_0 - 2a > 0$ and $\eta > d_1$.

Finally, we consider the second integral in (C.40). Performing computations similar to those that led to (C.30) (omitting the $(1+|k|^r)^2$ term) and using Lemma C.3, we find that the following bounds hold for $0 < \delta \leq \delta_m$:

$$\begin{aligned}
&\int_{-\infty}^\infty \int_{d_0}^{d_1} |\widehat{V}_m(x, k)|^2 dx dk \\
&\leq 2\tilde{C}_m(\delta) \left[\tilde{C}_c(\delta) C_I^2 \int_0^1 \int_{d_0}^{d_1} e^{-2k(x-2a)} dx dk + C_c(\delta) \int_1^\infty \int_{d_0}^{d_1} \frac{e^{-2k(x-2a+d_0)}}{k^2} dx dk \right] \\
&\quad + \int_0^1 \int_{d_0}^{d_1} C_H^2 dx dk + 2(d_1 - d_0) \|\rho\|_{L^2(\mathcal{M})}^2 \int_1^\infty \int_{d_0}^{d_1} \frac{1}{k^2} dx dk. \\
&= 2\tilde{C}_m(\delta) \left[\tilde{C}_c(\delta) C_I^2 \int_0^1 \frac{e^{-2k(d_0-2a)} - e^{-2k(d_1-2a)}}{2k} dk \right. \\
&\quad \left. + C_c(\delta) \int_1^\infty \frac{e^{-4k(d_0-a)} - e^{-2k(d_1+d_0-2a)}}{2k^3} dk \right] + \int_0^1 C_H^2 (d_1 - d_0) dk \\
&\quad + 2(d_1 - d_0)^2 \|\rho\|_{L^2(\mathcal{M})}^2 \int_1^\infty \frac{1}{k^2} dx dk.
\end{aligned}$$

The first integral above converges since $(2k)^{-1}[e^{-2k(d_0-2a)} - e^{-2k(d_1-2a)}] \rightarrow d_1 - d_0$ as $k \rightarrow 0^+$; the second integral converges since $d_0 > a$ and $d_1 + d_0 > 2a$; the third and fourth integrals converge as well. This completes the proof.

C.6.4 Summary

The results from Lemmas C.8–C.10 lead immediately to the following theorem.

Theorem C.7 *Let $\rho \in \mathcal{P}$, $\beta > 0$, and λ be feasible. Then for every $0 < \delta \leq \delta_m$ (where δ_m is defined in Lemma C.4), $V \in L^2_{\text{loc}}(\mathbb{R}^2) \cap H^1(\mathring{\mathcal{S}})$.*

C.7 Properties of the Fourier Transform

In this section, we provide a heuristic justification of (4.17) based on the theory of tempered distributions. See the book by Freidlander and Joshi [36] for more details.

Let $\phi : \mathbb{R}^2 \rightarrow \mathbb{C}$ be a *Schwartz Function*, i.e., an infinitely differentiable function that, together with all of its derivatives, decays to zero faster than any polynomial as $x^2 + y^2 \rightarrow \infty$. The set of tempered distributions is defined as the topological dual space of the set of Schwartz Functions; i.e., the set of tempered distributions is the set of all continuous (equivalently, bounded) linear functionals acting on Schwartz Functions. The pairing between a tempered distribution T and a Schwartz Function ϕ is denoted $\langle T, \phi \rangle$.

The distributional partial derivative of a tempered distribution T is the tempered distribution $\frac{\partial T}{\partial x_i}$ such that

$$\left\langle \frac{\partial T}{\partial x_i}, \phi \right\rangle = - \left\langle T, \frac{\partial \phi}{\partial x_i} \right\rangle \quad (\text{C.41})$$

for all Schwartz Functions ϕ . Similarly, the Fourier Transform of a tempered distribution T is defined as the tempered distribution \widehat{T} that satisfies

$$\langle \widehat{T}, \phi \rangle = \langle T, \widehat{\phi} \rangle \quad (\text{C.42})$$

for all Schwartz Functions ϕ .

Since $\widehat{V}(x, k) \in L^2_{\text{loc}}(\mathbb{R}^2)$ (by Theorem C.7 — the proof we used for V holds for \widehat{V} as well by the Plancherel Theorem), \widehat{V} and all of its distributional partial derivatives are tempered distributions. Thus, by the definitions of distributional

partial derivatives and Fourier Transforms given in (C.41) and (C.42), we have, for any Schwartz Function ϕ , that

$$\left\langle \frac{\partial \widehat{V}}{\partial x}, \phi \right\rangle = - \left\langle \widehat{V}, \frac{\partial \phi}{\partial x} \right\rangle = - \left\langle V, \frac{\partial \widehat{\phi}}{\partial x} \right\rangle. \quad (\text{C.43})$$

Since Schwartz Functions behave very nicely (in particular Schwartz Functions and all of their partial derivatives are integrable), Theorem 4.2 implies

$$\frac{\partial \widehat{\phi}}{\partial x}(x, k) = \int_{-\infty}^{\infty} \frac{\partial \phi}{\partial x}(x, y) e^{-iky} dy = \frac{\partial}{\partial x} \int_{-\infty}^{\infty} \phi(x, y) e^{-iky} dy = \frac{\partial \widehat{\phi}}{\partial x}(x, k). \quad (\text{C.44})$$

Inserting (C.44) into (C.43) and using the definitions of distributional partial derivative and Fourier Transforms in (C.41) and (C.42), respectively, gives

$$\left\langle \frac{\partial \widehat{V}}{\partial x}, \phi \right\rangle = - \left\langle V, \frac{\partial \widehat{\phi}}{\partial x} \right\rangle = - \left\langle V, \frac{\partial \widehat{\phi}}{\partial x} \right\rangle = \left\langle \frac{\partial V}{\partial x}, \widehat{\phi} \right\rangle = \left\langle \frac{\partial \widehat{V}}{\partial x}, \phi \right\rangle$$

for all Schwartz Functions ϕ . Hence

$$\frac{\partial \widehat{V}}{\partial x} = \frac{\partial \widehat{V}}{\partial x}.$$

A similar proof with $\frac{\partial}{\partial x}$ replaced by $\frac{\partial}{\partial y}$ shows that

$$-ik\widehat{V} = \frac{\partial \widehat{V}}{\partial y}.$$

REFERENCES

- [1] R. ADAMS, *Sobolev Spaces*, vol. 65 of Pure and Applied Mathematics Series, Academic Press, Inc., New York, 1975.
- [2] G. ALESSANDRINI, A. MORASSI, AND E. ROSSET, *Detecting an inclusion in an elastic body by boundary measurements*, SIAM Journal on Mathematical Analysis, 33 (2002), pp. 1247–1268.
- [3] —, *Detecting cavities by electrostatic boundary measurements*, Inverse Problems, 18 (2002), pp. 1333–1353.
- [4] —, *Detecting an inclusion in an elastic body by boundary measurements*, SIAM Review, 46 (2004), pp. 477–498.
- [5] G. ALESSANDRINI, L. RONDI, E. ROSSET, AND S. VESSELLA, *The stability for the Cauchy problem for elliptic equations*, Inverse Problems, 25 (2009), p. 123004.
- [6] G. ALESSANDRINI, E. ROSSET, AND J. K. SEO, *Optimal size estimates for the inverse conductivity problem with one measurement*, Proceedings of the American Mathematical Society, 128 (2000), pp. 53–64.
- [7] —, *Optimal size estimates for the inverse conductivity problem with one measurement*, Proceedings of the American Mathematical Society, 128 (2000), pp. 53–64.
- [8] H. AMMARI, G. CIRAULO, H. KANG, H. LEE, AND G. W. MILTON, *Anomalous localized resonance using a folded geometry in three dimensions*, Proceedings of the Royal Society A, 469 (2013).
- [9] —, *Spectral theory of a Neumann–Poincaré-type operator and analysis of cloaking due to anomalous localized resonance*, Archive for Rational Mechanics and Analysis, 208 (2013), pp. 667–692.
- [10] —, *Spectral theory of a Neumann–Poincaré-type operator and analysis of cloaking due to anomalous localized resonance II*, Contemporary Mathematics, 615 (2014), pp. 1–14.
- [11] H. AMMARI AND H. KANG, *Polarization and Moment Tensors With Applications to Inverse Problems and Effective Medium Theory*, vol. 162 of Applied Mathematical Sciences, Springer, New York, 2007.
- [12] K. ASTALA AND L. PÄIVÄRINTA, *Calderón’s inverse conductivity problem in the plane*, Annals of Mathematics, 263 (2006), pp. 265–299.

- [13] R. J. ATKIN AND N. FOX, *An Introduction to the Theory of Elasticity*, Longman Inc., New York, 1980.
- [14] E. BERETTA, E. FRANCINI, AND S. VESSELLA, *Size estimates for the EIT problem with one measurement: the complex case*, *Revista Matemática Iberoamericana*, (2011). Also see arXiv:1108.0052v2 [math.AP].
- [15] D. J. BERGMAN, *Perfect imaging of a point charge in the quasistatic regime*, *Physical Review A*, 89 (2014), p. 015801.
- [16] J. G. BERRYMAN AND R. V. KOHN, *Variational constraints for electrical-impedance tomography*, *Physical Review Letters*, 65 (1990), pp. 325–328.
- [17] V. BONNAILLIE-NOËL, M. DAMBRINE, F. HÉRAU, AND G. VIAL, *On generalized Ventcel's type boundary conditions for Laplace operator in a bounded domain*, *SIAM Journal on Mathematical Analysis*, 42 (2010), pp. 931–945.
- [18] —, *Artificial conditions for the linear elasticity equations*, to appear in *Mathematics of Computation*, (2014).
- [19] L. BORCEA, *Electrical impedance tomography*, *Inverse Problems*, 18 (2002), pp. R99–R136.
- [20] G. BOUCHITTÉ AND B. SCHWEIZER, *Cloaking of small objects by anomalous localized resonance*, *The Quarterly Journal of Mechanics and Applied Mathematics*, 63 (2010), pp. 437–463.
- [21] S. BOYD AND L. VANDENBERGHE, *Convex Optimization*, Cambridge University Press, Cambridge, UK, 2004.
- [22] R. BROWN AND G. UHLMANN, *Uniqueness in the inverse conductivity problem for nonsmooth conductivities in two dimensions*, *Communications in Partial Differential Equations*, 22 (1997), pp. 1009–1027.
- [23] O. P. BRUNO AND S. LINTNER, *Superlens-cloaking of small dielectric bodies in the quasistatic regime*, *Journal of Applied Physics*, 102 (2007), p. 124502.
- [24] A. P. CALDERÓN, *On an inverse boundary value problem*, in *Seminar on Numerical Analysis and its Applications to Continuum Physics*, W. H. Meyer and M. A. Raupp, eds., Rio de Janeiro, 1980, Sociedade Brasileira de Matematica, pp. 65–73.
- [25] Y. CAPDEBOSCQ AND H. KANG, *Improved Hashin–Shtrikman bounds for elastic moment tensors and an application*, *Applied Mathematics and Optimization*, 57 (2008), pp. 263–288.
- [26] Y. CAPDEBOSCQ AND M. S. VOGELIUS, *Optimal asymptotic estimates for the volume of internal inhomogeneities in terms of multiple boundary measurements*, *Mathematical Modelling and Numerical Analysis (Modelisation mathématique et analyse numérique: M²AN)*, 37 (2003), pp. 227–240.

- [27] M. CHENEY, D. ISAACSON, AND J. C. NEWELL, *Electrical impedance tomography*, SIAM Review, 41 (1999), pp. 85–101.
- [28] A. V. CHERKAEV AND L. V. GIBIANSKY, *Variational principles for complex conductivity, viscoelasticity, and similar problems in media with complex moduli*, Journal of Mathematical Physics, 35 (1994), pp. 127–145.
- [29] E. CHERKAEVA AND K. GOLDEN, *Inverse bounds for microstructural parameters of composite media derived from complex permittivity measurements*, Waves in Random Media, 8 (1998), pp. 437–450.
- [30] A. H. ENGLAND, *Complex Variable Methods in Elasticity*, Wiley-Interscience, New York, 1971.
- [31] H. ERICKSON, *Size and shape of protein molecules at the nanometer level determined by sedimentation, gel filtration, and electron microscopy*, Biological Proceedings Online, 11 (2009), pp. 32–51.
- [32] L. C. EVANS, *Partial Differential Equations*, vol. 19 of Graduate Studies in Mathematics, American Mathematical Society, Providence, 2010.
- [33] L. C. EVANS AND R. F. GARIEPY, *Measure Theory and Fine Properties of Functions*, Studies in Advanced Mathematics, CRC Press, New York, 1992.
- [34] H. FLANDERS, *Differentiation under the integral sign*, The American Mathematical Monthly, 80 (1973), pp. 615–627.
- [35] E. FRANCINI, *Recovering a complex coefficient in planar domain from the Dirichlet-to-Neumann map*, Inverse Problems, 16 (2000), pp. 107–119.
- [36] G. FRIEDLANDER AND M. JOSHI, *Introduction to the Theory of Distributions*, Cambridge University Press, Cambridge, UK, 1998.
- [37] N. GARCIA AND M. NIETO-VESPERINAS, *Left-handed materials do not make a perfect lens*, Physical Review Letters, 88 (2002), p. 207403.
- [38] D. GIVOLI, *Non-reflecting boundary conditions*, Journal of Computational Physics, 94 (1991), pp. 1–29.
- [39] Y. GRABOVSKY, *Exact relations for effective tensors of polycrystals. I. Necessary conditions*, Archive for Rational Mechanics and Analysis, 143 (1998), pp. 309–329.
- [40] Y. GRABOVSKY AND G. W. MILTON, *Exact relations for composites: towards a complete solution*, Documenta Mathematica, Journal der Deutschen Mathematiker-Vereinigung, Extra Volume ICM III (1998), pp. 623–632.
- [41] —, *Rank one plus a null-Lagrangian is an inherited property of two-dimensional compliance tensors under homogenization*, Proceedings of the Royal Society of Edinburgh, 128A (1998), pp. 283–299.

- [42] Y. GRABOVSKY, G. W. MILTON, AND D. S. SAGE, *Exact relations for effective tensors of composites: necessary conditions and sufficient conditions*, Communications on Pure and Applied Mathematics, 53 (2000), pp. 300–353.
- [43] Y. GRABOVSKY AND D. S. SAGE, *Exact relations for effective tensors of polycrystals. II. Applications to elasticity and piezoelectricity*, Archive for Rational Mechanics and Analysis, 143 (1998), pp. 331–356.
- [44] A. GREENLEAF, M. LASSAS, AND G. UHLMANN, *On non-uniqueness for Calderón’s inverse problem*, Mathematical Research Letters, 10 (2003), pp. 685–693.
- [45] D. J. GRIFFITHS, *Introduction to Electrodynamics*, Prentice-Hall, Inc., Upper Saddle River, NJ, third ed., 1999.
- [46] H. GRIFFITHS, *Tissue spectroscopy with electrical impedance tomography: computer simulations*, IEEE Transactions on Biomedical Engineering, 42 (1995), pp. 948–953.
- [47] B. HABERMAN AND D. TATARU, *Uniqueness in Calderón’s problem with Lipschitz conductivities*, Duke Mathematical Journal, 162 (2013), pp. 497–516.
- [48] S. J. HAMILTON, *A direct D -bar reconstruction algorithm for complex admittivities in $W^{2,\infty}(\Omega)$ for the 2-D EIT problem*, Ph.D. thesis, Colorado State University, Fort Collins, CO, 2012.
- [49] S. J. HAMILTON AND J. L. MUELLER, *Direct EIT reconstructions of complex admittivities on a chest-shaped domain in 2-D*, IEEE Transactions on Medical Imaging, 32 (2013), pp. 757–769.
- [50] S. J. HAMILTON AND S. SILTANEN, *Nonlinear inversion from partial EIT data: computational experiments*, in Inverse Problems and Applications, P. Stefanov, A. Vasy, and M. Zworski, eds., vol. CONM/615, Providence, RI, 2014, American Mathematical Society, pp. 105–129.
- [51] H. HAN AND W. BAO, *Error estimates for the finite element approximation of linear elastic equations in an unbounded domain*, Mathematics of Computation, 70 (2000), pp. 1437–1459.
- [52] H. HAN AND X. WU, *Approximation of infinite boundary condition and its application to finite element methods*, Journal of Computational Mathematics, 3 (1985), pp. 179–192.
- [53] —, *The approximation of the exact boundary conditions at an artificial boundary for linear elastic equations and its application*, Mathematics of Computation, 59 (1992), pp. 21–37.
- [54] Z. HASHIN, *Analysis of composite materials — A survey*, Journal of Applied Mechanics, 50 (1983), pp. 481–505.
- [55] Z. HASHIN AND S. SHTRIKMAN, *A variational approach to the theory of the effective magnetic permeability of multiphase materials*, Journal of Applied Physics, 33 (1962), pp. 3125–3131.

- [56] M. HEGG, *Exact relations and links for fiber-reinforced elastic composites*, PhD thesis, Temple University, Philadelphia, Pennsylvania, 2012.
- [57] —, *Links between effective tensors for fiber-reinforced elastic composites*, *Comptes Rendus Mécanique*, 341 (2013), pp. 520–532.
- [58] R. HILL, *The elastic behavior of a crystalline aggregate*, *Proceedings of the Physical Society, A*, 65 (1952), pp. 349–354.
- [59] —, *Discontinuity relations in mechanics of solids*, in *Progress in Solid Mechanics*, I. N. Sneddon and R. Hill, eds., vol. II, North-Holland Publishing Co., Amsterdam, 1961, ch. VI, pp. 247–276.
- [60] —, *Elastic properties of reinforced solids: some theoretical principles*, *Journal of the Mechanics and Physics of Solids*, 11 (1963), pp. 357–372.
- [61] —, *Theory of mechanical properties of fibre-strengthened materials: I. Elastic behaviour*, *Journal of the Mechanics and Physics of Solids*, 12 (1964), pp. 199–212.
- [62] M. IKEHATA, *Size estimation of inclusion*, *Journal of Inverse and Ill-Posed Problems*, 6 (1998), pp. 127–140.
- [63] J. D. JACKSON, *Classical Electrodynamics*, John Wiley & Sons, Inc., Hoboken, NJ, third ed., 1999.
- [64] H. KANG, E. KIM, AND G. W. MILTON, *Sharp bounds on the volume fractions of two materials in a two-dimensional body from electrical boundary measurements: the translation method*, *Calculus of Variations and Partial Differential Equations*, 45 (2012), pp. 367–401.
- [65] H. KANG, K. KIM, H. LEE, X. LI, AND G. W. MILTON, *Bounds on the size of an inclusion using the translation method for two-dimensional complex conductivity*, to appear in *SIAM Journal on Applied Mathematics*, (2014). Also see arXiv:1310.2439 [math.AP].
- [66] H. KANG AND G. W. MILTON, *Bounds on the volume fractions of two materials in a three dimensional body from boundary measurements by the translation method*, *SIAM Journal on Applied Mathematics*, 73 (2013), pp. 475–492.
- [67] H. KANG, G. W. MILTON, AND J.-N. WANG, *Bounds on the volume fraction of the two-phase shallow shell using one measurement*, *Journal of Elasticity*, 114 (2014), pp. 41–53.
- [68] H. KANG, J. K. SEO, AND D. SHEEN, *The inverse conductivity problem with one measurement: stability and estimation of size*, *SIAM Journal on Mathematical Analysis*, 28 (1997), pp. 1389–1405.
- [69] W. KAPLAN, *Advanced Calculus*, Addison-Wesley Publishing Company, Reading, Massachusetts, third ed., 1984.

- [70] Y. KATZNELSON, *An Introduction to Harmonic Analysis*, Dover Publications, Inc., New York, second corrected ed., 1976.
- [71] A. KLENKE, *Probability Theory: A Comprehensive Course*, Universitext, Springer-Verlag, London, UK, 2008.
- [72] R. V. KOHN, J. LU, B. SCHWEIZER, AND M. I. WEINSTEIN, *A variational perspective on cloaking by anomalous localized resonance*, Communications in Mathematical Physics, 328 (2014), pp. 1–27.
- [73] R. V. KOHN, H. SHEN, M. S. VOGELIUS, AND M. I. WEINSTEIN, *Cloaking via change of variables in electric impedance tomography*, Inverse Problems, 24 (2008), p. 015016.
- [74] R. V. KOHN AND M. S. VOGELIUS, *Determining conductivity by boundary measurements*, Communications on Pure and Applied Mathematics, 37 (1984), pp. 289–298.
- [75] ———, *Determining conductivity by boundary measurements II. Interior results*, Communications on Pure and Applied Mathematics, 38 (1985), pp. 643–667.
- [76] S. LEE, R. E. CAFLISCH, AND Y.-J. LEE, *Exact artificial boundary conditions for continuum and discrete elasticity*, SIAM Journal on Applied Mathematics, 66 (2006), pp. 1749–1775.
- [77] U. LEONHARDT AND T. G. PHILBIN, *General relativity in electrical engineering*, New Journal of Physics, 8 (2006), p. 247.
- [78] U. LEONHARDT AND T. TYC, *Broadband invisibility by non-Euclidean cloaking*, Science, 323 (2009), pp. 110–112.
- [79] R. LIPTON, *Inequalities for electric and elastic polarization tensors with applications to random composites*, Journal of the Mechanics and Physics of Solids, 41 (1993), pp. 809–833.
- [80] K. A. LURIE AND A. V. CHERKAEV, *Accurate estimates of the conductivity of mixtures formed of two materials in a given proportion (two-dimensional problem)*, Doklady Akademii Nauk SSSR, 264 (1982), pp. 1128–1130. English translation in *Soviet Phys. Dokl.* 27:461–462 (1982).
- [81] ———, *Exact estimates of conductivity of composites formed by two isotropically conducting media taken in prescribed proportion*, Proceedings of the Royal Society of Edinburgh. Section A, Mathematical and Physical Sciences, 99 (1984), pp. 71–87.
- [82] ———, *Effective characteristics of composite materials and the optimal design of structural elements*, Uspekhi Mekhaniki (Advances in Mechanics), 9 (1986), pp. 3–81. English translation in *Topics in the Mathematical Modelling of Composite Materials*, pp. 175–258, ed. by A. Cherkhev and R. Kohn. ISBN 0-8176-3662-5.

- [83] K. A. LURIE, A. V. CHERKAEV, AND A. V. FEDOROV, *On the existence of solutions to some problems of optimal design for bars and plates*, Journal of Optimization Theory and Applications, 42 (1984), pp. 247–281.
- [84] G. MATHERON, *Quelques inégalités pour la perméabilité effective d'un milieu poreux hétérogène. (French) [Some inequalities for the effective permeability of a heterogeneous porous medium]*, Cahiers de Géostatistique, 3 (1993), pp. 1–20.
- [85] R. C. MCPHEDRAN, D. R. MCKENZIE, AND G. W. MILTON, *Extraction of structural information from measured transport properties of composites*, Applied Physics A, 29 (1982), pp. 19–27.
- [86] R. C. MCPHEDRAN AND G. W. MILTON, *Inverse transport problems for composite media*, Materials Research Society Symposium Proceedings, 195 (1990), pp. 257–274.
- [87] G. W. MILTON, *Composites: a myriad of microstructure independent relations*, in Theoretical and Applied Mechanics 1996: Proceedings of the XIXth International Congress of Theoretical and Applied Mechanics, Kyoto, Japan, 25–31 August 1996, T. Tatsumi, E. Watanabe, and T. Kambe, eds., Amsterdam, 1997, Elsevier, pp. 443–459.
- [88] —, *The Theory of Composites*, vol. 6 of Cambridge Monographs on Applied and Computational Mathematics, Cambridge University Press, Cambridge, United Kingdom, 2002.
- [89] —, *Universal bounds on the electrical and elastic response of two-phase bodies and their application to bounding the volume fraction from boundary measurements*, Journal of the Mechanics and Physics of Solids, 60 (2012), pp. 139–155.
- [90] G. W. MILTON AND L. H. NGUYEN, *Bounds on the volume fraction of 2-phase, 2-dimensional elastic bodies and on (stress, strain) pairs in composites*, Comptes Rendus Mécanique, 340 (2012), pp. 193–204.
- [91] G. W. MILTON AND N.-A. P. NICOROVICI, *On the cloaking effects associated with anomalous localized resonance*, Proceedings of the Royal Society A, 462 (2006), pp. 3027–3059.
- [92] G. W. MILTON, N.-A. P. NICOROVICI, AND R. C. MCPHEDRAN, *Opaque perfect lenses*, Physica B, 394 (2007), pp. 171–175.
- [93] G. W. MILTON, N.-A. P. NICOROVICI, R. C. MCPHEDRAN, K. CHEREDNICHENKO, AND Z. JACOB, *Solutions in folded geometries, and associated cloaking due to anomalous resonance*, New Journal of Physics, 10 (2008), p. 115021.
- [94] G. W. MILTON, N.-A. P. NICOROVICI, R. C. MCPHEDRAN, AND V. A. PODOLSKIY, *A proof of superlensing in the quasistatic regime, and limitations of superlenses in this regime due to anomalous localized resonance*, Proceedings of the Royal Society A, 461 (2005), pp. 3999–4034.

- [95] J. MINKEL, *Left-handed materials debate heats up*, *Physical Review Focus*, 9 (2002), p. 23.
- [96] A. MORASSI, E. ROSSET, AND S. VESSELLA, *Detecting general inclusions in elastic plates*, *Inverse Problems*, 25 (2009), p. 045009.
- [97] J. L. MUELLER AND S. SILTANEN, *Linear and Nonlinear Inverse Problems with Practical Applications*, SIAM Series on Computational Science and Engineering, SIAM, Philadelphia, 2012.
- [98] F. MURAT AND L. TARTAR, *Calcul des variations et homogénéisation. (French) [Calculus of variation and homogenization]*, in *Les méthodes de l'homogénéisation: théorie et applications en physique*, vol. 57 of *Collection de la Direction des études et recherches d'Électricité de France*, Paris, 1985, Eyrolles, pp. 319–369. English translation in *Topics in the Mathematical Modelling of Composite Materials*, pp. 139–173, ed. by A. Cherkaev and R. Kohn.
- [99] N. I. MUSKHELISHVILI, *Some Basic Problems of the Mathematical Theory of Elasticity: Fundamental Equations, Plane Theory of Elasticity, Torsion, and Bending*, P. Noordhoff, Groningen, The Netherlands, 1963.
- [100] A. I. NACHMAN, *Reconstructions from boundary measurements*, *Annals of Mathematics*, 128 (1988), pp. 531–576.
- [101] ———, *Global uniqueness for a two-dimensional inverse boundary value problem*, *Annals of Mathematics*, 143 (1996), pp. 71–96.
- [102] S. NEMAT-NASSER AND M. HORI, *Micromechanics: Overall Properties of Heterogeneous Materials*, vol. 37 of *North-Holland Series in Applied Mathematics and Mechanics*, North-Holland Publishing Co., Amsterdam, first ed., 1993.
- [103] H.-M. NGUYEN, *Superlensing using complementary media*, to appear in *Annales de l'Institut Henri Poincaré (C) Non Linear Analysis*, (2014). Also see arXiv:1311.5700v1 [math-AP].
- [104] N. A. NICOROVICI, R. C. MCPHEDRAN, AND G. W. MILTON, *Optical and dielectric properties of partially resonant composites*, *Physical Review B*, 49 (1994), pp. 8479–8482.
- [105] N.-A. P. NICOROVICI, R. C. MCPHEDRAN, AND L. C. BOTTEN, *Relative local density of states and cloaking in finite clusters of coated cylinders*, *Waves in Random and Complex Media*, 21 (2011), pp. 248–277.
- [106] N.-A. P. NICOROVICI, R. C. MCPHEDRAN, L. C. BOTTEN, AND G. W. MILTON, *Cloaking by plasmonic resonance among systems of particles: cooperation or combat?*, *Comptes Rendus Physique*, 10 (2009), pp. 391–399.
- [107] N.-A. P. NICOROVICI, R. C. MCPHEDRAN, S. ENOCH, AND G. TAYEB, *Finite wavelength cloaking by plasmonic resonance*, *New Journal of Physics*, 10 (2008), p. 115020.

- [108] N.-A. P. NICOROVICI, G. W. MILTON, R. C. MCPHEDRAN, AND L. C. BOTTEN, *Quasistatic cloaking of two-dimensional polarizable discrete systems by anomalous resonance*, *Optics Express*, 15 (2007), pp. 6314–6323.
- [109] J. B. PENDRY, *Negative refraction makes a perfect lens*, *Physical Review Letters*, 85 (2000), pp. 3966–3969.
- [110] J. B. PENDRY AND S. A. RAMAKRISHNA, *Near-field lenses in two dimensions*, *Journal of Physics: Condensed Matter*, 14 (2002), pp. 8463–8479.
- [111] N. PHAN-THIEN AND G. W. MILTON, *A possible use of bounds on effective moduli of composite materials*, *Journal of Reinforced Plastics and Composites*, 1 (1982), pp. 107–114.
- [112] E. ROSSET AND G. ALESSANDRINI, *The inverse conductivity problem with one measurement: bounds on the size of the unknown object*, *SIAM Journal on Applied Mathematics*, 58 (1998), pp. 1060–1071.
- [113] W. RUDIN, *Real and Complex Analysis*, McGraw-Hill, New York, third ed., 1987.
- [114] J. L. SCHIFF, *The Laplace Transform: Theory and Applications*, Undergraduate Texts in Mathematics, Springer-Verlag, New York, 1999.
- [115] J. SYLVESTER AND G. UHLMANN, *A uniqueness theorem for an inverse boundary value problem in electrical prospection*, *Communications on Pure and Applied Mathematics*, 39 (1986), pp. 91–112.
- [116] —, *A global uniqueness theorem for an inverse boundary value problem*, *Annals of Mathematics*, 125 (1987), pp. 153–169.
- [117] —, *Inverse boundary value problems at the boundary — continuous dependence*, *Communications on Pure and Applied Mathematics*, 41 (1988), pp. 197–219.
- [118] L. TARTAR, *Estimation de coefficients homogénéisés. (French) [Estimation of homogenization coefficients]*, in *Computing Methods in Applied Sciences and Engineering: Third International Symposium, Versailles, France, December 5–9, 1977*, R. Glowinski and J.-L. Lions, eds., vol. 704 of *Lecture Notes in Mathematics*, Berlin / Heidelberg / London / etc., 1979, Springer-Verlag, pp. 364–373. English translation in *Topics in the Mathematical Modelling of Composite Materials*, pp. 9–20, ed. by A. Cherkaev and R. Kohn. ISBN 0-8176-3662-5.
- [119] —, *Estimations fines des coefficients homogénéisés. (French) [Fine estimations of homogenized coefficients]*, in *Ennio de Giorgi Colloquium: Papers Presented at a Colloquium Held at the H. Poincaré Institute in November 1983*, P. Krée, ed., vol. 125 of *Pitman Research Notes in Mathematics*, London, 1985, Pitman Publishing Ltd., pp. 168–187.

- [120] A. E. THALER AND G. W. MILTON, *Bounds on the volume of an inclusion in a body from a complex conductivity measurement*, to appear in *Communications in Mathematical Sciences*, (2014). Also see arXiv:1306.6608 [math.AP].
- [121] V. G. VESELAGO, *The electrodynamics of substances with simultaneously negative values of ϵ and μ* , *Uspekhi Fizicheskikh Nauk*, 92 (1967), pp. 517–526. English translation in *Soviet Physics Uspekhi* 10:509–514 (1968).
- [122] M. XIAO, X. HUANG, J. W. DONG, AND C. T. CHAN, *On the time evolution of the cloaking effect of a metamaterial slab*, *Optics Letters*, 37 (2012), pp. 4594–4596.
- [123] A. D. YAGHJIAN AND T. B. HANSEN, *Plane-wave solutions to frequency-domain and time-domain scattering from magnetodielectric slabs*, *Physical Review E*, 73 (2006), p. 046608.
- [124] M. YAN, W. YAN, AND M. QIU, *Cylindrical superlens by a coordinate transformation*, *Physical Review B*, 78 (2008), p. 125113.
- [125] E. ZEIDLER, *Nonlinear Functional Analysis and its Applications II/A: Linear Monotone Operators*, Springer-Verlag, New York, 1990.